
Diazo Compounds in Continuous Flow Technology



A Thesis Submitted to Cardiff University
in Fulfilment of the Requirements for the
Degree of Doctor of Philosophy
by Simon Mueller

PhD Thesis December 2015

Cardiff University

DECLARATION

This work has not been submitted in substance for any other degree or award at this or any other university or place of learning, nor is being submitted concurrently in candidature for any degree or other award.

Signed (candidate) Date

STATEMENT 1

This thesis is being submitted in partial fulfillment of the requirements for the degree of(insert MCh, MD, MPhil, PhD etc, as appropriate)

Signed (candidate) Date

STATEMENT 2

This thesis is the result of my own independent work/investigation, except where otherwise stated.

Other sources are acknowledged by explicit references. The views expressed are my own.

Signed (candidate) Date

STATEMENT 3

I hereby give consent for my thesis, if accepted, to be available online in the University's Open Access repository and for inter-library loan, and for the title and summary to be made available to outside organisations.

Signed (candidate) Date

STATEMENT 4: PREVIOUSLY APPROVED BAR ON ACCESS

I hereby give consent for my thesis, if accepted, to be available online in the University's Open Access repository and for inter-library loans **after expiry of a bar on access previously approved by the Academic Standards & Quality Committee.**

Signed (candidate) Date

Acknowledgements

This thesis would have been unimaginable without the great support and help of many people. Unfortunately, my poor memory will probably lead to some important people being missed on this list but I will try my best to name all the important influences I had during these three years. It has been an exciting and intense journey which was made special by all the people who contributed to this work and made the time in Cardiff & Gaillac unforgettable.

Firstly, I want to thank my two excellent supervisors, Thomas Wirth and Paul Hellier. During my time in Cardiff, Thomas challenged me constantly to become a better scientist with a critical mind. His on-going passion for chemistry and his thorough knowledge of synthetic transformations were an inspiration during my PhD. Paul welcomed me in France during my stay at Pierre Fabre and he was a great motivator, constantly positive and excited about new results. His experience and insights into chemistry and the work in an international pharmaceutical company were invaluable. Thanks to both of them, I had the chance to learn so much about chemistry on all levels.

Next, I want to express my gratitude to the students who worked with me. Daniel Smith, my first MChem student, was already waiting for me here on my first day in Cardiff. Dan worked with a lot of motivation on using ethyl diazoacetate as nucleophile in flow chemistry (Chapter 3.2). Special credit has to go to Dan as he was around in the very beginning when my motivation to work 12 hours days was still at its peak. He survived it and is now already a third year PhD student himself. Thanks Dan! My next student was Ana Folgueiras, an Erasmus student from Spain who started in January 2013 and who brought some engineering experience into our little team. She worked with me on the synthesis of some heterocyclic structures (parts of Chapter 5.3 and parts of the Outlook section) with great dedication. Ana has a sharp mind and was a great help during our project together. Svenja Ehrmann and Tobias Hokamp were two German Erasmus students who worked with me on the lithiations of ethyl diazoacetate (Chapter 3.3), a very challenging project. Svenja was probably more organised than I am, I am still impressed by how much she did in just three months. Tobias was around when I was already writing up and without him, I would have struggled to do a proper substrate scope on the lithiation reactions. Not being very shy, Tobias asked me questions at any time of the day but we had a really good time and some in-depth discussions on basketball. Micol Santi was my Italian Erasmus student who spent nine months in our group and who worked on heterocycles (Chapter 5.3). I have never seen anybody work harder than Micol who, at times, seemed to live in the Uni. Being the daughter of a chemistry professor, her future can only be bright! Finally, Jasmine Lyster spent several weeks as a Bachelor

student with me and it was fun to have her around! I am grateful to all of them for their hard work but mostly for the great time we had together.

In fact, all the people in our research group at Cardiff University have to be thanked. The atmosphere in the group was really good the entire time. Thanks to Umar, Mike, Pushpak, Nida, Kenta, Ravi, Basil, Pete, Rebecca, Alessandra, Joel, Martin, Fabian, Anne, Sam, Seb, Jordan, Jonathan, Christiane, Joey, Duncan, Louis, Céline, Xiaoping, Filipa, Wilke, Marion, Michele, Erika, Kirara, Aragorn, Jihan, Daniel, Kai, Christina and Baker. My special gratitude to our social secs Ana and Florence for organising so many cool events. Florence also needs to get a big thank you from me for proof-reading parts of my thesis. Also a thank you to Dan and Rich for proof-reading some parts of my thesis. Matt and Rich also deserve a special thanks for being such good friends during my time in Cardiff and living with me for a year.

I was also very lucky during my time in France at Pierre Fabre where I worked with some great people in the lab. Special thanks to Aurélien Murat who worked with me on some of the flow projects (Chapter 5.2). It was a really fun time together in the lab and I am also really grateful that I could stay in his house for 6 months, merci Aurélien! Merci also to Manu, Delphine, Patrick, Cédrine, Eric, Gilles, Vincent, Stéphanie, Romain L., Roman A., Gautier, and all the others at the CDCI in Gaillac. It is a shame that the site is now closing down, the atmosphere was really exceptional.

My acknowledgements also have to be extended to the people from the School of Chemistry who helped me during my PhD. Alun Davies from the work-shop helped us with developing our FLLEX system. Rob Jenkins, Robin Hicks, Tom Williams, Sham Ali, Gary Coleman, Moira Northam, Benson Kariuki and Simon James have to be thanked for all their support for NMR, Mass spec, X-Ray and safety.

Finally, I need to say thank you to all my friends and my family who have been supporting me during the entire time. Thanks to my Cardiff & Toulouse friends Alex, Nic, Trygve, Roman, Carla, Ali, Ramu, Mylène, Dana, Pauline, Simone, and Jeremy. Thanks to my father Andreas and my mother Hélène as well as to my two awesome brothers Paul and Matze. And then I still need to thank the most important person who has been with me really day and night during this PhD, especially during the final writing up she was my biggest comfort and help. Thank you so much Christine, without you I would never have managed this. I'm so happy to have you in my life and I'm looking forward to our exciting future!

Dedicated to Hélène, Andreas, Paul and Mathias

List of Abbreviations

°C	Degree Celsius
μL	Microlitre
Å	Angström
anhydr.	anhydrous
APC	Alkylidene cyclopropane
APCI	atmospheric pressure chemical ionisation
aq.	aqueous
Ar	Aryl
bpr	back-pressure regulator
cat	catalytic
cm	Centimeter
conv	Conversion
CV	Column volumes
<i>d.r.</i>	Diastereomeric ratio
DBU	1,8-Diazabicyclo[5.4.0]undec-7-ene
DIBAL-H	Diisobutylaluminium hydride
DMF	<i>N,N</i> -Dimethylformamide
DMSO	Dimethylsulfoxide
DoE	Design of experiment
DSC	Differential scanning calorimetry
<i>ee</i>	Enantiomeric excess
<i>e.r.</i>	Enantiomeric ratio
EDA	Ethyl diazoacetate
EDG	electron donating group
EI	Electron ionisation

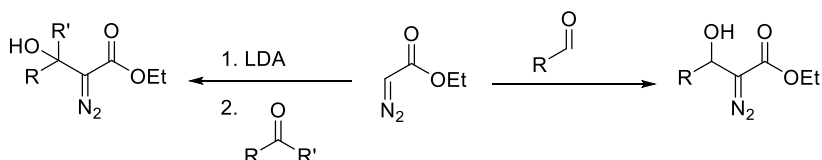
equiv.	Equivalents
ES	Electrospray ionisation
EtOAc	ethyl acetate
EWG	electron withdrawing group
Fe(TPP)Cl	Iron(III) tetraphenylporphine chloride
g	gramm
h	hour(s)
HOMO	Highest occupied molecular orbital
HPLC	High pressure liquid chromatography
HRMS	High resolution mass spectrometry
Hz	Hertz
i.d.	inner diameter
IBX	2-Iodoxybenzoic acid
IR	Infrared
J	Coupling constant (NMR)
Kg	Kilogramm
L	Litre
LDA	Lithium diisopropylamide
m.p.	Melting point
m/z	Mass over charge ratio
M	Molarity [mol/L]
mg	Milligramm
MHz	Megahertz
min	minute(s)
mL	Millilitre
mm	Millimeter

mmol	Millimol
MTSR	Maximum temperature of synthesis reaction
MTT	Maximum temperature for technical reasons
<i>n</i> -BuLi	<i>n</i> -butyllithium
nm	nanometer
NMR	Nuclear magnetic resonance
NSI	nanospray ionisation
<i>p</i> -ABSA	<i>p</i> -Acetamidobenzenesulfonyl azide
Pd/C	Palladium on charcoal
PDMS	Polydimethylsiloxane
PEEK	Polyether ether ketone
pm	picometer
<i>p</i> -NBSA	<i>p</i> -Nitrobenzenesulfonyl azide
ppm	parts per million
psi	pounds per square inch
PTFE	Polytetrafluoroethylene
r.t.	room temperature
RBF	round bottom flask
sat.	saturated
S-DOSP	S-(<i>N</i> -dodecylbenzenesulfonyl)prolinate
SNRI	serotonin-norepinephrine reuptake inhibitor
THF	Tetrahydrofuran
TLC	Thin layer chromatography
TMR	Time to maximum rate

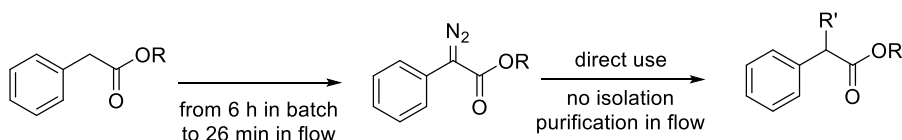
Abstract

Diazo compounds are highly reactive carbene precursors which can be used to generate molecular complexity rapidly. However, diazo compounds are highly energetic and dangerous compounds and therefore, their use in large-scale applications remains rare.

In this work, the use of continuous flow technology for the safe, efficient and scalable use of diazo compounds is described. By using flow chemistry, diazo compounds were safely generated within small diameter devices and directly used in subsequent reactions without a hazardous isolation of the diazo reagents. This thesis describes five new protocols for the use of diazo compounds. In the first project, ethyl diazoacetate (EDA) was generated safely in flow and used in subsequent aldol addition reactions to aldehydes with high yields (right). The preparation of the organometallic ethyl lithiodiazoacetate species in flow was achieved in the second project and used for the addition to ketones (left).



Detailed kinetic and thermal studies on aryl diazoacetates were performed in the third project which yielded a new, multistep continuous flow protocol for the use of donor / acceptor carbenes. Rapid reaction optimisation was achieved using in-line infrared spectroscopy. Purification of the diazo species was performed in flow using in-line liquid / liquid extraction methodology.



The fourth protocol entails the rapid assembly of complex lactone-cyclopropane structures of biological interest from diazo compounds in a combination of flow and batch technologies (left). In the final project, the stereoselective preparation of indolines using diazo compounds is discussed (right).

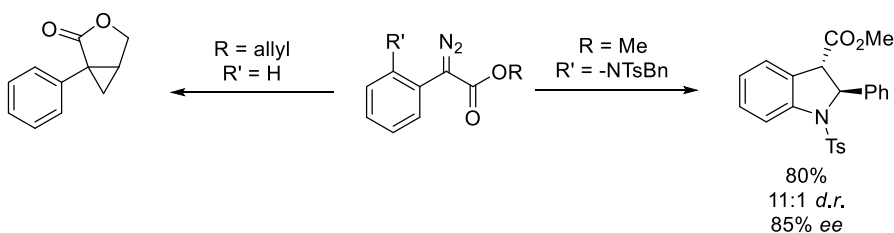


Table of Contents

1	Diazo compounds in continuous flow technology – Introduction	1
1.1	Diazo compounds – General properties	1
1.2	Diazo compounds – Preparation	4
1.2.1	Diazotization of primary amines	4
1.2.2	Diazo transfer reaction	5
1.2.3	Base treatment of sulfonyl hydrazones (Bamford-Stevens reaction)	6
1.2.4	Base-mediated cleavage of N-alkyl-N-Nitrosamides	7
1.2.5	Miscellaneous	7
1.3	Reactions of diazo compounds	10
1.3.1	Non-carbene based reactions	10
1.3.2	Diazo compounds to generate carbenes	11
1.3.2.1	Metal carbenes derived from diazo compounds	11
1.3.2.2	Catalyst systems for carbene reactions	13
1.3.2.3	C-H insertion reactions	14
1.3.2.4	X-H insertion reactions	15
1.3.2.5	Cyclopropanation	16
1.3.2.6	Cross-Coupling reactions	18
1.4	Continuous flow technology – General properties	19
1.4.1	Chemical hazards in flow	21
1.4.2	In-line analysis in flow	24
1.4.3	Multistep synthesis in flow	25
1.4.4	Diazo compounds in continuous flow technology	25
2	Objectives & Outline of the thesis	33
3	Ethyl diazoacetate as nucleophile	35
3.1	Introduction – EDA as nucleophile	35
3.2	Generation and direct use of ethyl diazoacetate in flow chemistry	38
3.2.1	Synthesis of ethyl diazoacetate	39
3.2.2	Aldol addition in continuous flow	42
3.2.3	Two-step continuous flow approach	44
3.2.3.1	Upscale	48
3.2.3.2	Limitations of the two-step continuous flow method	49
3.2.4	Three-step approach	50
3.3	Lithiation of ethyl diazoacetate in flow chemistry	54
3.3.1	Introduction into organometallics in flow	55
3.3.2	Reactions of ethyl lithiodiazoacetate in batch	56

3.3.3	Lithiation of ethyl diazoacetate in flow	59
3.4	Conclusion & Outlook	65
4	Donor / Acceptor Carbenes derived from Aryldiazoacetates	67
4.1	General Introduction	67
4.1.1	Diazo transfer reaction	70
4.1.1.1	Diazo transfer reagents	72
4.2	Standard protocol diazo transfer	73
4.3	Risk assessment diazo transfer	74
4.4	Reaction kinetics diazo transfer	79
4.4.1	Reaction kinetics in batch	79
4.4.2	Reaction kinetics in flow	81
4.5	Extraction of diazo reagent	84
4.6	Reaction optimization of carbene reactions	87
4.6.1	General kinetic properties of diazo decomposition	93
4.6.2	Comparison of catalysts for diazo decomposition	94
4.7	Multistep Process	96
4.8	Conclusion & Outlook	101
5	Synthesis of heterocycles using diazo compounds	103
5.1	General Introduction	103
5.2	Intramolecular Cyclopropanation	104
5.2.1	Introduction – Intramolecular cyclopropanation to bicyclic lactone	104
5.2.2	Diazo transfer in flow	106
5.2.3	Intramolecular cyclopropanation in flow	109
5.2.4	Two-step protocol	111
5.2.5	Side product and error analysis	116
5.2.6	Modified two-step protocol	120
5.2.7	Upscale	122
5.3	Formation of dihydroindoles	123
5.3.1	Introduction	123
5.3.2	Synthesis of diazo transfer precursor	127
5.3.3	Diazo transfer	130
5.3.4	C-H insertion for dihydroindoles	137
5.4	Conclusion & Outlook	142
6	Conclusion & Outlook	146
7	Experimental Section	156
7.1	General Methods	156
7.2	Experimentals Chapter 3	156

7.2.1	Synthesis of ethyl diazoacetate in batch <i>via</i> diazotization	156
7.2.2	Synthesis of ethyl diazoacetate in batch from ethyl 2-bromoacetate	157
7.2.3	Synthesis of ethyl diazoacetate in flow	158
7.2.4	Two-step continuous flow system for α -diazo- β -hydroxyester	158
7.2.5	Cyclopropanation with styrene	163
7.2.6	Oxidation of α -diazo- β -hydroxyester to α -diazo- β -ketoester	163
7.2.7	Three-step process	165
7.2.8	Lithiation reactions in batch	166
7.2.9	Lithiation of ethyl diazoacetate in flow	167
7.2.10	Ring-expansion reaction of diazoalcohol	172
7.3	Experimentals Chapter 4	173
7.3.1	Calculation of rate constant of batch reaction	173
7.3.2	Calculation of rate constant for different temperature in flow	174
7.3.3	Calculation of activation energy	174
7.3.4	Calculation of T_{D24}	175
7.3.5	Procedure thermal studies	175
7.3.6	Kinetic studies of diazo transfer	175
7.3.7	Procedure batch reaction diazo transfer	177
7.3.8	Procedure flow reaction diazo transfer	178
7.3.9	Diazo decomposition reactions	178
7.3.10	Multistep process in flow	192
7.4	Experimentals Chapter 5	200
7.4.1	Experimentals intramolecular cyclopropanation	200
7.4.2	Experimentals Dihydroindoles	207
7.4.2.1	Synthesis of tosyl protected amine 257	207
7.4.2.2	Benzylation of tosyl protected amine 257	208
7.4.2.3	Diazo transfer	213
7.4.2.4	C-H insertion reaction	218
7.4.2.5	^1H NMR studies	224
7.4.2.5.1	Diazo transfer with methyl phenylacetate 186	224
7.4.2.5.2	Diazo transfer with ester 258	225

1 Diazo compounds in continuous flow technology – Introduction

Organic chemistry strives for the rapid assembly of complex molecules with multiple stereocenters. Some functional groups stand out in their ability to generate such a complexity quickly. The diazo functionality is among the most useful of these functional groups. Through the cleavage of the carbon-nitrogen bond releasing dinitrogen, diazo compounds generate carbenes which are highly reactive, and in case of metal-carbenes also very selective. Consequently, diazo compounds have been studied intensely in laboratory scale reactions. However, large scale applications of diazo compounds remain scarce. This is due to their thermal properties, as they are highly energetic and prone to explosion. Continuous flow chemistry has emerged as a safe technology for handling highly energetic reagents due to the large surface-to-volume ratio of continuous flow microreactors. Herein, the use of continuous flow technology for the safe and scalable generation of diazo compounds is presented.

1.1 Diazo compounds – General Properties

Diazo compounds **1** are reagents with linear dinitrogen as a functional group connected to a substituted carbon atom. The first diazo reagent made by Curtius in 1883 was ethyl diazoacetate.¹ In the reaction of glycine ethyl ester with sodium nitrite in acidic conditions, a yellow liquid could be obtained. Shortly after, diazomethane was produced by von Pechmann in a reaction of *N*-methyl-*N*-nitrosourethane with a base.² Interestingly, the structure of the diazo reagents was unclear in the beginning as a cyclic structure of type **2** could not be excluded (Figure 1).³ In 1911, Thiele argued against structure **2** as diazo compounds could be obtained by dehydrogenation of hydrazones which were known to possess a linear structure.⁴ Later, Boersch demonstrated the open chain structure of diazomethane using electron diffraction experiments.⁵ The linear structure of ethyl diazoacetate was demonstrated by Clusius in 1957 in a ¹⁵N-labeling experiment.⁶ Using ¹⁵N-labeled sodium nitrite for the preparation of ethyl diazoacetate (EDA), a subsequent reductive cleavage of EDA with zinc in acetic acid provided exclusively ¹⁵N ammonia. In a cyclic structure, a mixture of ¹⁵N and ¹⁴N ammonia would have to be expected. The cyclic equivalent **2** is now well established as functional class called diazirines.⁷ Diazirines are prepared by the Graham reaction, a hypohalite oxidation of amidines.

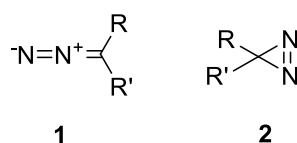
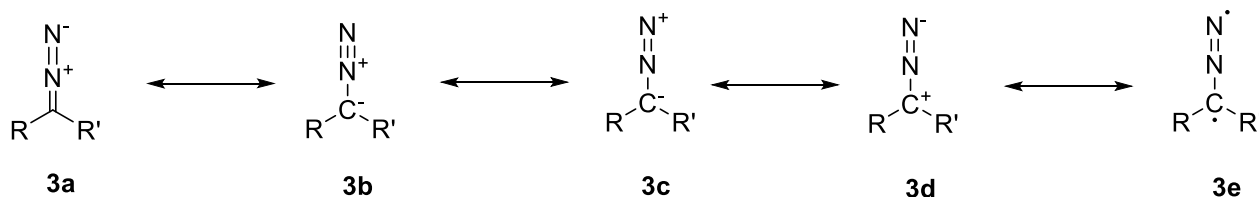


Figure 1: Diazo compounds **1** and diazirines **2**



Scheme 1: Mesomeric structures of diazo compounds

The structure of diazo compounds is generally described with resonance forms **3a** – **3e** (Scheme 1). Of these, structures **3a** and **3b** fit best with bond lengths and angles. In the structurally most simple diazo reagent, diazomethane, the C-N bond is 132 pm long and therefore shorter than a normal C-N single bond (147 pm). The N-N bond however is slightly longer than a normal N-N triple bond (109.8 pm) with 112 pm.⁸ The molecule has a C_{2v} symmetry and is therefore linear. Hybridisation is best described as $C(sp^2)$ - $N(sp)$ - $N(sp)$ system.⁹ The highest occupied molecular orbital (HOMO) is the nonbonding three-centre orbital **4** (Figure 2).¹⁰

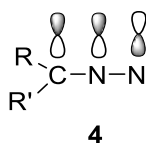


Figure 2: Highest occupied molecular orbital (HOMO) of diazoalkanes

The importance of a particular resonance form **3a** – **3e** to the overall structure depends on the carbon substituents R and R'. For example, in the case of R = EWG (electron withdrawing group), resonance structures **3b** and **3c** contribute more to the overall structure of the diazo reagent as the negative charge on the carbon atom can be further stabilised by the electron withdrawing group (–M effect).

The delocalised electron system of the diazo functional group is also responsible for its spectroscopical properties. Diazo compounds absorb energy of the electromagnetic spectrum within the range of visible light resulting in a strong yellow to red colour. They display two peaks in a UV/Vis spectrum, one weak peak at around 410-460 nm and a stronger one around 270 nm.¹¹ Interestingly, in case of α -diazoketones, the UV/Vis spectrum is highly solvent dependent. This was attributed to hydrogen bonding effects of the α -carbonyl group.¹² Diazo compounds exhibit a characteristic infrared absorption in the region from 1950 to 2300 cm^{-1} . The peak is strong in intensity and can be attributed to the N-N stretch of the nitrogen-nitrogen triple bond.¹³ ^{13}C spectra provide a good argument for the importance of structure **3b** and **3c** mentioned above. Compared to other sp^2 hybridised carbon atoms diazo reagents have a ^{13}C

peak shifted upfield i.e. diazomethane has a ^{13}C peak at 23 ppm and ethyl diazoacetate at 46 ppm.¹⁴ ^{15}N spectra have shown that N1 next to the carbon is more shielded than the terminal N2 (Figure 3). This finding seems to contradict the importance of structures **3a** and **3b** for describing the structures of diazo compounds as the positive charge on N1 should lead to a downfield shift. However, it has been shown that quaternary nitrogen species that lack the lone pair on nitrogen are shifted significantly upfield.¹⁵

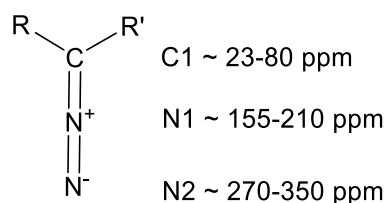


Figure 3: Typical ^{13}C and ^{15}N NMR shifts of diazo compounds

Diazo compounds are highly reactive species due to the possible loss of dinitrogen as a stabilised leaving group. Although providing synthetically valuable carbenes, this cleavage of nitrogen is also dangerous as it occurs highly exothermally and with a quick pressure build-up. The stability of diazo compounds depends on the substituents R and R' on the carbon atom. Overall, three classes of diazo compounds can be identified: (1) diazo compounds without any electron withdrawing group i.e. diazomethane **5** or phenyldiazomethane **6**; (2) diazo compounds with one electron withdrawing group i.e. ethyl diazoacetate **7** or diazo ethyl phenylacetate **8**; (3) diazo compounds with two electron withdrawing groups such as diazo diethyl malonate **9**. The stability increases with more electron withdrawing groups as substituents on the carbon atom of the diazo group (Figure 4). The impact of electron donating and withdrawing groups for the reactivity of these reagents will be discussed in section 1.3.2.1 on the topic of carbenes.

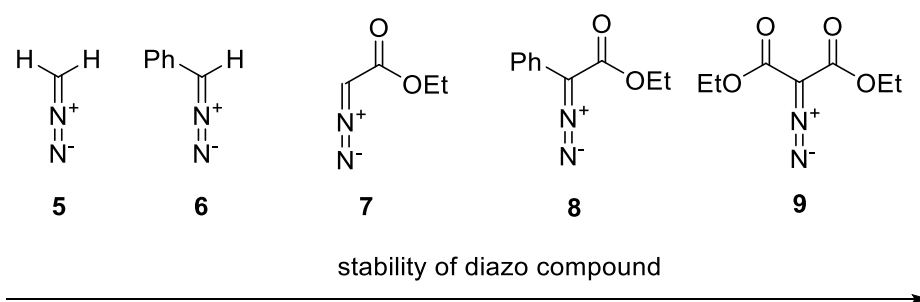


Figure 4: Stability of different classes of diazo compounds

Several spontaneous explosions of diazomethane **5** have been reported¹⁶ and even stabilised diazo compounds such as ethyl diazoacetate **7** are still highly energetic.¹⁷ Diazoalkanes such as diazomethane **5** are also toxic as they are classified as alkylation reagents and can

therefore lead to tumorigenesis. The toxicity of **5** is so acute that von Pechmann remarked in his original paper²:

“Scheinbar geruchlos, besitzt es höchst giftige Eigenschaften, welche zunächst Atemnoth, Brustschmerzen und Abgeschlagenheit hervorrufen und das Arbeiten damit äusserst unangenehm machen.”

“Seemingly odourless, this compound possesses highly toxic properties which cause breathlessness, breast pain and lassitude. This makes working with diazomethane very unpleasant.”

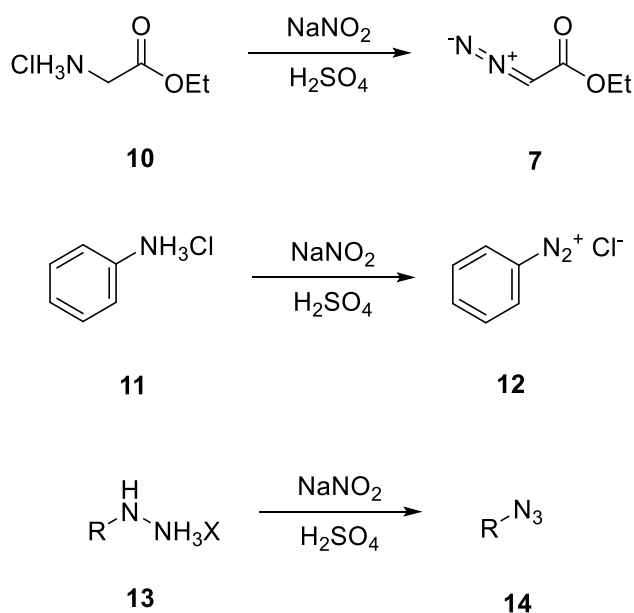
Nevertheless, diazo compounds have received immense interest by the scientific community in the last 130 years due to their exceptional reactivity. Industrial applications however remain rare as the use of such highly energetic compounds on large scale poses several challenges and risks in batch reaction conditions. In section 1.2 and 1.3 the preparation and utility of diazo reagents will be discussed. Section 1.4 will deal with continuous flow technology as a potential enabling methodology for the safe handling of large quantities of energetic diazo reagents.

1.2 Diazo compounds – Preparation

Diazo compounds can be made *via* different routes and it depends on the exact structure of the diazo reagent and the desired subsequent use which protocol should be employed.¹⁸ The most important synthetic pathways to diazo compounds are: (1) diazotization of primary amines with α -acceptor substituents; (2) diazo transfer onto an activated methylene group; (3) base treatment of sulfonylhydrazones and; (4) base mediated cleavage of *N*-alkyl-*N*-nitroso sulfonamides. Apart from these four most important methods there are several useful but less regularly employed techniques that will be discussed in section 1.2.5 under miscellaneous.

1.2.1 Diazotization of primary amines

Curtius made ethyl diazoacetate **7** in 1883 by using the diazotization of glycine ethyl ester **10**. The reaction can also be used in very similar fashion to make diazonium salts and azides depending on the substituents of the amine (Scheme 2).

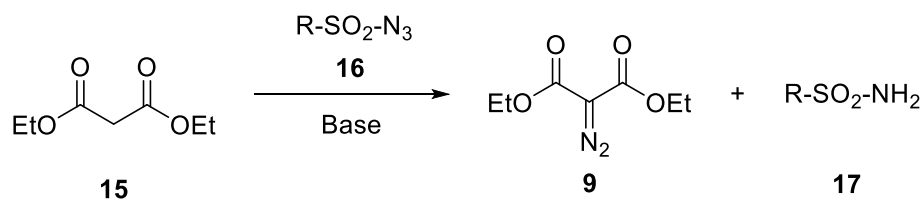


Scheme 2: Diazotization to make ethyl diazoacetate **7**, diazonium salt **12** and azide **14**; R = alkyl, aryl

Whilst this method is regularly used in the preparation of diazo reagents from amino acids, it is rarely used for introducing diazo groups into more complex molecules. A detailed discussion of diazotization reactions will be performed in chapter 3.

1.2.2 Diazo transfer reaction

The diazo transfer reaction was discovered by Regitz in 1967.¹⁹ The reaction transfers a diazo species from an organoazide **16** with an electron withdrawing group on the azide (usually a sulfonyl azide) onto an activated methylene or methine group **15** (Scheme 3). The reaction is used to make compounds bearing electron withdrawing groups such as phenyl diazoacetate **8** and diazo diethyl malonate **9**.



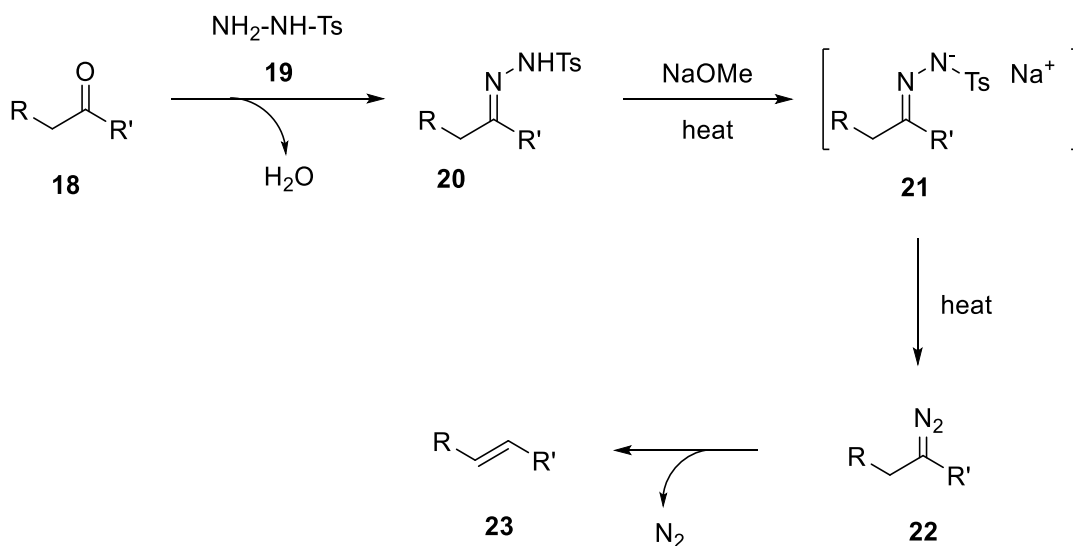
Scheme 3: Diazo transfer reaction onto diethyl malonate **15**; R = *p*-tosyl, *p*-acetamidobenzyl, trifluoromethyl, methyl

Diazo group transfer reactions are frequently employed to introduce diazo species late within a natural product synthesis as selectivity can be tuned.²⁰ In contrast to diazotization reactions, diazo transfer reactions tend to be clean reactions. However, diazo transfer reactions are not atom economic reactions as many sulfonyl azides **16** are large molecules for safety reasons. The reaction is also commonly used in the synthesis of azides using similar conditions but with

a primary amine instead of an activated methylene group as nucleophile. A detailed discussion on this reaction can be found in chapter 4.

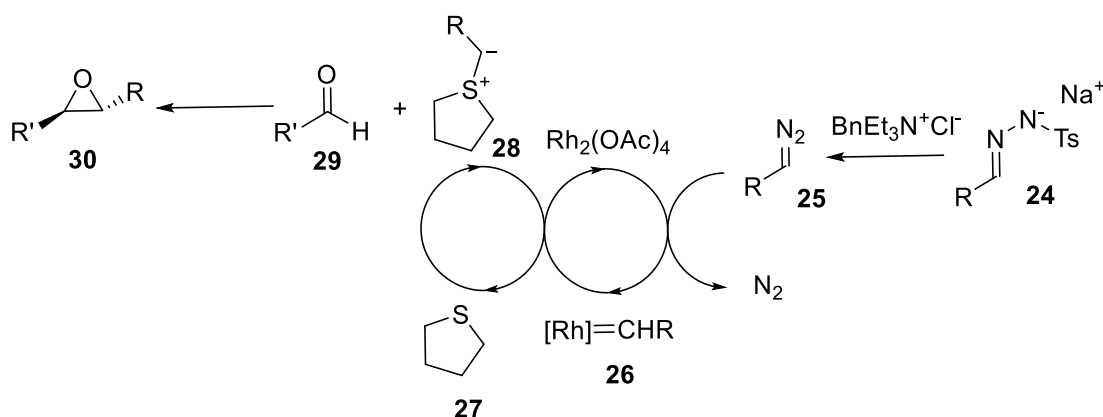
1.2.3 Base treatment of sulfonyl hydrazones (Bamford-Stevens reaction)

The base-induced decomposition of sulfonyl hydrazones was discovered by Bamford and Stevens in 1952.²¹ Tosyl hydrazones **20** can be obtained from the condensation of aldehydes and ketones **18** with tosyl hydrazine **19**. When these tosyl hydrazones **20** are heated in basic conditions, diazo species **22** can be formed. Typical diazo reagents obtained *via* this route are aryl diazomethane reagents such as **6** (Figure 4)y. In the standard protocol from Bamford and Stevens, the diazo compound decomposed immediately *via* an 1,2-hydride shift into the corresponding alkenes **23** (Scheme 4). Albeit useful for the regioselective synthesis of highly substituted olefins, the reaction lacked the versatility of normal diazo reactions.²²



Scheme 4: Bamford-Stevens reaction; R = alkyl; R' = alkyl

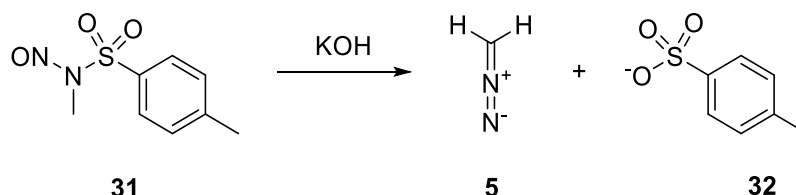
This has changed dramatically in the last 15 years. Aggarwal and co-workers developed a phase-transfer approach to trap diazo reagent **22** before alkene **23** was formed.²³ Quickly, this method was used for homologation of aldehydes,²⁴ highly stereoselective cyclopropanation of alkenes²⁵ and epoxidation of aldehydes (Scheme 5).²⁶ Tosyl hydrazone salt **24** is transferred into the solution using a phase-transfer catalyst ($\text{BnEt}_3\text{N}^+\text{Cl}^-$) to subsequently furnish diazo reagent **25**. The diazo reagent is then decomposed *via* rhodium catalysis to give the metal carbene **26** which reacts with thiophene **27** to the sulfur ylide **28**. This then attacks aldehyde **29** to give the *trans* epoxide **30** in high selectivity. The reaction can be highly enantioselective when a chiral sulfide is used. The decomposition of tosyl hydrazones is now the most common synthetic method for substituted diazo compounds in cases where none of the substituents are electron withdrawing groups.



Scheme 5: *In situ* formation of diazo reagent **25** for epoxidation; R = aryl, heteroaryl; R' = alkyl, aryl

1.2.4 Base-mediated cleavage of *N*-alkyl-*N*-nitrosamides

In 1894, von Pechmann published his work on the synthesis of diazomethane. The general strategy of preparation, using a strongly alkaline solution of sodium or potassium hydroxide to prepare a diazoalkane from *N*-alkyl-*N*-nitrosamides is still frequently used. The commercially available Diazald® **31** is used to generate diazomethane **5** in 6 M KOH which is subsequently distilled as an ethereal solution (Scheme 6). Compounds such as phenyl diazomethane **6** can also be obtained in a similar fashion, although the modified Bamford-Stevens reaction is clearly advantageous from a safety point of view as the diazo reagent does not have to be distilled.



Scheme 6: Formation of diazomethane from Diazald®

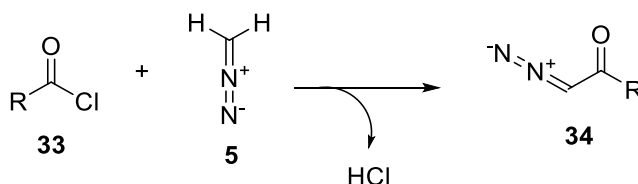
Recently, a powerful *in situ* method of formation and consumption of diazomethane was developed by Morandi and Carreira.²⁷ An iron porphine catalyst was able to promote cyclopropanations of styrenes with diazomethane even in a 6 M alkali solution.

1.2.5 Miscellaneous

There are many other pathways to diazo reagents of which some could gain importance whereas others are only useful for niche applications.

Historically, the acylation of diazoalkanes was of great importance for the synthesis of terminal diazo species type **34** (Scheme 7). This reaction is also part of the Arndt-Eistert homologation.²⁸ However, yields tend to be low with longer chain diazoalkanes²⁹ and the

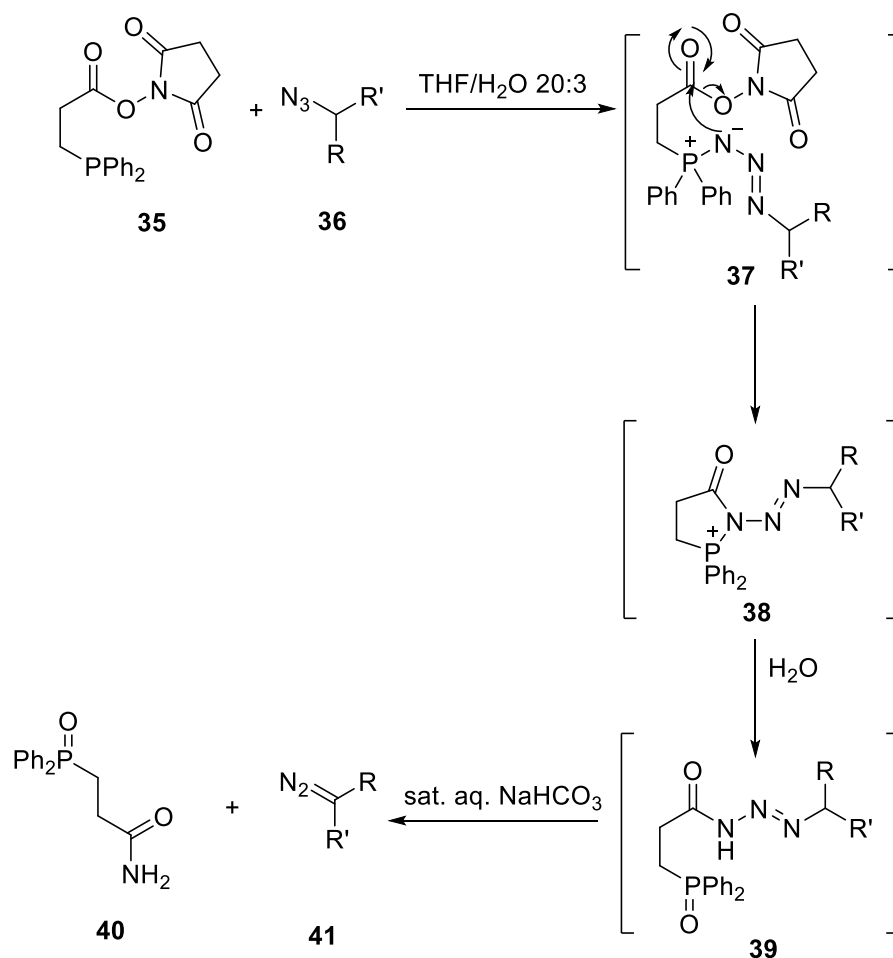
requirement of handling highly explosive diazoalkanes make this method less attractive than a deacylation type diazo transfer (see section 1.2.2) or an *in situ* Bamford-Stevens reaction (see section 1.2.3).



Scheme 7: Acylation of diazomethane; R = aryl, alkyl

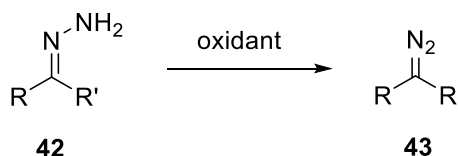
It should further be mentioned that an excess of diazomethane is required when acyl chlorides are used as HCl is liberated that will react with diazomethane to form methyl chloride.

An elegant strategy was developed by Myers and Raines in 2009, in which was found that organoazides can react with phosphines to generate diazo reagents.³⁰ This is a remarkable finding considering the use of organoazides and phosphines for the preparation of amines and amides *via* Staudinger reaction and Staudinger ligation, respectively. Phosphine **35** reacts with organoazide **36** to form acyl triazene **39** *via* five-membered transition state **38**. Acyl triazene **39** can be isolated and characterized *via* X-ray crystallography. Compound **39** can be decomposed selectively into amide **40** and diazo **41** when treated with sodium hydrogen carbonate solution (Scheme 8). This reaction can be performed in water³¹ and has promoted the use of diazo compounds for bio-orthogonal chemistry.³² Even terminal diazo compounds such as **34** can be obtained *via* this method in moderate to good yields (49-85%).



Scheme 8: Diazo compounds from azides; R = amide, ester, ketone, aryl; R' = H, alkyl, aryl

From an atom economy point of view, the dehydrogenation of hydrazones **42** is a very interesting route to diazo compounds (Scheme 9). The reaction was first developed by Curtius who has therefore developed two major syntheses of diazo compounds.³³ Common oxidants for this reaction are heavy metal based such as HgO or Pb(OAc)₄.³⁴ Recently, Javed and Brewer developed a method using *Swern* conditions³⁵ and Myers *et al.* used iodine (III) reagent difluoroiodobenzene as the oxidant.³⁶ Findings by Ley *et al.*³⁷ and Hayes *et al.*³⁸ on the development of efficient flow protocols for the oxidation of hydrazones could make this route to diazo compounds much more popular (see section 1.4.4).



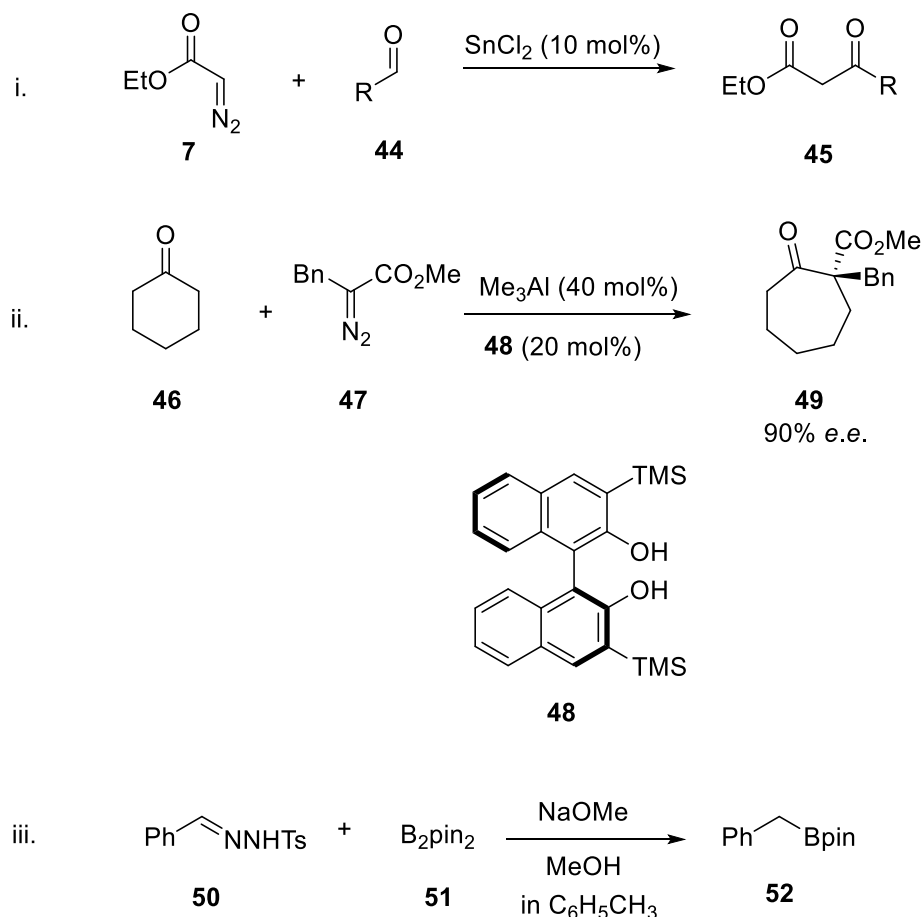
Scheme 9: Oxidation of hydrazones; R = aryl, vinyl; R' = H, alkyl, aryl, ester

1.3 Reactions of diazo compounds

Diazo compounds are extremely versatile reagents for organic synthesis.³⁹ Considering the vast number of transformations performed with diazo compounds only a small fraction can be discussed here. Diazo compounds have been used in C-H insertion reactions,⁴⁰ X-H insertion reactions⁴¹ (X = O, N, S, Si, B, P), cyclopropanations,⁴² ylide formation and reaction,⁴³ and cross-coupling reactions among others.⁴⁴ Most reactions of diazo compounds are based on the generation of carbenes. However, some useful reactions of diazo compounds without the formation of carbenes exist.⁴⁵ Only reactions in which nitrogen is a leaving group will be discussed herein.

1.3.1 Non-carbene based reactions

The carbon atom of diazo reagents is nucleophilic as can be inferred from structures **3b** and **3c** (Scheme 1). This reactivity can be used to promote reactions with electrophiles in the presence of activating Lewis acids. The Roskamp reaction was developed in 1989 for the formation of β -ketoesters from diazo reagents.⁴⁶ Ethyl diazoacetate **7** reacts with aldehyde **44** under tin(II) chloride catalysis to generate β -ketoester **45** (Scheme 10 i). Enantioselective versions of the Roskamp reaction have been published recently.⁴⁷ The homologation of cyclohexanone **46** to cycloheptanone **49** using diazo reagent **47** can be performed with high stereocontrol when a binol type ligand **48** is used (Scheme 10 ii).⁴⁸ Diazo compounds can also perform a nucleophilic attack onto boranes and boronic esters⁴⁹ to give access to new boron reagents. This was done by Wang *et al.* by treating tosyl hydrazone **50** and B₂pin₂ **51** with sodium methanolate and methanol to give boronic ester **52** (Scheme 10 iii).⁵⁰



Scheme 10: i. Roskamp reaction; ii. Homologation of cyclohexanone; iii. Bamford-Stevens type reaction of tosyl hydrazones with boronic esters; R = aryl, alkyl

1.3.2 Diazo compounds to generate carbenes

Diazo compounds are mainly used as carbene precursors. The release of nitrogen to generate carbenes can be performed thermally,⁵¹ by UV irradiation⁵² or through metal catalysis. In modern synthetic chemistry, the use of metal catalysis to generate metal carbenes is by far the most important route to carbenes. Metals commonly used for the preparation of metal carbene species are copper,⁵³ palladium,⁵⁴ rhodium,⁵⁵ ruthenium,⁵⁶ cobalt⁵⁷ and iron.⁵⁸

1.3.2.1 Metal carbenes derived from diazo compounds

Metal carbenes derived from diazo compounds can be grouped into four groups of reactivity and selectivity (Figure 5). Metal carbenes possessing two acceptor substituents (EWG = electron withdrawing group) **53** are highly electrophilic and therefore the most reactive member of this group of metal carbenes. However, selectivity can be rather poor. Selectivity improves from compound **53** to **56** whereas reactivity decreases. This is an interesting trend when put in relation to the stability of the diazo precursors (Scheme 5) for which the reactivity of **9** (precursor for type **53** metal carbene) is lower than that of **8** (precursor

for type **54** metal carbene). In the last years, donor / acceptor carbenes **55** have received immense attention as the increased selectivity compared to **53** and **54** allows for much better chemo- and regioselectivity.⁵⁹

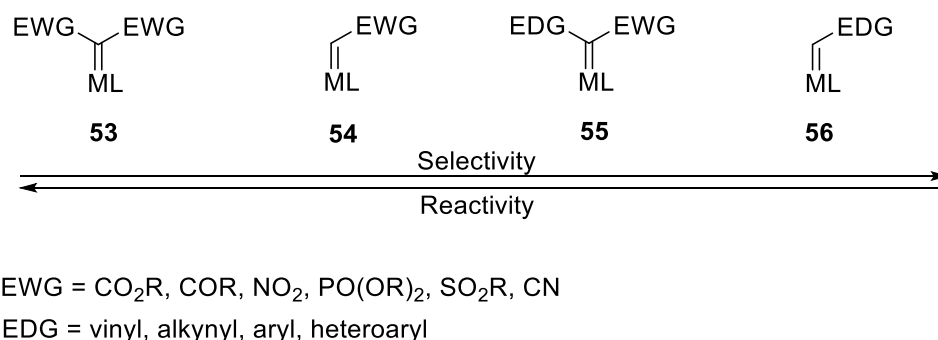
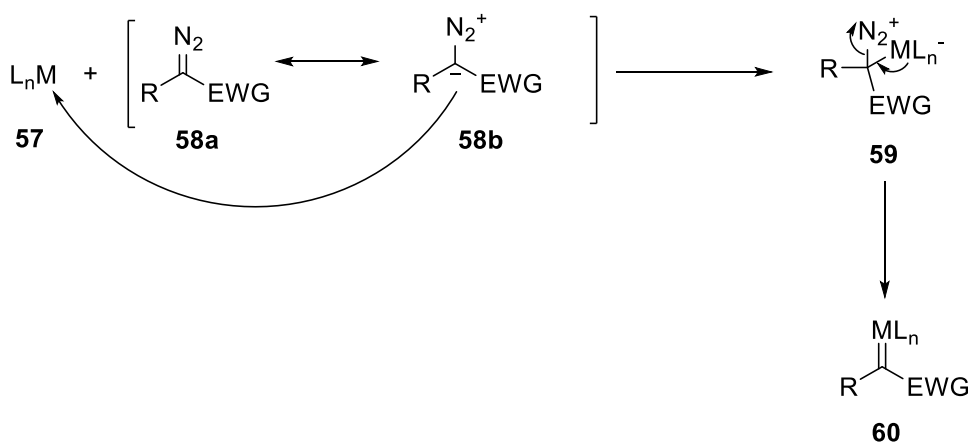


Figure 5: Classes of metal carbenes ordered in respect of their selectivity and reactivity

Metal carbenes derived from diazo compounds are generally electrophilic. Depending on the substituents, the metal as well as the ligands, electrophilicity of the metal carbene can be increased or reduced. Compared to Fischer and Schrock carbenes, metal carbenes derived from diazo compounds are less stable and in their reactivity more similar to naked carbenes. They are also significantly more electrophilic than Fischer and Schrock carbenes. The carbon-metal bond is characterised by a strong σ -bonding from the carbene to the metal and a weak π -backbonding from the metal into the free p orbital of the carbene. These metal carbenes are generated by the reaction of the ylide form of the diazo reagent **58b**, which attacks metal complex **57** to generate intermediate **59**, leading to metal carbenoid **60** under release of nitrogen (Scheme 11).⁶⁰ This scheme demonstrates further why diazo reagents with more electron withdrawing groups are more stable; the ylide form **58b** is more stabilised and will be less likely to react with metal complex **57**.



Scheme 11: Diazo decomposition and formation of metal carbene; R = aryl, alkyl, vinyl, heteroaryl

1.3.2.2 Catalyst systems for carbene reactions

As can be expected from the metal carbene structure **60**, the metal and ligand have a major impact on the reactivity and selectivity of the compound. For example, in C-H insertion reactions, rhodium (II) catalysts provide the best balance of reactivity and selectivity whereas copper catalysts are more reactive but generally also less selective.⁶¹ The level of stereocontrol that chiral ligands can induce depends significantly on the reaction studied. For example, rhodium (II) catalysts dominate the field of enantioselective C-H insertion reactions whereas copper catalysts with chiral ligands are used for enantioselective O-H and N-H insertion reactions. Cyclopropanations have been performed with high stereoselectivities with numerous metals. Figure 6 shows some of the most important catalyst systems in the literature.

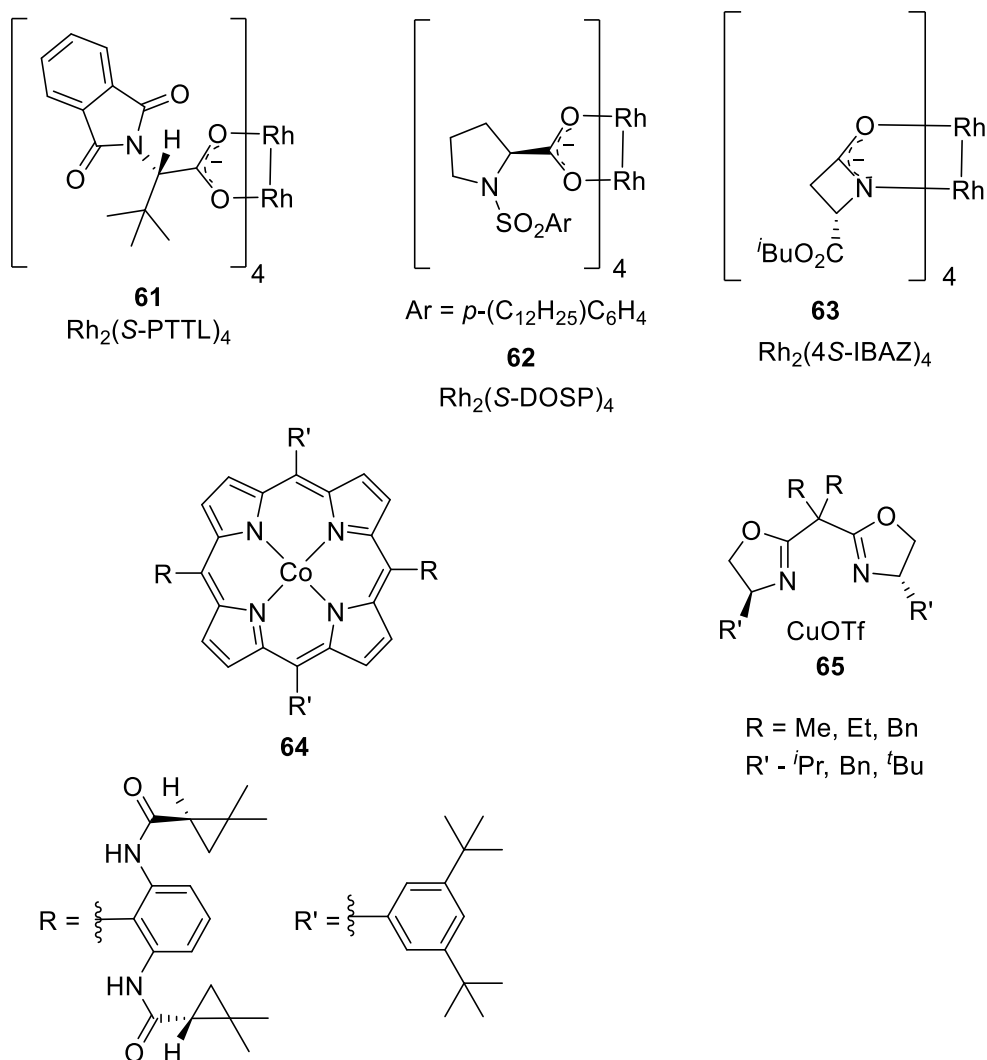
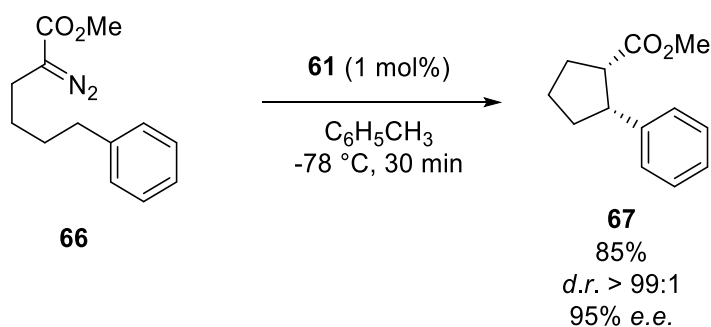


Figure 6: A selection of catalysts used for stereoselective reactions with diazo compounds

1.3.2.3 C-H insertion reactions

C-H insertion reactions belong to the most important and synthetically useful reactions of diazo compounds. The field of C-H insertion of metal carbenoids gained importance after Teyssié *et al.* discovered the efficiency of rhodium carboxylate-derived metal carbenes for the insertion into unactivated C-H bonds.⁶² Since then, rhodium catalysts have been used for highly regio- and stereoselective inter- and intramolecular C-H insertions. Generally, functionalities that can stabilise a positive charge on the carbon involved promote C-H insertion whereas electron withdrawing groups deactivate such a reactivity. Methine C-H bonds are more reactive for C-H insertions than methylene C-H bonds which are more reactive than methyl groups. In intramolecular reactions, 5-membered rings are preferably formed⁶³ even in the presence of oxygen-activated and benzylic C-H bonds at different positions within the molecule.⁶⁴ The reactions can provide excellent enantiomeric excess as in case of the cyclization of compound **66** using catalyst **61** providing **67** with great diastereo- and enantioselectivity (Scheme 12).⁶⁵

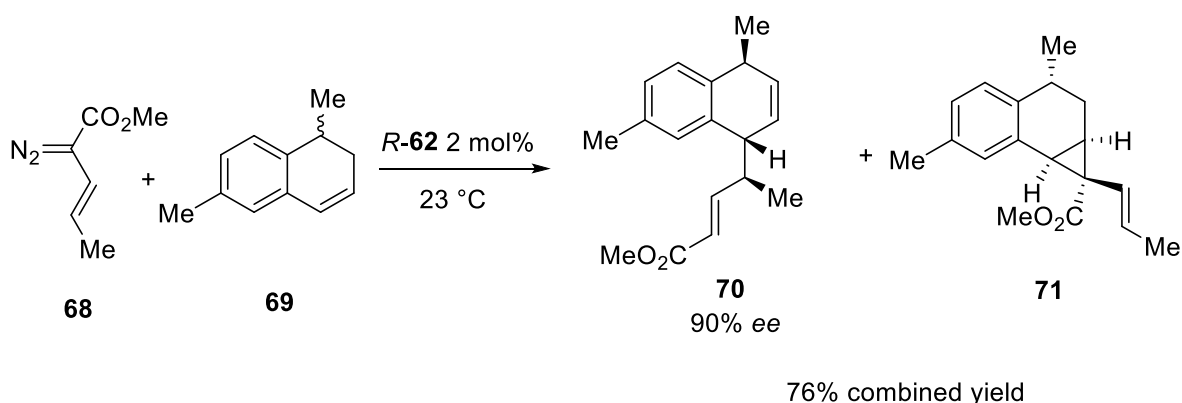


Scheme 12: Cyclopentane formation using chiral rhodium catalyst **61**

Intermolecular C-H insertion reactions were considered too unselective for a long time. In their review in 1994, Ye and McKervy state:

*“From the synthetic point of view, intermolecular C-H insertion is not generally useful because of low selectivity and competition from intramolecular reactions”*⁶⁶

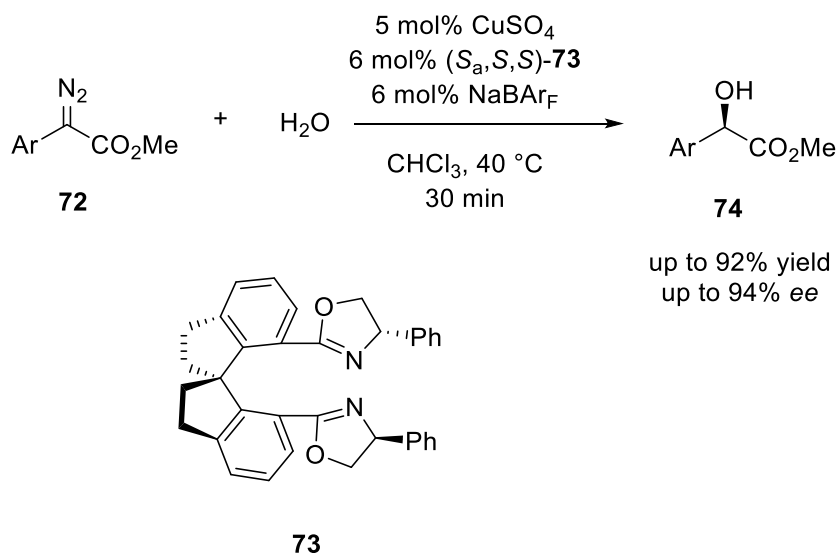
This has changed significantly within the last two decades, making intermolecular C-H insertion a rapid strategy for the functionalisation of organic molecules. Great enantiocontrol can be achieved when vinyl diazo reagents **68** are used to go through a combined C-H functionalisation / Cope rearrangement mechanism.⁶⁷ Such an approach was implemented in the synthesis of (+)-Erogorgiaene in a kinetic enantiodifferentiating step (Scheme 13). As the combined C-H functionalisation / Cope rearrangement is very diastereoselective,⁶⁸ Davies and co-workers were able to react racemic **69** in a highly selective way providing only C-H insertion / Cope rearrangement product **70** with 90% ee. The other enantiomer of **69** reacted under rhodium catalysis with vinyl diazo reagent **68** to form cyclopropane product **71**.⁶⁹



Scheme 13: Asymmetric C-H functionalisation / Cope rearrangement for kinetic resolution

1.3.2.4 X-H insertion reactions

Metal carbenes readily undergo a broad range of X-H insertion reactions. Although these reactions are very fast and have been known for a long time,⁷⁰ it took considerable time until enantioselective protocols were developed. This is due to the fact that chiral rhodium catalysts only induce very moderate enantioselectivities in most of these reactions.⁷¹ Maier and Fu developed the first O-H insertion reaction with high enantiomeric excess (up to 98%) using a copper catalyst coordinated by a chiral bisazaferrocene ligand.⁷² Zhou and co-workers expanded the scope of stereoselective O-H insertions to challenging substrates such as water⁷³ (Scheme 14) and phenols using spirobox ligand **73**.⁷⁴



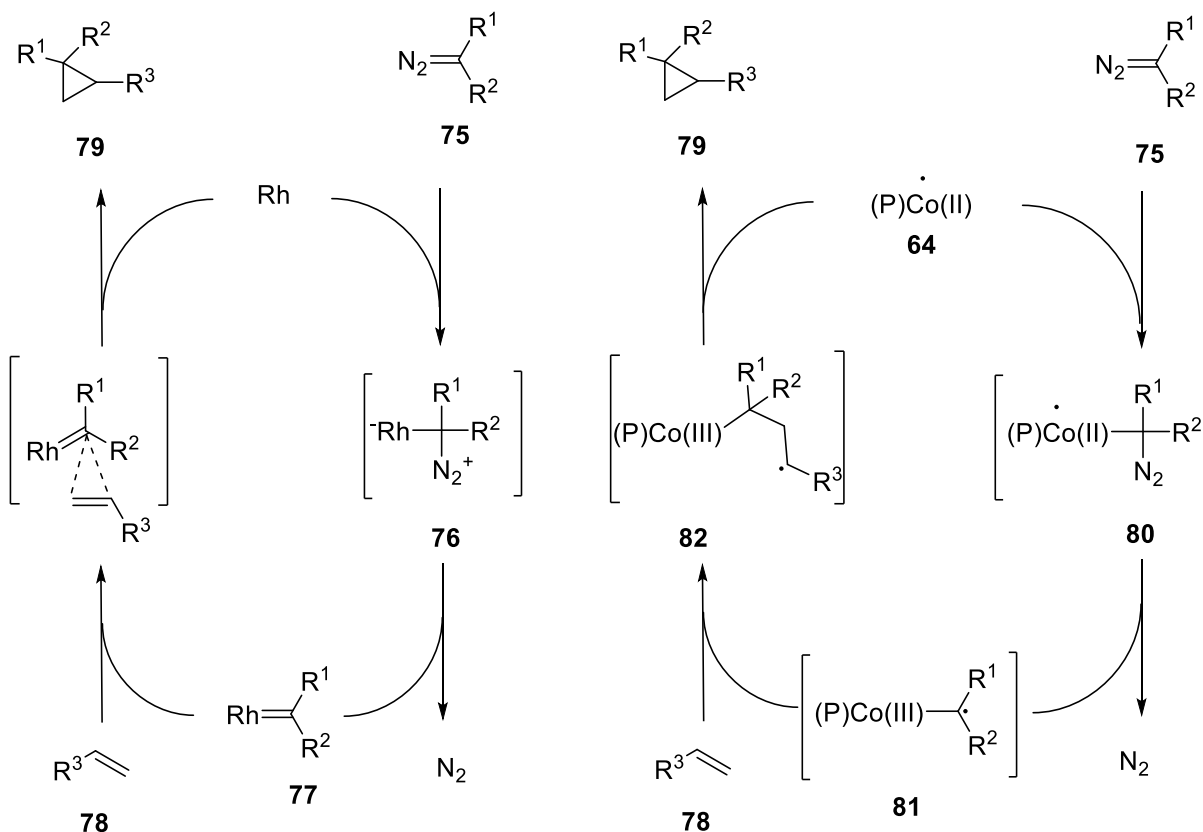
Scheme 14: Enantioselective water insertion of donor / acceptor copper carbenes

Spirobox catalysts of this type also give access to highly stereoselective N-H insertion reactions,⁷⁵ S-H insertion reactions,⁷⁶ Si-H insertion reactions,⁷⁷ and B-H insertion reactions.⁷⁸ Unfortunately, the preparation of these ligands is synthetically demanding and expensive.

1.3.2.5 Cyclopropanation

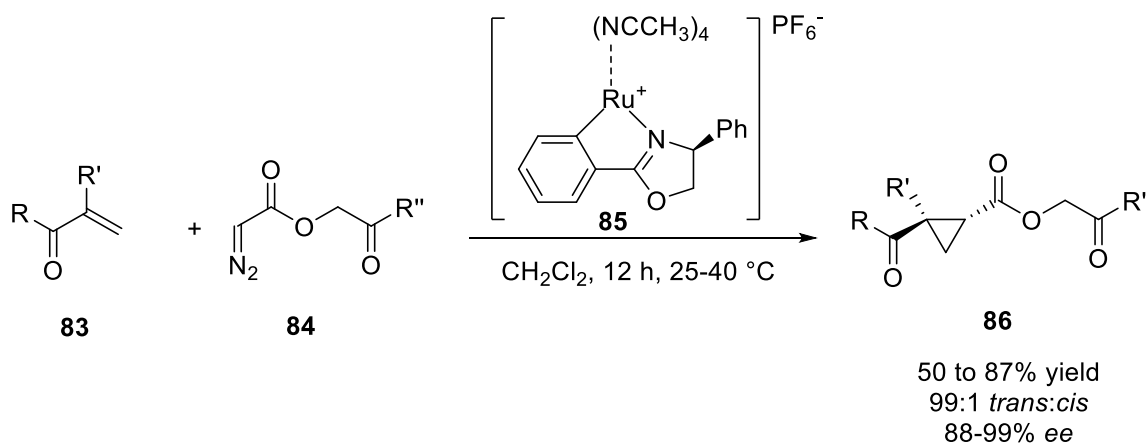
Cyclopropane moieties are found in several natural products⁷⁹ and drug molecules such as Ciprofloxacin as well as in pyrethrins,⁸⁰ an important class of insecticides. They are also versatile synthetic building blocks that can be used for example in cycloaddition⁸¹ and rearrangement reactions.⁸² However, the synthesis of cyclopropanes is difficult as a highly strained three-membered ring is formed. Metal catalysis of diazo compounds with alkenes is one of the most efficient and selective ways to achieve this goal. In contrast to C-H insertion and X-H insertion reactions, stereoselective cyclopropanations have been achieved with many different metals. Among them are rhodium,⁸³ copper,⁸⁴ cobalt,⁸⁵ iron,⁸⁶ palladium,⁸⁷ ruthenium⁸⁸ and gold.⁸⁹

An interesting example is the use of cobalt porphyrins as catalysts for diazo decomposition. Mechanistic studies by Zhang *et al.* on the cyclopropanation of olefines using cobalt porphyrin catalysts provided evidence for a radical based mechanism.⁹⁰ This stands in contrast to the mechanisms most diazo derived metal carbene reactions are thought to react by. Scheme 15 compares the cyclopropanation mechanism for rhodium with that of cobalt porphyrin complex **64**. In the case of rhodium catalysis (Scheme 15, left) the metal carbene **77** is formed from diazo species **75** via intermediate **76**. Alkene **78** subsequently interacts with the empty p orbital of the metal carbene to furnish cyclopropane **79**. In the case of cobalt porphyrin catalyst **64**, the catalytic cycle begins with the coordination of the cobalt catalyst to the carbon atom of the diazo compound (Scheme 15, right). After cleavage of dinitrogen, radical **81** is formed as the reactive species. Compound **81** then attacks olefin **78** which finally ring closes from radical structure **82** to cyclopropane **79** with cobalt(II) being regenerated. Excellent stereocontrol is possible through this route with up to 99:1 diastereomeric ratio and up to 99% enantiomeric excess.⁹¹ In contrast to reactions of highly electrophilic metal carbenes, the substrate scope of alkenes of this method is not limited to electron rich double bonds. However, the high complexity of the porphyrin ligand of cobalt catalyst **64** prevents this approach from becoming a standard protocol for the cyclopropanation of electron poor alkenes.



Scheme 15: Mechanism for cyclopropanation for rhodium catalysis (left) and cobalt porphyrin catalysis (right)

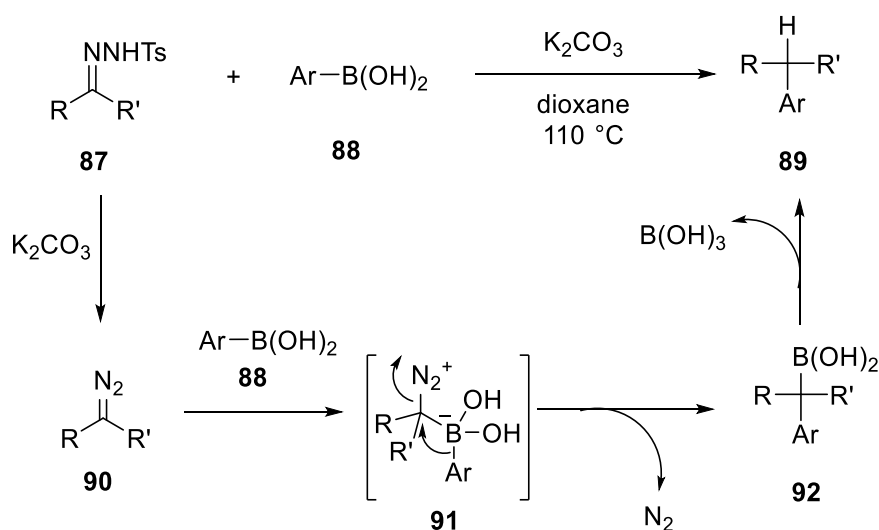
For this purpose, Iwasa and co-workers developed the relatively simple ruthenium pheox catalyst **85** (Scheme 16).⁹² Cyclopropanation of electron poor alkene **83** proceeds smoothly with acetyl diazoacetate and methyl (diazoacetoxymethyl)acetate **84** in excellent enantiomeric and diastereomeric excess using 1 mol% of **85**. This catalyst can also promote intramolecular cyclopropanation in very high yield and enantiomeric excess.⁹³



Scheme 16: Cyclopropanation of electron poor alkenes using a ruthenium(II) pheox catalyst;
R = alkoxy, amino, alkyl; R' = H, methyl; R'' = methyl, methoxy

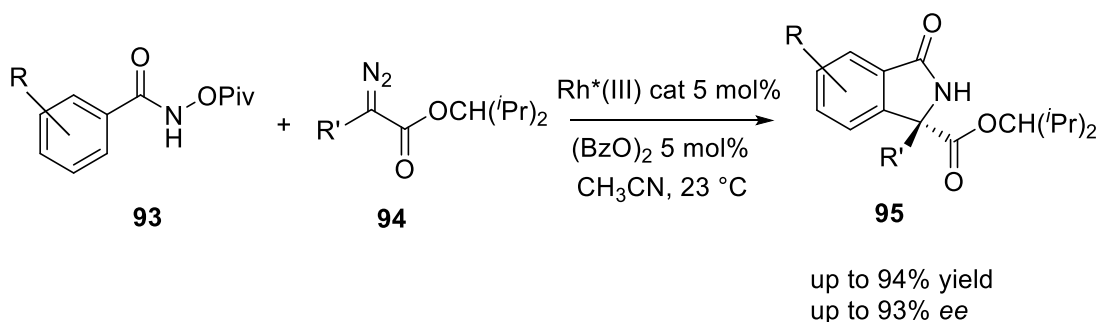
1.3.2.6 Cross-coupling reactions

A recent development in diazo chemistry is the use of tosylhydrazones as diazo precursor for cross-coupling reactions. The reaction gained importance when Barluenga and co-workers found that tosylhydrazones react smoothly with aryl halides in presence of LiO^tBu as base under palladium catalysis.⁹⁴ The choice of the metal is crucial as a too Lewis acidic catalyst would decompose the diazo reagent before inserting into the aryl halide bond. In the case of palladium(0), it is in fact the oxidative addition into the aryl halide bond that makes the palladium species an effective reagent for the decomposition of the diazo species.⁹⁵ When boronic acids are used as coupling partners to tosyl hydrazones, the use of any metal becomes superfluous. Barluenga *et al.* found that treating tosyl hydrazone **87** with potassium carbonate at 110 °C in dioxane in the presence of boronic acid **88** provides coupling products **89** in good to excellent yields (Scheme 17).⁹⁶ In a first step, the base induced decomposition of tosyl hydrazone **87** leads to the formation of diazo reagent **90**. This diazo reagent then attacks boronic acid **88** to form intermediate **91**. After cleavage of nitrogen and 1,2-aryl migration, reagent **92** is obtained that leads to the final product *via* protodeboronation.



Scheme 17: Metal-free cross-coupling reaction of tosyl hydrazones with boronic acids; R = aryl, heteroaryl, alkyl; R' = H, alkyl

A slightly modified approach using the same principle was used by Cramer *et al.* for the stereoselective assembly of isoindolones. Rhodium(III) is used to insert into an aromatic C-H bond using an amide directing group. Only then, the rhodium catalyst decomposes the diazo species and leads to the formation of **95** with up to 93% enantiomeric excess (Scheme 18).⁹⁷



Scheme 18: Stereoselective synthesis of isoindolones; R = alkyl, alkoxy, halide; R' = aryl, alkyl

1.4 Continuous flow technology – General properties

Section 1.3 describes the broad synthetic utility of diazo compounds. As mentioned above, these reagents are highly energetic and upscaling reactions with diazo reagents poses several risks. In this regard, continuous flow technology provides a promising platform to safely produce and use large quantities of diazo compounds.

Flow chemistry, especially that conducted in microreactors, has received immense interest in academia and industry recently.⁹⁸ Microreactor technology is based on small diameter devices (≤ 1 mm inner diameter) made out of materials such as metals, metal alloys, ceramics, glass, silicon or organic polymer based materials such as PTFE and PEEK. In continuous flow chemistry, fluids are pushed into these microreactor devices at well-defined flow rates. Within the microreactor, reactions can then be performed. In organic chemistry, the microreactor can therefore be compared to a round bottom flask usually used to perform reactions.

The main interest in continuous flow chemistry arises from the properties these micro-sized devices possess. The small diameters of the channels of microreactors lead to excellent mass- and heat transfer which leads to several benefits of conducting organic synthesis in flow chemistry:⁹⁹

- **Safety:** Most interestingly for this work, microreactor technology leads to an improved safety profile for organic reactions. This is due to the high surface-to-volume ratio of a microreactor compared to a batch reactor. The safety benefits of flow reactors will be discussed in detail in section 1.4.1.
- **Selectivity:** The uniformity of the flow stream within a microreactor leads to much better control of reaction selectivity. In batch reactors the concentration of reagents is not completely homogeneous. This can be a problem in rapid reactions leading to hot spots and undesired side reactions. In microreactors, the rapid diffusion leads to uniform reagent distributions. Therefore, improved

selectivity within microreactors can be attributed to the more efficient mixing within these devices.

- *Speed:* There are two distinct ways in which flow chemistry can speed up reactions. They relate to the first two points of this list. Firstly, flow chemistry can allow reactions to be performed safely at higher temperatures which leads to faster reaction kinetics. It is further possible to superheat solvents above their boiling point by pressurising the system. Secondly, reactions in which the reaction rate is faster than the traditional mixing in batch can be sped up using microreactors. An important area taking advantage of this effect is called flash chemistry.¹⁰⁰ Flash chemistry describes extremely fast reactions (≤ 1 s reaction time) performed in microstructured devices that would not be possible in batch. Several organometallic reactions fall into this realm. Although repeatedly done, it is important not to interchange these two effects. Slow reactions (reaction rate \ll diffusion time) will provide the same kinetics in flow as in batch reactors if the reaction temperature is the same.
- *Information:* Continuous flow chemistry can provide a very efficient and rapid way for reaction optimisation and detection of optimal reaction conditions. This is due the small amount of reagents necessary for each experiment, the possibility of rapid change of reaction conditions as well as high levels of reproducibility. In recent years, several in-line analysis techniques were developed to take advantage of these benefits of flow chemistry. They will be discussed in section 1.4.2.
- *Scalability:* Flow chemistry can provide a good platform for scaling of reactions as parameters can be very well controlled. Two often mentioned methods of scaling up flow reactions are numbering up and scaling out. Numbering up means that several reactors are placed in parallel. Although already used practically, this approach has the disadvantage of requiring immense investment costs especially if multiple pumps are required for the numbering up. Scaling out is the process of running a system over a longer period of time to obtain more product. Although very useful for scaling a reaction by one order of magnitude, this approach cannot be used to make multikilogram quantities of materials. For example, a reaction that provides 100 mg of product within ten minutes will give 6 g of product in 10 hours. A third option of scaling up flow reactions is by increasing the diameter of the flow reactors and switching from micro- to mesoflow systems (i.d. > 1 mm). It depends on the specific needs of the process which of these three approaches will be most useful.

It is beyond the scope of this work to discuss all the techniques, developments and properties of flow chemistry. The most important aspects of flow chemistry for this thesis are discussed: safe use of hazards in flow (section 1.4.1), inline analysis techniques (section 1.4.2) and multistep synthesis (section 1.4.3). In the final section, recent work utilising diazo reagents in flow by other research groups will be reviewed.

1.4.1 Chemical hazards in flow

Continuous flow chemistry provides several advantages for the use of highly energetic materials such as diazo compounds. These benefits arise from two main features of flow chemistry: (1) excellent heat exchange of flow reactors and (2) small total volumes of dangerous materials at any given time.

To understand the improved efficiency of heat removal for microreactors compared to batch systems, a short discussion of the underlying thermodynamics is necessary. The heat balance of a synthetic reaction is described by Equation 1. For a stable heat balance of a reaction it is important that the heat removal Q_{ex} is sufficient for the heat created in the reaction Q_r .

$$\Delta Q = Q_{ex} - Q_r$$

Equation 1: Heat balance ΔQ of a chemical reaction with Q_{ex} being the heat removed from the system and Q_r being the heat produced by the reaction

The heat removal Q_{ex} depends on the difference between the temperature of the reaction T_r and the temperature outside the reactor (e.g. the cooling fluid or open air, T_c) as well as the heat transfer coefficient U and the heat transfer area A (see Equation 2).

$$Q_{ex} = UA(T_c - T_r)$$

Equation 2: Newtonian cooling describes the heat loss of an object, here the reaction mixture with U being a heat transfer coefficient, A being the heat transfer area, T_c being the temperature of the surrounding environment and T_r being the temperature in the reactor

The heat release rate behaves as an exponential function of the temperature $Q_{ex} = f(T)$. This can be plotted in a Semenov diagram (Figure 7). The slope of the straight line is UA and the intersection with the x-axis is the temperature of the cooling system T_c . The curved line is the heat produced within the reaction Q_r . There are two intersection points for the two lines at which the heat balance is in an equilibrium ($Q_{ex} = Q_r$). The one at lower temperatures (S) describes a stable equilibrium point. This means that when the temperature within the reaction increases, Q_{ex} dominates and reduces the temperature again to the point of the intersection S. If the temperature decreases, Q_r dominates and the reaction returns again to the stable equilibrium point S. However, for the higher intersection point (I) small changes can lead to

more drastic outcomes. If the temperature drops slightly below intersection point *I*, the temperature will decrease down to the intersection point *S* as the heat removal Q_{ex} dominates until that point. However, if the temperature increases slightly from point *I* a thermal runaway will occur as the heat of the reaction medium outperforms the heat removal ($Q_r > Q_{ex}$). The dashed lines Q_{ex2} and Q_{ex3} describe the effect of a higher temperature of the cooling system (i.e. in case of a failure of the cooling systems) which can make the heat removal completely insufficient for the heat generated within the temperature.

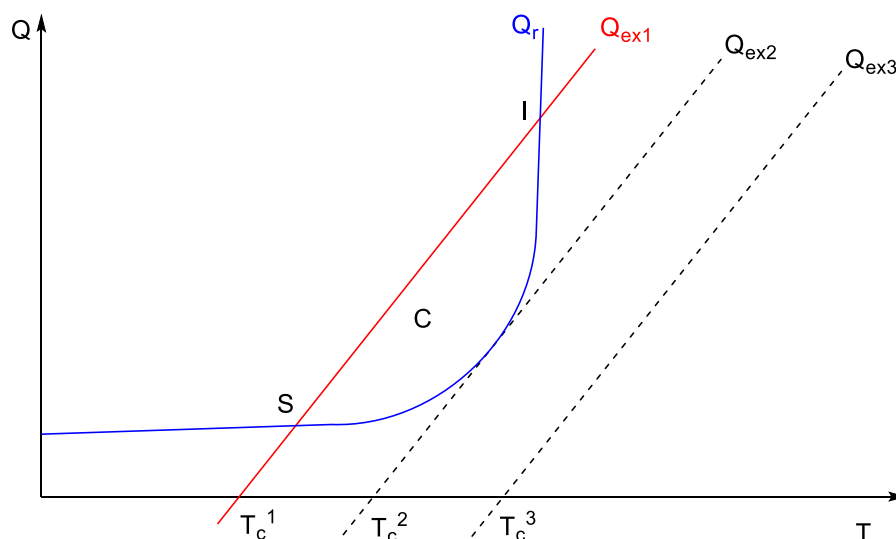


Figure 7: Semenov diagram

The aspect of this diagram on which microreactor technology has an impact is the slope of the heat removal Q_{ex1} . As Figure 8 shows this can dramatically influence the outcome of an unexpected increase in temperature. The slope of the heat removal Q_{ex} is the product of the heat coefficient U and the heat transfer area A . The heat transfer area A changes in an upscale as the surface-to-volume ratio decreases for bigger objects. This is a common issues as the cooling temperature in a batch upscale must be chosen lower than in the batch experiment. The opposite is true for a microreactor. As the surface-to-volume ratio is greater for small objects, $Q_{exMicroreactor}$ has a much greater slope UA and can therefore remove heat much more efficiently.

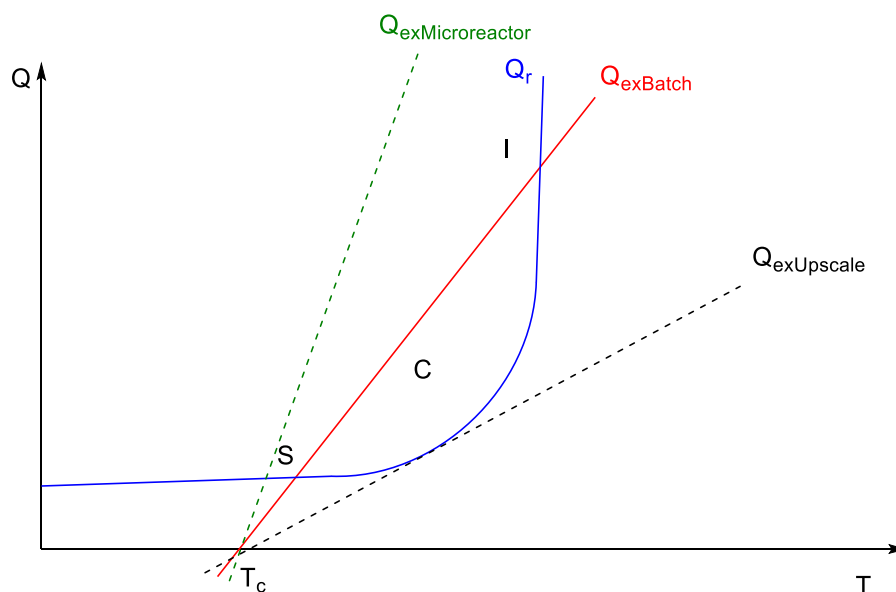


Figure 8: Semenov diagram in dependence of the heat transfer area A

Table 1.1 compares the heat removal capacity of a 2 litre round bottom flask with a tubular flow system of 10 mm diameter and a microreactor of 0.1 mm diameter. The increased surface-to-volume ratio A/V goes together with an increased heat removal Q_{ex} .

Table 1.1: Comparison of round bottom flask, tubular mesoflow reactor and microreactor for heat removal¹⁰¹

Reactor	Dimension	A/V [m ² /m ³]	Q_{ex} [kW/m ³]
Round bottom flask	2 L	40	400
Tubular i.d. 10 mm	10 mm	400	4000
Microreactor i.d. 0.1 mm	0.1 mm	40000	400000

It is therefore not surprising that many highly exothermic reactions and reactions involving explosive or aggressive reagents have been performed in microreactors.¹⁰² Among these reactions are organometallic chemistry,¹⁰³ hydrogenations,¹⁰⁴ ozonolysis,¹⁰⁵ nitrations,¹⁰⁶ diazonium salts as well as reactions with diazo compounds,¹⁰⁷ azides,¹⁰⁸ hydrazines,¹⁰⁹ fluorine gas,¹¹⁰ phosgene,¹¹¹ and conc. sulfuric acid.¹¹²

1.4.2 In-line analysis in flow

The small quantities of reagents required for experiments and the high level of control over the reaction conditions as well as a high level of reproducibility makes flow chemistry the ideal platform for rapid optimisation and analysis of reactions. For this purpose, several techniques for in-line analytics in flow chemistry have been developed. The spectroscopic analysis techniques utilised for this include UV/Vis and Raman spectroscopy,¹¹³ NMR spectroscopy,¹¹⁴ infrared spectroscopy,¹¹⁵ mass spectrometry,¹¹⁶ gas chromatography,¹¹⁷ and HPLC analysis.¹¹⁸ Of these, infrared spectroscopy has received most attention as it combines a rapid analysis frequency (measurements can take < 15 s) with detailed chemical information. Especially in cases where characteristic functional groups such as azides,¹¹⁹ diazonium salts,¹²⁰ diazo compounds¹²¹ or carbonyls¹²² are formed or consumed, infrared spectroscopy provides excellent in-line analysis. The results obtained *via* in-line infrared spectroscopy can be used for detailed kinetic analysis of reactions as shown by Jensen and co-workers.¹²³ In a recent report,¹²⁴ infrared analysis in flow is used to mimic “batch kinetics”. An advantage of batch kinetic analysis is that many time points can be analysed from one experiment. In flow chemistry, reaction time corresponds to the time that one molecule requires to pass the entire flow reactor. By using a ramp which increases the residence time gradually instead of stepwise, instantaneous residence times τ_{ins} can be obtained without the need to wait for a steady-state (Figure 9). With this method, exact kinetics of a Paal-Knorr reaction were obtained.

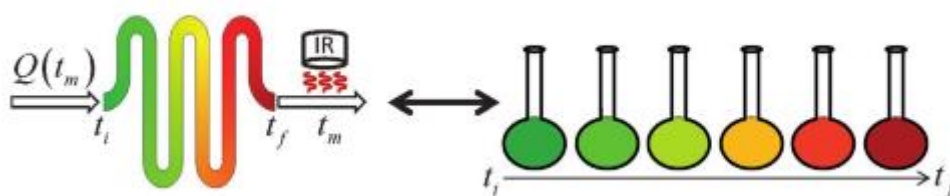


Figure 9: Flow kinetics to mimic batch kinetics using gradual change of flow rate; from J. S. Moore, K. F. Jensen, “Batch” Kinetics in Flow: Online IR Analysis and Continuous Control, *Angew. Chem. Int. Ed.* **2014**, 53, 470-473; Copyright Wiley-VCH Verlag GmbH & Co. KGaA. Reproduced with permission.

An interesting application of in-line analysis tools in flow chemistry is its use in automated synthesis. The idea of automated synthesis has received increasing attention in recent years.¹²⁵ Jensen *et al.* were able to design a self-optimising flow system that enabled the straight-forward upscale from micro- to mesoscale flow reactors for an intermolecular Heck reaction. The analysis tool (in-line HPLC) was connected to a computer system that controlled the syringe pumps and the reactor temperature and thus optimised itself through an algorithm.

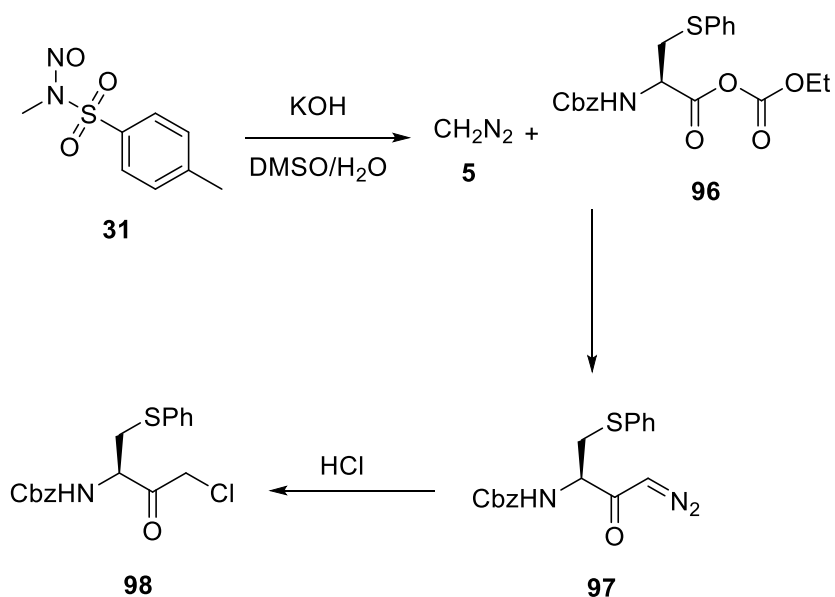
The system automatically found the optimum conditions which were stable when scaled by 50-fold.¹²⁶

1.4.3 Multistep synthesis in flow

An important development in continuous flow chemistry has been the integration of separation and purification methods to enable multistep synthesis in continuous fashion. Potentially, this could lead to a very flexible and rapid design to manufacture small quantities of drugs or similar molecules on-demand. Technologies that were developed to enable multistep synthesis are: solvent switching systems,¹²⁷ liquid / liquid separation,¹²⁸ in-line chromatography,¹²⁹ in-line filtration,¹³⁰ as well as crystallography.¹³¹ Using such technologies some impressive multistep synthesis have been accomplished. Ley *et al.* have synthesised natural products such as Spiragnien A¹³² and Oxomaritidine¹³³ as well as drug molecules such as Tamoxifen.¹³⁴ End-to-end manufacturing of pharmaceuticals has even been achieved which integrated the final dosage formation of the drug pills in the system.¹³⁵

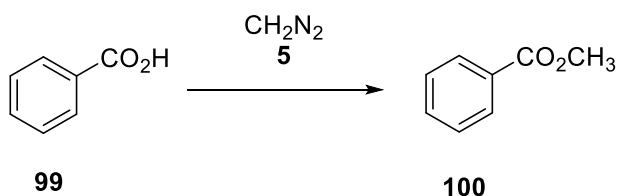
1.4.4 Diazo compounds in continuous flow technology¹³⁶

Prior to this work, first studies into the use of diazo reagents in continuous flow technology had been performed. Most of these have dealt with the *in situ* formation and direct use of diazomethane **5**. This is not surprising considering the synthetic utility of **5** as a C1 building block in combination with its toxic and explosive properties. The first report of the formation of diazomethane **5** in flow was published as early as 2002 (Scheme 19). Proctor and Warr described a large scale approach to **98** generating 90-93 g diazomethane per hour but limited the maximum quantity of diazomethane present at any given time to 110 mg. In their approach, diazomethane **5** is formed from Diazald® **31** in a solvent mixture of DMSO/H₂O and then carried into the solution of **96** using a flow of nitrogen gas.¹³⁷ The resulting α -diazoketone **97** is treated with hydrochloric acid to generate α -chloroketone **98**.



Scheme 19: Continuous production of diazomethane for the formation of chloromethyl ketone **98**

Another large scale approach was presented by Stark *et al.* in which diazomethane **5** was made in a microreactor and used for the methylation of benzoic acid **99** to provide methyl ester **100** (Scheme 20). With this method up to 2.5 mol of **5** could be generated safely in a day. However, no base sensitive materials such as anhydrides can be employed through this method as 6 M KOH is needed for the generation of diazomethane.¹³⁸

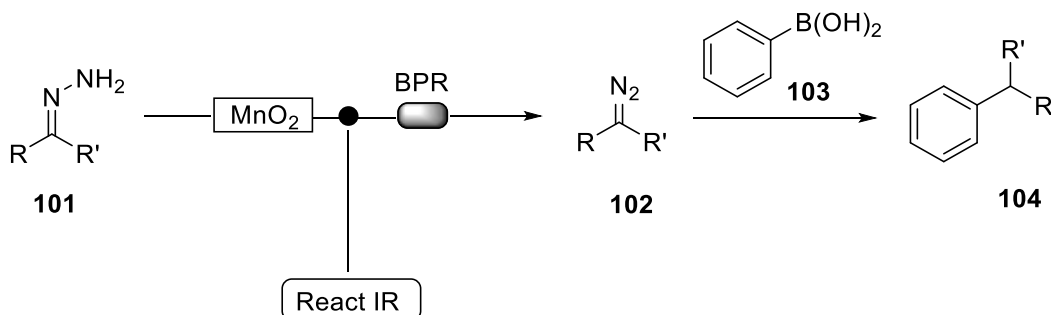


Scheme 20: Methylation of benzoic acid **99**

Therefore, methods to transfer diazomethane safely from the aqueous potassium hydroxide solution into an organic solvent in flow were needed. An elegant solution to this challenge was provided by Kim and co-workers who used a hydrophobic PDMS membrane through which the gaseous diazomethane can pass from the aqueous solution into an organic solvent. Albeit this method solved the problem of separating **5** from the aqueous KOH solution, the approach was limited to a daily output of 3 mmol of diazomethane.¹³⁹ Finally, Kappe *et al.* have used the AF-2400 tube-in-tube reactor to overcome the limitation of Kims method. Here, diazomethane is formed *in situ* in one tube and quenched with different substrates (e.g. alkenes for cyclopropanations) in the second tube. With this approach up to 35 mmol of diazomethane can be generated within a day.¹⁴⁰

Beside the safe generation of diazomethane, some one-step protocols of other diazo reagents have been developed. Rutjes *et al.* optimised the formation of ethyl diazoacetate **7** using design of experiments (DoE) algorithms.¹⁴¹ Martínez-Merino and co-workers looked into the asymmetric cyclopropanation of ethyl diazoacetate with styrene derivatives using heterogeneous copper catalysis in flow.¹⁴² Hayes *et al.* developed semi-batch protocols in which diazo reagents are generated from tosyl hydrazones in flow and subsequently passed through a scavenger column to trap sulfinic acid byproducts. The reaction solution is then directly used for X-H insertion reactions using rhodium or copper catalysis in semi-batch mode.¹⁴³

As mentioned in section 1.2.5, Ley³⁷ and Hayes³⁸ independently published methods for the in-flow generation of diazo reagents from hydrazones. Both groups used solid-supported oxidants that can be easily recycled and are based on cheap materials. For this purpose, Ley *et al.* used MnO_2 to generate diazo species **102** from hydrazone **101**. By this method, unstabilised diazo reagents such as phenyl diazomethane **6** could be generated. They can subsequently be utilised for sp^2 - sp^3 cross coupling reactions with boronic acids **103** to generate disubstituted benzyl moieties **104** (Scheme 21).



Scheme 21: MnO_2 based dehydrogenation of hydrazones to diazo compounds; R = aryl, vinyl; R' = H, methyl

Although first studies into the use of diazo reagents in continuous flow have been explored, several major challenges are still unsolved. In the following chapter, objectives to this work will be defined.

References

- 1 T. Curtius, *Chem. Ber.* **1883**, 16, 2330.
- 2 a) H. V. Pechmann, *Chem. Ber.* **1894**, 27, 1888; b) H. V. Pechmann, *Chem. Ber.* **1895**, 28, 855.
- 3 M. O. Forster, D. Cardwell, *J. Chem. Soc., Trans.* **1913**, 103, 861.
- 4 J. Thiele, *Chem. Ber.* **1911**, 44, 2522.
- 5 H. Boersch, *Monatsh. Chem.* **1934**, 65, 311.
- 6 K. Clusius, U. Lüthi, *Helv. Chim. Acta* **1957**, 40, 445.
- 7 R. A. Moss, *Acc. Chem. Res.* **2006**, 39, 267.
- 8 M. Regitz, *Diazo Compounds: Properties and Synthesis*, Academic Press. Inc., Orlando, Florida (**1986**), p. 11.
- 9 P. Schuster, O. E. Polansky, *Monatsh. Chem.* **1965**, 96, 396.
- 10 R. Hoffmann, *Tetrahedron* **1966**, 22, 539.
- 11 a) E. Heilbronner, H-D. Martin, *Chem. Ber.* **1973**, 106, 3376; b) J. Bastide, J. P. Maier, *Chem. Phys.* **1976**, 12, 177.
- 12 E. Fahr, *Chem. Ber.* **1959**, 92, 398.
- 13 B. L. Crawford Jr., W. H. Fletcher, D. A. Ramsay, *J. Chem. Phys.* **1951**, 19, 406.
- 14 a) J. Firl, W. Runge, W. Hartmann, *Angew. Chem. Int. Ed. Engl.* **1974**, 13, 270; b) T. A. Albright, W. J. Freeman, *Org. Magn. Res.* **1977**, 9, 75; c) R. O. Duthaler, H. G. Förster, J. D. Roberts, *J. Am. Chem. Soc.* **1978**, 100, 4974.
- 15 M. Regitz, *Diazo Compounds: Properties and Synthesis*, Academic Press. Inc., Orlando, Florida (**1986**), p. 52.
- 16 T. J. de Boer, H. J. Backer, *Org. Synth.* **1956**, 36, 16.
- 17 J. D. Clark, A. S. Shah, J. C. Petereson, L. Patelis, R. J. A. Kersten, A. H. Heemskerk, *Therm. Acta* **2002**, 386, 73.
- 18 G. Maas, *Angew. Chem. Int. Ed.* **2009**, 48, 8186.
- 19 M. Regitz, *Angew. Chem. Int. Ed. Engl.* **1967**, 6, 733.
- 20 J. P. Olson, H. M. L. Davies, *Org. Lett.* **2008**, 10, 573.
- 21 W. R. Bamford, T. S. M. Stevens, *J. Chem. Soc.* **1952**, 4735.
- 22 J. J. Li, *Name Reactions*, 3rd edition, Springer-Verlag, Berlin Heidelberg (**2006**), p. 20-21
- 23 J. R. Fulton, V. K. Aggarwal, J. de Vincente, *Eur. J. Org. Chem.* **2005**, 1479.
- 24 V. K. Aggarwal, J. de Vicente, B. Pelotier, I. P. Holmes, R. V. Bonnert, *Tetrahedron Lett.* **2000**, 41, 10327.
- 25 a) V. K. Aggarwal, E. Alonso, G. Fang, M. Ferrara, G. Hynd, M. Porcelloni, *Angew. Chem. Int. Ed.* **2001**, 40, 1433; b) V. K. Aggarwal, J. de Vincente, R. V. Bonnert, *Org. Lett.* **2001**, 3, 2785.
- 26 V. K. Aggarwal, E. Alonso, G. Hynd, K. M. Lydon, M. J. Palmer, M. Porcelloni, J. R. Studley, *Angew. Chem. Int. Ed.* **2001**, 40, 1430.
- 27 B. Morandi, E. M. Carreira, *Science* **2012**, 335, 1471.
- 28 J. J. Li, *Name Reactions*, 3rd edition, Springer-Verlag, Berlin Heidelberg (**2006**).
- 29 A. L. Wilds, A. L. Meader, *J. Org. Chem.* **1948**, 13, 763.
- 30 E. L. Myers, R. T. Raines, *Angew. Chem. Int. Ed.* **2009**, 48, 2359.
- 31 H.-H. Chou, R. T. Raines, *J. Am. Chem. Soc.* **2013**, 135, 14936.
- 32 K. A. Andersen, M. R. Aronoff, N. A. McGrath, R. T. Raines, *J. Am. Chem. Soc.* **2015**, 137, 2412.
- 33 T. Curtius, *Chem. Ber.* **1889**, 22, 2161.
- 34 T. L. Holton, H. Schechter, *J. Org. Chem.* **1995**, 60, 4725.

- 35 M. I. Javed, M. Brewer, *Org. Lett.* **2007**, *9*, 1789.
- 36 M. E. Furrow, A. G. Myers, *J. Am. Chem. Soc.* **2004**, *126*, 12222.
- 37 D. N. Tran, C. Battilocchio, S.-B. Lou, J. M. Hawkins, S. V. Ley, *Chem. Sci.* **2015**, *6*, 1120.
- 38 S. M. Nicolle, C. J. Hayes, C. J. Moody, *Chem. Eur. J.* **2015**, *21*, 4576.
- 39 a) T. Ye, M. A. McKerver, *Chem. Rev.* **1994**, *94*, 1091; b) Z. Zhang, J. Wang, *Tetrahedron* **2008**, *64*, 6577.
- 40 Selected reviews on C-H insertion reactions: a) H. M. L. Davies, R. E. J. Beckwith, *Chem. Rev.* **2003**, *103*, 2861; b) M. M. Díaz-Requejo, T. R. Belderrain, M. C. Nicasio, P. J. Pérez, *Dalton Trans.* **2006**, 5559; c) H. M. L. Davies, S. J. Hedley, *Chem. Soc. Rev.* **2007**, *36*, 1109; d) H. M. L. Davies, J. R. Manning, *Nature* **2008**, *451*, 417; e) M. P. Doyle, R. Duffy, M. Ratnikov, L. Zhou, *Chem. Rev.* **2010**, *110*, 704; f) C. N. Slattery, A. Ford, A. R. Maguire, *Tetrahedron* **2010**, *66*, 6681; g) H. M. L. Davies, D. Morton, *Chem. Soc. Rev.* **2011**, *40*, 1857; h) H. Lu, X. P. Zhang, *Chem. Soc. Rev.* **2011**, *40*, 1899; i) F. J. Lombard, M. J. Coster, *Org. Biomol. Chem.* **2015**, *13*, 6419.
- 41 Selected reviews on X-H insertion reactions: a) D. J. Miller, C. J. Moody, *Tetrahedron* **1995**, *51*, 10811; b) S.-F. Zhu, Q.-L. Zhou, *Acc. Chem. Res.* **2012**, *45*, 1365; c) D. Gillingham, N. Fei, *Chem. Soc. Rev.* **2013**, *42*, 4918.
- 42 Selected reviews on cyclopropanations and cyclopropanes: a) H.-U. Reissig, R. Zimmer, *Chem. Rev.* **2003**, *103*, 1151; b) H. Lebel, J.-F. Marcoux, C. Molinaro, A. B. Charette, *Chem. Rev.* **2003**, *103*, 977; c) G. Maas, *Chem. Soc. Rev.* **2004**, *33*, 183; d) M. Yu, B. L. Pagenkopf, *Tetrahedron* **2005**, *61*, 321.
- 43 Selected reviews on ylide type reactions of diazo compounds: a) A. Padwa, S. F. Hornbuckle, *Chem. Rev.* **1991**, *91*, 263; b) D. M. Hodgson, F. Y. T. M. Pierard, P. A. Stupple, *Chem. Soc. Rev.* **2001**, *30*, 50; c) P. Müller, *Acc. Chem. Res.* **2004**, *37*, 243; d) A. Padwa, *Helv. Chim. Acta* **2005**, *88*, 1357; e) G. K. Murphy, C. Stewart, F. G. West, *Tetrahedron* **2013**, *69*, 2667; f) X. Guo, W. Hu, *Acc. Chem. Res.* **2013**, *46*, 2427.
- 44 Selected reviews on cross-coupling reactions: a) J. Barluenga, C. Valdés, *Angew. Chem. Int. Ed.* **2011**, *50*, 7486; b) Z. Shao, H. Zhang, *Chem. Soc. Rev.* **2012**, *41*, 560; c) Z. Liu, J. Wang, *J. Org. Chem.* **2013**, *78*, 10024; d) Q. Xiao, Y. Zhang, J. Wang, *Acc. Chem. Res.* **2013**, *46*, 236; e) F. Hu, Y. Xia, C. Ma, Y. Zhang, J. Wang, *Chem. Commun.* **2015**, *51*, 7986.
- 45 R. Kumar, D. Nair, I. N. N. Namboothiri, *Tetrahedron* **2014**, *70*, 1794.
- 46 C. R. Holmquist, E. J. Roskamp, *J. Org. Chem.* **1989**, *54*, 3258.
- 47 a) T. Hashimoto, H. Miyamoto, Y. Naganawa, K. Maruoka, *J. Am. Chem. Soc.* **2009**, *131*, 12290; b) W. Li, J. Wang, X. Hu, K. Shen, W. Wang, Y. Chu, L. Lin, X. Liu, X. Feng, *J. Am. Chem. Soc.* **2010**, *132*, 8532; c) L. Gao, B. C. Kang, G.-S. Hwang, D. H. Ryu, *Angew. Chem. Int. Ed.* **2012**, *51*, 8322.
- 48 T. Hashimoto, Y. Naganawa, K. Maruoka, *J. Am. Chem. Soc.* **2011**, *133*, 8834.
- 49 H. Li, Y. Zhang, J. Wang, *Synthesis* **2013**, *45*, 3090.
- 50 H. Li, L. Wang, Y. Zhang, J. Wang, *Angew. Chem. Int. Ed.* **2012**, *51*, 2943.
- 51 S. R. Ovalles, J. H. Hansen, H. M. L. Davies, *Org. Lett.* **2011**, *13*, 4284.
- 52 N. R. Candeias, C. A. M. Afonso, *Curr. Org. Chem.* **2009**, *13*, 763.
- 53 X. Zhao, Y. Zhang, J. Wang, *Chem. Commun.* **2012**, *48*, 10162.
- 54 Y. Zhang, J. Wang, *Eur. J. Org. Chem.* **2011**, 1015.
- 55 C. A. Merlic, A. L. Zechman, *Synthesis* **2003**, *8*, 1137.
- 56 C.-Y. Zhou, J.-S. Huang, C.-M. Che, *Synlett* **2010**, 2681.
- 57 a) M. P. Doyle, *Angew. Chem. Int. Ed.* **2009**, *48*, 850; b) S. Zhu, X. Ciu, P. X. Zhang, *Eur. J. Inorg. Chem.* **2012**, 430.
- 58 S.-F. Zhu, Q.-L. Zhou, *Acc. Chem. Res.* **2012**, *45*, 1365.
- 59 H. M. L. Davies, D. Morton, *Chem. Soc. Rev.* **2011**, *40*, 1857.

- 60 F. Z. Dörwald, *Metal Carbenes in Organic Synthesis*, Wiley-VCH, Weinheim (1999).
- 61 H. M. L. Davies, R. E. J. Beckwith, *Chem. Rev.* **2003**, 103, 2861.
- 62 A. Demonceau, A. F. Noels, A. J. Hubert, P. Teyssié, *J. Chem. Soc., Chem. Commun.* **1981**, 688.
- 63 D. F. Taber, E. H. Petty, *J. Org. Chem.* **1995**, 47, 4808.
- 64 J. W. Bode, M. P. Doyle, M. N. Protopopova, Q.-L. Zhou, *J. Org. Chem.* **1996**, 61, 9146.
- 65 K. Minami, H. Saito, H. Tsutsui, H. Nambu, M. Anada, S. Hashimoto, *Adv. Synth. Catal.* **2005**, 347, 1483.
- 66 T. Ye, M. A. McKerver, *Chem. Rev.* **1994**, 94, 1091.
- 67 H. M. L. Davies, D. G. Stafford, T. Hansen, *Org. Lett.* **1999**, 1, 233.
- 68 Y. Lian, K. I. Hardcastle, H. M. L. Davies, *Angew. Chem. Int. Ed.* **2011**, 50, 9370.
- 69 The paper states no details on the ee of the cyclopropane ring for this substrate; however in the test reaction in the same paper the cyclopropane was formed in 98% ee.
- 70 P. Yates, *J. Am. Chem. Soc.* **1952**, 74, 5376.
- 71 a) C. F. García, M. A. McKerver, T. Ye, *Chem. Commun.* **1996**, 1465; b) P. Bulugahapitiya, Y. Landais, L. Parra-Rapado, D. Planchenault, V. Weber, *J. Org. Chem.* **1997**, 62, 1630; c) R. T. Buck, C. J. Moody, A. G. Pepper, *Arkivoc* **2002**, viii, 16.
- 72 T. C. Maier, G. C. Fu, *J. Am. Chem. Soc.* **2006**, 128, 4594.
- 73 S.-F. Zhu, C. Chen, Y. Cai, Q.-L. Zhou, *Angew. Chem. Int. Ed.* **2008**, 47, 932.
- 74 C. Chen, S.-F. Zhu, B. Liu, L.-X. Wang, Q.-L. Zhou, *J. Am. Chem. Soc.* **2007**, 129, 12616.
- 75 B. Liu, S.-F. Zhu, W. Zhang, C. Chen, Q.-L. Zhou, *J. Am. Chem. Soc.* **2007**, 129, 5834.
- 76 B. Xu, S.-F. Zhu, Z.-C. Zhang, Z.-X. Yu, Y. Ma, Q.-L. Zhou, *Chem. Sci.* **2014**, 5, 1442.
- 77 Y.-Z. Zhang, S.-F. Zhu, L.-X. Wang, Q.-L. Zhou, *Angew. Chem. Int. Ed.* **2008**, 47, 8496.
- 78 Q.-Q. Cheng, S.-F. Zhu, Y.-Z. Zhang, X.-L. Xie, Q.-L. Zhou, *J. Am. Chem. Soc.* **2013**, 135, 14094.
- 79 W. A. Donaldson, *Tetrahedron* **2001**, 57, 8589.
- 80 M. Elliott, A. W. Farnham, N. F. Janes, P. H. Needham, D. A. Pulman, *Nature* **1973**, 244, 456.
- 81 P. A. Wender, L. O. Haustedt, J. Lim, J. A. Love, T. J. Williams, J.-Y. Yoon, *J. Am. Chem. Soc.* **2006**, 128, 6302.
- 82 A. Fürstner, C. Aïssa, *J. Am. Chem. Soc.* **2006**, 128, 6306.
- 83 H. M. L. Davies, P. R. Bruzinski, D. H. Lake, N. Kong, M. J. Fall, *J. Am. Chem. Soc.* **1996**, 118, 6897.
- 84 J. Li, S.-H. Liao, H. Xiong, Y.-Y. Zhou, X.-L. Sun, Y. Zhang, X.-G. Zhou, Y. Tang, *Angew. Chem. Int. Ed.* **2012**, 51, 8838.
- 85 B. Morandi, B. Mariampillai, E. M. Carreira, *Angew. Chem. Int. Ed.* **2011**, 50, 1101.
- 86 J.-J. Shen, S.-F. Zhu, Y. Cai, H. Xu, X.-L. Xie, Q.-L. Zhou, *Angew. Chem. Int. Ed.* **2014**, 53, 13188.
- 87 Diastereoselective: S. Chen, J. Ma, J. Wang, *Tetrahedron Lett.* **2008**, 49, 6781. (with Pd only very low enantioselectivities have been obtained so far: S. E. Denmark, R. A. Stavenger, A.-M. Faucher, J.P. Edwards, *J. Org. Chem.* **1997**, 62, 3375.)
- 88 S. Chanthamath, S. Ozaki, K. Shibatomi, S. Iwasa, *Org. Lett.* **2014**, 16, 3012.
- 89 Z.-Y. Cao, X. Wang, C. Tan, X.-L. Zhao, J. Zhou, K. Ding, *J. Am. Chem. Soc.* **2013**, 135, 8197.
- 90 H. Lu, W. I. Dzik, X. Xu, L. Wojtas, B. de Bruin, X. P. Zhang, *J. Am. Chem. Soc.* **2011**, 133, 8518.
- 91 S. Zhu, X. Xu, J. A. Perman, X. P. Zhang, *J. Am. Chem. Soc.* **2010**, 132, 12796.
- 92 S. Chanthamath, S. Takaki, K. Shibatomi, S. Iwasa, *Angew. Chem. Int. Ed.* **2013**, 52, 5818.
- 93 Y. Nakagawa, S. Chanthamath, K. Shibatomi, S. Iwasa, *Org. Lett.* **2015**, 17, 2792.
- 94 J. Barluenga, P. Moriel, C. Valdés, F. Aznar, *Angew. Chem. Int. Ed.* **2007**, 46, 5587.
- 95 Q. Xiao, Y. Zhang, J. Wang, *Acc. Chem. Res.* **2013**, 46, 236.

- 96 J. Barluenga, M. Tomás-Gamasa, F. Aznar, C. Valdés, *Nat. Chem.* **2009**, *1*, 494.
- 97 B. Ye, N. Cramer, *Angew. Chem. Int. Ed.* **2014**, *53*, 7896.
- 98 For books on continuous flow chemistry and flow chemistry in microreactors: T. Wirth (Editor), *Microreactors in Organic Chemistry and Catalysis*, 2nd edition, Wiley-VCH, Weinheim (**2013**); F. Darvas, G. Dormán, V. Hessel (Editors), *Flow Chemistry*, Walter de Gruyter GmbH, Berlin/Boston (**2014**);
- 99 There are several excellent reviews discussing the benefits of continuous flow chemistry in microreactors: a) R. L. Hartman, J. P. McMullen, K. F. Jensen, *Angew. Chem. Int. Ed.* **2011**, *50*, 7502; b) C. Wiles, P. Watts, *Green Chem.* **2012**, *14*, 38; c) K. S. Elvira, X. C. I. Solvas, R. C. R. Wootton, A. J. deMello, *Nature Chem.* **2014**, *5*, 905.
- 100 J.-i. Yoshida, A. Nagaki, T. Yamada, *Chem. Eur. J.* **2008**, *14*, 7450.
- 101 Modified from: F. Stoessel, *Thermal Safety of Chemical Processes*, Wiley-VCH, Weinheim (**2008**), page 199.
- 102 B. Gutmann, D. Cantillo, C. O. Kappe, *Angew. Chem. Int. Ed.* **2015**, *54*, 6688.
- 103 P. R. D. Murray, D. L. Browne, J. C. Pastre, C. Butters, D. Guthrie, S. V. Ley, *Org. Process Res. Dev.* **2012**, *16*, 1131.
- 104 M. Irfan, T. N. Glasnov, C. O. Kappe, *ChemSusChem* **2011**, *4*, 300.
- 105 a) Y. Wada, M. A. Schmidt, K. F. Jensen, *Ind. Eng. Chem. Res.* **2006**, *45*, 8036; b) F. Lévesque, P. H. Seeberger, *Angew. Chem. Int. Ed.* **2012**, *51*, 1706.
- 106 J. R. Gage, X. Guo, J. Tao, C. Zheng, *Org. Process Res. Dev.* **2012**, *16*, 930.
- 107 B. J. Deadman, S. G. Collins, A. R. Maguire, *Chem. Eur. J.* **2015**, *21*, 2298.
- 108 a) P. B. Palde, T. F. Jamison, *Angew. Chem. Int. Ed.* **2011**, *50*, 3525; b) B. Gutmann, D. Obermayer, J.-P. Roduit, D. M. Roberge, C. O. Kappe, *J. Flow Chem.* **2012**, *1*, 8.
- 109 A. DeAngelis, D.-H. Wang, S. L. Buchwald, *Angew. Chem. Int. Ed.* **2013**, *52*, 3434.
- 110 C. B. McPake, G. Sandford, *Org. Process Res. Dev.* **2012**, *16*, 884.
- 111 S. Fuse, N. Tanabe, T. Takahashi, *Chem. Commun.* **2011**, *47*, 12661.
- 112 L. Audinger, K. Watts, S. C. Elmore, R. I. Robinson, T. Wirth, *ChemSusChem* **2012**, *5*, 257.
- 113 W. Ferstl, T. Klahn, W. Schweikert, G. Billeb, M. Schwarzer, S. Loebbecke, *Chem. Eng. Technol.* **2007**, *30*, 370.
- 114 A. V. Gomez, H. H. J. Verputten, A. Díaz-Ortiz, A. Moreno, A. de la Hoz, A. H. Velders, *Chem. Commun.* **2010**, *46*, 4514.
- 115 C. F. Carter, H. Lange, S. V. Ley, I. R. Baxendale, B. Wittkamp, J. G. Goode, N. L. Gaunt, *Org. Process Res. Dev.* **2010**, *14*, 393.
- 116 D. L. Browne, S. Wright, B. J. Deadman, S. Dunnage, I. R. Baxendale, R. M. Turner, S. V. Ley, *Rapid Commun. Mass Spectrom.* **2012**, *26*, 1999.
- 117 P. L. Mills, J. F. Nicole, *Ind. Eng. Chem. Res.* **2005**, *44*, 6435.
- 118 M. Rasheed, T. Wirth, *Chem. Today* **2011**, *29*, 54.
- 119 C. J. Smith, N. Nikbin, S. V. Ley, H. Lange, I. R. Baxendale, *Org. Biomol. Chem.* **2011**, *9*, 1938.
- 120 L. Malet-Sanz, J. Madrzak, S. V. Ley, I. R. Baxendale, *Org. Biomol. Chem.* **2010**, *8*, 5324.
- 121 S. T. R. Müller, A. Murat, D. Maillos, P. Lesimple, P. Hellier, T. Wirth, *Chem. Eur. J.* **2015**, *21*, 7016.
- 122 P. Koos, U. Gross, A. Polyzos, M. O'Brien, I. R. Baxendale, S. V. Ley, *Org. Biomol. Chem.* **2011**, *9*, 6903.
- 123 a) B. J. Reizman, K. F. Jensen, *Org. Process Res. Dev.* **2012**, *16*, 1770; b) J. S. Moore, K. F. Jensen, *Org. Process Res. Dev.* **2012**, *16*, 1409.
- 124 J. S. Moore, K. F. Jensen, *Angew. Chem. Int. Ed.* **2014**, *53*, 470.
- 125 J. Li, S. G. Ballmer, E. P. Gillis, S. Fujii, M. J. Schmidt, A. M. E. Palazzolo, J. W. Lehmann, G. F. Morehouse, M. D. Burke, *Science* **2015**, *347*, 1221.

- 126 a) J. P. McMullen, M. T. Stone, S. L. Buchwald, K. F. Jensen, *Angew. Chem. Int. Ed.* **2010**, 49, 7076; b) M. Rasheed, T. Wirth, *Angew. Chem. Int. Ed.* **2011**, 50, 357.
- 127 B. J. Deadman, C. Battilocchio, E. Sliwinski, S. V. Ley, *Green Chem.* **2013**, 15, 2050.
- 128 A. E. Cervera-Padrell, S. T. Morthensen, D. J. Lewandowski, T. Skovby, S. Kiil, K. V. Gernaey, *Org. Process Res. Dev.* **2012**, 16, 888.
- 129 A. G. O'Brien, Z. Horváth, F. Lévesque, J. W. Lee, A. Seidel-Morgenstern, P. H. Seeberger, *Angew. Chem. Int. Ed.* **2012**, 51, 7028.
- 130 R. J. Ingham, C. Battilocchio, D. E. Fitzpatrick, E. Sliwinski, J. M. Hawkins, S. V. Ley, *Angew. Chem. Int. Ed.* **2015**, 54, 144.
- 131 H. Zhang, R. Lakerveld, P. L. Heider, M. Tao, M. Su, C. J. Testa, A. N. D'Antonio, P. I. Barton, R. D. Braatz, B. L. Trout, A. S. Myerson, K. F. Jensen, J. M. B. Evans, *Cryst. Growth Des.* **2014**, 14, 2148.
- 132 C. F. Carter, H. Lange, D. Sakai, I. R. Baxendale, S. V. Ley, *Chem. Eur. J.* **2011**, 17, 3398.
- 133 I. R. Baxendale, J. Deeley, C. M. Griffiths-Jones, S. V. Ley, S. Saaby, G. K. Trammer, *Chem. Commun.* **2006**, 2566.
- 134 P. R. D. Murray, D. L. Browne, J. C. Pastre, C. Butters, D. Guthrie, S. V. Ley, *Org. Process Res. Dev.* **2013**, 17, 1192.
- 135 S. Mascia, P. L. Heider, H. Zhang, R. Lakerveld, B. Benyahia, P. I. Barton, R. D. Braatz, C. L. Cooney, J. M. B. Evans, T. F. Jamison, K. F. Jensen, A. S. Myerson, B. L. Trout, *Angew. Chem. Int. Ed.* **2013**, 52, 12359.
- 136 A comprehensive overview of this chapter has been published: S. T. R. Müller, T. Wirth, *ChemSusChem* **2015**, 8, 245.
- 137 L. D. Procter, A. J. Warr, *Org. Process Res. Dev.* **2002**, 6, 884.
- 138 M. Struempel, B. Ondruschka, R. Daute, A. Stark, *Green Chem.* **2008**, 10, 41.
- 139 R. A. Maurya, C. P. Park, J. H. Lee, D.-P. Kim, *Angew. Chem. Int. Ed.* **2011**, 50, 5952.
- 140 a) F. Mastronardi, B. Gutmann, C. O. Kappe, *Org. Lett.* **2013**, 15, 5590; b) V. D. Pinho, B. Gutmann, L. S. M. Miranda, R. O. M. A. de Souza, C. O. Kappe, *J. Org. Chem.* **2014**, 79, 1555.
- 141 M. M. E. Delville, J. C. M. van Hest, F. P. J. T. Rutjes, *Beilstein J. Org. Chem.* **2013**, 9, 1813.
- 142 a) M. I. Burguete, A. Cornejo, E. García-Verdugo, J. García, M. J. Gil, S. V. Luis, V. Martínez-Merino, J. A. Mayoral, M. Sokolova, *Green Chem.* **2007**, 9, 1091; b) C. Aranda, A. Cornejo, J. M. Fraile, E. García-Verdugo, M. J. Gil, S. V. Luis, J. A. Mayoral, V. Martínez-Merino, Z. Ochoa, *Green Chem.* **2011**, 13, 983.
- 143 a) H. E. Bartrum, D. C. Blakemore, C. J. Moody, C. J. Hayes, *Chem. Eur. J.* **2011**, 17, 9586; b) H. E. Bartrum, D. C. Blakemore, C. J. Moody, C. J. Hayes, *Tetrahedron* **2013**, 69, 2276.

2 Objectives & Outline of the thesis

The ability of diazo compounds to generate metal carbenes which undergo numerous reactions with high selectivities make this class of reagents an attractive group for applied synthetic chemistry. The thermal properties of diazo compounds, however, hinder the safe use of large quantities of these compounds in process chemistry. The aim of this work is to develop protocols using continuous flow technology for the safe, efficient and versatile use of diazo compounds.

Four main targets were set at the beginning of this work:

- (1) Development of efficient continuous flow protocols for the preparation and direct use of diazoesters
- (2) Scalability of the developed processes to make them interesting for use on industrial scale
- (3) Application of the newly developed continuous flow protocols to the synthesis of biologically active molecules
- (4) Investigation of novel reactions of diazo compounds

The development of novel continuous flow protocols for diazo compounds (1) is the underlying theme of this thesis. Consequently, four of the five projects that are being discussed deal with the preparation and direct use of diazo compounds in flow. The scalability (2) of the flow methods developed is used to generate gram quantities of valuable synthetic targets. The application of these systems for the preparation of biologically active molecules (3) will be discussed, mainly in chapter 5. The development of a new stereochemically defined C-H insertion reaction of diazo compounds (4) will also be discussed in chapter 5.

This work is divided into five projects that are discussed in three chapters. The first two projects (Chapter 3) deal with the use of ethyl diazoacetate as nucleophile. In the first project (Section 3.2), ethyl diazoacetate is prepared in flow and directly used in an aldol addition reaction to aldehydes. The scope of this reactivity is then extended in the second project (Section 3.3) by preparing ethyl lithiodiazoacetate which is added to a diverse set of ketones in flow.

In the third project (Chapter 4), the formation and use of aryl diazoacetates in flow is discussed. Thermal and kinetic studies aid in the development of a multistep continuous flow method. The rapid generation of data on the formation of these diazo compounds is achieved through in-line analytics (infrared spectroscopy). Purification of the diazo compound in flow is accomplished by a liquid / liquid extraction in flow.

In the fourth project (Chapter 5, Section 5.2), diazo compounds are used to generate complex cyclopropanes in a safe fashion using continuous flow technology. Competing side-reactions

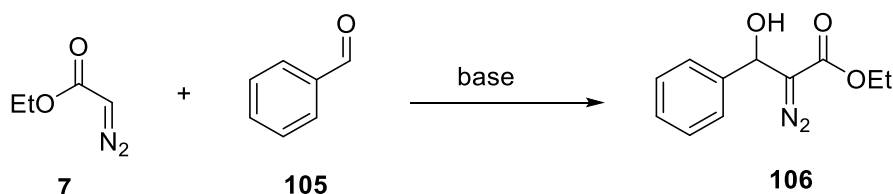
are studied and strategies to avoid the side-reactions are investigated. The final project discusses the use of diazo compounds for the highly stereoselective formation of indolines (Section 5.3). A six step synthesis is designed in which a diazo transfer reaction is followed by an intramolecular C-H insertion reaction to generate *trans*-indolines in high yields and selectivities.

In the conclusion (Chapter 6), an overview of some preliminary investigations into other projects using diazo compounds is presented. Albeit these projects have not been finished in this thesis, they represent interesting avenues for further explorations into diazo compounds. Finally, detailed experimental information can be found in Chapter 7.

3 Ethyl diazoacetate as nucleophile

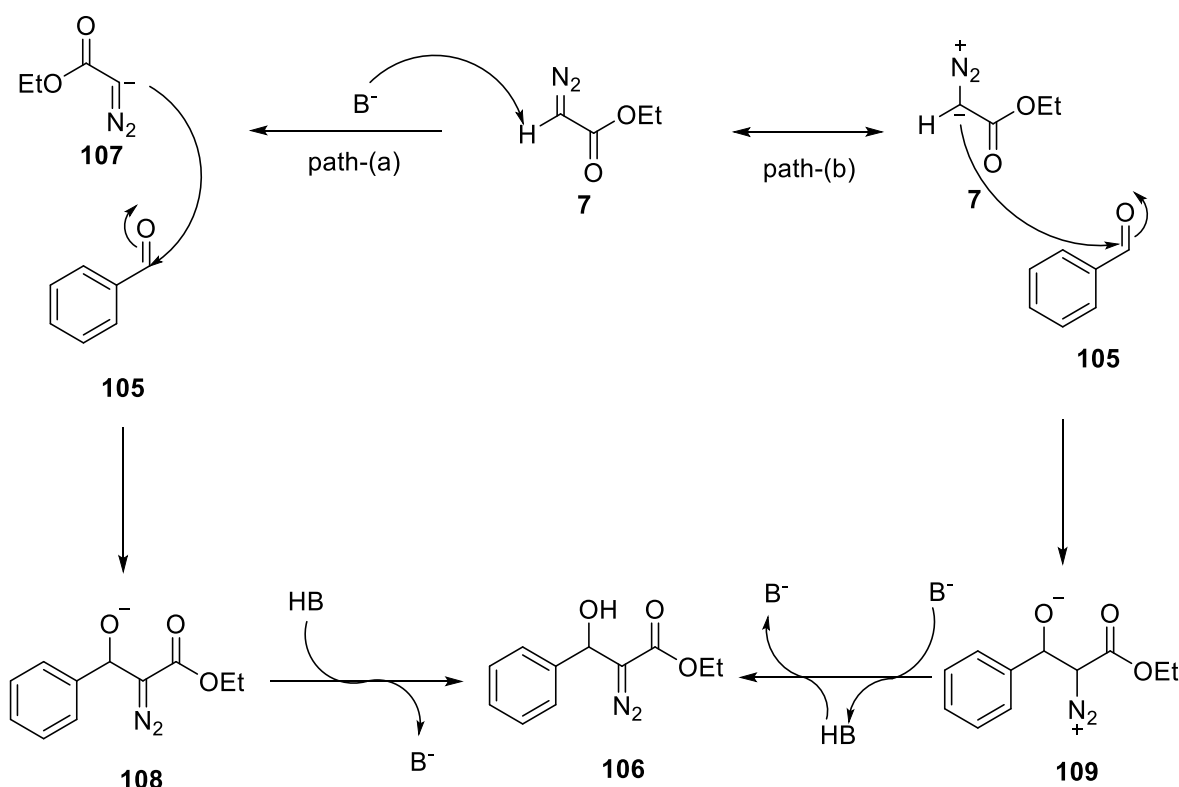
3.1 Introduction – EDA as nucleophile

Ethyl diazoacetate (EDA) **7** was not only the first diazo compound discovered, it has also been one of the most intensely studied diazo reagents. The vast majority of reactions for which ethyl diazoacetate has been used are based on the metal-based decomposition of the diazo species (see section 1.3.2). However, ethyl diazoacetate can also be deprotonated and used as nucleophilic species with retention of the dinitrogen functionality.¹ The first relevant synthetic reports of this strategy appeared in the late 1960s² and early 1970s.³ Ethyl diazoacetate **7** was found to react smoothly with aldehydes such as benzaldehyde **105** under base catalysis to afford β -hydroxy- α -diazo compound **106** (Scheme 22). This reaction can be considered to be an aldol addition.



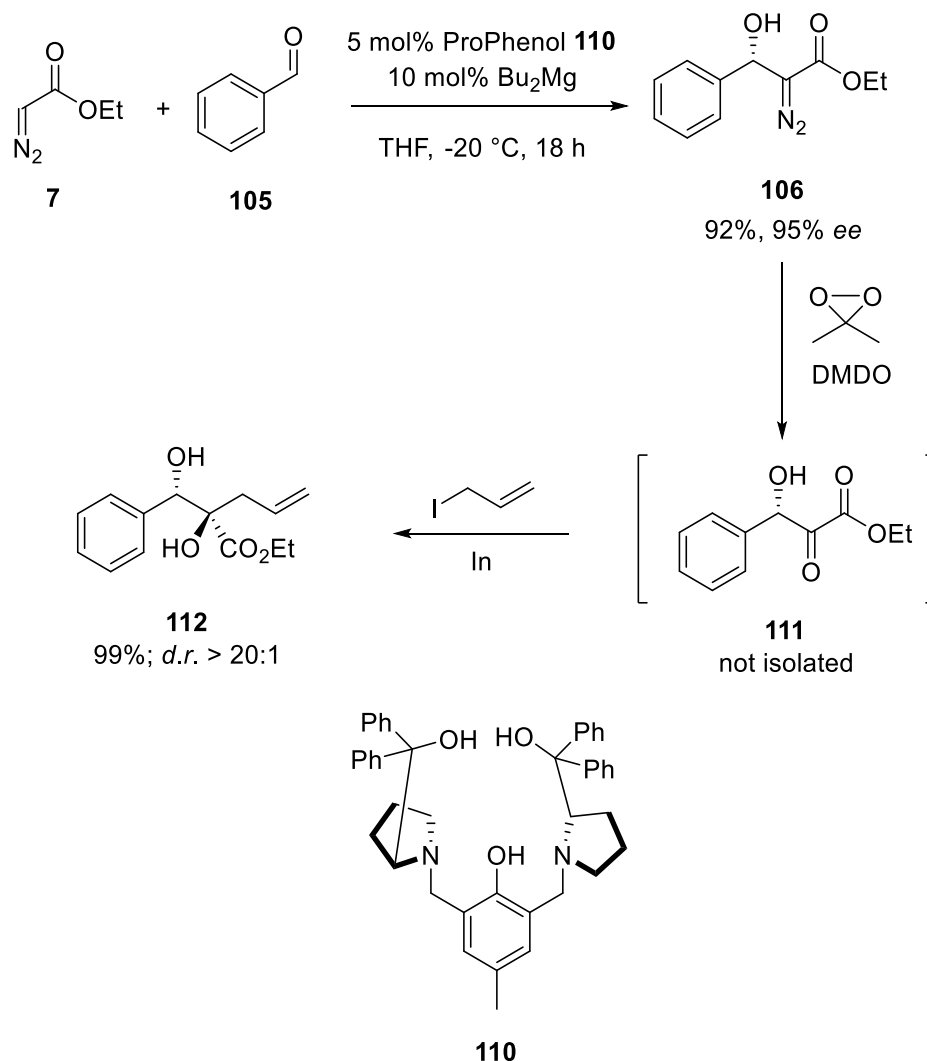
Scheme 22: Aldol addition of ethyl diazoacetate onto benzaldehyde

An interesting question in this reaction scheme is the role of the base. One could imagine two possible pathways for the formation of **106** out of starting materials **7** and **105** (Scheme 23). In the first case (a), the base deprotonates **7** to generate anion **107** which then attacks aldehyde **105**. In the second case (b), ethyl diazoacetate **7** reacts with benzaldehyde **105** first which is then followed by a deprotonation of intermediate **109**. It depends on the base employed and the pKa of the nucleophile which of the two pathways will dominate. No report of the exact pKa value of **7** was found. However, the following considerations can provide an idea of the acidity of ethyl diazoacetate **7**: A) Ethyl diazoacetate **7** has a much higher electron density on the carbon atom of the diazo group than its non-diazo counterpart ethyl acetate (due to resonance forms; see section 1.1). Therefore, deprotonation of ethyl diazoacetate **7** can be expected to require stronger bases than deprotonation of ethyl acetate. Ethyl acetate has a pKa of 25.⁴ B) It is well known that lithium diisopropylamide (LDA) can however, deprotonate ethyl diazoacetate **7** readily to generate ethyl lithiodiazoacetate. It can be concluded that relatively strong organometallic bases will be needed to favour reaction path- (a) in case of ethyl diazoacetate **7**.



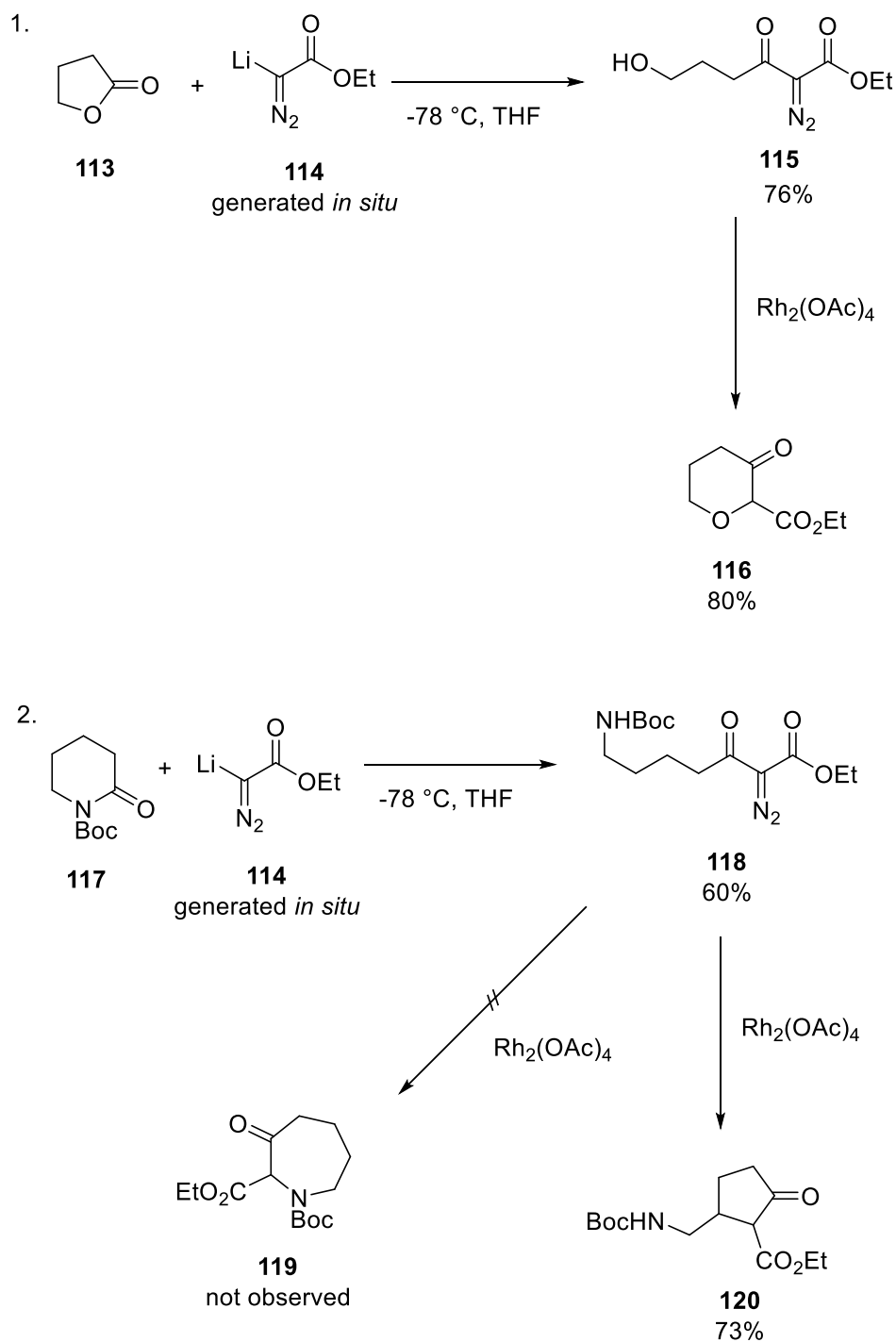
Scheme 23: Mechanistic analysis for aldol addition of ethyl diazoacetate

The use of ethyl diazoacetate as nucleophilic species has found several interesting applications. In case of the addition to aldehydes, many different bases can be used such as sodium hydride,⁵ potassium hydroxide,⁶ tetrabutylammonium hydroxide,⁷ DBU,⁸ *n*-butyllithium⁹, and LDA¹⁰. Recently, asymmetric versions of this transformation have been developed. Arai *et al.* investigated the use of a chiral phase transfer catalyst for this reaction, resulting in moderate to good enantiomeric excess (up to 79% *ee*).¹¹ Yao and Wang achieved higher enantiomeric excess utilising a chiral Binol ligand on zirconium providing up to 87% *ee*.¹² Very high selectivities were then recorded by Trost and coworkers using ProPhenol ligand **110** and magnesium as catalytic system (up to 97% *ee*).¹³ This catalytic system was used for the elegant asymmetric synthesis of 1,2 diols (Scheme 24).¹⁴ After the stereoselective reaction of benzaldehyde **105** with ethyl diazoacetate **7**, β -hydroxy- α -diazoester **106** was selectively oxidised to β -hydroxy- α -ketoester **111**. This compound was immediately trapped using indium and allyl iodide to furnish 1,2-diol **112** with high diastereomeric excess.



Scheme 24: Stereoselective generation of 1,2-diols using asymmetric aldol reaction of EDA **7**

Another synthetically useful application of using ethyl diazoacetate as nucleophile is the ring opening of lactones and similar functionalities. In this case, ethyl lithiodiazoacetate **114** is generated first and then trapped using lactone **113**. These reactions are performed at very low temperatures ($\leq -78\text{ }^\circ\text{C}$) due to the instability of ethyl lithiodiazoacetate.^{3a} Subsequent treatment of diazo alcohol **115** with rhodium acetate provides the ring-expanded ether **116** (Scheme 25, 1.). The ring opening can also be performed on lactams and thiolactones. Interestingly, in case of the *N*-Boc lactam **117**, the subsequent treatment with rhodium acetate did not provide cyclic amine **119** but instead the cyclopentane structure **120** through C-H insertion chemistry (Scheme 25, 2.).¹⁰

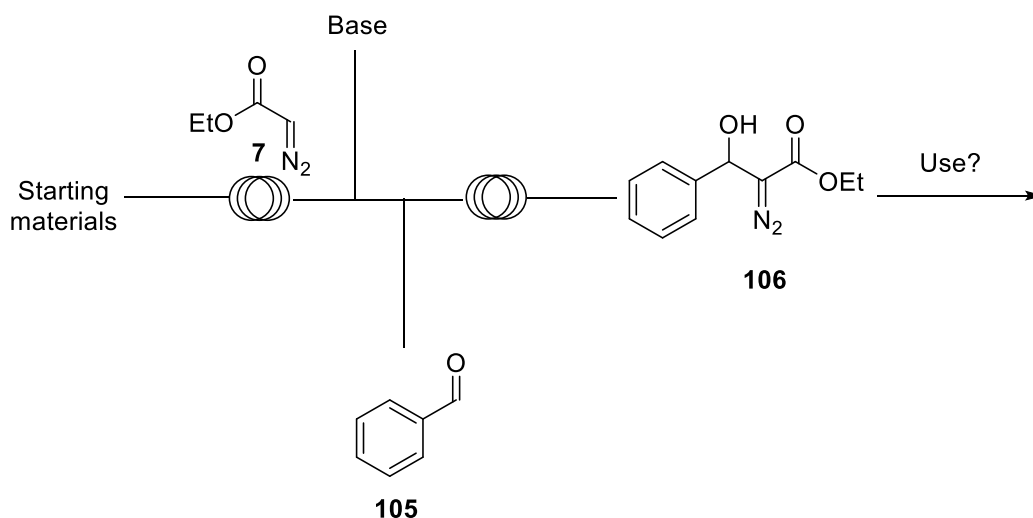


Scheme 25: Use of ethyl lithiodiazoacetate **114** for ring opening of lactones **113** (1.) and lactams **117** (2.)

3.2 Generation and direct use of ethyl diazoacetate in flow chemistry

At the start of this project, no reports on the generation of ethyl diazoacetate in continuous flow had been published.¹⁵ Therefore, a continuous flow protocol was anticipated in which ethyl diazoacetate **7** would be generated *in situ* within a first continuous flow reactor to then

be quenched using the base-catalysed aldol addition with benzaldehyde **105** in a second flow reactor (Scheme 26). The β -keto- α -diazoester **106** could then be used for the generation of a carbene species in a third reaction step.

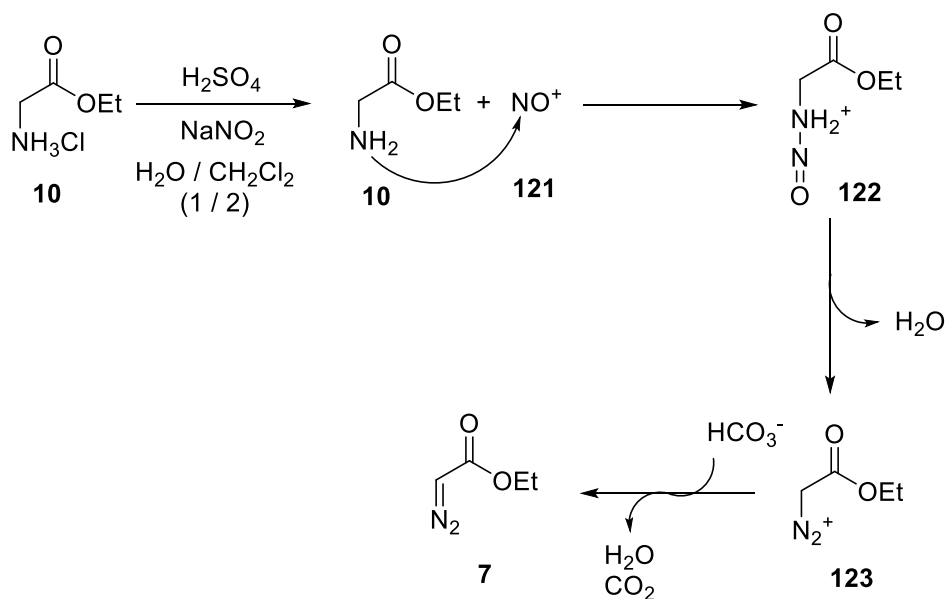


Scheme 26: General scheme of the flow set-up for the formation and consumption of ethyl diazoacetate **7**

To develop such a system, first a reaction for the generation of ethyl diazoacetate had to be chosen.

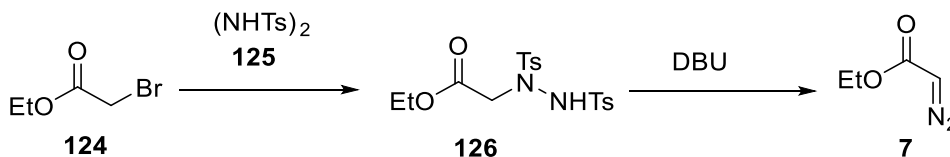
3.2.1 Synthesis of ethyl diazoacetate

Some of the synthetic strategies to diazo reagents were discussed in section 1.2. Two strategies to access ethyl diazoacetate **7** were investigated in batch first. The first one is the diazotization of glycine ethyl ester hydrochloride **10** under acidic conditions (Scheme 27). In this reaction, a highly reactive nitrosonium ion **121** is generated from the protonation of sodium nitrite with sulfuric acid. Compound **121** is then trapped by the amine group of glycine ethyl ester **10** to form diazonium salt **123**. Quenching with sodium hydrogen carbonate solution provides ethyl diazoacetate **7**. The reaction is performed at $-10\text{ }^{\circ}\text{C}$ and the work-up has to be performed at low temperatures, too. This is due to the instability of diazonium compound **123**.



Scheme 27: Diazotization of glycine ethyl ester **10** to prepare ethyl diazoacetate **7**

The second approach was recently described by Fukuyama and co-workers.¹⁶ α -Bromo reagent **124** is treated with *N,N'*-ditosylhydrazine **125** to generate hydrazone intermediate **126** which then eliminates two toluenesulfonic acid groups to furnish ethyl diazoacetate **7** (Scheme 28).

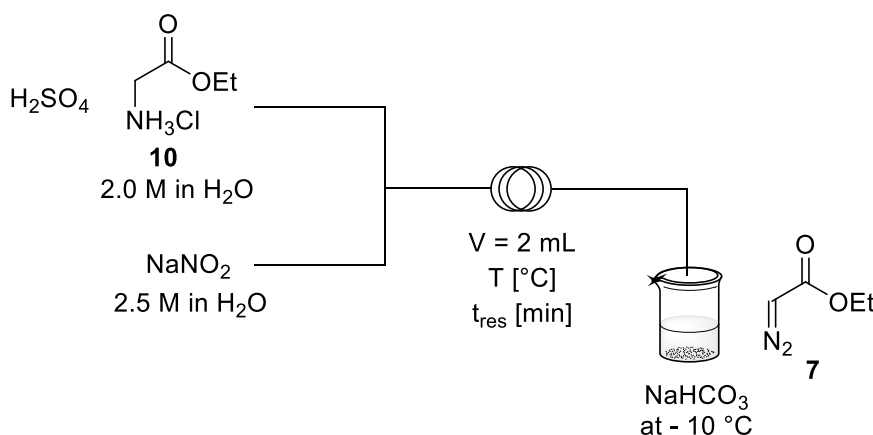


Scheme 28: Preparation of ethyl diazoacetate **7** from α -bromoethyl acetate **124**

When tested, both reactions worked well providing ethyl diazoacetate in 86% and 77% yield, respectively. Diazotization of glycine ethyl ester hydrochloride **10** however, provided a slightly higher yield as well as a higher purity of the diazo reagent after a simple work-up. Therefore, this method was transferred into continuous flow to test the efficiency of the formation of ethyl diazoacetate **7** in flow. This strategy also allowed for the safe preparation of multigram quantities of ethyl diazoacetate **7**.

The set-up used for the flow synthesis of **7** is shown in Scheme 29. Glycine ethyl ester hydrochloride **10** reacts with the *in situ* generated nitrosium ion in the flow reactor. The reaction mixture is then quenched in a beaker containing a saturated aqueous sodium hydrogen carbonate solution at $-10\text{ }^{\circ}\text{C}$. One of the main modifications to the batch protocol was the switch from a biphasic $\text{CH}_2\text{Cl}_2/\text{H}_2\text{O}$ solvent mixture to water as reaction solvent. This solvent switch allowed for the direct addition of a second step (e.g. aldol addition to an aldehyde)

without the need of an initial extraction. In this set-up relatively high concentrations of reagents were employed (2.5 M solution of NaNO_2 and 2 M solution of glycine ethyl ester hydrochloride **10**).



Scheme 29: Continuous flow set-up for the preparation of ethyl diazoacetate **7**

Results from this approach are shown in Table 3.1. It should be noted that there is a certain standard deviation in the yields obtained as ethyl diazoacetate **7** forms an azeotrope with most solvents (CH_2Cl_2 , Et_2O) and some residual solvent is still observed in the ^1H NMR (see value in brackets in Table 3.1). Consequently, commercially available EDA **7** also contains around 13% dichloromethane. The first finding from the flow experiment was the improved purity of the isolated EDA **7** compared to batch experiments. In fact, EDA **7** obtained *via* this route was of higher purity than EDA **7** obtained from the commercial source. The first parameter evaluated in the flow experiment was the residence time. A very short residence time of one minute was already sufficient to form significant amounts of ethyl diazoacetate **7**, albeit in reduced yield compared to the batch experiment (Table 3.1, entry 1). The increase of the residence time to three minutes led to a significant improvement in yield (Table 3.1, entry 2). However, further extension of the residence time to four and five minutes did not lead to any further changes (Table 3.1, entries 3-4). Changes in temperature had a strong effect on the efficiency of the process. At 0 °C, a sharp drop in yield was observed compared to the experiment at room temperature (Table 3.1, entry 6). In contrast, performing the reaction at slightly elevated temperature (40 °C) led to an increased formation of EDA **7** (Table 3.1, entry 5). As a significant formation of gas was observed in the microreactor tubing, therefore the impact of a back-pressure regulator on the system was studied. However, the reaction yield improved only slightly when a back-pressure regulator with 40 psi was utilised (Table 3.1, entry 7). In conclusion, the transfer from batch to continuous flow was easily achieved using mild reaction conditions.

Table 3.1: Continuous flow optimisation of ethyl diazoacetate **7** formation

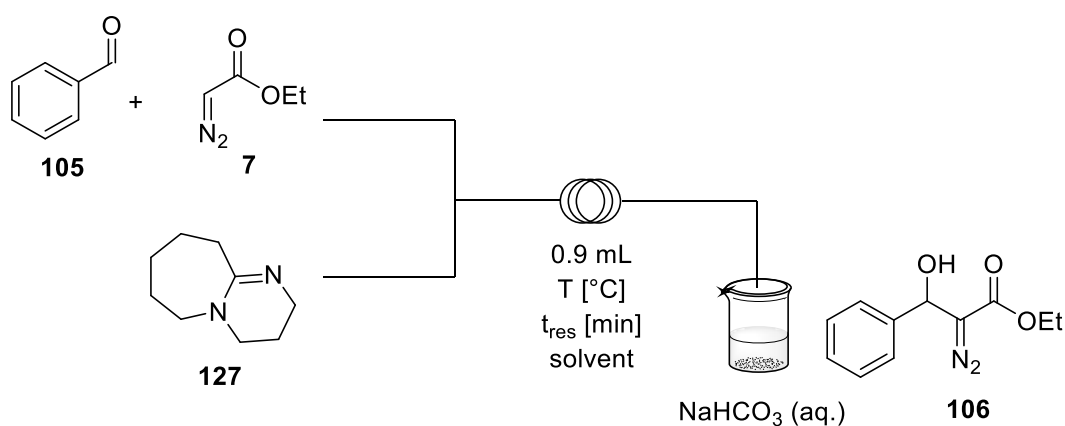
Entry	T [°C]	Flow rate [mL/min]	t _{res} [min]	Yield [%] ^a (% of CH ₂ Cl ₂) ^b
1	22	2	1	45 (7)
2	22	0.66	3	68 (8)
3	22	0.5	4	68 (10)
4	22	0.4	5	68 (6)
5	40	0.66	3	78 (16)
6	0	0.66	3	28 (12)
7 ^c	22	0.66	3	71 (12)

^a isolated yield; ^b mol% of CH₂Cl₂ in the sample determined by ¹H NMR; ^c use of back-pressure regulator 2.7 bar (40 psi)

Having established that the formation of EDA **7** worked rapidly and cleanly, the next step of the two-step process was optimised.

3.2.2 Aldol addition in continuous flow

Next, the reaction of ethyl diazoacetate **7** with benzaldehyde **105** was investigated. Therefore, the following set-up was utilised (Scheme 30). A short 0.9 mL reactor coil was used for the reaction. DBU **127** was selected as base since it combines a high yield in the aldol addition with a relative simplicity in usage compared to lithium bases such as LDA. DBU **127** was added to a stream of benzaldehyde **105** with ethyl diazoacetate **7**. One equivalent of each, DBU and benzaldehyde, was used. The focus of this approach was to determine the solvent which would be used for the two-step protocol.

Scheme 30: Continuous flow experiment of aldol addition of diazo reagent **7** onto benzaldehyde **105**

The results of the aldol addition in flow are shown in Table 3.2. The reaction was evaluated via offline ^1H NMR analysis. This was possible as no side-products were formed and therefore the conversion of the reaction was a good indicator of the yields that could be expected. The first solvent investigated in this reaction was water. A recent publication described water as solvent for the aldol addition of ethyl diazoacetate to aldehydes.¹⁷ As the synthesis of ethyl diazoacetate **7** has been achieved in water, this was an intriguing option. At room temperature, the formation of β -hydroxy- α -diazoester **106** was observed in 13.5 minutes albeit with poor conversion (Table 3.2, entry 1). Increasing the temperature or the residence time led to improvements in the conversion (Table 3.2, entries 2-3). A further improvement was achieved with dimethylsulfoxide (DMSO) as solvent which gave 83% conversion (^1H NMR) at the conditions in which water had given 31% (compare Table 3.2, entries 1 and 5). Even at shorter residence times the product was still obtained in good conversion in DMSO (Table 3.2, entry 4). A very long residence time of almost two hours gave the highest conversion observed (Table 3.2, entry 6). Shorter reaction times were investigated at an elevated temperature (60 °C) which gave moderate yields even at a residence time of just 0.5 minutes (entries 7-9). Dimethylsulfoxide was also a better solvent than acetonitrile (Table 3.2, entry 10) and dichloromethane (Table 3.2, entry 11). The most promising reaction conditions were those using DMSO at room temperature with a residence time of 13.5 minutes (Table 3.2, entry 5) as they were a good compromise between reaction time and conversion.

Table 3.2: Solvent, temperature and residence time screening of aldol addition

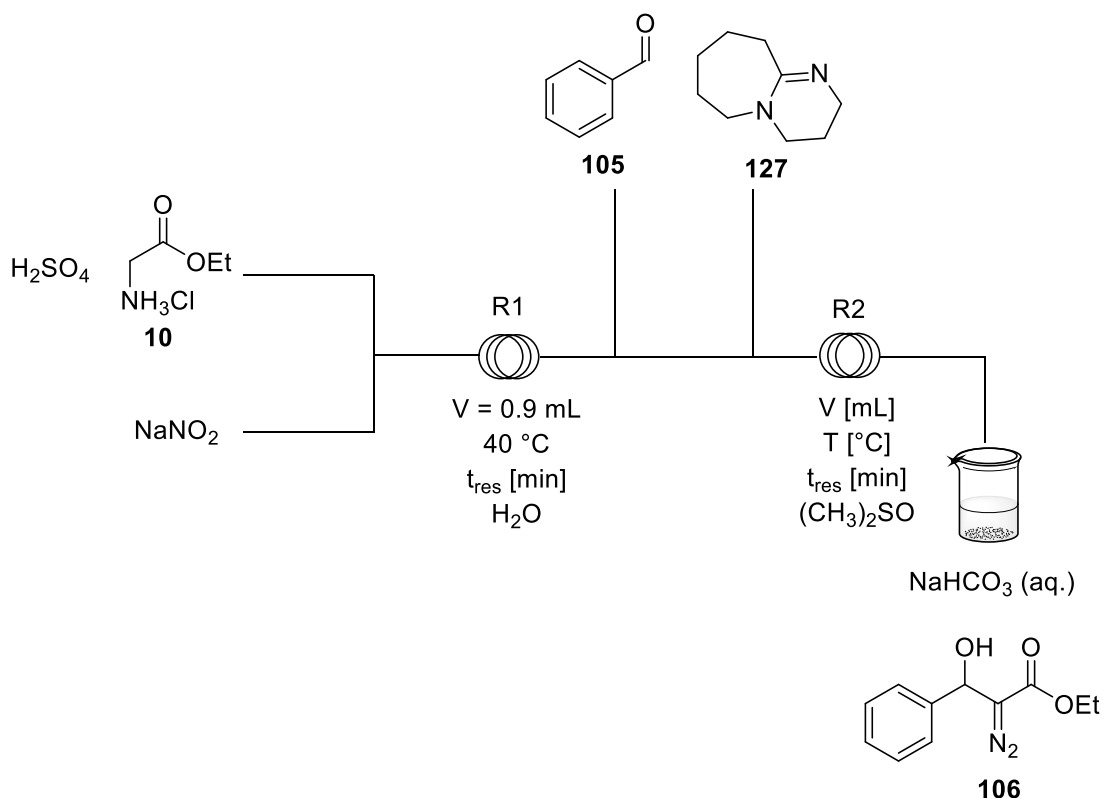
Entry	solvent	t_{res} [min]	T [°C]	Conversion [%] ^a
1	H ₂ O	13.5	22	31
2	H ₂ O	13.5	40	63
3	H ₂ O	27.3	22	71
4	(CH ₃) ₂ SO	6.8	22	71
5	(CH ₃) ₂ SO	13.5	22	83
6	(CH ₃) ₂ SO	108	22	93
7	(CH ₃) ₂ SO	3.7	60	57
8	(CH ₃) ₂ SO	1.8	60	56
9	(CH ₃) ₂ SO	0.5	60	60
10	CH ₃ CN	2.3	60	45
11	CH ₂ Cl ₂	27.3	22	9

^a conversion determined by ^1H NMR comparing peaks of starting material and product

The two separate reaction steps of i) the formation of ethyl diazoacetate **7** and ii) the subsequent aldol addition to benzaldehyde **105** to generate β -hydroxy- α -diazoester **106** had been successfully transferred to continuous flow conditions. With this in hand, a two-step protocol could be envisioned in which the diazo reagent **7** was generated within a first reactor and directly used for the aldol addition with aldehydes in the second reactor.

3.2.3 Two-step continuous flow approach

To optimise such an approach, the set-up shown in Scheme 31 was used. It is noteworthy that the order of addition of benzaldehyde **105** and DBU **127** to the stream of *in situ* formed ethyl diazoacetate **7** is counterintuitive. However, it was necessary to add benzaldehyde **105** first as ethyl diazoacetate **7** forms with DBU **127** a brownish gel that is extremely insoluble in organic solvents but readily dissolves in water. However, this gel formation is not observed when benzaldehyde **105** is present to trap the nucleophilic diazo species. The parameters investigated in this set-up were residence time, equivalents of *in situ* formed EDA **7** and DBU **127** as well as the temperature of the aldol addition reaction.



Scheme 31: Two-step optimisation set-up

The results of the reaction optimisation are shown in Table 3.3. At 60°C , a residence time of 0.5 and 0.2 minutes per reactor provided a low conversion to the β -hydroxy- α -diazoester **106** (Table 3.3, entry 1). However, the same conditions using a large excess of glycine ethyl ester

hydrochloride **10** (3 equivalents) gave a good conversion (69%) indicating that the formation of EDA **7** was not complete in 0.5 minutes at 60 °C (Table 3.3, entry 2). Slightly longer reaction times at these elevated temperatures did not improve the yield when only one equivalent of glycine ethyl ester hydrochloride **10** was used (Table 3.3, entries 3-5). At room temperature, the reaction gave promising results (74% conversion) when 2.3 equivalents of DBU **127** were utilised (Table 3.3, entry 6). The conversion was further improved by slightly increasing the temperature (40 °C) and the equivalents of glycine ethyl ester hydrochloride **10** (2 equivalents) to give 83% conversion (Table 3.3, entry 7). At this temperature, the reduction of equivalents of DBU **127** and glycine ethyl ester hydrochloride **10** led to a drop in product formation (Table 3.3, entries 8-10, 12). However, reducing the equivalents of glycine ethyl ester HCl **10** was more detrimental to the reaction outcome than reducing the equivalence of DBU **127**. Consequently, the reaction gave good results when one equivalent of DBU **127** and two equivalents of glycine ethyl ester HCl **10** were used at 40 °C (80%, Table 3.3, entry 11). A further reduction of the residence time to make the process more efficient led to a lower conversion (Table 3.3, entry 13). In contrast, an excellent result was obtained when the residence time in the second reactor was increased to 7.5 minutes, providing β -hydroxy- α -diazoester **106** in 96% ¹H NMR conversion (Table 3.3, entry 14). The relatively low amount of base required (1 equivalent) in the short overall reaction time (total residence time: 14.3 min) made this an efficient process.

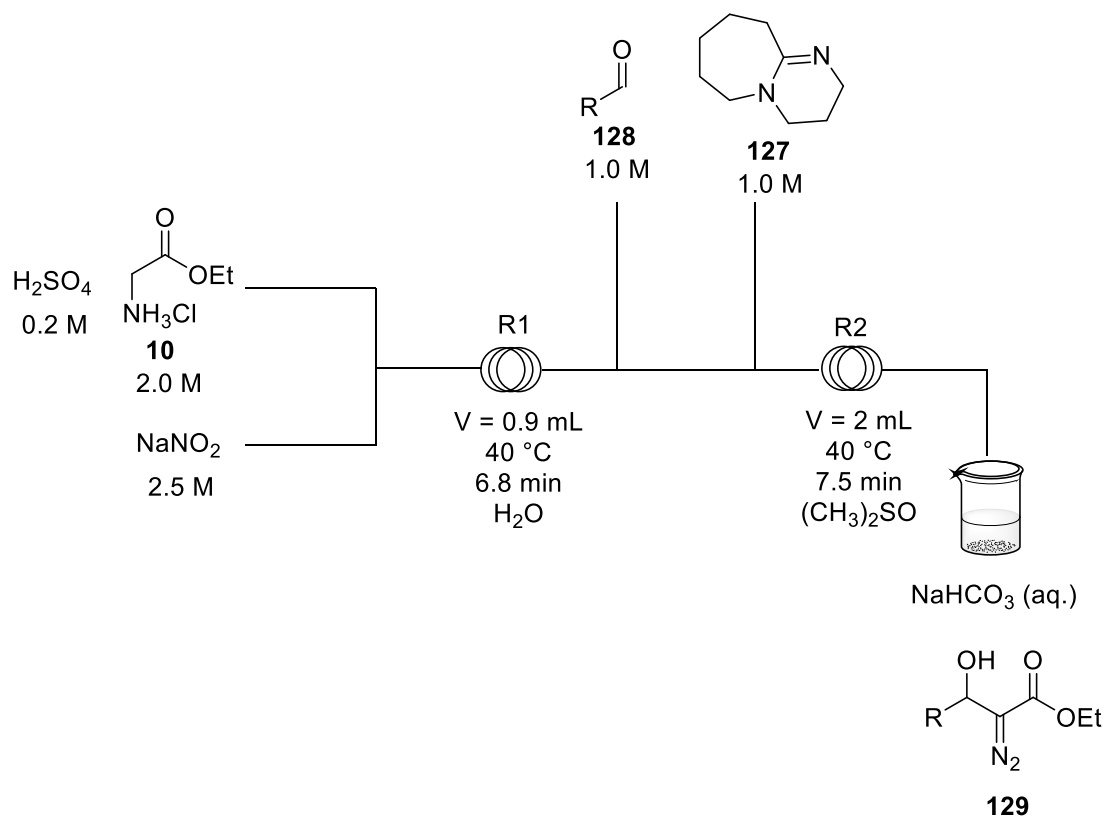
Table 3.3: Optimisation studies in continuous flow on two-step process to β -hydroxy- α -diazoester **106**

Entry	t _{res} [min] R1	t _{res} [min] R2	T [°C] R2	Glycine ethyl ester/DBU (equiv.)	Conversion [%] ^a
1	0.5	0.2	60	1:1.7	28
2	0.5	0.2	60	3:1	69
3	1.3	0.7	60	1:1.7	45
4	2.3	1.1	60	1:1.7	43
5	2.3	1.1	75	1:1.7	40
6	6.8	3.4	22	1:2.3	74
7	6.8	3.4	40	2:2.3	83
8	6.8	3.4	40	1.5:2	73
9	6.8	3.4	40	1.7:0.7	57
10	6.8	3.4	40	1.7:1	75

11	6.8	3.4	40	2:1	80
12	6.8	3.4	40	1.5:1	76
13	4.5	2.3	40	2:1	56
14	6.8	7.5	40	2:1	96

^a determined by ¹H NMR comparing peak of benzaldehyde to product peak

Having developed the two-step protocol, the substrate scope was examined. The set-up for the screening of the substrate scope is depicted in Scheme 32. The relatively high concentrations of reagents were desirable from an industrial point of view as they gave access to a high space-time yield. The reaction was stabilised for 28 minutes which equals 2 reactor volumes and then the reaction was performed for 20-30 minutes collection time.

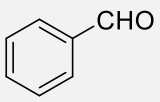
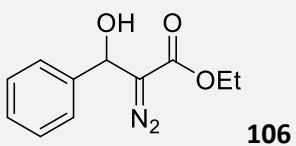
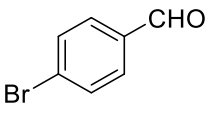
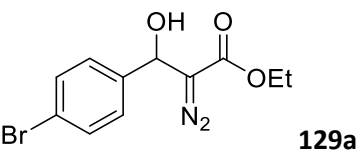
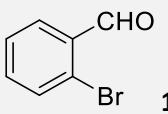
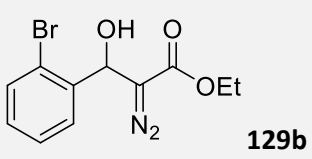
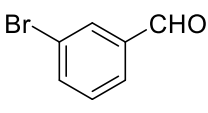
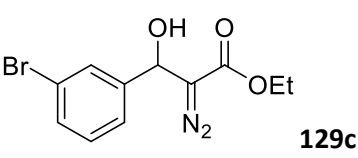
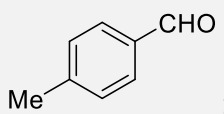
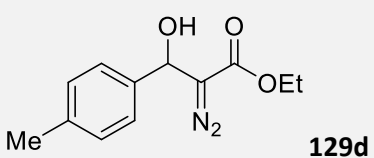
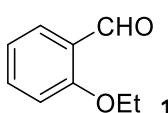
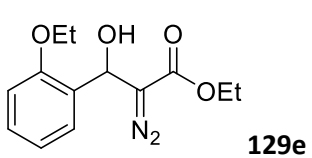
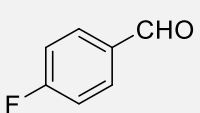
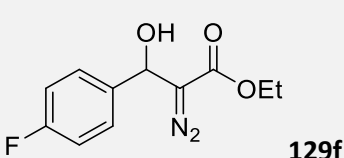
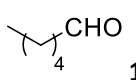
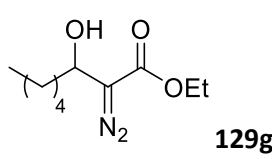


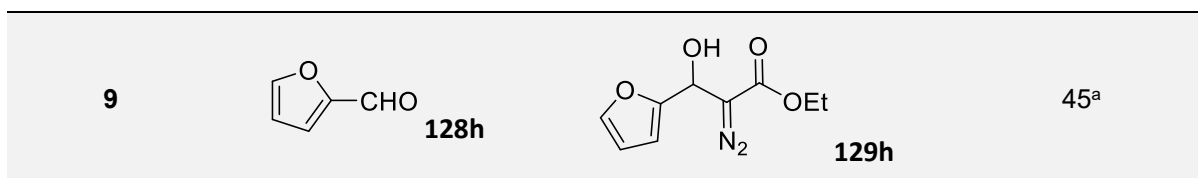
Scheme 32: Set-up used for the substrate scope for the two-step process

The scope of substrates accessed *via* this protocol is shown in Table 3.4. The substitution on the aromatic ring seems to have only a minor impact on the yield (Table 3.4, entries 1-7). Aromatic substrates worked well, giving good to excellent yields (74-96%), providing access to electron-rich aromatic β -hydroxy- α -diazoester (Table 3.4, entries 5-6) as well as electron-poor substrates (Table 3.4, entry 7). An electron-rich heteroaromatic system such as furyl aldehyde worked less well than the other substrates, however still giving an acceptable 45% yield (Table 3.4, entry 9). Aliphatic hexanal was also usable *via* this two-step continuous flow

protocol, giving 66% (Table 3.4, entry 8). Overall the new continuous flow methodology proved applicable to a broad range of aldehyde substrates.

Table 3.4: Substrate scope of two-step aldol addition protocol

Entry	Aldehyde	Product	Yield [%]
1	 105	 106	82
2	 128a	 129a	74 ^a
3	 128b	 129b	96
4	 128c	 129c	82
5	 128d	 129d	77
6	 128e	 129e	85
7	 128f	 129f	82 ^a
8	 128g	 129g	66 ^a



^a Reaction conditions Table 3.3, entry 11 were used

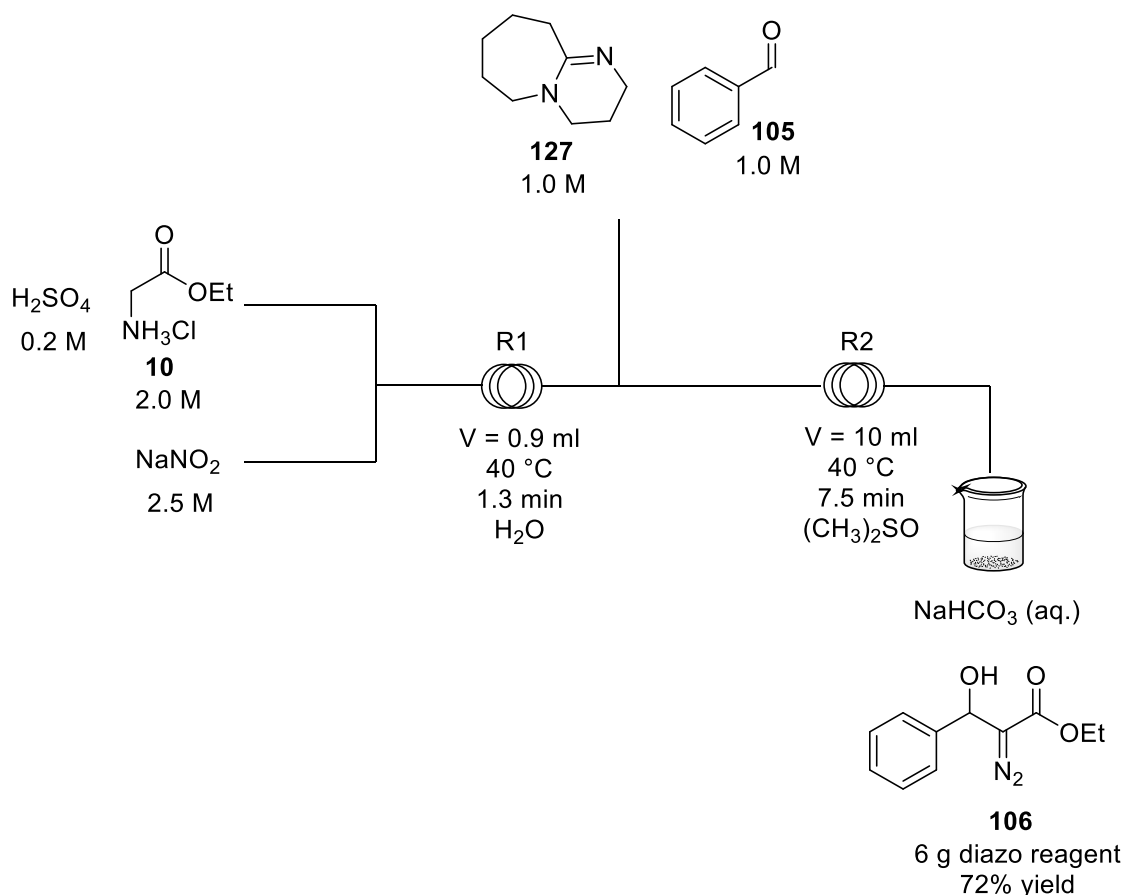
3.2.3.1 Upscale

The reactions mentioned above all gave β -hydroxy- α -diazoesters in quantities of around 100-400 mg. To test the scalability of the system, a large scale approach (multigram quantities) was designed. Continuous pumping was achieved using the Vapourtec® E-Series (Figure 10). In contrast to a syringe pump, the Vapourtec® system uses peristaltic pumps to pump continuously. The common problem of peristaltic pumps, the sinusoidal intervals with which the reagents are pumped through the system, is circumvented by the use of a non-linear rotor system leading to a steady and reliable flow of reagents.¹⁸



Figure 10: Vapourtec® E-Series

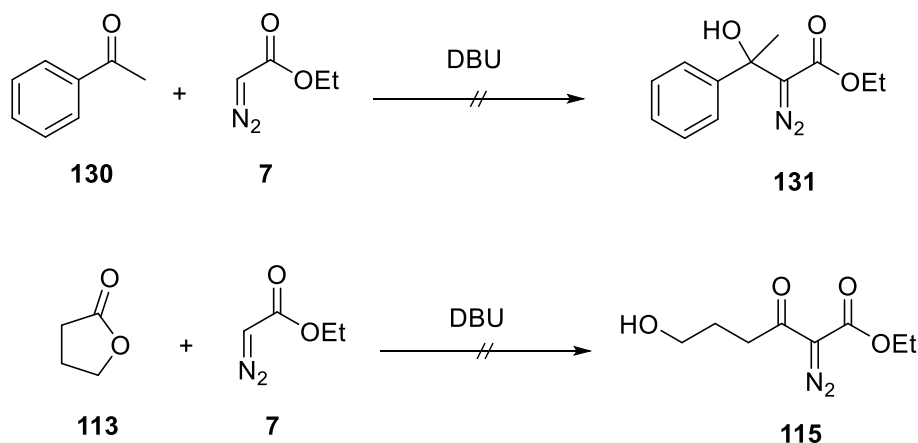
The flow rates and reactor sizes had to be altered to efficiently generate the required quantities of diazo reagent (Scheme 33). In the first reactor, ethyl diazoacetate **7** was generated in 1.3 minutes at 40 °C. In contrast to the small scale approach, DBU **127** and benzaldehyde **105** were added from the same pump as the Vapourtec® E-Series has three pumps in total. The reaction time of the second reactor was not altered, remaining at 7.5 minutes. With this approach, 6 g (27 mmol) of ethyl 2-diazo-3-hydroxy-3-phenylpropanoate **106** was synthesised in less than two hours (115 minutes, 72%).



Scheme 33: Scale-up reaction for two-step protocol

3.2.3.2 Limitations of the two-step continuous flow method

The newly designed two-step continuous protocol worked well with a variety of aldehydes (Table 3.4, entries 1-9). However, the method also proved to be restricted to aldehydes as carbonyl electrophiles. The reactions of ethyl diazoacetate **7** with acetophenone **130** or γ -butyrolactone **113** (Scheme 34) did not provide any product and the starting materials were recovered completely after work-up. Acetophenone **130** and γ -butyrolactone **113** are both less reactive electrophiles than aldehydes **128a-128h** and therefore not reactive enough for the rapid nucleophilic attack of ethyl diazoacetate **7**. In this case, the generation of ethyl lithiodiazoacetate **114** would be needed for a quick product formation. This approach will be discussed in Section 3.3.

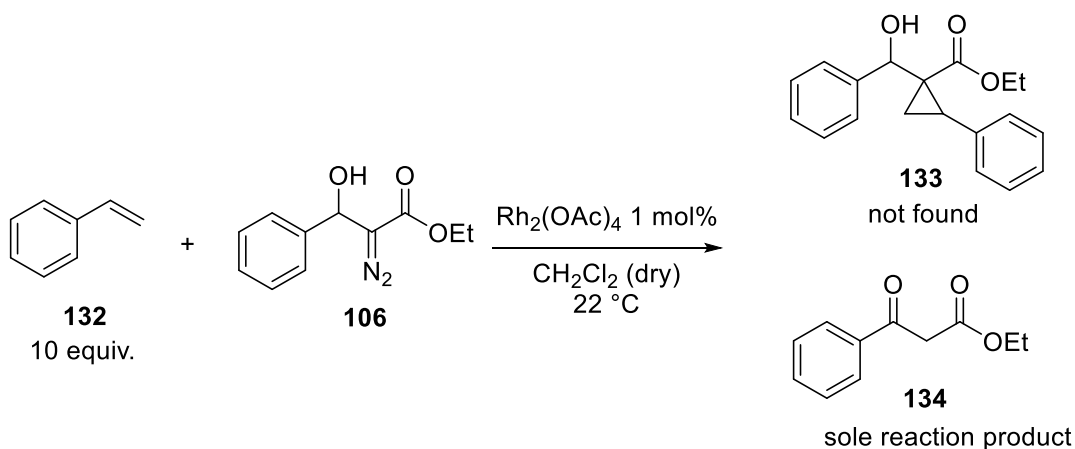


Scheme 34: Unsuccessful reaction of EDA **7** with acetophenone **130** and γ -butyrolactone **113**

Another disadvantage of the developed method is the need to isolate the β -hydroxy- α -diazoester **106** after the continuous flow synthesis. For safety reasons it would thus be preferential to add a third step to the continuous flow system in which the diazo functionality is consumed in one of the diverse reactions of β -hydroxy- α -diazoesters. Selection and evaluation of a third step as well as the implementation into a three-step continuous flow method is discussed in the next section.

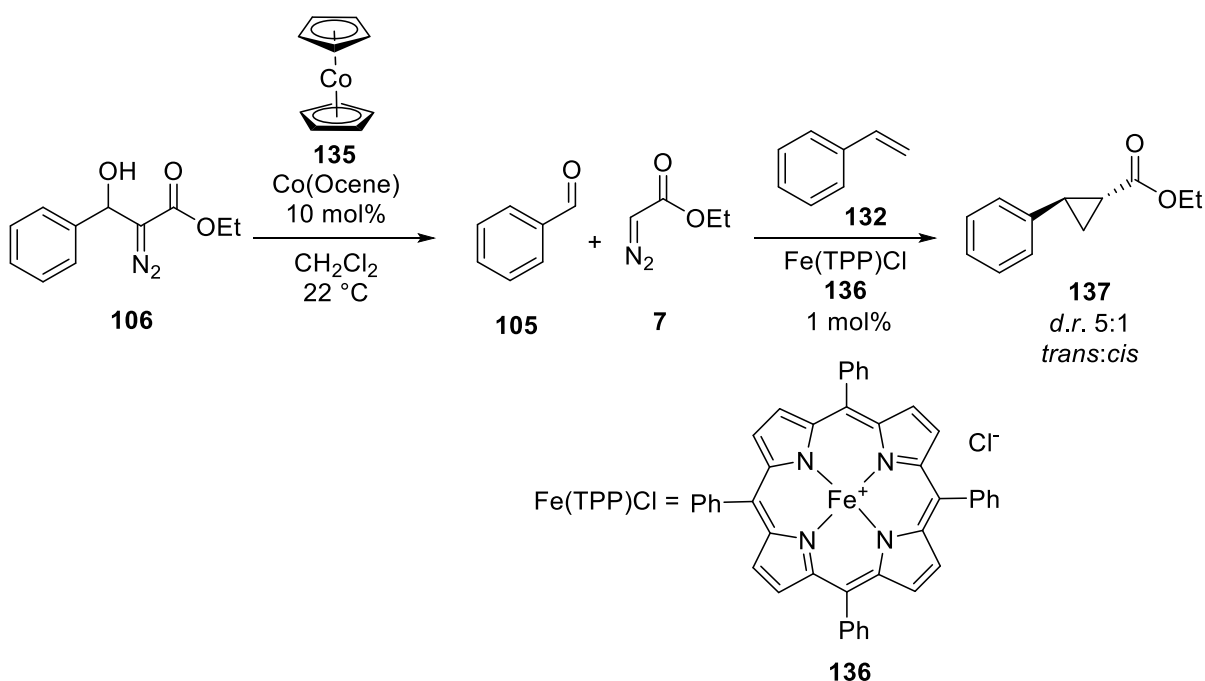
3.2.4 Three-step approach

The cyclopropanation of β -hydroxy- α -diazoester **106** with styrene **132** was investigated first. Ethyl diazoacetate **7** has been frequently used in cyclopropanation reactions.¹⁹ In contrast, no reports on the cyclopropanation of alcohol **106** were found. The reason for this became apparent when testing this reaction in dry dichloromethane under rhodium catalysis (Scheme 35). The intramolecular 1,2-hydride shift to generate β -ketoester **134** is a very rapid reaction that occurs preferentially even in the presence of a large excess of styrene **132**.



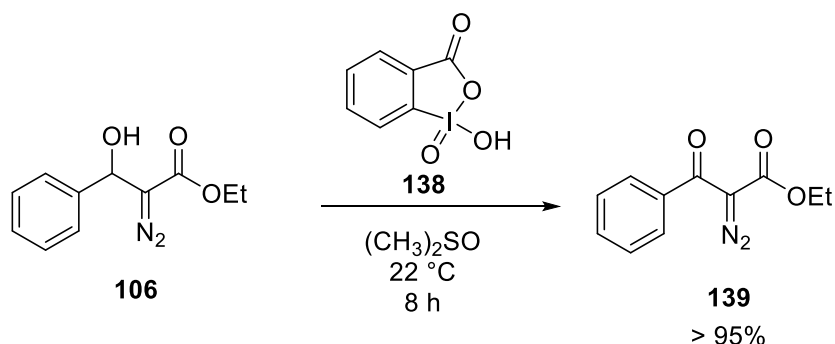
Scheme 35: Reaction of β -hydroxy- α -diazoester **106** in presence of large excess of styrene **132**

During the studies on the cyclopropanation of alcohol **106**, a surprising reaction product was discovered when a catalyst mixture of Co(Ocene) **135** and Fe(TPP)Cl **136** was utilised. In this case, characteristic ^1H NMR shifts of a cyclopropane moiety were observed after the work-up. However, the cyclopropane isolated did not correspond to the β -hydroxy system **106** but was the simple cyclopropane derived from ethyl diazoacetate **7** in reaction with styrene **132**. As further investigations showed, cobalt ocene **135** induced a retro-aldol reaction on β -hydroxy- α -diazoester **106** which led to the formation ethyl diazoacetate **7** and benzaldehyde **105**. In presence of catalytic Fe(TPP)Cl **136** and styrene **132**, ethyl diazoacetate **7** underwent then cyclopropanation of the styrene double bond (Scheme 36, *d.r.* 5:1 *trans:cis*). The diastereomeric ratio for this cyclopropanation is slightly lower than that described by Woo *et al.* (8.8:1 *trans:cis*).²⁰ Further investigations would be needed to find out how to put the retro-aldol reaction of β -hydroxy- α -diazoester **106** into synthetic use.



Scheme 36: Retro aldol reaction of β -hydroxy- α -diazoester **106** with subsequent cyclopropanation

The oxidation of the alcohol functionality of **106** whilst retaining the diazo group was another reaction investigated. β -Hydroxy- α -diazoester **106** can be oxidised using hypervalent iodine reagent IBX **138** (Scheme 37).²¹ This reaction proceeds in excellent yield (> 95%) in around eight hours.

Scheme 37: Oxidation of β -hydroxy- α -diazoester **106**

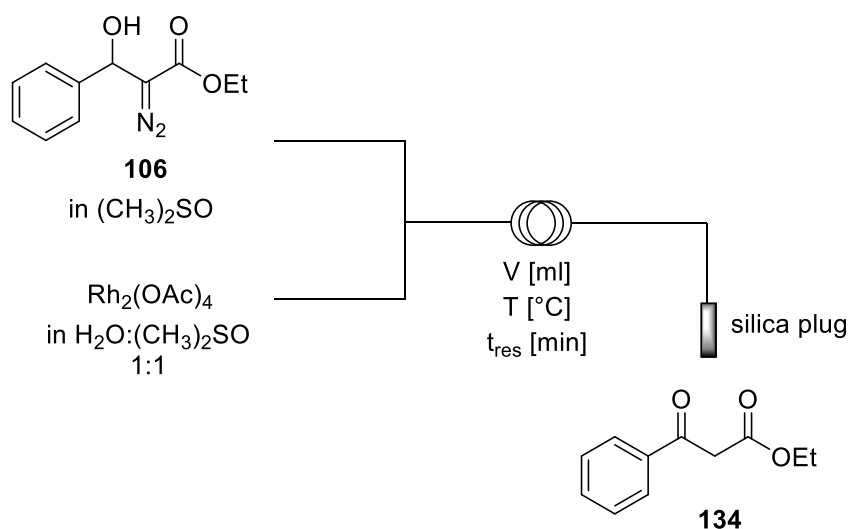
The reaction was next studied under continuous flow conditions (Table 3.5). Elevated temperatures led to a good ^1H NMR conversion in just 5.3 minutes residence time (Table 3.5, entry 2). As this reaction would however retain the diazo functionality and reagent **139** is also easily accessible *via* diazo transfer reaction, diazo decomposition reactions were next investigated in flow.

Table 3.5: Continuous flow reaction of IBX mediated oxidation of β -hydroxy- α -diazoester **106**

Entry	t_{res} [min]	T [$^\circ\text{C}$]	Conversion [%] ^a
1	5.3	22	20
2	5.3	60	85

^a conversion determined by ^1H NMR comparing peaks of starting material and product

The formation of β -ketoester **134** had dominated the previously desired cyclopropanation (Scheme 35) and was a very fast reaction under rhodium catalysis. Consequently, it was an excellent candidate for a three-step continuous flow protocol of ethyl diazoacetate **7** formation, aldol addition to β -hydroxy- α -diazoester **106** and then 1,2 hydride shift to give β -ketoester **134**. To develop such a system, first the decomposition of alcohol **106** to β -ketoester **134** was performed in flow (Scheme 38).

Scheme 38: Formation of β -ketoester **134** in flow

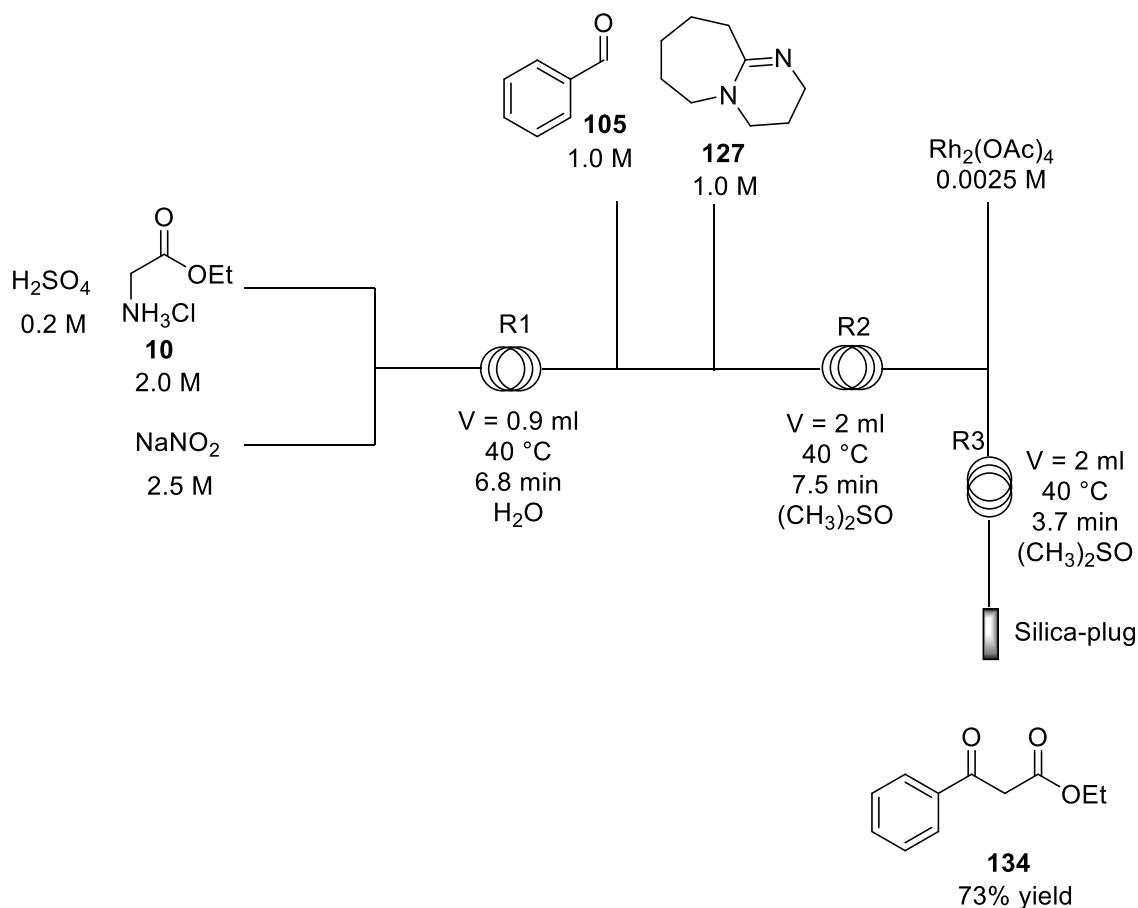
Conversions were good in short reaction times (Table 3.6, entries 1-3), although doubling the residence time led to a slight improvement in conversion (Table 3.6, entry 3). A reaction temperature of 40 °C turned out to be a better operating temperature than 60 °C (Table 3.6, entries 1-2).

Table 3.6: Continuous flow optimisation of 1,2 hydride shift

Entry	t _{res} [min]	T [°C]	Conversion[%] ^a
1	7.5	40	84
2	7.5	60	79
3	15	40	88

^a conversion determined by ¹H NMR comparing peaks of starting material and product

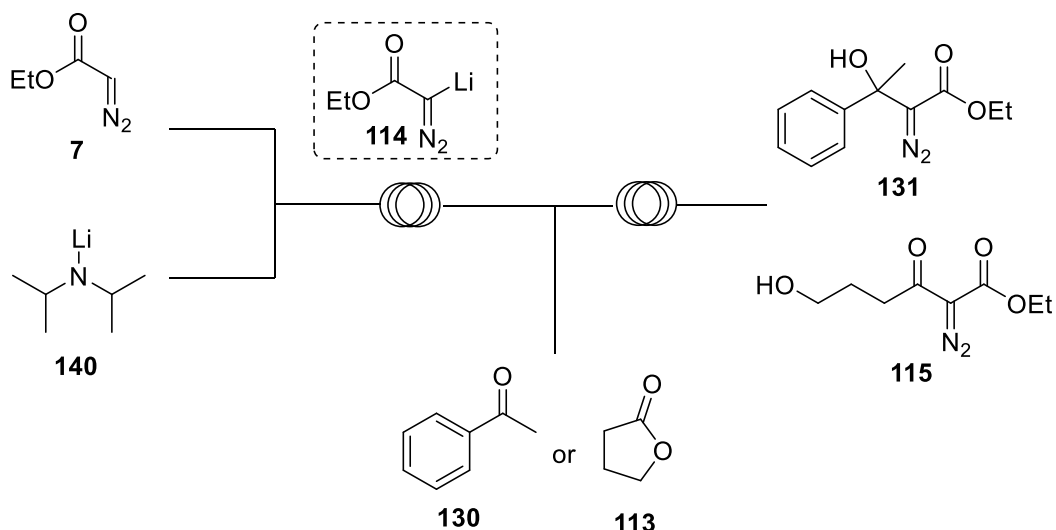
With these results in hand, a three-step continuous flow process was established (Scheme 39). Three reactors were coupled one after another with no need for in-line extraction. The overall yield over three steps was good (73%). However, it should be noted that the work-up under these reaction conditions is tedious as the β -ketoester **134** and the corresponding enol tautomer partly dissolve in the DMSO / water mixture which is the aqueous phase in a dichloromethane work-up. Regardless, the three step protocol provides a powerful method of handling diazo reagents in a safe fashion.



Scheme 39: Three-step continuous flow protocol

3.3 Lithiation of ethyl diazoacetate in flow chemistry

As mentioned in section 3.2.3.2, the DBU-mediated two-step protocol of an aldol addition of ethyl diazoacetate to a carbonyl electrophile was limited to aldehydes as electrophiles. To expand the scope of electrophiles accessible to continuous flow addition of ethyl diazoacetate, a system with the *in situ* generation of the highly nucleophilic ethyl lithiodiazoacetate **114** was sought. This species could then be trapped using electrophiles less reactive than aldehydes such as acetophenone **130** or γ -butyrolactone **113** (Scheme 40).

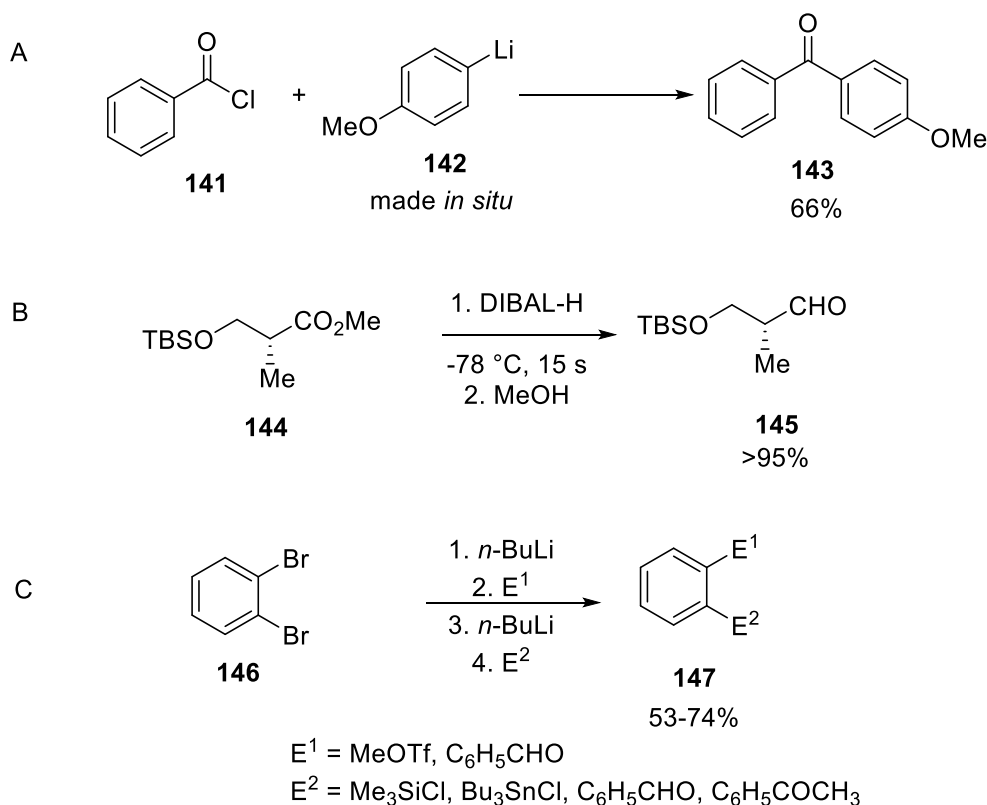


Scheme 40: In-situ formation of ethyl lithiodiazoacetate **114**

Before discussing the results obtained in this project, a short introduction into the use of organometallics and lithiated reagents in continuous flow is given.

3.3.1 Introduction into organometallics in flow

Two main features of flow chemistry in microreactors makes them the ideal platform for the use of organometallics. Firstly, continuous flow chemistry reduces the potential risks of hazardous reagents due to the excellent heat transfer (see Section 1.4.1). Secondly, mixing can be precisely controlled and rapid reactions can be performed selectively. For example, the addition of lithiated aromatics **142** to acyl chloride **141** was achieved selectively without the batch-problems of over-addition onto the resulting ketone **143** (Scheme 41, A).²² DIBAL-H reduction of ester **144** to aldehyde **145** was achieved in a very short reaction time (15 s) without the formation of the corresponding alcohol (Scheme 41, B).²³ *o*-Dibromobenzene **146** was functionalised with two different electrophiles selectively in a cascade of lithium-halogen exchange – electrophilic trapping – lithium halogen exchange – electrophilic trapping without the formation of benzyne which had occurred in the batch experiment (Scheme 41, C).²⁴



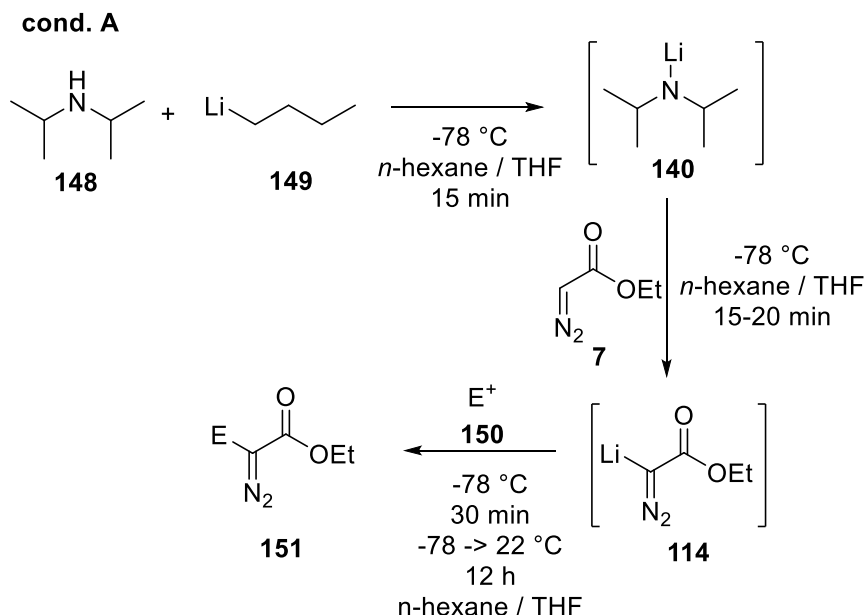
Scheme 41: Use of organometallics in flow chemistry; addition of lithium arene **142** to acyl chloride **141** (A); DIBAL-H reduction of ester **144** to aldehyde **145** (B); Cascade of lithium-halogen exchange and electrophilic trapping (C)

There are, however, also challenges in using organometallics in continuous flow systems. One of these problems stems from the high moisture sensitivity of most organometallic reagents. *n*-Butyllithium, for example, reacts readily with residual water to form LiOH, insoluble in the organic solvents used to handle *n*-BuLi. This can therefore clog the reactor. Furthermore, the aggressive nature of many organometallics poses a great challenges to the equipment used in the flow reactions, e.g. the pumps and tubes used. In a recent report, Ley and coworkers described in detail a very efficient method to handle *n*-BuLi and other organometallics in continuous flow using the Vapourtec® E-Series.¹⁸ The pumps are resistant to the aggressive *n*-BuLi solutions and an efficient drying procedure for handling moisture sensitive reagents was described. Hence, this method was considered a good potential platform for the lithiation of ethyl diazoacetate **7**.

3.3.2 Reactions of ethyl lithiodiazoacetate in batch

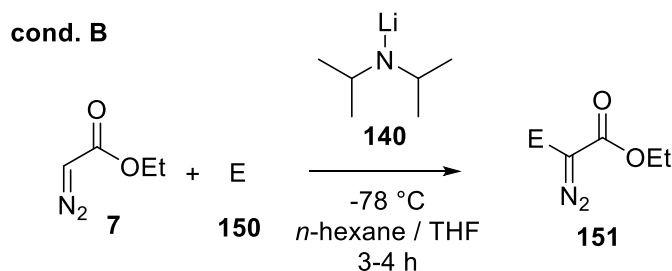
The reaction of ethyl lithiodiazoacetate with ketones and lactones has been known in synthetic chemistry for around thirty years.²⁵ To get used to this chemistry, two different protocols were employed for the electrophilic trapping of ethyl lithiodiazoacetate **114** in batch. Esters, lactones and ketones were investigated as electrophiles. In the first set of conditions (**cond. A**; Scheme

42), ethyl diazoacetate **7** was added to a solution of diisopropylamine **148** and *n*-butyllithium **149** at $-78\text{ }^{\circ}\text{C}$. The reaction mixture was then kept at $-78\text{ }^{\circ}\text{C}$ for 15-20 min. Subsequently, the corresponding electrophile was added to the reaction mixture and stirred at $-78\text{ }^{\circ}\text{C}$ for 30 minutes before the mixture was warmed up slowly to room temperature.



Scheme 42: Order of addition for conditions A

For the second set of conditions, ethyl diazoacetate **7** and the electrophile **150** were pre-mixed at $-78\text{ }^{\circ}\text{C}$. Then, a solution of freshly prepared lithium diisopropylamide **140** was added slowly to this mixture and the reaction was left stirring at $-78\text{ }^{\circ}\text{C}$ for 3-4 hours (Scheme 43).

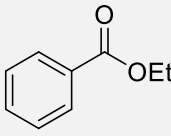
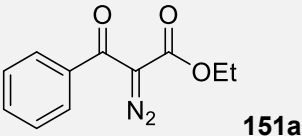
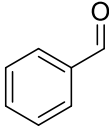
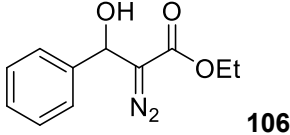
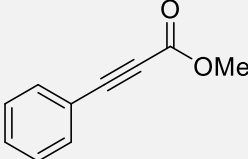
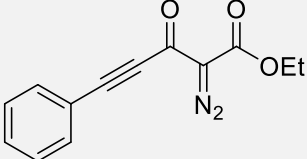
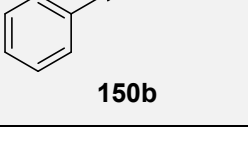
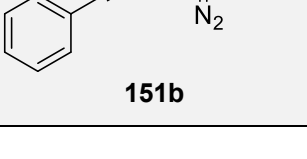


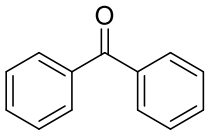
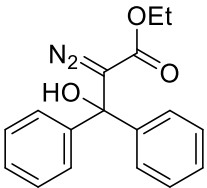
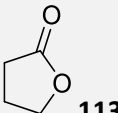
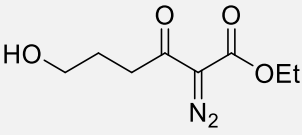
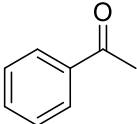
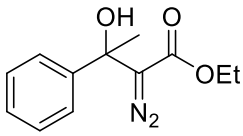
Scheme 43: Reaction conditions B

Reaction conditions A were unsuccessful for the reaction of ethyl lithiodiazoacetate **114** with ethyl benzoate **150a** (Table 3.7, entry 1), benzophenone **150c** (Table 3.7, entry 5) and γ -butyrolactone **113** (Table 3.7, entry 6). In two cases, the reaction provided no reaction product and the starting material was recovered (Table 3.7, entries 1 and 5). For γ -butyrolactone a complex mixture of products was obtained containing only traces of the desired product (Table 3.7, entry 6). Reaction conditions A, however, were relatively successful for the ethyl lithiodiazoacetate **114** addition to benzaldehyde **105** (Table 3.7,

entry 2) and to phenyl propiolic ester **150b** (Table 3.7, entry 3). Unfortunately, the isolation of diazo reagent **151b** was not successful as product and starting material could not be separated *via* column chromatography. Conditions A provided overall relatively poor results. Whilst little is known on ethyl lithiodiazoacetate **114** additions to esters, the γ -butyrolactone **113** ring-opening reaction has been used repeatedly. Therefore, conditions B were applied onto this reaction to investigate if the presence of the electrophile at the time of the formation of ethyl lithiodiazoacetate **114** was beneficial. Conditions B led to a good conversion of lactone **113** to diazo alcohol **115** (66% ^1H NMR conversion), albeit with a low yield due to issues in the purification (Table 3.7, entry 7). These conditions also promoted the addition of ethyl lithiodiazoacetate **114** to acetophenone **130** (Table 3.7, entry 8) and phenyl propiolic ester **150b** (Table 3.7, entry 4). For the ring opening of lactone **113**, conditions B were superior to conditions A, possibly due to the instability of the *in situ*-formed ethyl lithiodiazoacetate **114** (stable only $< -55\text{ }^\circ\text{C}$)^{3a} or due to the longer stirring time at $-78\text{ }^\circ\text{C}$ (compare Table 3.7, entries 6 and 7). However, in both sets of conditions the yields were lower than expected and repeated experiments on substrates **113** and **130** showed that the reactions were not very reliable. Small alterations in the reaction procedure had a strong impact on the yield of the transformation. Continuous flow chemistry should be able to lead to a higher yielding and much more reliable process for the addition of ethyl lithiodiazoacetate **114** to diverse electrophiles.

Table 3.7: Batch experiments for trapping of ethyl lithiodiazoacetate **114**

Entry	Electrophile	Product	Conditions	Conversion [%] ^a
1	 150a	 151a	A	0
2	 105	 106	A	91
3	 150b	 151b	A	62
4	 150b	 151b	B	50

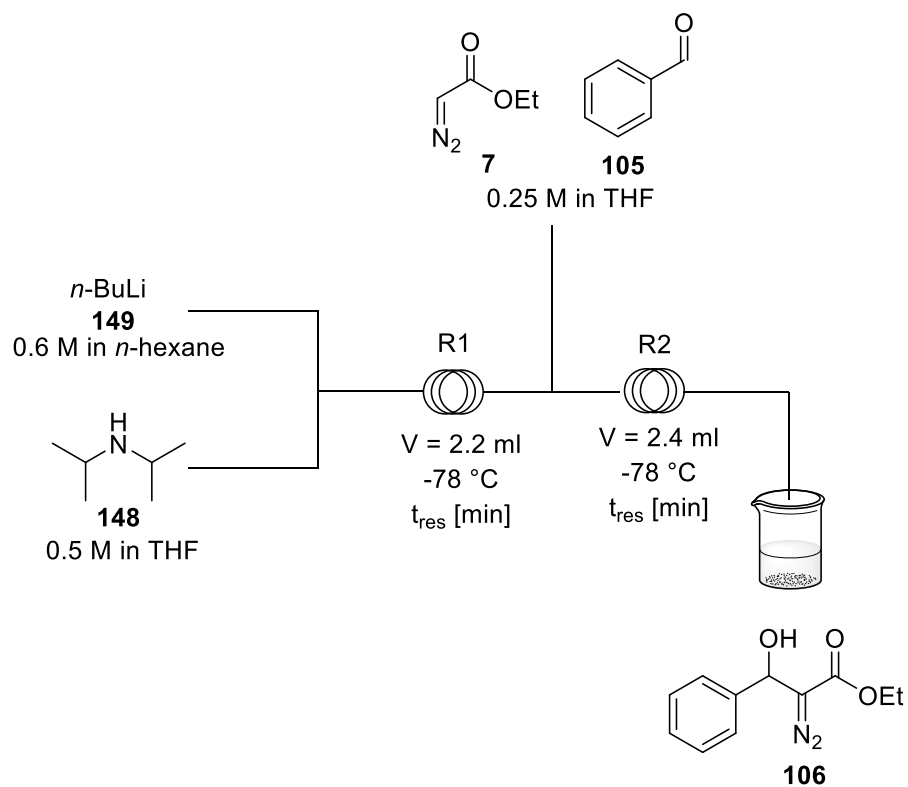
5			A	0
6			A	Complex product mixture; traces of 115
7			B	66 (21% yield)
8			B	54 (41% yield)

^a conversion determined by ¹H NMR comparing peaks of starting material and product

3.3.3 Lithiation of ethyl diazoacetate in flow

For the development of a continuous flow protocol for the formation and use of ethyl lithiodiazoacetate **114** two main challenges had to be overcome. First, clogging of the tubes due to moisture in the presence of *n*-BuLi had to be circumvented. Second, the unstable ethyl lithiodiazoacetate **114** had to be trapped effectively. Unfortunately, the decomposition of ethyl lithiodiazoacetate **114** at any temperature above $-55\text{ }^{\circ}\text{C}$ led to the instantaneous formation of a brownish gel completely insoluble in organic solvents that clogged the microreactor immediately.

The first flow experiment was performed on the ethyl lithiodiazoacetate **114** addition to benzaldehyde **105** as this had given the best result in the batch experiment (Table 3.7, entry 2). The drying protocol described by Ley *et al.*²⁵ was applied to the Vapourtec® E-Series system. In this protocol, the flow system is first flushed with ⁱPrOH to wash out residual water and then the dried solvents used in the reaction (THF, *n*-hexane) are pumped into the systems under argon atmosphere. The set-up used for the ethyl lithiodiazoacetate **114** addition to benzaldehyde **105** consisted of two reactors (Scheme 44). In the first one, lithium diisopropylamide **140** was generated from *n*-BuLi **149** and diisopropylamine **148**. Then, a solution containing ethyl diazoacetate **7** and benzaldehyde **105** in THF was added to the LDA solution. For this set-up, a total of five flasks under argon atmosphere was needed to flush the lines with dry solvents and then have the dry reagent solutions ready for addition to the flow reactor (Figure 11).



Scheme 44: Lithiation of EDA **7** in flow and addition to benzaldehyde **105**

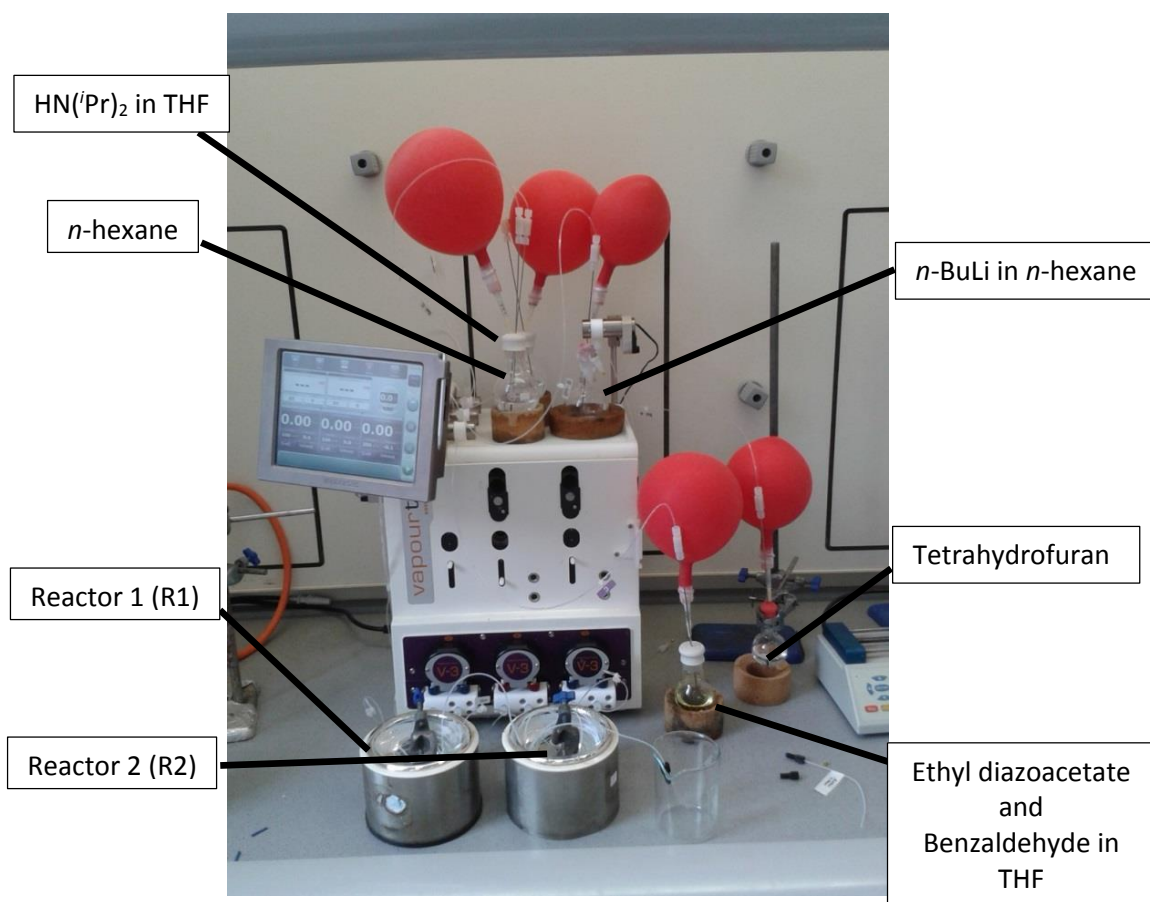


Figure 11: Continuous flow set-up for the use of ethyl lithiodiazoacetate **114**

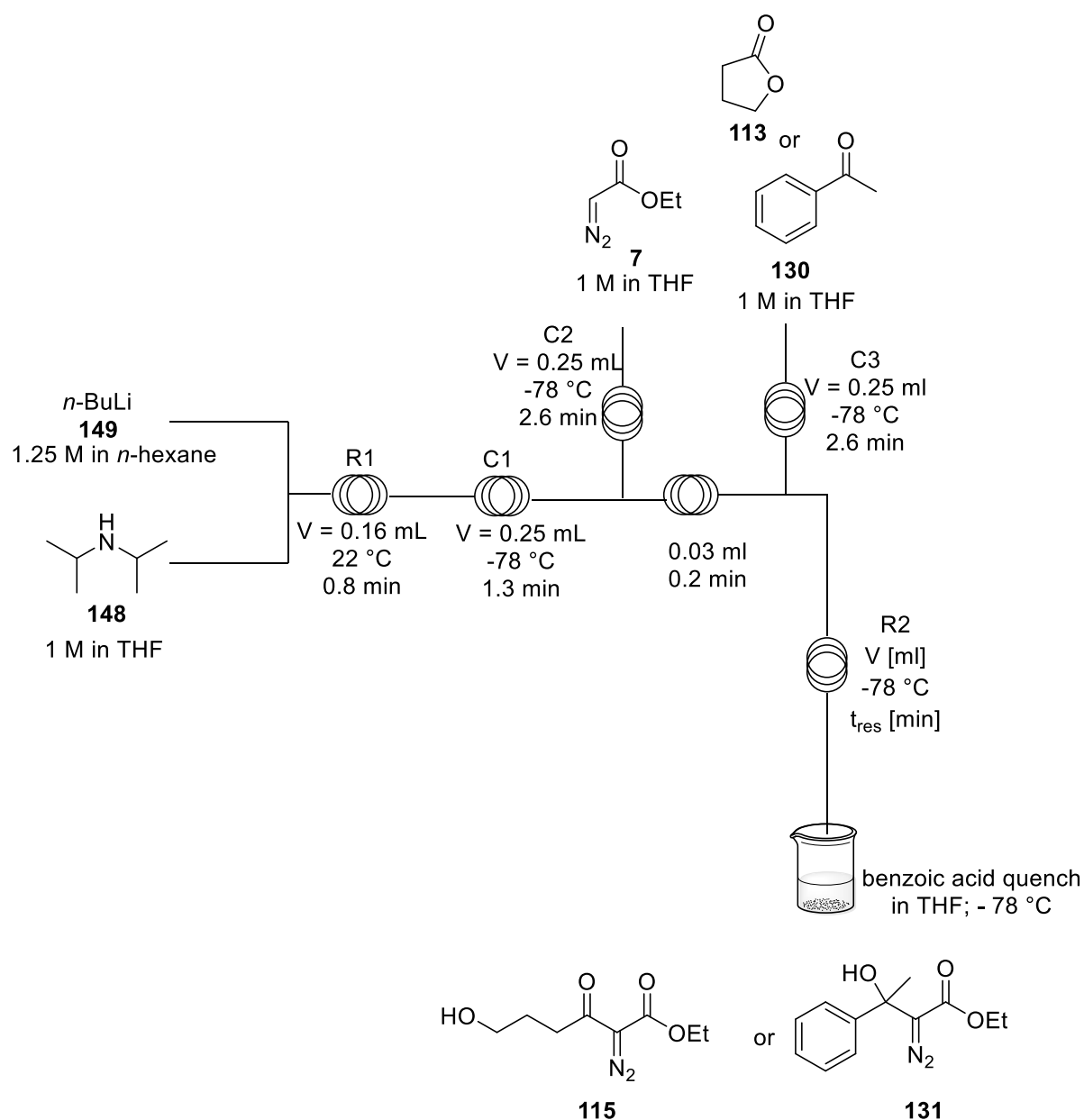
The results of this experiment are shown in Table 3.8. The reaction worked smoothly at $-78\text{ }^{\circ}\text{C}$ at all three residence times tested (Table 3.8, entries 1-3). Longer residence times worked slightly better than short residence times. However, even at just over one minute residence time in the second reactor, the conversion into the β -hydroxy- α -diazoester **106** worked smoothly (Table 3.8, entry 3).

Table 3.8: Continuous flow experiment of ethyl lithiodiazoacetate **114** addition onto benzaldehyde **105**

Entry	R1 t_{res} [min]	R2 t_{res} [min]	Conversion [%] ^a
1	11	6	87
2	4.4	2.4	85
3	2.2	1.2	79

^a conversion determined by ^1H NMR comparing peaks of starting material and product

After these first promising results, the set-up was next applied onto γ -butyrolactone **113** as electrophile. However, complex product mixtures were found and difficulties with the reaction set-up were encountered. Especially problematic was the decomposition reaction of ethyl lithiodiazoacetate **114** into the brownish gel as it occurred readily as soon as any parts of the tubings (e.g. the collection vial) were not kept strictly at $-78\text{ }^{\circ}\text{C}$. For these reasons, a different set-up was designed (Scheme 45). The changes installed included a much shorter reactor length for the formation of lithium diisopropylamide (LDA) which was now kept at room temperature. Furthermore, cooling coils were implemented into the system to cool down the reagent streams before reacting with each other. Finally, the collection vial was fixed into the cooling bath so that all parts of the equipment were kept at $-78\text{ }^{\circ}\text{C}$.



Scheme 45: Set-up used for the optimisation of the lithiation of ethyl diazoacetate **7**

The results of this reaction are shown in Table 3.9. At the beginning, γ -butyrolactone **113** was used as electrophile (Table 3.9, entries 1-2). A reaction time of 5.5 minutes for the second reactor was too short at -78°C providing only very small quantities of alcohol **115** (Table 3.9, entry 1). This is a noteworthy observation as many lithiation reactions take place in the realm of seconds and less. A longer residence time in the second reactor by increasing its length from 2.2 mL to 12.2 mL led to a great improvement in conversion (Table 3.9, entry 2). Next, acetophenone **130** was used as electrophile to see if the transformation of a ketone would work more easily. At the same conditions, 41% conversion into the product was observed (Table 3.9, entry 3). A great improvement in the conversion was achieved when 1.3 equivalents of ethyl diazoacetate **7** were employed (Table 3.9, entry 4). Using an excess

of base led to further improvements in yield (Table 3.9, entries 5-6). Interestingly, increasing the reaction temperature slightly to $-72\text{ }^{\circ}\text{C}$ led to a slight drop in conversion, presumably due to the instability of ethyl lithiodiazoacetate **114** (Table 3.9, entry 7). In all cases, the yield was significantly lower than the conversion of the reaction which was somewhat surprising as the crude ^1H NMR spectrum showed only starting material and product. However, separation of the acetophenone and the product proved to be difficult.

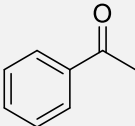
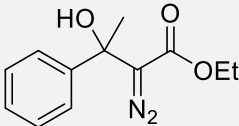
Table 3.9: Results of the optimisation of the lithiation of ethyl diazoacetate **7**

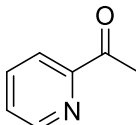
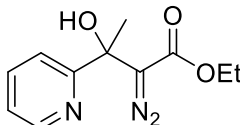
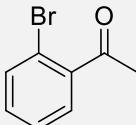
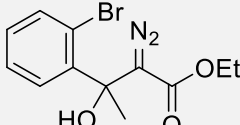
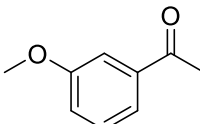
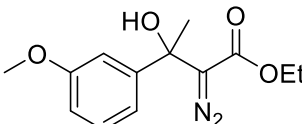
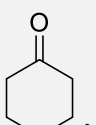
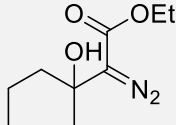
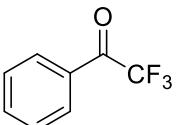
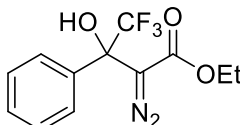
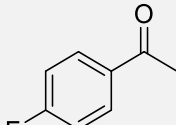
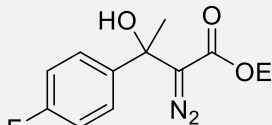
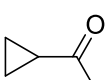
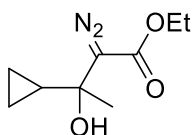
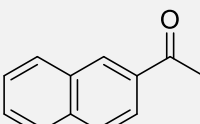
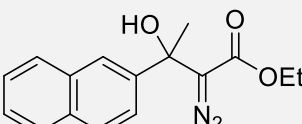
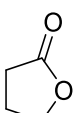
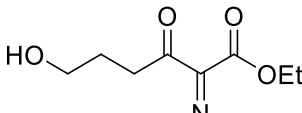
Entry	Electrophile	EDA 7 (equiv.)	LDA (equiv.)	R2 t_{res} [min]	T [$^{\circ}\text{C}$]	Conversion [%] ^a (Yield [%])
1	113	0.9	1	5.5	-78	3
2	113	0.9	1	31	-78	31
3	130	0.9	1	31	-78	46 (28)
4	130	1.3	1	31	-78	71 (58)
5	130	1.3	1.25	31	-78	80 (62)
6	130	1.3	1.5	31	-78	84 (62)
7	130	1.3	1.5	31	-72	79

^a conversion determined by ^1H NMR comparing peaks of starting material and product

As efficient reaction conditions for the generation of ethyl lithiodiazoacetate **114** and the subsequent reaction with acetophenone **130** had been found (Table 3.9, entry 6), the substrate scope was investigated. Overall yields were moderate to good, with aromatic and aliphatic ketones giving similar yields. Pyridine substituted ketone **152a** worked slightly less well than acetophenone (Table 3.10, entry 2) whereas 2-bromoacetophenone **152b** was more reactive than acetophenone (Table 3.10, entry 3). Electron-rich 3-methoxyacetophenone was a sufficiently good electrophile to provide β -hydroxy- α -diazoester **153c** in good yield (Table 3.10, entry 4). The best yield was obtained for trifluoroacetophenone **152e** (Table 3.10, entry 6) as substrate. The ring-opening reaction of γ -butyrolactone **113** provided the corresponding diazo alcohol **115** in very low yield (Table 3.10, entry 10).

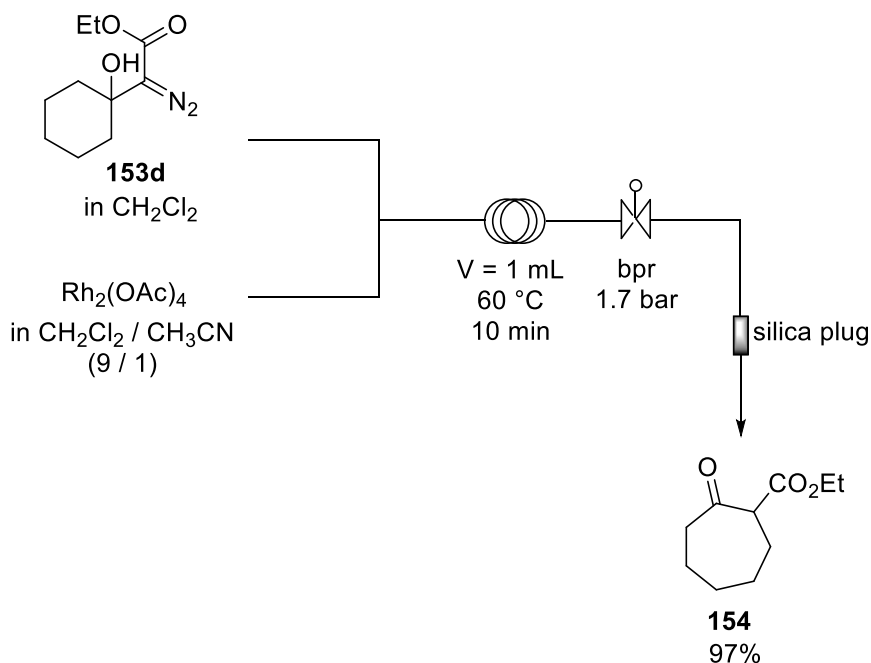
Table 3.10: Substrate scope for the lithiation reaction

Entry	Electrophile	Product	Yield [%]
1	 130	 131	62

2	 152a	 153a	53
3	 152b	 153b	70
4	 152c	 153c	66
5	 152d	 153d	65
6	 152e	 153e	71
7	 152f	 153f	60
8	 152g	 153g	48
9	 152h	 153h	40
10	 113	 115	12

The resulting β -hydroxy- α -diazoester products can undergo migration reaction similar to those discussed in section 3.2.4. However, in the cases of products **131**, **153a-153c**, **153e-153h**, there is a competition between the two possible migratory groups. This is not the case in the ring expansion of cyclohexanol product **153d**. It was therefore studied if the migration reaction

could be performed in a short flow system (Scheme 46). The ring expansion worked well (97%) in a short reaction time (10 min).



Scheme 46: Diazo decomposition of **153d**

3.4 Conclusion & Outlook

In this chapter, the formation of ethyl diazoacetate **7** and its use as nucleophilic species was investigated using continuous flow technologies. The work was divided into two segments. The first one was the *in situ* generation of ethyl diazoacetate **7** combined with the subsequent aldol addition with aldehydes using DBU as base. Yields were high in this flow set-up, the reaction proved scalable and a third step of diazo decomposition was added in flow. However, this continuous flow set-up was limited to aldehydes as electrophiles. To make ketones and lactones accessible to the addition of ethyl diazoacetate in flow, another approach was investigated. Using unstable but highly reactive ethyl lithiodiazoacetate **114**, multiple ketones were reacted. The reaction set-up required the careful control of temperature and moisture in the system, then however, diazo alcohols were obtained in moderate to good yields.

In the next chapter, focus will be laid on a different class of diazo compounds, aryl diazoacetates. These reagents are precursors of flexible donor / acceptor carbenes. Flow chemistry will be used to study their preparation with detailed kinetic studies, the purification of these reagents in flow systems as well as a diverse set of carbene reactions to produce valuable synthetic targets.

References

- 1 For reviews see: a) O. A. Kruglaya, N. S. Vyazankin, *Russ. Chem. Rev.* **1980**, 49, 357; b) Y. Zhang, J. Wang, *Chem. Commun.* **2009**, 5350.
- 2 a) H. Plieninger, D. vor der Brück, *Tetrahedron Lett.* **1968**, 4371; b) T. L. Burkoth, *Tetrahedron Lett.* **1969**, 5049.
- 3 a) U. Schöllkopf, H. Frasnelli, *Angew. Chem. Int. Ed.* **1970**, 9, 301; b) E. Wenkert, C. A. McPherson, *J. Am. Chem. Soc.* **1972**, 94, 8084.
- 4 T. L. Amyes, J. P. Richard, *J. Am. Chem. Soc.* **1996**, 118, 3129.
- 5 N. Jiang, Z. Qu, J. Wang, *Org. Lett.* **2001**, 3, 2989
- 6 N. F. Woolsey, M. H. Khalil, *J. Org. Chem.* **1972**, 37, 2405.
- 7 R. Varala, R. Enugala, S. Nuvula, S. R. Adapa, *Tetrahedron Lett.* **2006**, 47, 844.
- 8 N. Jiang, J. Wang, *Tetrahedron Lett.* **2002**, 43, 1285.
- 9 U. Schöllkopf, B. Bándhidai, H. Frasnelli, R. Meyer, H. Beckhaus, *Liebigs Ann. Chem.* **1974**, 1767.
- 10 C. J. Moody, R. J. Taylor, *Tetrahedron Lett.* **1987**, 28, 5351.
- 11 A. Arai, K. Hasegawa, A. Nishida, *Tetrahedron Lett.* **2004**, 45, 1023.
- 12 W. Yao, J. Wang, *Org. Lett.* **2003**, 5, 1527.
- 13 B. M. Trost, S. Malhotra, B. A. Fried, *J. Am. Chem. Soc.* **2009**, 131, 1674.
- 14 B. M. Trost, S. Malhotra, P. Koschker, P. Ellerbrock, *J. Am. Chem. Soc.* **2012**, 134, 2075.
- 15 The start of this project was autumn 2012
- 16 T. Toma, J. Shimokawa, T. Fukuyama, *Org. Lett.* **2007**, 9, 3195.
- 17 F. Xiao, Y. Liu, J. Wang, *Tetrahedron Lett.* **2007**, 48, 1147.
- 18 P. R. D. Murray, D. L. Browne, J. C. Pastre, C. Butters, D. Guthrie, S. V. Ley, *Org. Process Res. Dev.* **2013**, 17, 1192.
- 19 a) M. P. Doyle, R. L. Dorow, W. E. Buhro, J. H. Griffin, W. H. Tambllyn, M. L. Trudell, *Organometallics* **1984**, 3, 44; b) M. L. Rosenberg, A. Krivokapic, M. Tilset, *Org. Lett.* **2009**, 11, 547.
- 20 J. R. Wolf, C. G. Hamaker, J.-P. Djukic, T. Kodadek, L. K. Woo, *J. Am. Chem. Soc.* **1995**, 117, 9194.
- 21 M. O. Erhunmwunse, P. G. Steel, *J. Org. Chem.* **2008**, 73, 8675.
- 22 S.-Y. Moon, S.-H. Jung, U. B. Kim, W.-S. Kim, *RSC Adv.* **2015**, 5, 79385.
- 23 a) D. Webb, T. F. Jamison, *Org. Lett.* **2012**, 14, 568; b) D. Webb, T. F. Jamison, *Org. Lett.* **2012**, 14, 2465.
- 24 H. Usutani, Y. Tomida, A. Nagaki, H. Okamoo, T. Nokami, J.-i. Yoshida, *J. Am. Chem. Soc.* **2007**, 129, 3046.
- 25 K. Nagao, M. Chiba, S.-W. Kim, *Synthesis* **1983**, 197.

4 Donor / Acceptor Carbenes derived from Aryldiazoacetates

4.1 General Introduction

In chapter 3, the nucleophilic addition of ethyl diazoacetate **7** with aldehydes and ketones was discussed. In this chapter, focus is put on the generation and use of diazo arylacetates in flow. These are precursors to donor / acceptor carbenes which are highly selective reagents for organic synthesis (see section 1.3.2.1). Donor / acceptor carbenes give rise to more selective reactions than acceptor / acceptor or acceptor substituted carbenes. They are therefore commonly employed as reagents in total synthesis, often installing key stereocenters *en route* to the target molecule (Figure 12).¹ In particular, their ability to perform intermolecular C-H insertion reactions with very high stereoselectivity has made donor / acceptor substituted carbenes popular reagents in organic chemistry. Acceptor groups are typically ester, keto, nitro, cyano, phosphonyl and sulfonyl groups. Donor groups can be vinyl, aryl or heteroaryl functionalities.

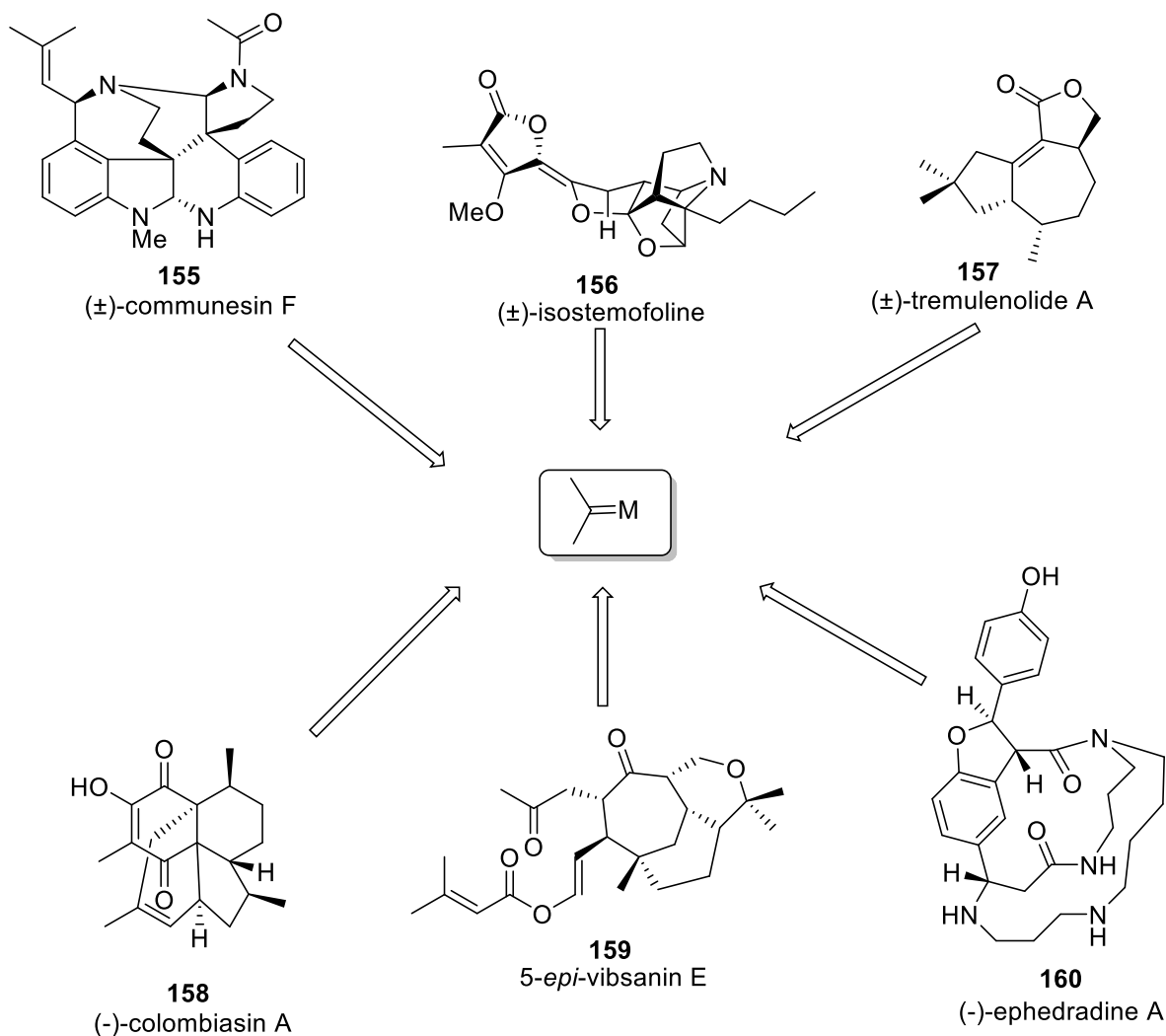
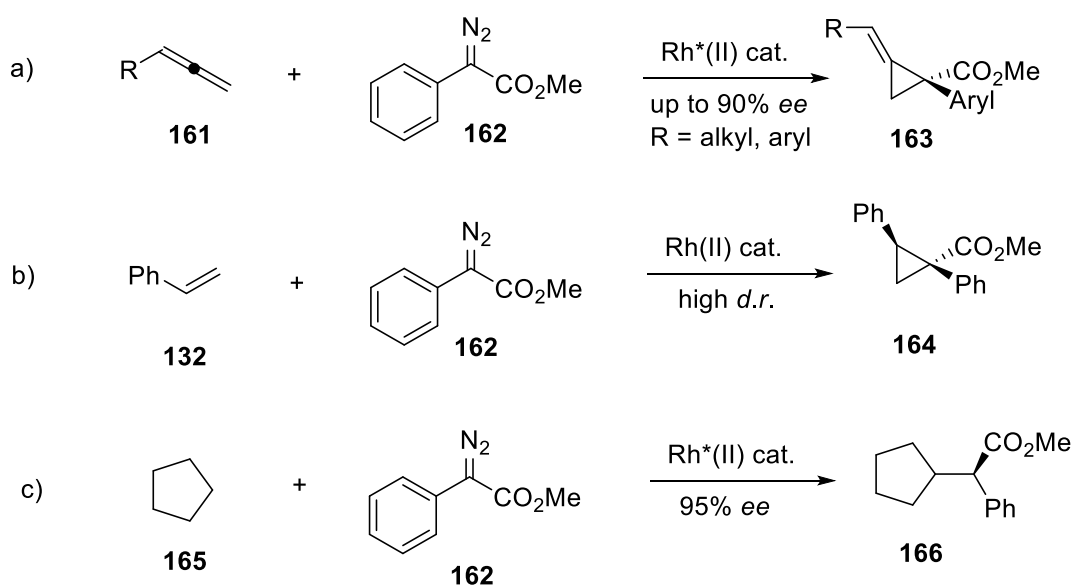


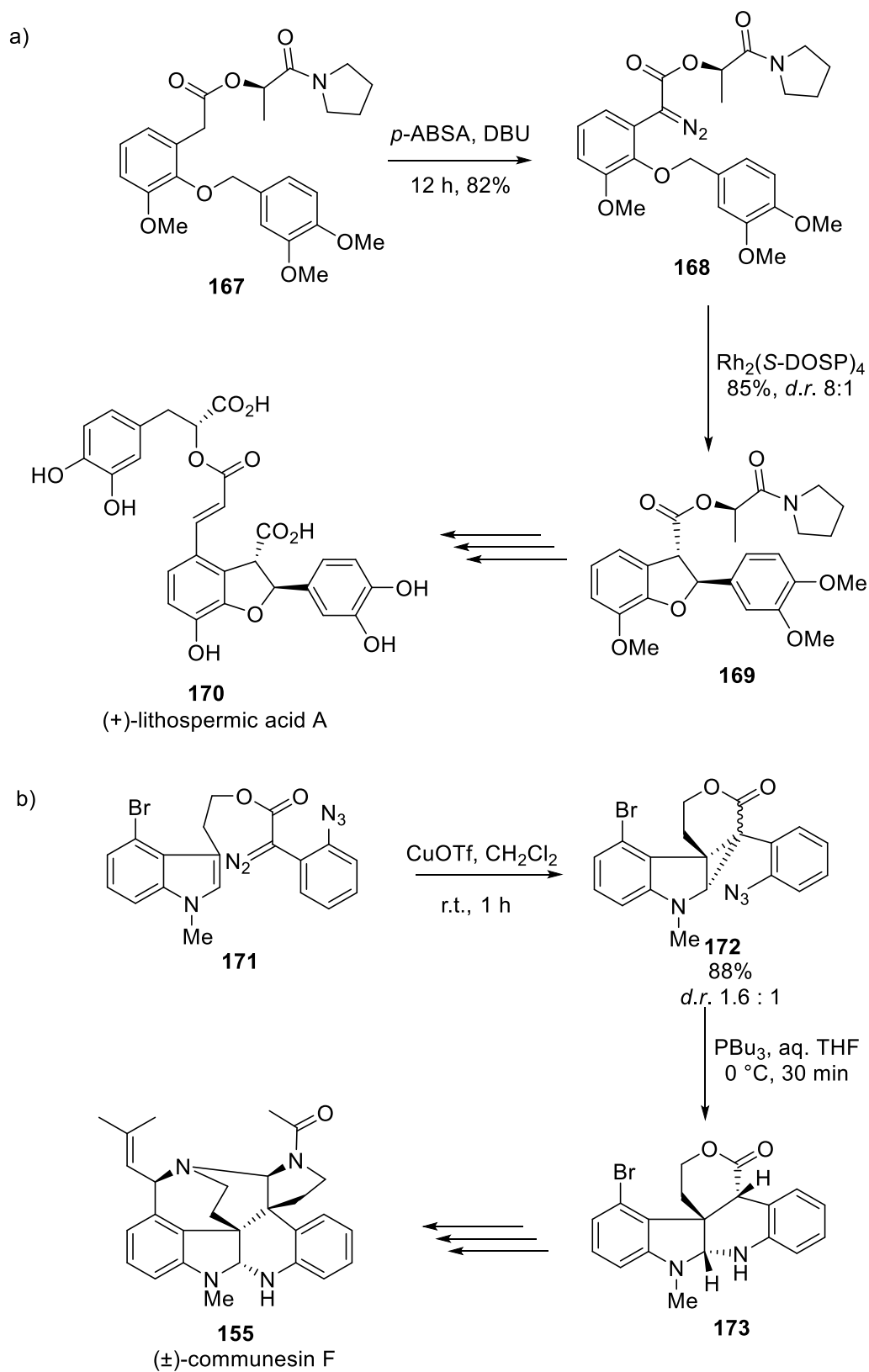
Figure 12: Synthetic targets made via donor / acceptor carbene chemistry¹

Diazo phenylacetates **162** are versatile and popular precursors for this donor / acceptor carbene reactivity. They can be used in the stereoselective formation of alkylidene cyclopropanes **163** (APCs) *via* allene cyclopropanation with up to 90% ee (Scheme 47, a).² Alkene cyclopropanation of diazo phenylacetates **162** is highly diastereoselective, a feat difficult to achieve with ethyl diazoacetate (Scheme 47, b).³ The increased selectivity of these reagents compared to acceptor / acceptor substituted diazo compounds gives access to highly regio- and enantioselective intermolecular C-H insertion reactions (Scheme 47, c) even with rather simple rhodium(II) proline catalysts such as $\text{Rh}_2(\text{DOSP})_4$ **62**.⁴



Scheme 47: Diverse reactivity of diazo phenylacetates: a) Enantioselective cyclopropanation of allenes; b) Diastereoselective cyclopropanation of alkenes; c) Enantioselective C-H insertion in unactivated C-H bonds

Considering the impressive reactivity and selectivity of diazo phenylacetates, it is no surprise that these reagents have been used in the total synthesis of natural products. Yu and Wang used a double C-H insertion and C-H activation strategy to rapidly assemble lithospermic acid A (Scheme 48, a).⁵ Qin *et al.* described an intramolecular cyclopropanation with an adjacent indole **171** in their total synthesis of (\pm)-communesin F with subsequent diastereoselective amine induced cyclopropane ring opening to **173** (Scheme 48, b).⁶

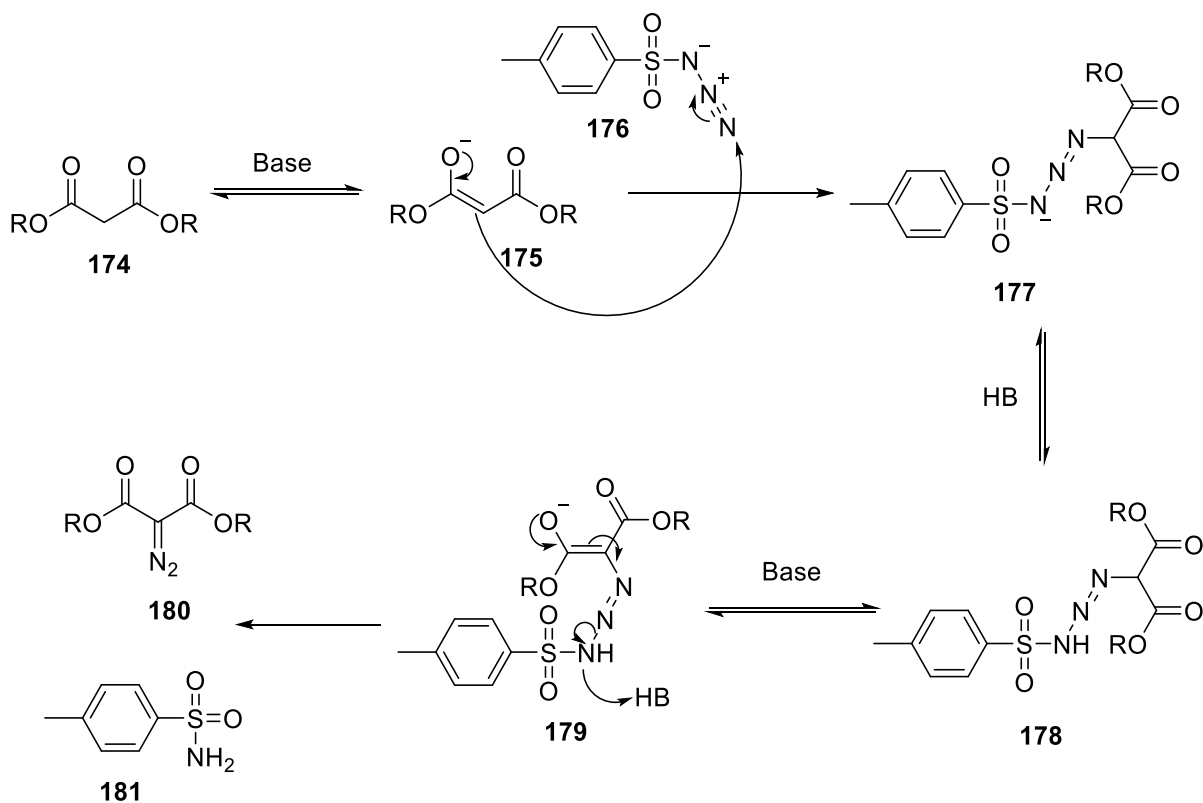


Scheme 48: a.) Total synthesis of (+)-lithospermic acid A via C-H insertion strategy; b.) Total synthesis of (±)-communesin F via cyclopropanation

Whilst the reactivity of donor / acceptor carbenes is well developed, much less attention has been given to the formation of the diazo species necessary for the subsequent carbene reactivity. Phenyl diazoacetates are commonly made *via* diazo group transfer reactions of sulfonyl azides with the activated methylene group of an α -phenylester. Other routes are the decomposition of tosyl hydrazones, the oxidation of hydrazones or the diazotization of phenylalanine esters (see Section 1.2). The first two methods have the disadvantage of requiring functionalisation *prior* to the formation of the diazo species whereas the latter usually provides relatively low yields and several byproducts. This makes the diazo group transfer reaction the most popular and efficient method to form phenyl diazoacetates.

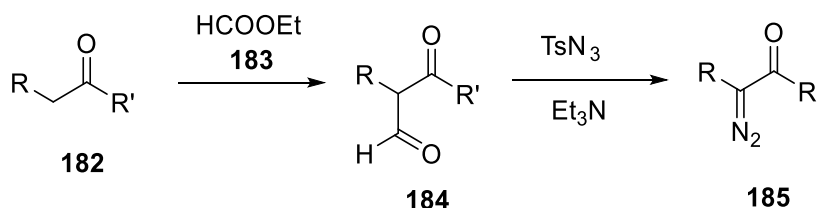
4.1.1 Diazo transfer reaction

The diazo group transfer reaction was first discovered by the German chemist Regitz in 1967.⁷ The standard protocol Regitz developed required the use of acceptor / acceptor substituted methylene groups that were sufficiently acidic to be deprotonated with a mild base such as triethylamine. The mechanism is depicted in Scheme 49. In the first step, the enolate **175** of the diester **174** is formed. Enolate **175** does a nucleophilic attack onto sulfonyl azide **176** to furnish intermediate **177**. Subsequent protonation and deprotonation cascade leads to triazene intermediate **178** which decomposes into diazo compound **180** and sulfonyl amide **181**.



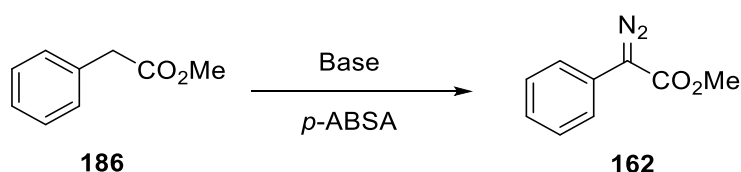
Scheme 49: Proposed mechanism for diazo group transfer reaction; R = alkyl

Compounds bearing only one acceptor functionality next to the methylene group are not acidic ($pK_a \sim 25$) enough to be deprotonated by triethylamine. For this class of compounds, Regitz developed a deformylation strategy using pre-functionalisation of the α -methylene group using a Claisen condensation with ethyl formate **183**.⁸ This pre-functionalisation leads to a much more acidic proton in the α -position ($pK_a \sim 14$), so that compound **184** can be easily transformed into diazo reagent **185** (Scheme 50). Several modifications from Regitz deformylation strategy were developed over the years.⁹



Scheme 50: Regitz deformylation strategy for less activated methylene groups; R = alkyl, aryl;
R' = alkyl, alkoxy, amino

The formation of diazo phenylacetates can be achieved in a more direct way, using DBU as base. In contrast to simple α -diazoketones, diazo phenylacetates can be made *via* diazo group transfer without pre-functionalisation. This reaction does not work with triethylamine (Et_3N), whereas the reaction proceeds with good yields (around ~ 75 -85% yield for most aryl diazoacetates) when DBU is employed as base. Figure 13 shows the difference between the use of DBU and Et_3N as base in the diazo transfer reaction on methyl phenylacetate **186** after 12 hours reaction time. In the case of DBU as base, a strong yellow colour can be observed. The reaction with triethylamine does not promote the formation of the yellow coloured diazo product **162**.



Scheme 51: Diazo transfer onto methyl phenylacetate **186**

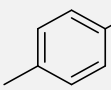
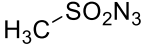
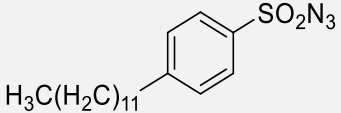


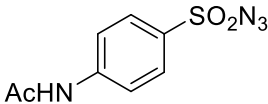
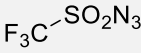
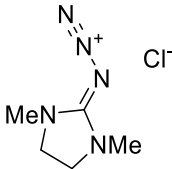
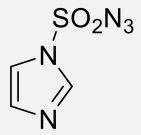
Figure 13: Comparison of DBU (left) and Et_3N (right) as base to promote diazo group transfer on methyl phenylacetate

4.1.1.1 Diazo transfer reagents

The diazo group transfer reaction requires a donor of the diazo functionality. This is always an azide, usually a sulfonyl azide. The most common diazo transfer reagents are listed in Table 4.1. Sulfonyl azides are highly energetic compounds.¹⁰ Tosyl azide **176** (Table 4.1, entry 1) and mesyl azide **187** (Table 4.1, entry 2) were the most commonly employed diazo transfer reagents until *p*-acetamidobenzenesulfonyl azide **189** (Table 4.1, entry 4) received more attention in the last 20 years. This is quite remarkable considering the immense safety hazards associated with these reagents. Mesyl azide **187** has the highest detonation energy of all reagents discussed in Table 4.1. Tosyl azide **176** has been reported to have been the cause of several explosions in the past.¹¹ It has explosive properties similar to those of trinitrotoluene (TNT). Triflyl azide **190** (Table 4.1, entry 5) has, in fact, an even worse safety profile than mesyl azide **187** as the neat substance is prone to explosion.¹² *p*-Dodecylsulfonyl azide **188** and *p*-acetamidebenzenesulfonyl azide **189** (*p*-ABSA) show similar thermal properties, however only *p*-ABSA **189** has been employed frequently in diazo transfer reactions. Both compounds are much safer than tosyl azide **176**, mesyl azide **187** and triflyl azide **190**, however they are still highly energetic molecules that should be handled carefully. Diazo transfer reagents **191** (Table 4.1, entry 6) and **192** (Table 4.1, entry 7) are rather recent additions to the pool of diazo transfer reagents. They have the advantage of providing water soluble by-products which helps to circumvent column chromatography. Unfortunately, there has been a report of an explosion of **192** (Table 4.1, entry 7) recently.¹³ Safer analogues (e.g. the corresponding hydrogen sulfate salt) have now been developed.¹⁴

Table 4.1: Selected list of diazo transfer reagents

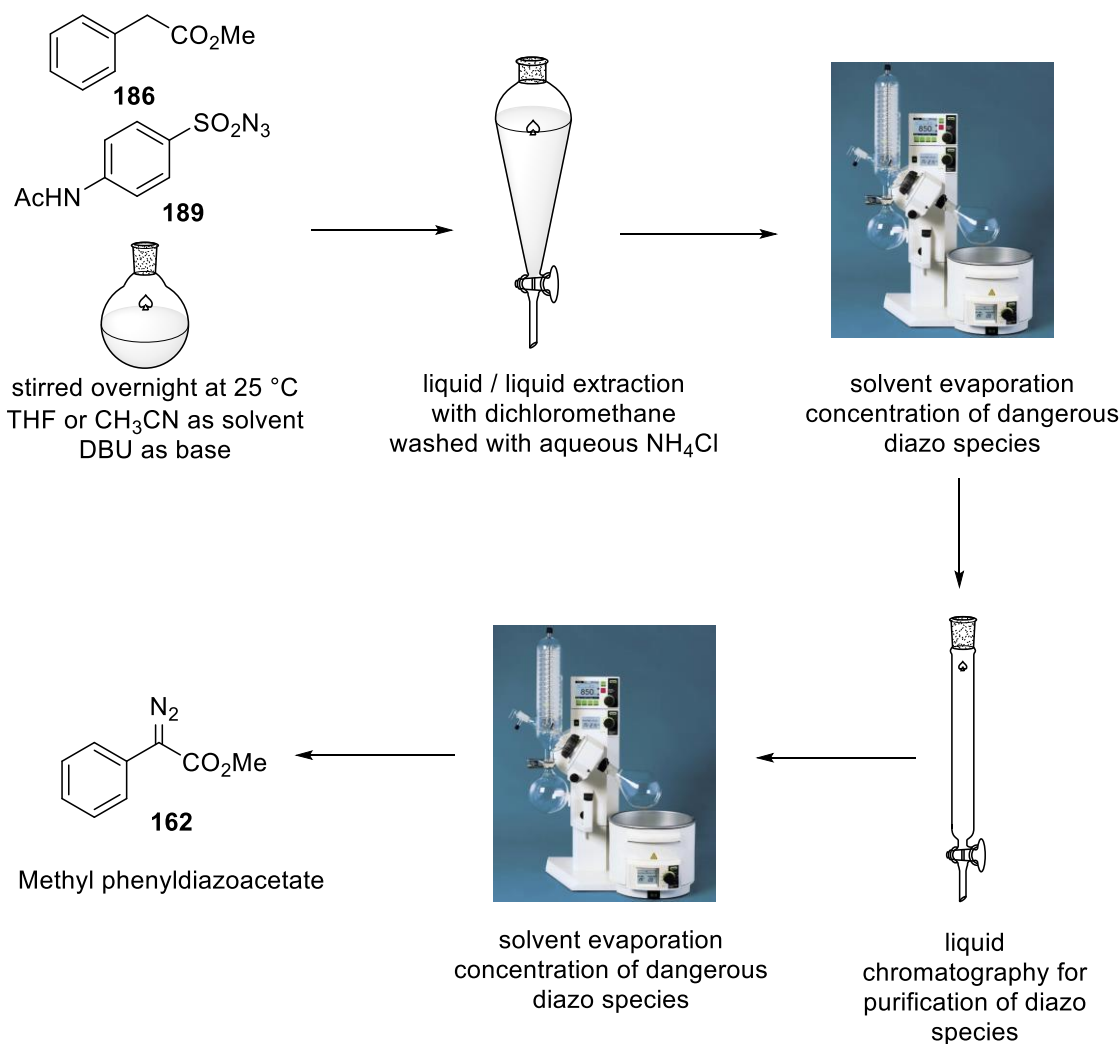
Entry	Compound	ΔH_D [cal/g]	Approx. initiation temperature [°C]	Impact Sensitivity [kg x cm]
1 ¹⁰	 176	-405	120	50
2 ¹⁰	 187	-557	125	50
3 ¹⁰	 188	-168	151	Negative to 150

4 ¹⁵	 <chem>CC(=O)Nc1ccc(S(=O)(=O)N=[N+]=[N-])cc1</chem> 189	-172	120	Negative to 136
5	 <chem>Fc1ccccc1C(F)(F)F(S(=O)(=O)N=[N+]=[N-])</chem> 190	n.A.	n.A.	n.A.
6 ¹⁶	 <chem>CN1CCN(C)C1[N+]#N.[Cl-]</chem> 191	n.A.	200	Negative to 255
7 ¹⁴	 <chem>C1=CN=C(C=N1)CN=[N+]=[N-]</chem> 192	n.A.	102	60

4.2 Standard protocol diazo transfer

As described, alkyl phenyldiazoacetates type **162** are derived from alkyl phenylacetates and a diazo transfer reagent using DBU as base. The detailed process is shown in Scheme 52. The reaction shows a compromise between safety and efficiency. The addition of the base (DBU) is performed at 0 °C, whereas the reaction is then left to warm to room temperature overnight. Subsequently, the reaction is extracted with dichloromethane and washed with aqueous ammonium chloride solution. This is done to separate DBU out of the dichloromethane / acetonitrile mixture into the aqueous layer. However, there is a risk of residual free azide moieties resulting from an aqueous cleavage of the sulfonyl azide functionality of diazo transfer reagent *p*-ABSA **189**. These free azides can form hydrazoic acid (HN₃) under acidic conditions provided by the ammonium chloride washing. Hydrazoic acid (HN₃) is a highly potent explosive and very toxic.

After the extraction, the organic layer is dried over MgSO₄ and the solvent is evaporated *in vacuo*. Therefore, highly concentrated diazo compounds with potentially significant left-over quantities of *p*-ABSA have to be handled carefully. In the next step, the mixture has to be purified *via* flash column chromatography to separate the sulfonyl amide from the diazo transfer reagent. In a last step, the pure collected fractions have to be concentrated again. The repeated concentration of the diazo species as well as the long reaction time (12 h) make this process highly unattractive for industrial applications.

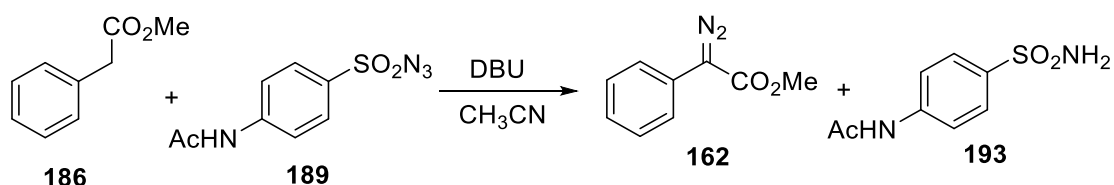


Scheme 52: Standard protocol for the formation of diazo phenylacetates

Herein, the development of a superior protocol is described. In order to develop a more powerful and safer protocol, it was first necessary to understand the thermal properties of the transformation and the risks associated with the diazo group transfer onto alkyl phenylacetates.

4.3 Risk assessment diazo transfer

In Section 4.1.1.1, the thermal properties of some diazo transfer reagents were discussed. To further understand the risks associated with the diazo transfer reaction, a risk class assessment was performed. Risk class assessments of chemical reactions require thermal measurements on the risk provoking materials of the reaction as well as of the reaction medium itself. It is important to determine adiabatic temperature rises due to the desired transformation and due to unwanted side- and decomposition reactions. In the diazo group transfer reaction of interest (Scheme 53), thermal risk arises from diazo transfer reagent *p*-acetamidobenzenesulfonyl azide (*p*-ABSA) **189** and diazo product **162**.



Scheme 53: General scheme of diazo group transfer studied

First, differential scanning calorimetry (DSC) of **189** and **162** was performed. In a DSC experiment, the difference in the amount of heat necessary to increase the temperature linearly of the sample is compared against a well-known reference. The DSC graph for *p*-ABSA **189** is shown in Figure 14. The blue coloured peak with negative energy values that starts at approximately 98 °C describes the melting of the solid reagent **189**, a process that requires energy. However, the sharp rising red coloured peak next to it is a highly exothermal decomposition of the diazo transfer reagent. The energy released in this process is $\Delta H = -1378 \text{ J/g}$ which equals $\Delta H = -331 \text{ kJ/mol}$. This is around 400 J/g more than the value obtained by Baum *et al.* (see Table 4.1 in Section 4.1.1.1).

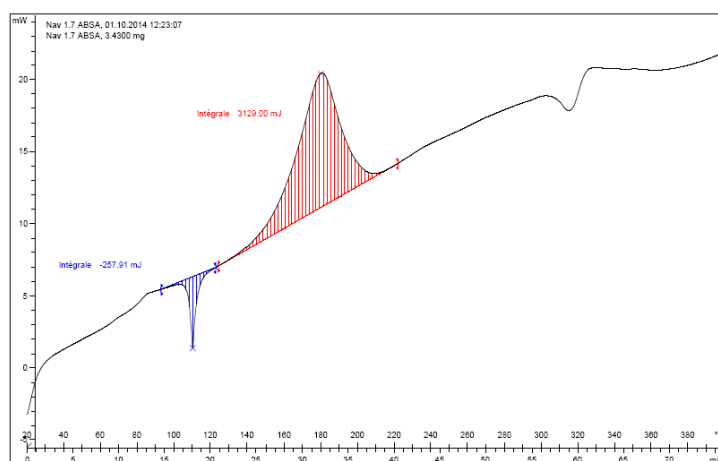


Figure 14: DSC measurement of *p*-acetamidobenzenesulfonyl azide **189**

With the enthalpy of the decomposition in hand, one can calculate the adiabatic temperature rise according to Formula 4.1.

$$\Delta T_{ad} = \frac{Q'}{c'_p}$$

Formula 4.1: Calculation of adiabatic temperature rise by division of heat per mass unit Q' through specific heat capacity c'_p ¹⁷

Using the standard specific heat capacity for non-halogenated organic compounds (c'_p) of 1.7 kJ/(kg K), one obtains an adiabatic temperature rise of $\Delta T_{ad} = 810 \text{ °C}$. This immense energy release should be considered when working with larger quantities of *p*-ABSA **189**. However,

the on-set temperature of 140 °C makes it possible to store laboratory quantities of **189** at room temperature. An important information for the thermal properties of a reagent as well as of a reaction is the T_{D24} value. The T_{D24} is the temperature at which it takes the decomposition reaction 24 hours, in adiabatic conditions, to reach the maximum rate of the decomposition reaction. It is assumed that at this point a thermal runaway cannot be stopped anymore.¹⁸ The T_{D24} can be calculated via the equation for the time to maximum rate in adiabatic conditions (TMR_{ad}) given in Formula 4.2.

$$TMR_{ad} = \frac{c_p R T_0^2}{q_0 E_A} [s]$$

Formula 4.2: Time to maximum rate under adiabatic conditions, solved for T with 24 hours as TMR_{ad} this gives T_{D24} . TMR_{ad} = time to maximum rate under adiabatic conditions [s]; c_p = specific heat capacity [kJ/(kg K)]; R = gas constant [J/(mol K)]; T_0 = initial temperature of runaway [K]; q_0 = heat release rate at T_0 [W/kg]; E_A = activation energy [J/mol]

It is important to mention that several assumptions are made routinely when this formula is used. (i) The activation energy of the transformation is set to 50 kJ/mol which is a conservative estimate. However, it is quite accurate for the diazo transfer reaction in discussion (Scheme 53) as will be shown in Section 4.4. (ii) It is assumed that the decomposition reaction follows 0th order kinetics. (iii) The specific heat capacity is again considered to be 1.7 kJ/(kg K). For *p*-acetamidobenzenesulfonyl azide **189** this calculation reveals a T_{D24} of 45 °C.

Diazo reagent **162** shows a different energy profile than the diazo transfer reagents *p*-ABSA **189** (Figure 15). The energy released in the diazo decomposition reaction is $\Delta H = -861$ J/g and $\Delta H = -151$ kJ/mol, respectively. This corresponds to $\Delta T_{ad} = 506$ °C, which is around 300 °C lower than **189** but still a very high energy profile. The biggest issue of diazo product **162** lies in the low on-set temperature of the decomposition reaction at 77 °C. Using formula 4.1, this translates into a T_{D24} of 6 °C. It is therefore absolutely mandatory to store the diazo reagent **162** at low temperatures, but it would be preferential to use it immediately without any storage time.

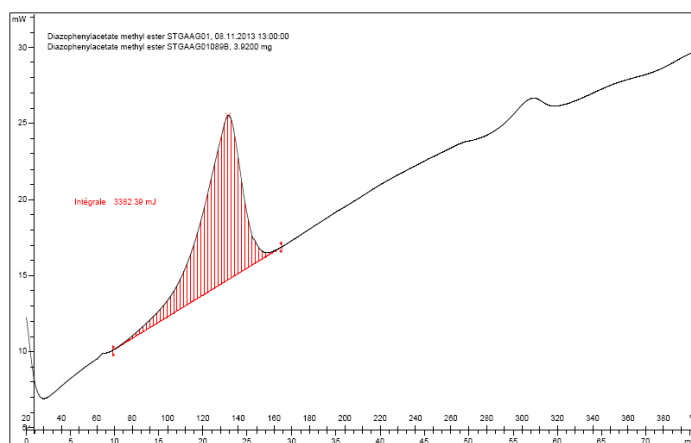


Figure 15: DSC of methyl phenyldiazoacetate **162**

Having established a good understanding of the risk provoking materials in the diazo transfer reaction, risk class assessment could be performed using C80 Calvet-type calorimeter measurements. First, the reaction enthalpy was recorded (Figure 16). An exothermic reaction of $\Delta H = -86 \text{ J/g}$ or $\Delta H = -138 \text{ kJ/mol}$ was found. This corresponds to a ΔT_{ad} of 39°C . In the case of a cooling failure, the heat of the reaction would hence lead to a temperature rise of 39°C . As the standard reaction temperature for a diazo transfer is 25°C , the reaction would attain 64°C .

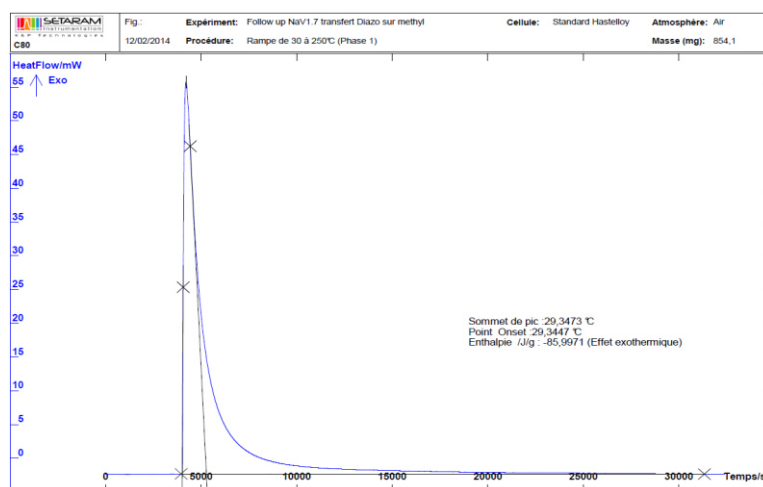


Figure 16: C80 measurement of reaction enthalpy

Next, the reaction decomposition energy was determined for the calculation of T_{D24} of the process (Figure 17). The decomposition reaction gives an enthalpy of ΔH of -133 J/g corresponding to a ΔT_{ad} of 60°C and a T_{D24} of 54°C . This means that the time to maximum rate of 24 hours is not provided if the reaction enthalpy itself is completely released in adiabatic conditions. The further exothermic decomposition reaction would lead to an increase to an operating temperature of 124°C ($64^\circ\text{C} + 60^\circ\text{C}$). This is far above the boiling point of the reaction solvent acetonitrile (81°C).

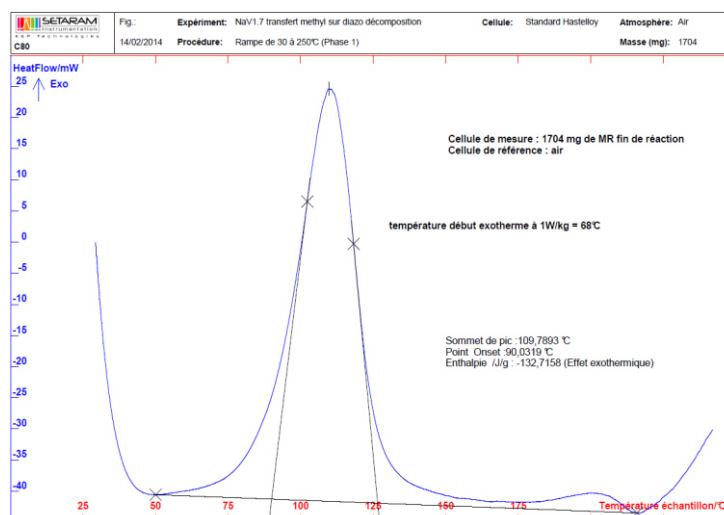


Figure 17: C80 measurement of decomposition reaction

With the results obtained, a risk class assessment was performed. The different risk classes and their definition are shown in Figure 18. Risk class 1-3 have all a maximum temperature of the chemical reaction (MTSR) that is below the T_{D24} of the reaction. This means that even in case of adiabatic reaction conditions, process chemists have more than 24 hours to react before there is a risk of a thermal runaway. In risk class 4, the maximum temperature for technical reasons (MTT), which is often the boiling point of the reaction solvent, is lower than the T_{D24} but the MTSR is higher than the T_{D24} . In these cases careful planning is required to perform these reactions. It is desirable to find ways to either increase the T_{D24} or reduce the MTSR. In case of risk class 5, the MTSR and the MTT are higher than the T_{D24} . A thermal runaway can therefore happen in less than 24 hours after adiabatic conditions occurred. Reactions of risk class 5 need significant safety planning and usually require specialised equipment. A detailed discussion of the different risk classes is outside the scope of this work.¹⁹ Diazo transfer reaction from Scheme 53 clearly falls into risk class 5, the highest risk class. The T_{D24} of 54 °C is lower than MTSR = 64 °C and MTT = 81 °C. This reaction would therefore be a great challenge to perform in classical batch chemistry on industrial scale.

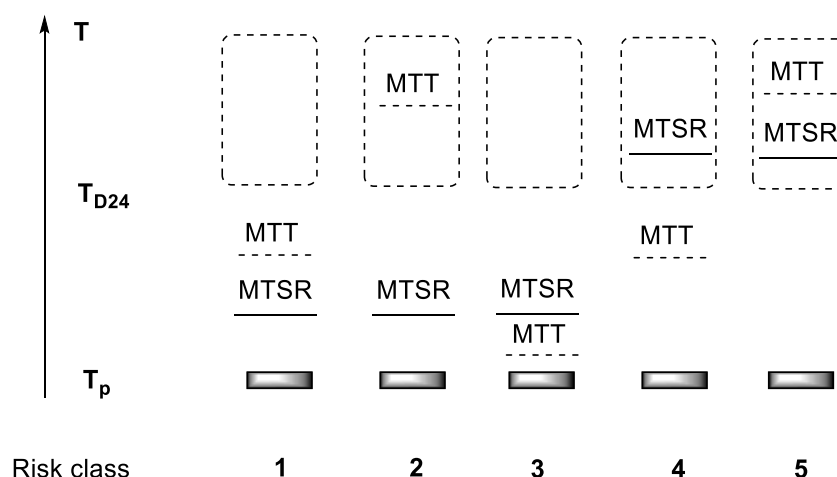


Figure 18: Risk class definitions; MTSR: maximum temperature of synthesis reaction; MTT: maximum temperature for technical reasons; T_p : process temperature¹⁷

4.4 Reaction kinetics of diazo transfer

After establishing the thermal properties of the diazo transfer reaction and the reagents involved, reaction kinetics of the diazo transfer onto methyl phenylacetate **186** using *p*-ABSA **189** was studied. First, this was done in batch (Section 4.4.1) and subsequently, continuous flow was tested as a platform to speed the reaction up safely (Section 4.4.2).

4.4.1 Reaction kinetics in batch

It was mentioned in Section 4.2 that standard protocols for the diazo transfer reaction on phenylacetates usually need around 12 hours reaction time. In Section 4.3 it was described that these are dangerous reaction conditions for larger scale applications as a thermal runaway could occur. It is also a rather inefficient reaction time. Therefore, a better understanding of the kinetic properties of the reaction was desirable. For this purpose, in-line analysis techniques in form of in-line infrared spectroscopy using ReactIR from Mettler Toledo were used (Figure 19).

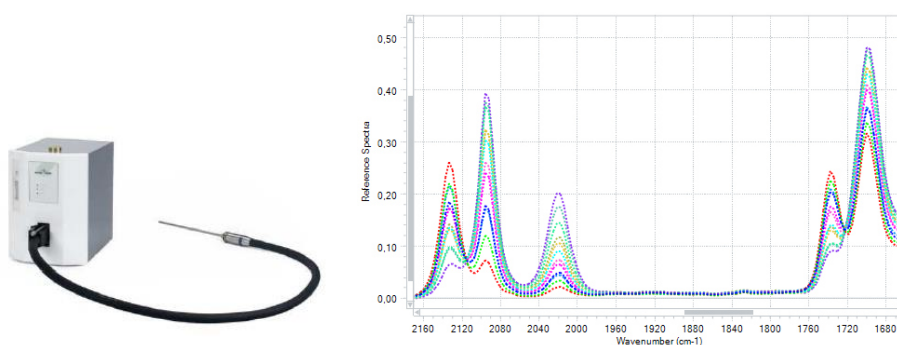


Figure 19: ReactIR system with diamond batch probe (left); absorption infrared spectrum observed at different reaction times with ReactIR systems (right)

The reaction was performed at 0.5 M concentration of methyl phenylacetate **186** in acetonitrile at 25 °C. Starting materials **186** and **189** were calibrated using well separated IR bands at wave numbers of 1741 cm^{-1} and 2135 cm^{-1} . Diazo product **162** was calibrated using the well-defined C=N stretch at 2097 cm^{-1} . R^2 values for each calibration exceeded 0.99. A three dimensional view on the reaction progress over time is shown in Figure 20 (left). The reaction progress for methyl phenylacetate **186** (red), *p*-ABSA **189** (blue) and methyl phenyldiazoacetate **162** (green) is shown in Figure 20 (right). The reaction starts fast but slows down with time more and more. To completion of the diazo transfer reaction (> 90% yield) it takes around six hours.

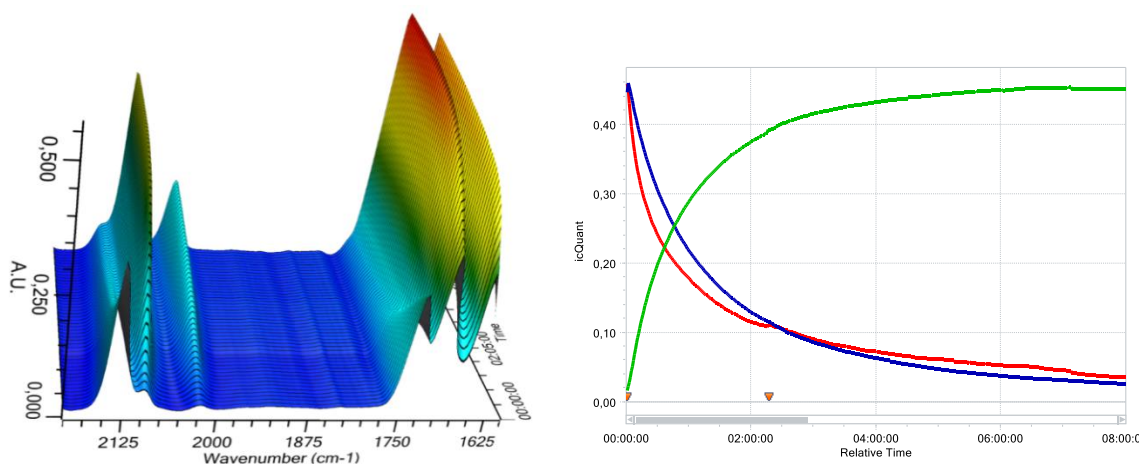


Figure 20: three dimensional view on the reaction process (left); reaction progress in the first eight hours of the reaction; methyl phenylacetate **186** (red), *p*-ABSA **189** (blue), and methyl phenyldiazoacetate **162** (green)

Starting materials ester **186** and *p*-ABSA **189** behave similarly in respect to their consumption rate during the reaction. Therefore the following assumptions could be made for calculation of the rate constant: (i) The starting concentrations of the two starting materials are not the same: $[\text{Ester } \mathbf{186}]_0 \neq [\text{ABSA } \mathbf{189}]_0$ but (ii) their concentrations change at the same rate over time: $[\text{Ester } \mathbf{186}]/dt \sim [\text{ABSA } \mathbf{189}]/dt$. Following on this assumption, plotting for 2nd order kinetics gave a linear relation between time [s] against $\ln([[\mathbf{186}]_0 * [\mathbf{189}]] / ([\mathbf{186}] * [\mathbf{189}]_0))$ (Figure 21).

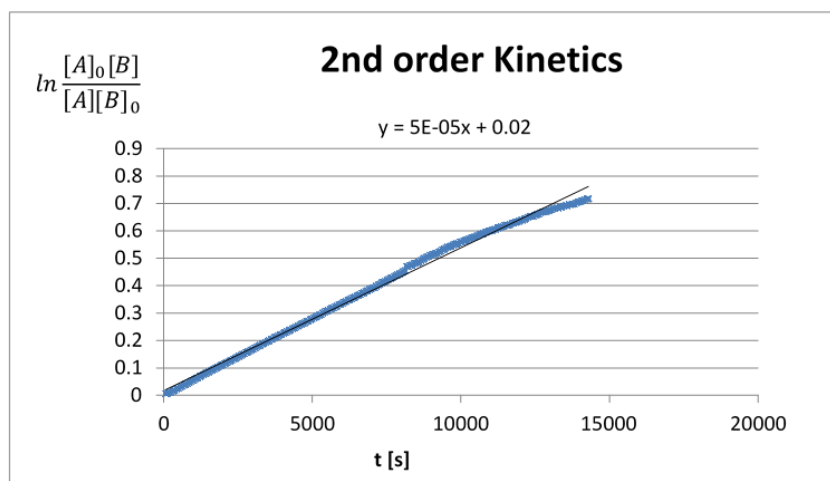


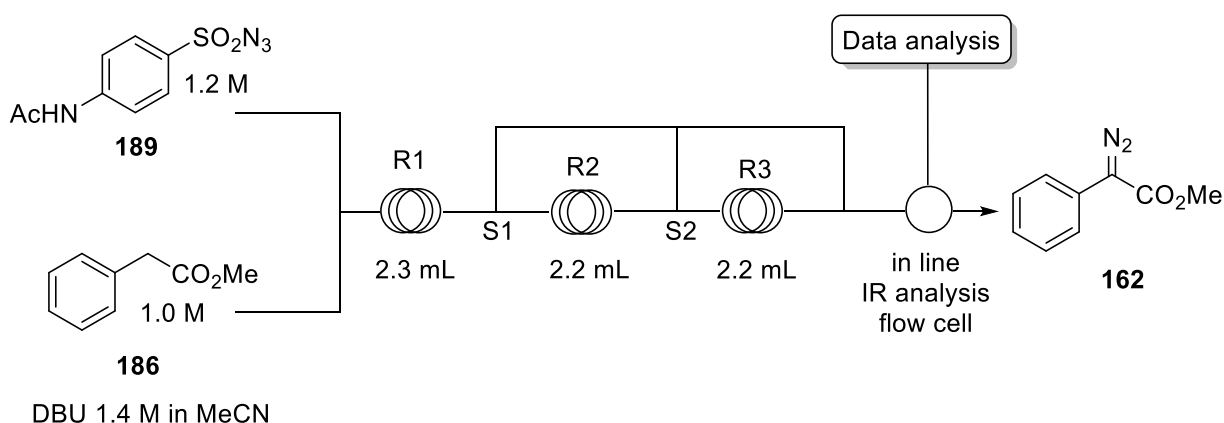
Figure 21: Plotting for 2nd order kinetics with [ester **186**]/dt ~ [*p*-ABSA **189**]/dt

Solving the resulting equation, a rate constant of $k = 5 \times 10^{-4} \text{ M}^{-1} \text{ s}^{-1}$ was found.

4.4.2 Reaction kinetics in flow

In Section 1.4, the benefits of flow chemistry for the use of highly energetic compounds as well as for reaction kinetics were briefly discussed. Therefore, a comparison of batch and flow reaction kinetics of this diazo transfer reaction was performed. It was speculated that the improved safety profile of continuous flow systems would give access to higher operating temperatures and hence, faster reaction times. Furthermore, reaction kinetics might be improved by better mixing in the micro- or mesoreactor systems.

Reaction concentration of methyl ester **186** was 0.5 M and the calibration curves made for the batch system in section 4.4.1 were used again. A three reactor continuous flow set-up was designed (Scheme 54). The advantage of this two-valve (S1 and S2), three reactor (R1, R2 and R3) system is the faster optimisation time as well as a reduced consumption of reagents. This is due to the shorter stabilisation time (one stabilisation time for three data points) compared to a system without valves to switch reaction times. Residence times were 9 minutes (R1), 17 minutes (R1 + R2) and 26 minutes (R1 + R2 + R3).



Scheme 54: Continuous flow set-up for diazo transfer optimisation

In addition to different reaction times, different temperatures were screened. The first three data points were taken at 25 °C, then at 40 °C, 50 °C and finally at 60 °C. One data point for R1 + R2 + R3 was taken at 70 °C (Table 4.2, entry 13) but showed no further improvement to the data points at 60 °C (Table 4.2, entries 4, 8, 12). A table with all results is shown below (Table 4.2). Both factors, temperature and residence time, play a very important role in the yields of the diazo group transfer reaction. Whilst it requires 26 minutes at 25 °C to achieve a yield of 40% (Table 4.2, entry 9), a very similar yield (39%) can be achieved within 9 minutes when the reaction temperature is only raised by 15 °C to 40 °C (Table 4.2, entry 2). At even more elevated temperatures, good yields (72%) can be obtained in just 9 minutes (Table 4.2, entry 4). Increasing the residence time at the same temperature leads to higher yields, in 17 minutes (85%) and in 26 minutes (89%) (Table 4.2, entries 8 and 12). The rapid generation of the diazo reagent is therefore possible in continuous flow.

Table 4.2: Results from continuous flow experiment on kinetic properties of diazo transfer

Entry	t_{res} [min]	T [°C]	Yield [%]
1	9	25	18
2	9	40	39
3	9	50	59
4	9	60	72
5	17	25	28
6	17	40	55
7	17	50	73
8	17	60	85

9	26	25	40
10	26	40	68
11	26	50	83
12	26	60	89
13	26	70	90

A plot of the results obtained from the flow experiment against the results obtained from the batch experiment is shown in Figure 22. The continuous flow reaction at 25 °C is very similar to the batch reaction at the same temperature. This is an interesting finding considering the vast amount of literature on the effect of mixing in continuous flow compared to batch reactions. However, diazo transfer reactions are rather slow reactions and therefore the reaction kinetics are much slower than the mass transfer. Mixing has therefore only a minor impact on the speed of the reaction. This finding stands therefore in complete agreement with the findings of Blackmond *et al.*²⁰ Higher reaction temperature in flow chemistry however outperform the batch reaction at 25 °C dramatically. At 60 °C in continuous flow the reaction is complete (~ 90%) in just 26 minutes whereas it takes 6 hours in batch chemistry at room temperature to achieve this level of transformation. It is important to note that such operating temperatures could never be used in batch due to the safety concerns associated with the diazo transfer reaction in batch.

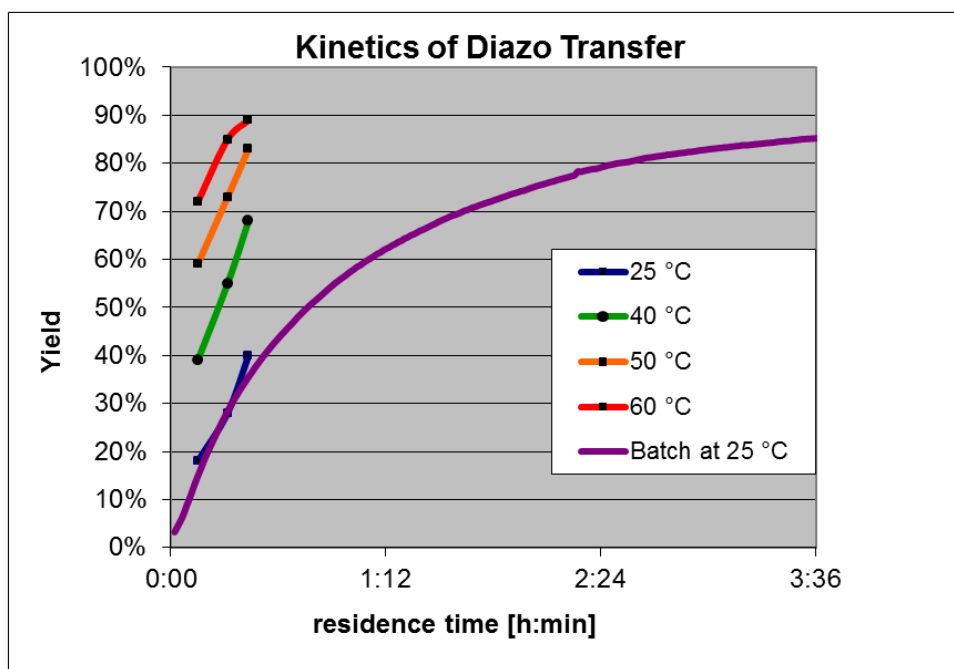


Figure 22: Comparison of continuous flow results with batch results for diazo transfer on methyl phenylacetate

Arrhenius plotting of rate constants at different reaction temperatures gives the possibility to determine the activation energy required for the diazo transfer reaction (Formula 4.3).

$$k = Ae^{-\frac{E_A}{RT}}$$

$$\Leftrightarrow \ln k = \ln A - \frac{1}{T} \frac{E_A}{R}$$

Formula 4.3: Determination of activation energy using reaction rates over different temperatures

Formula 4.3 can be plotted so that $\ln k$ is the y axis, $1/T$ the x axis, and $\ln A$ the intercept with the y axis. Therefore, $-E_A/R$ is the slope of the graph (Figure 23). The activation energy obtained is $E_A = 56$ kJ/mol. This is a relatively low activation energy for a chemical reaction. It is also very close to the estimate used in Section 4.3 to determine the time to maximum rate of the diazo transfer reaction.

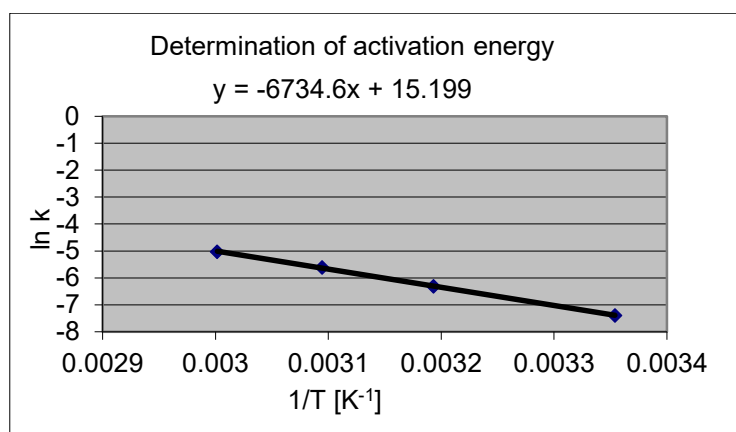


Figure 23: Arrhenius plotting to obtain the activation energy of diazo transfer

In summary of Section 4.3 and 4.4, a strong case can be made for the development of a continuous flow process for the diazo transfer reaction on phenylacetates. The following benefits arise from the use of continuous flow for the diazo transfer:

- (1) Reduced safety concerns due to improved heat exchange
- (2) Change of operating window due to improved heat exchange
- (3) Significantly reduced reaction time due to the higher temperature possible to use safely

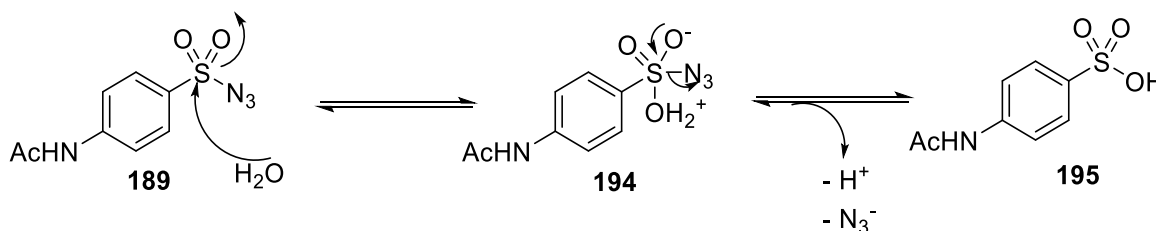
4.5 Extraction of diazo reagent

One of the major disadvantages of the standard batch process for diazo transfer reactions described in Section 4.2 is the need of column chromatography and concentrating the diazo species. It was evident that this had to be altered to make a continuous flow process attractive as otherwise the hazards from large quantities of neat diazo reagent would remain. Another issue was the use of ammonium chloride solution in the extraction because of the potential

formation of hydrazoic acid, a potent explosive. Therefore, the following goals for isolation of the diazo species were set:

- (1) Development of an effective quench of remaining traces of free azides
- (2) Development of a selective liquid / liquid separation to obtain diazo species in sufficient purity for metal promoted carbene reaction

Azides could be formed by a nucleophilic substitution of water on the sulfonyl azide (Scheme 55).



Scheme 55: Generation of azides species from *p*-acetamidobenzenesulfonyl azide

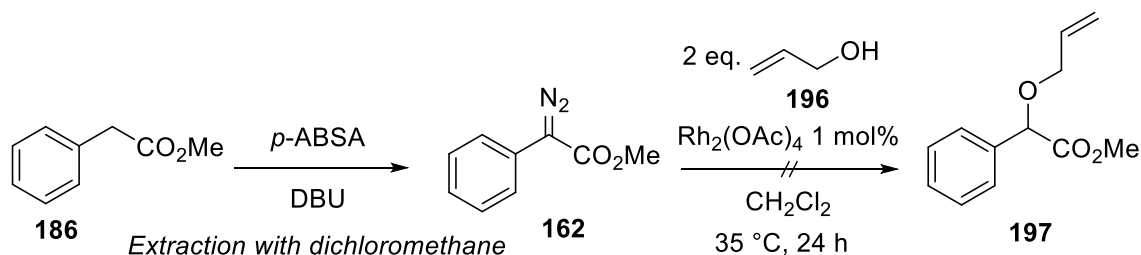
A powerful azide detection test which detects azides down to 5 mM concentrations uses iron(III) chloride. Iron(III) chloride forms strongly red coloured complexes with azides.²¹ The iron(III) chloride test was positive for the aqueous ammonium chloride solution after the first extraction of the diazo transfer reaction medium. Azides can be decomposed using bleach or sodium nitrite. However, bleach would be incompatible with the diazo species formed in the reaction, therefore aqueous sodium nitrite solution was tested as quench reagent. It was found that the use of aqueous sodium nitrite solution instead of the aqueous ammonium chloride solution reduced the concentration of free azides below the iron(III) chloride detection level (Figure 24).



Figure 24: Azide tests with FeCl₃: aqueous ammonium chloride used for extraction, azide test positive (left); aqueous sodium nitrite solution used for extraction, azide test negative (right)²²

Next, it was investigated if the organic layer of the extraction after the diazo transfer reaction could be utilised in a subsequent carbene reaction without purification and solvent

concentration. For this purpose, methyl phenyldiazoacetate **162** made *via* diazo transfer onto methyl phenylacetate **186** was extracted using dichloromethane (Scheme 56). The crude dichloromethane solution of methyl phenyldiazoacetate **162** was then treated in a subsequent reaction with allyl alcohol **196**. No product formation was observed and only starting material was recovered. The reaction does, however, work in high yield if a liquid column chromatography is performed to purify the diazo compound after the extraction in dichloromethane.



Scheme 56: No reaction observed when crude dichloromethane solution was used for carbene reaction

One possible reason for the lack of reactivity of the crude reaction mixture was that the rhodium acetate catalyst was poisoned by one of the side products of the diazo transfer reaction which were soluble in dichloromethane. This could have been traces of DBU or the sulfonyl amide side product. Therefore, a solvent that was less polar than dichloromethane was used. In a less polar solvent, acetonitrile would remain in the aqueous layer and so would side products formed in the diazo transfer reaction. It was found that hydrocarbon solvents such as *n*-hexane or *n*-heptane were highly efficient in extracting only diazo reagents and phenylacetate starting material out of the reaction mixture as long as the alkyl side chain of the ester was long enough. The right ratio of hydrocarbon solvent to aqueous sodium nitrite solution and reaction mixture had to be chosen as otherwise three layers were formed. The following ratio has proven ideal:

For each gram of phenylacetate starting material (0.5 M concentration in MeCN within the diazo transfer reaction) 15 ml *n*-hexane and 11 ml 1 M sodium nitrite solution were required. If these exact conditions are used, the separation of long chain alkyl chains ($n \geq 3$) is very efficient (Figure 25). Less than 3% of the allyl phenyldiazoacetate was in the aqueous layer.

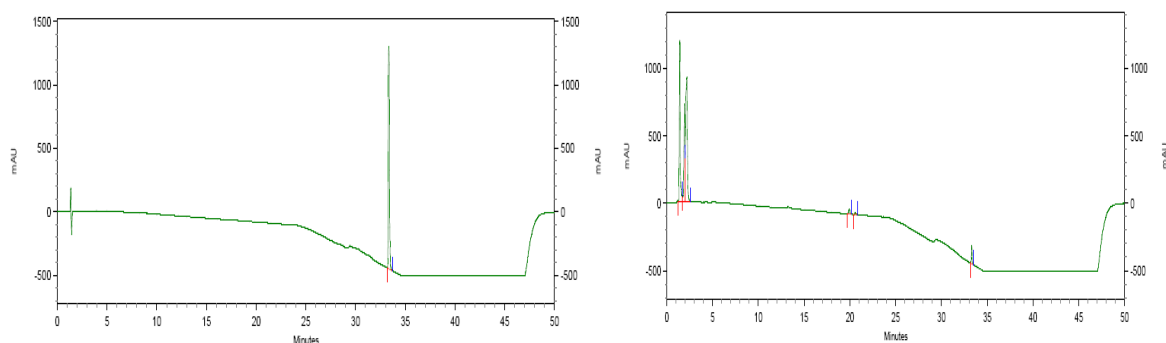
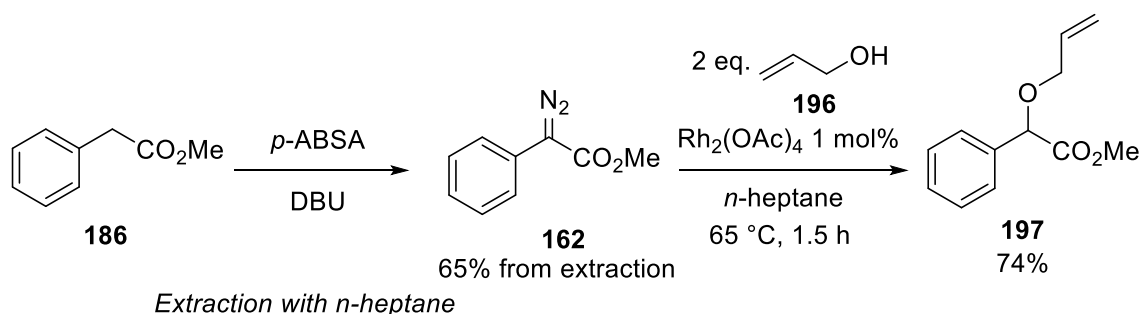


Figure 25: HPLC spectrum of organic layer after extraction of allyl phenyldiazoacetate (left); HPLC spectrum of aqueous layer of the same reaction (right); diazo at 33.5 minutes

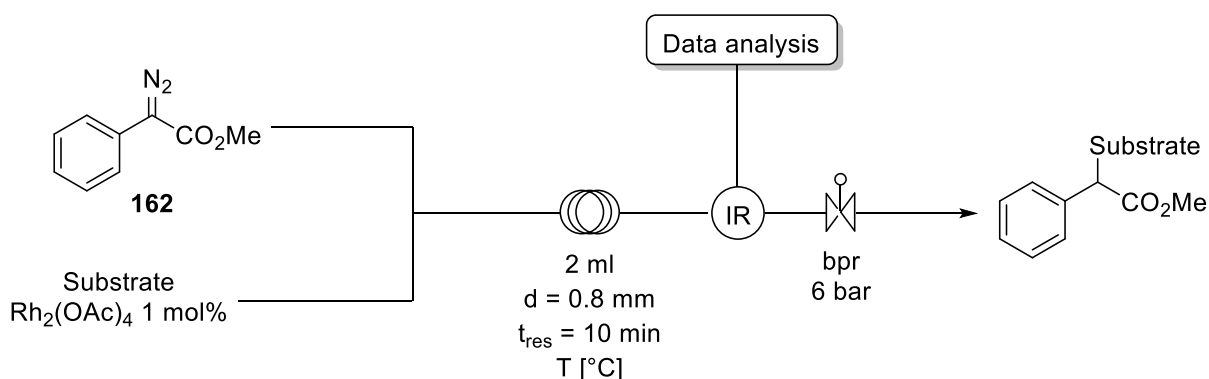
The obtained crude hydrocarbon solution with the diazo species readily undergoes carbene chemistry such as the O-H insertion into allyl alcohol in 74% yield (Scheme 57). Therefore, the extraction protocol developed was suitable for the direct use of diazo reagent **162** circumventing laborious column chromatography and hazardous concentration of the diazo reagent.



Scheme 57: Proof of concept for the direct use of extracted diazo species **162** in subsequent carbene reaction with allyl alcohol **196**

4.6 Reaction optimisation of carbene reactions

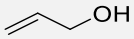
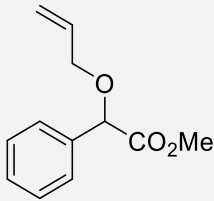
Having established an efficient way of isolated the diazo species, the next step was to optimise a diverse range of diazo decomposition reactions to use the versatile reactivity of diazo phenylacetates. Therefore, diazo compound **162** was reacted with different substrates under rhodium catalysis in a continuous flow set-up. Concentration of **162** in *n*-heptane was 0.27 M, the same concentration that the diazo compound has after extraction. Rhodium acetate was dissolved in a 9 / 1 mixture of chloroform / acetonitrile, a solvent mixture that has proven efficient to dissolve rhodium acetate and promote diazo reactions. The substrate was added to the chloroform / acetonitrile solution in a concentration of 0.32 M (1.2 eq.). Subsequently, the continuous flow was evaluated using in-line infrared spectroscopy (Scheme 58).

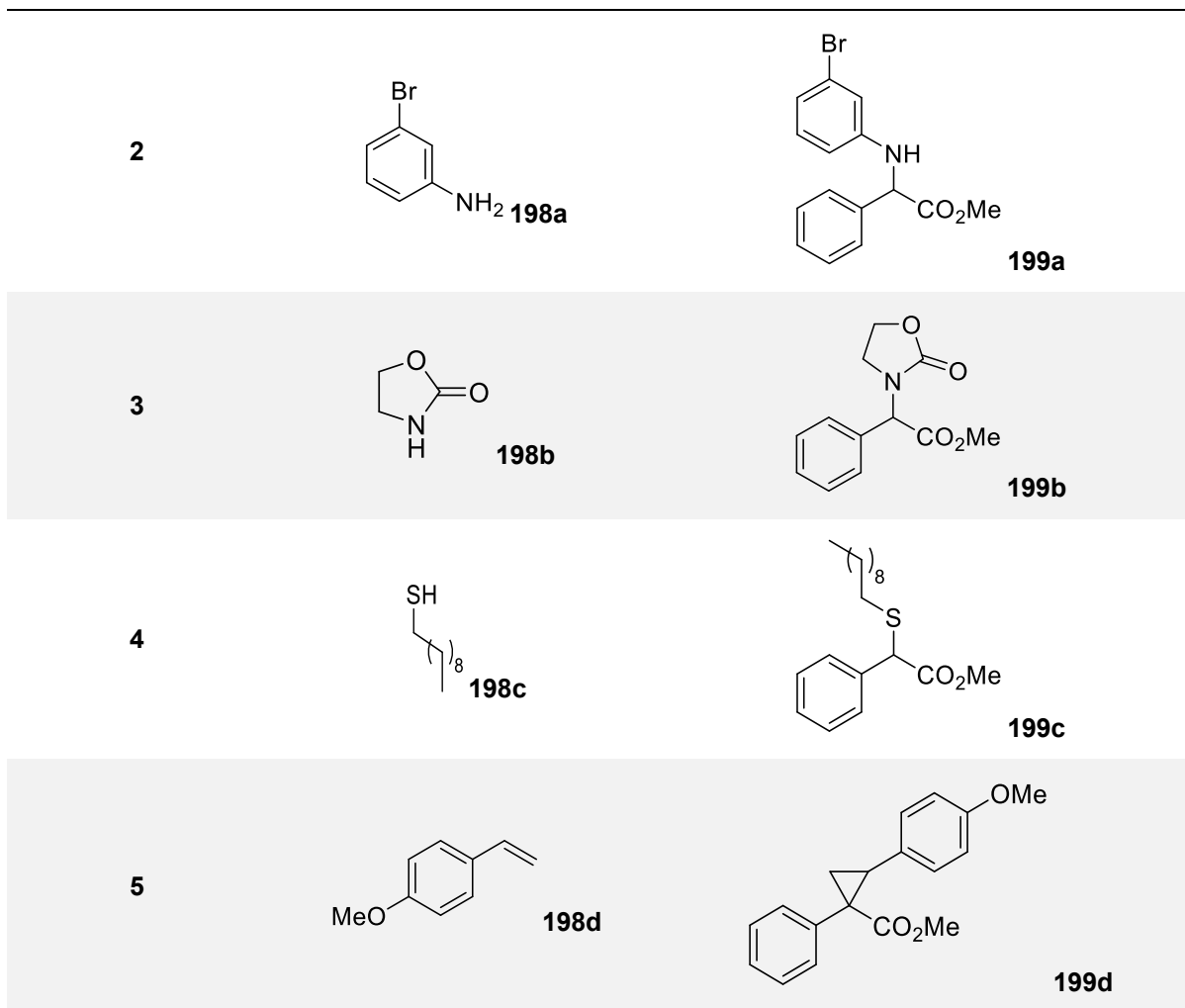


Scheme 58: General scheme of diazo decomposition optimization set-up

One of the bottlenecks of the use of in-line analysis technologies is the need to measure and calibrate all reagents and products involved in each reaction before the optimisation can be performed. To improve the efficiency and speed of the reaction optimisation, quantification of the reaction was performed by measuring the decomposition of the diazo starting material. Thus, it was possible to obtain detailed information of the reaction progress without the need of a spectroscopic analysis of the other starting materials and products. Diazo decomposition was studied using the IR band of the C=O carbonyl of the ester at 1704 cm^{-1} . In contrast to the kinetic experiments in Section 4.4, a diamond infrared probe was used to study the reaction progress. The reactions were also monitored qualitatively *via* offline HPLC to verify the infrared data. Five different substrates were used successfully in this set-up (Table 4.3). In all cases, structural changes could be observed in the in-line infrared analysis. The characteristic component for all reactions was a shift of the IR band of the carbonyl group of diazo reagent **162** from around 1704 cm^{-1} to around 1745 cm^{-1} . In four cases (Table 4.3, entries 1-4) this change could be quantified. At this stage of the project, the reactions were only studied using IR, HPLC and LC/MS analysis and no isolated yields were recorded.

Table 4.3: Substrates used for the diazo decomposition optimisation in flow

Entry	Substrate	Product
1	 196	 197



It was found that the reactions were highly temperature dependent and that the importance of temperature was much more significant than that of the residence time of the reaction mixture in the flow reactor. Two examples, the alcohol insertion of allyl alcohol **196** and the reaction of diazo reagent **162** with 3-bromoaniline **198a** are briefly discussed (details for the other three examples can be found in the experimental section).

For the alcohol insertion into allyl alcohol **196**, spectra were recorded at 25 °C, 50 °C, 60 °C, and 70 °C with a residence time of 10 minutes. The IR spectra recorded are shown in Figure 26. The most apparent change at higher temperature is the shift of the C=O stretch from 1704 cm⁻¹ to higher energies around 1752 cm⁻¹. Considering the structural change from a fully conjugated sp² system to a system with a sp³ carbon neighbouring the carbonyl, an increase in energy of the C=O stretch vibration would be expected. At 25 °C, none of the diazo compound **162** seems to have reacted as there is no peak at 1752 cm⁻¹ (red line). The reaction is however completed in 10 minutes at 70 °C which suggests that all diazo compound has been consumed as the carbonyl peak at 1704 cm⁻¹ has disappeared (blue line). Several peaks disappear with the consumption of the diazo species, these changes can be observed for all diazo consumption reactions in this section (at 1500 cm⁻¹, 1440 cm⁻¹, 1360 cm⁻¹, 1250 cm⁻¹,

1210 cm^{-1} , 1150 cm^{-1}). A broad band in the fingerprint region around 1070-1150 cm^{-1} is formed at increased temperatures. This is a region in which typically C-O-C stretch bands of ethers can be found.

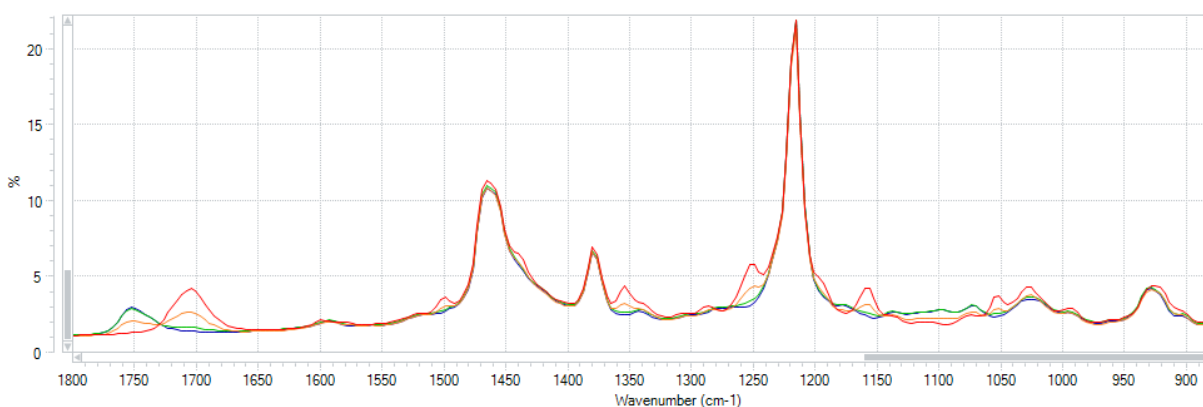
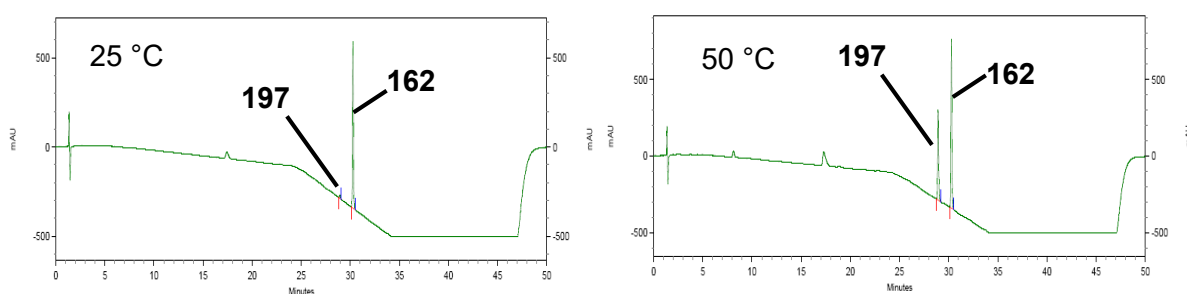


Figure 26: Infrared spectra for reaction between diazo compound and allyl alcohol; red line: 25 °C; orange line: 50 °C; green line: 60 °C; blue line: 70 °C

To verify the results obtained *via* in-line infrared analysis, qualitative offline HPLC analysis was done simultaneously. For the O-H insertion of allyl alcohol **196** these HPLC results will be discussed within this chapter (Figure 27; for the other substrates see experimental section). The HPLC spectra of the four different reaction conditions are shown in Figure 27. At 25 °C almost no insertion product **197** can be observed (2%) which is in accordance to the result observed in the in-line infrared spectrum. At 50 °C, significant quantities of diazo species **162** are already transformed into product **197**. Whilst there is still some methyl phenyldiazoacetate **162** left at 60 °C within 10 minutes reaction time, none is present when the reaction is conducted at 70 °C.



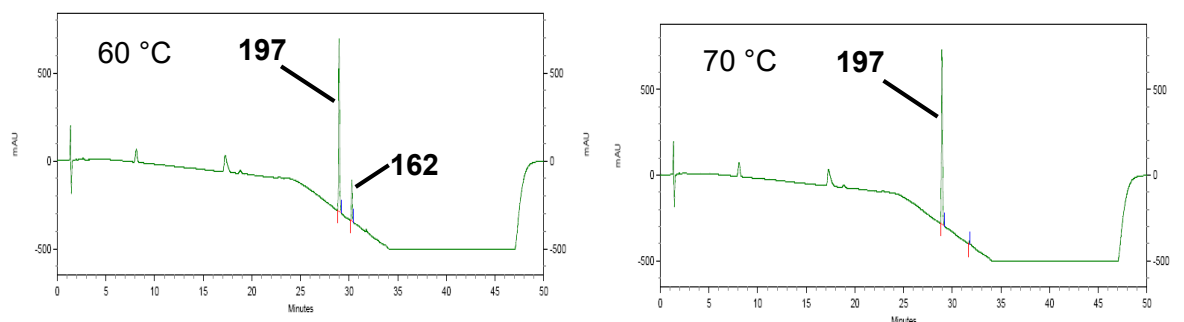


Figure 27: HPLC spectra of carbene insertion into allyl alcohol; 25 °C (left top); 50 °C (right top); 60 °C (left bottom); 70 °C (right bottom); 28.93 minutes compound **197**; 30.26 minutes methyl phenyldiazoacetate **162**

For N-H insertion into 3-bromoaniline **198a**, spectra were recorded at 25 °C, 40 °C, 50 °C, 60 °C and 70 °C with a residence time of 10 minutes (Figure 28). Again, a shift of the peak corresponding to the carbonyl group can be observed at higher temperatures. This happens in very similar fashion to the shift of the peak corresponding to the carbonyl group in the O-H insertion reaction. Significant changes in the amounts of diazo present were found between 40 °C and 50 °C (orange and green line) as well as between 50 °C and 60 °C (green and blue line). The N-H bend of primary amines at 1625 cm⁻¹ disappears at higher temperatures. Another change of shifts was observed between 1340 cm⁻¹ to 1280 cm⁻¹ which could be a change in the energy of the C-N bond between starting material and product. A peak at 880 to 840 cm⁻¹ decreases at higher temperature, presumably the N-H wag.

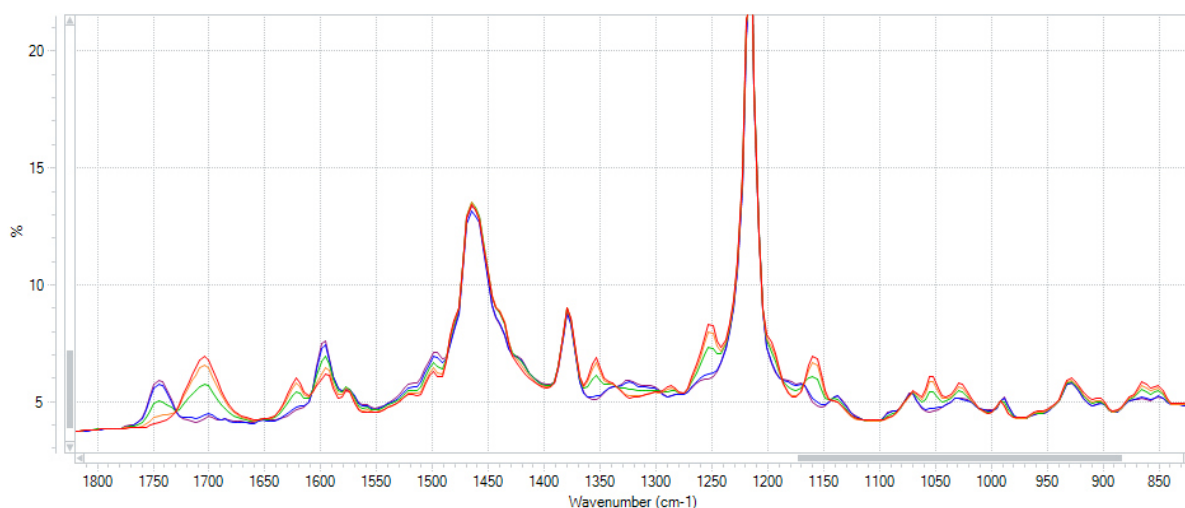


Figure 28: Infrared spectra for reaction between diazo compound and 3-bromoaniline; red line: 25 °C; orange line: 40 °C; green line: 50 °C; blue line: 60 °C; purple line: 70 °C

Although in-line infrared spectra were extremely useful for the examination of the progress of the reaction and to find ideal conditions for the diazo decomposition, side products are not always identified if they have strong structural similarities to the main products. HPLC analysis

showed the formation of a major side product when the reaction was performed at higher temperatures. LC-MS analysis provided the mass corresponding to amide **200** (Figure 29). This would not interfere with the N-H insertion as an excess of the aniline species was used (Scheme 58). This side product was only detected at temperatures above 50 °C.

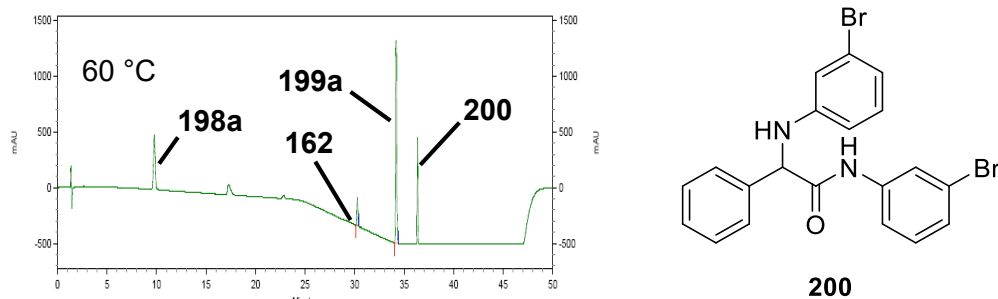
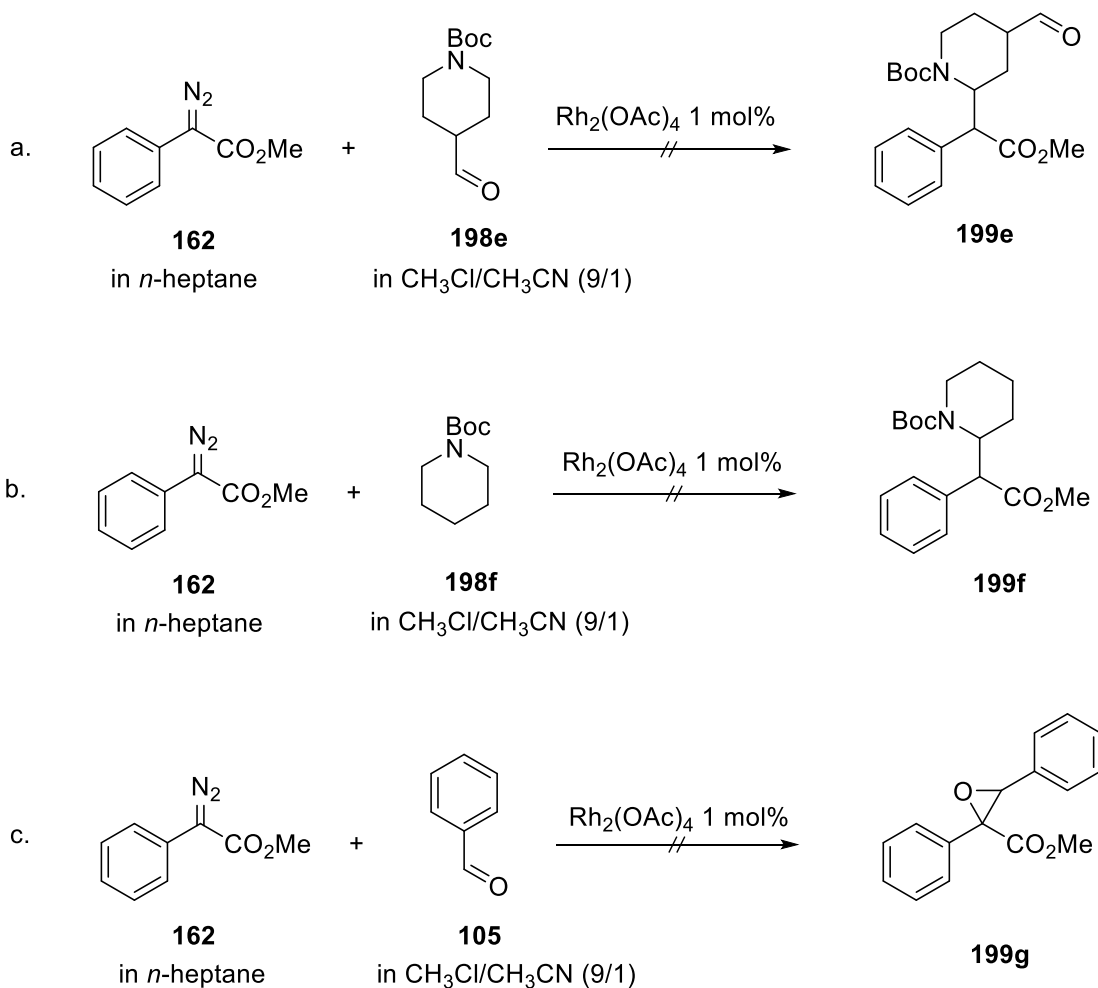


Figure 29: HPLC spectrum at 60 °C (left); 9.78 min 3-Bromoaniline **198a**; 30.26 min methyl phenyldiazoacetate **162**; 34.18 min N-H insertion product **199a**; 36.33 min side product **200**; structure amide **200** (right)

The five reactions shown (Table 4.3, entries 1-5) display a broad level of structural diversity. Discussions of the reactions of substrates **198b-198d** are in the experimental section. However, not all well-known transformations of phenyldiazoacetates were successful when employed in the reaction system shown in Scheme 58. The reactions of **162** in a C-H insertion with **198e** or **198f** gave none of the desired product, instead a variety of side products were found of which the most dominant ones were water insertion products and carbene dimerization. Epoxidation of **162** with benzaldehyde **105** did not furnish any of the desired epoxide (Scheme 59). In all of these reactions the diazo species was decomposed completely but gave a mixture of undesired products.

Scheme 59: Unsuccessful reactions of methyl phenyldiazoacetate **162** in flow

4.6.1 General kinetic properties of diazo decomposition

Four of the reactions discussed previously (Table 4.3, entries 1-4) provided quantitative data on the decomposition of the diazo species **162** in the infrared spectra. This quantitative analysis was achieved by using a calibrated value for the C=O stretch of the ester carbonyl. Interestingly, the rate of decomposition was substrate independent (Figure 30). In all cases, no diazo decomposition was observed at 25 °C within ten minutes reaction time. At 40 °C, diazo compound was still relatively stable in ten minutes reaction time (80-90% of diazo reagent **162** present). However, at 60 °C most of the diazo reagent **162** was decomposed in ten minutes. The percentage of diazo reagent **162** does not go down to 0% as a slight overlap of the formed ester carbonyl functionality in the infrared analysis was inevitable. The substrate independence of the diazo decomposition reaction can be rationalised by considering the formation of the metal carbene species as the rate-determining step. Once the metal carbene is formed from the diazo reagent, the subsequent insertion into an activated nucleophilic bond of one of the substrates is very rapid.

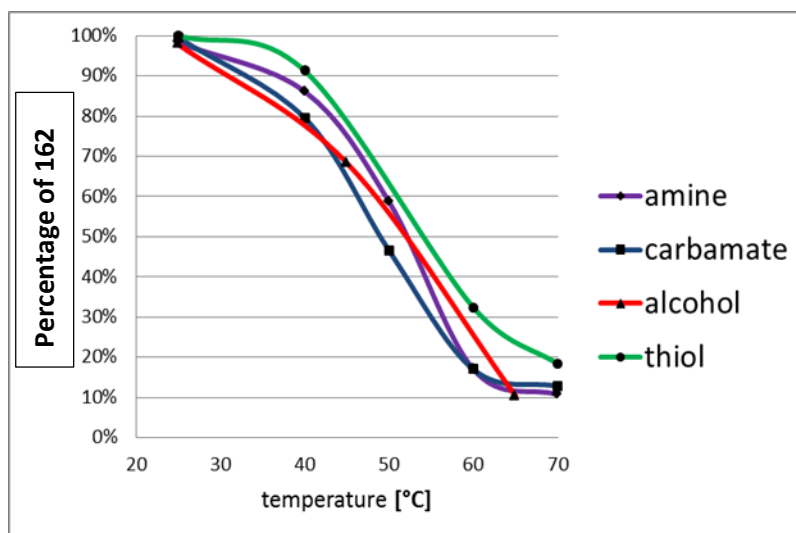
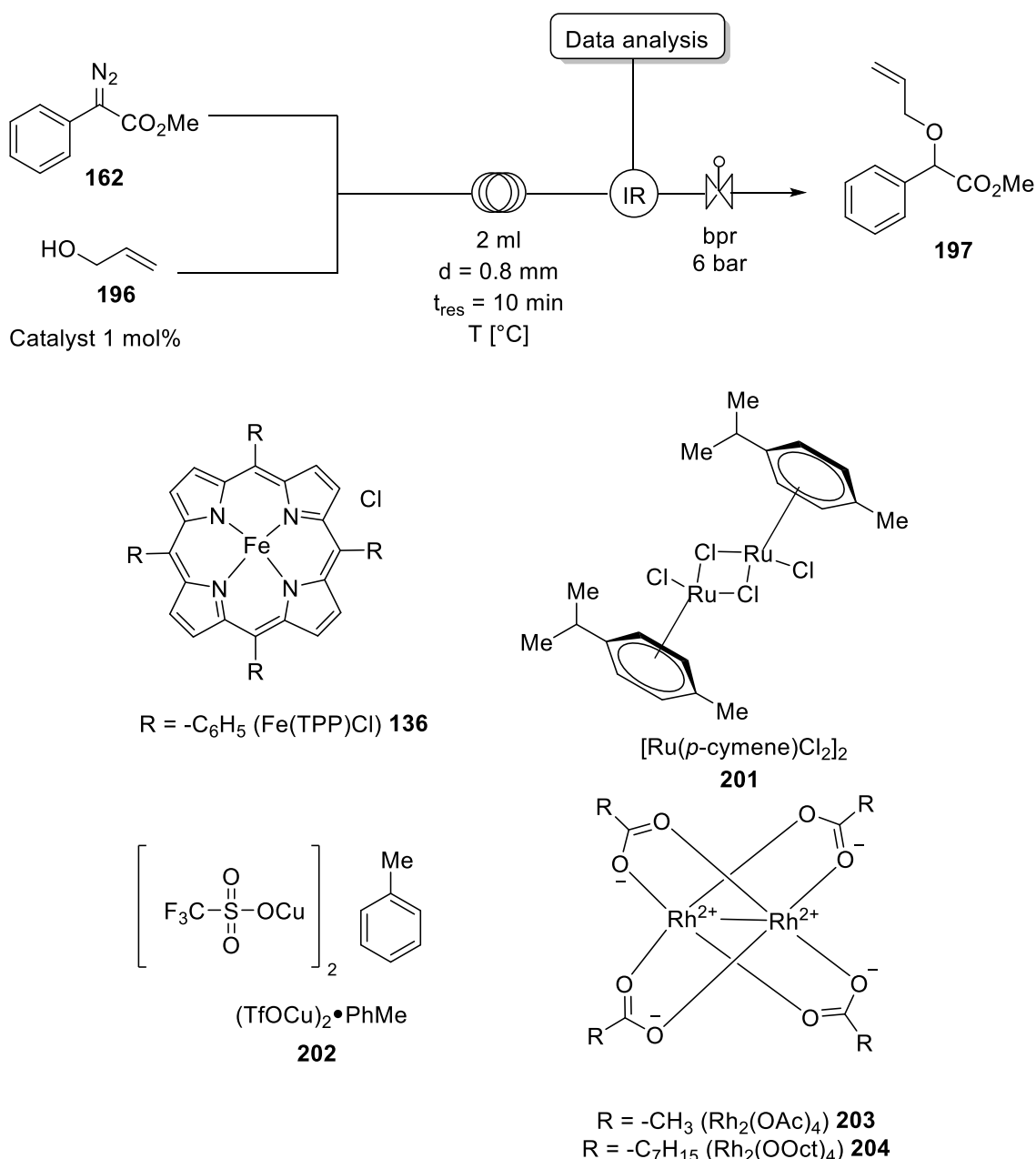


Figure 30: Carbene insertion with four different substrates

4.6.2 Comparison of catalysts for diazo decomposition

Many different metals have been employed for carbene reactions of diazo reagents. Whilst rhodium based catalysts are the most popular and versatile systems, they bear the disadvantage of being expensive. Therefore, metals such as copper, iron and ruthenium have received considerable attention in diazo chemistry. To test the efficiency of different metals for diazo decomposition, the insertion of methyl phenyldiazoacetate **162** into allyl alcohol **196** was investigated using different metal catalysts (Scheme 60). Two rhodium carboxylates were used, namely rhodium acetate dimer **203** and rhodium octanoate dimer **204**. Trifluorosulfonylcopper toluene complex (triflate copper toluene) **202** was used as copper source, iron(III) tetraphenylporphine chloride **136** as iron catalyst and dichloro(*p*-cymene)ruthenium(II) dimer **201** as ruthenium catalyst. For each catalyst, three different reaction temperatures were tested (25 °C, 45 °C and 65 °C). This resulted in 15 data points which were collected in approximately 6 hours. This demonstrates how rapidly reaction conditions can be screened using continuous flow systems.



Scheme 60: Catalyst screening for the allyl alcohol **196** insertion of methyl phenyldiazoacetate **162**

The first finding of this reaction was that neither the iron(III) **136** nor the copper(I) catalyst **202** were effective in decomposing the diazo species **162** under the reaction conditions screened (Figure 31). The ruthenium catalyst **201** promotes the decomposition of the diazo species but the reaction does not proceed to completion even at higher temperatures. Offline HPLC analysis showed that the decomposition of the diazo compound furnished relatively cleanly the desired product at 25 °C, however at 65 °C several by-products were formed. In contrast, both rhodium catalysts were able to efficiently and selectively promote the reaction of methyl phenyldiazoacetate **162** to methyl 2-(allyloxy)-2-phenylacetate **197**. Interestingly, rhodium octanoate **204** proved to be significantly more efficient in this reaction than rhodium

acetate **203**. It is unlikely that the difference between the two rhodium carboxylates derives from electronics as both rhodium catalysts have very similar electronic properties. Therefore, the difference in the reaction rate is likely related to the longer alkyl chain in the case of rhodium octanoate. One possible explanation would be a better solubility of rhodium octanoate **204** in the *n*-heptane / chloroform / acetonitrile solvent system (10 / 9 / 1).

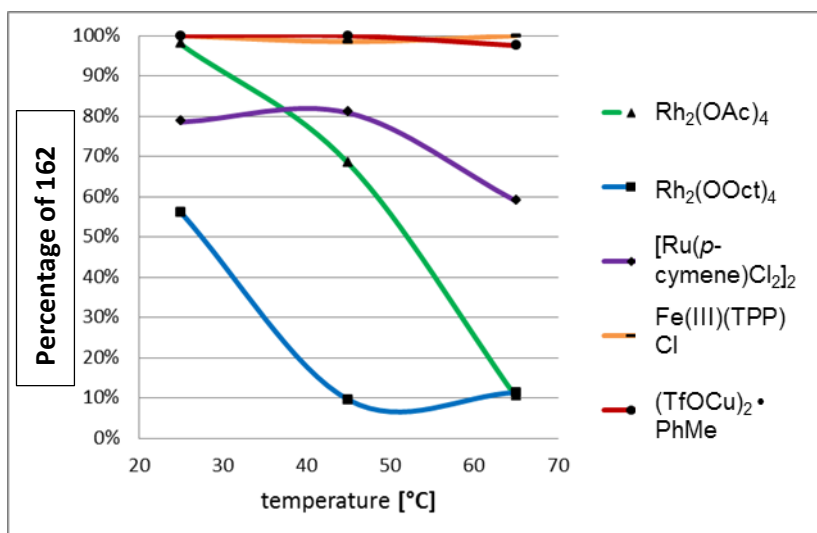
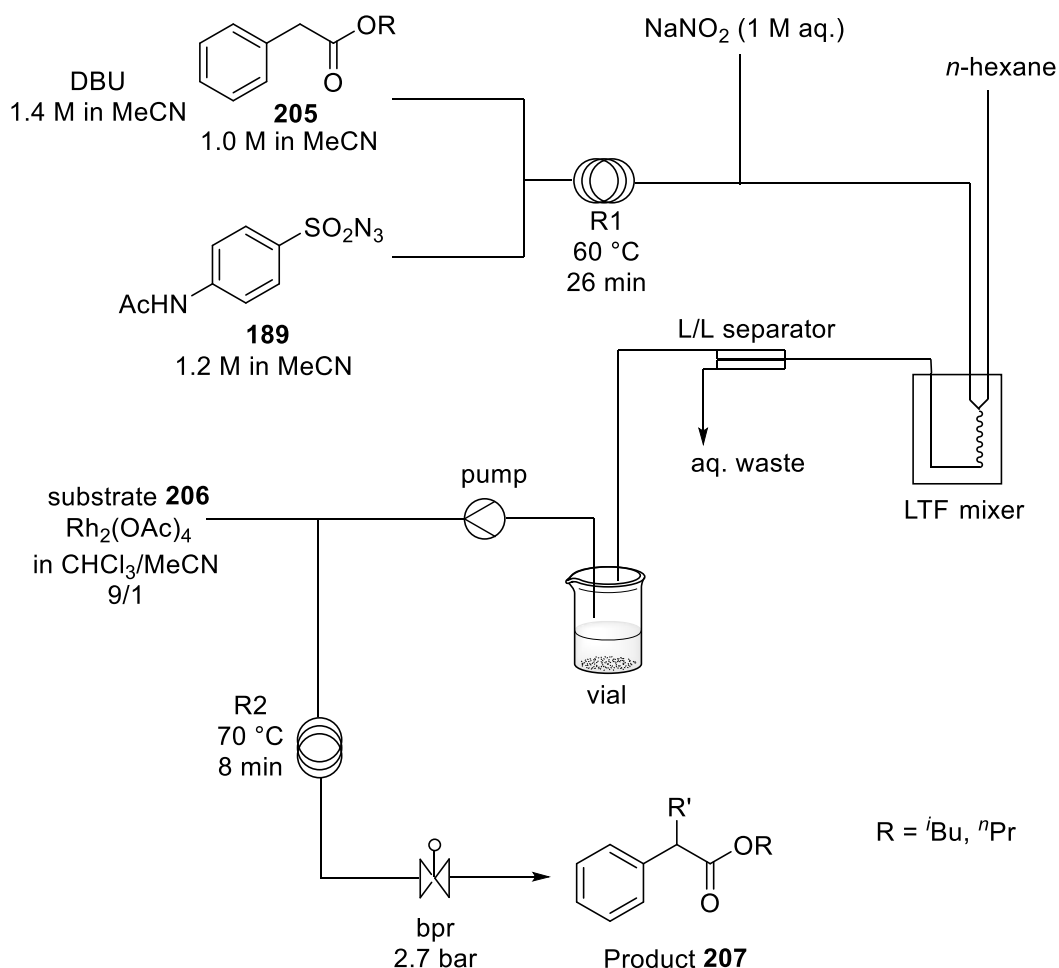


Figure 31: Comparison of different metal catalysts for allyl alcohol insertion into methyl phenyldiazoacetate

4.7 Multistep Process

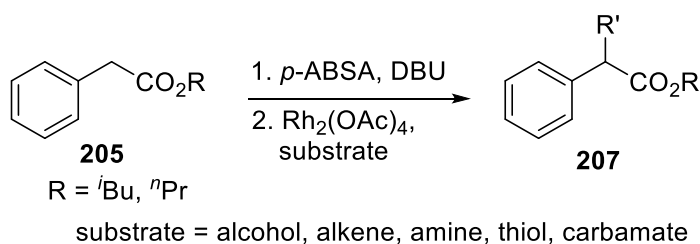
For the development of a safe, reliable and versatile method for the preparation and use of alkyl phenyldiazoacetates, several aspects of the process had been evaluated and optimised. First, the thermal and kinetic properties of the diazo transfer reactions had been investigated (Section 4.3 and 4.4). An optimised continuous flow approach led to a much faster formation of methyl phenyldiazoacetate **162** (Section 4.4.2). Subsequently, an efficient liquid / liquid extraction was developed as method of purification of the diazo species (Section 4.5). Finally, the intermolecular reaction of diazo compounds with a diverse set of substrates to prepare ethers, thioethers, amines, and cyclopropanes was optimised in flow (Section 4.6). With all the results in hand, a multistep continuous flow process was designed (Scheme 61). Instead of methyl phenylacetate, *iso*-butyl- and *n*-propyl phenylacetate were used as starting materials. This choice was made as the extraction was found to be much more efficient when longer alkyl chains ($n \geq 3$) were utilised for the ester group (see Section 4.5). In the first reactor, phenyldiazoacetate was generated in the optimised diazo transfer conditions. Then, a solution of aqueous one molar NaNO_2 was added to the stream which was pumped into a LTF[®] glass mixer. There, the diazo reagent was extracted using a stream of *n*-hexane and the two layers were separated using a membrane separator (also see Section 5.2.3 for details on the

separator). The organic layer was pumped from the collection vial into the next microreactor and combined with a solution of substrate **206** with $\text{Rh}_2(\text{OAc})_4$ as catalyst in a 9 / 1 mixture of chloroform and acetonitrile. The reagent stream was passed through a second reactor coil with a back-pressure regulator (bpr) to give a broad range of products **207**. The total residence time within the system was around 45 minutes.



Scheme 61: Multi-step continuous flow set-up for donor / acceptor carbenes

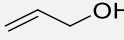
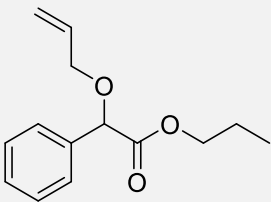
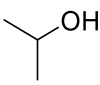
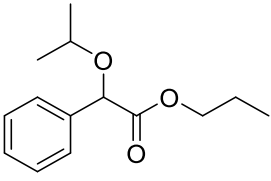
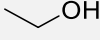
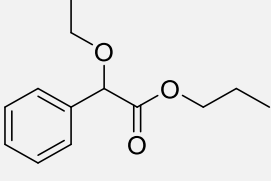
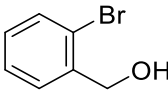
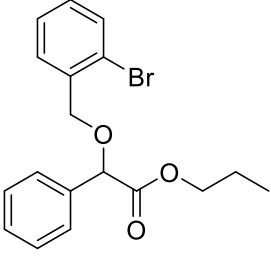
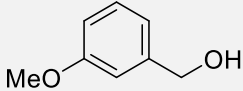
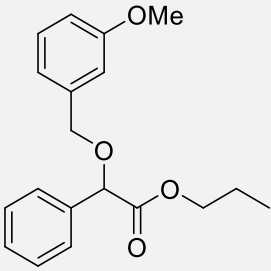
Using this system, a broad range of intermolecular carbene reactions were performed. Among the substrates tested were alcohols, alkenes, an amine, a thiol and a carbamate (Scheme 62).

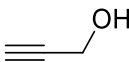
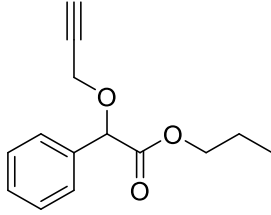
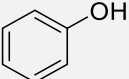
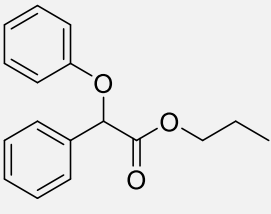
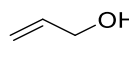
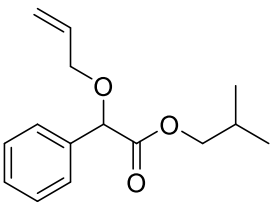


Scheme 62: Reaction scheme for multi-step process

Alcohol insertion reactions worked very well with high yields considering the complexity of the system (Table 4.4, entries 1-5, 71-78% yield). For this, it made no difference if it was a primary (Table 4.4, entries 1, 3-5) or secondary alcohol (Table 4.4, entry 2). Benzylic alcohols worked well (Table 4.4, entries 4-5) In contrast, using phenol as substrate did not give any of the desired product (Table 4.4, entry 7). Propargyl alcohol gave a slightly lower yield than aliphatic and allylic primary alcohols (Table 4.4, entry 6). The reaction of the *iso*-butyl ester starting material with allyl alcohol provided product **207h** in 62% yield (Table 4.4, entry 8).

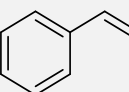
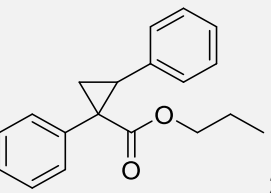
Table 4.4: Substrate scope for alcohol insertion of donor/acceptor carbenes

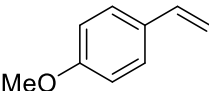
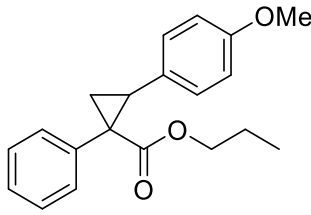
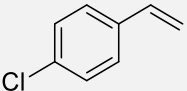
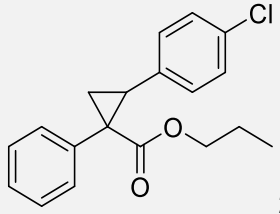
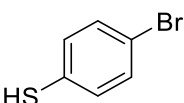
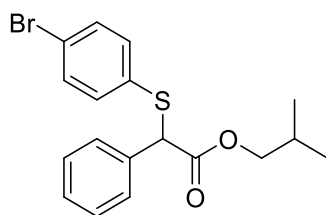
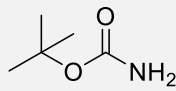
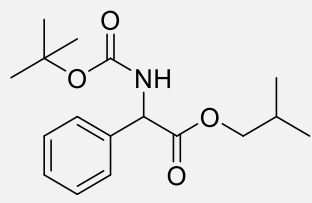
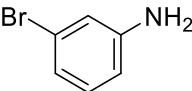
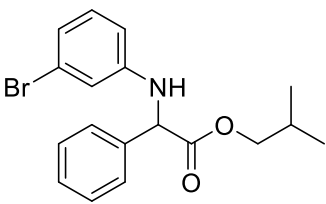
Entry	R of Ester	Substrate	Product	Yield [%]
1	<i>n</i> -Propyl	 196	 207a	72
2	<i>n</i> -Propyl	 206b	 207b	72
3	<i>n</i> -Propyl	 206c	 207c	77
4	<i>n</i> -Propyl	 206d	 207d	71
5	<i>n</i> -Propyl	 206e	 207e	72

6	<i>n</i> -Propyl	 206f	 207f	58
7	<i>n</i> -Propyl	 206g	 207g	0
8	<i>iso</i> -butyl	 196	 207h	62

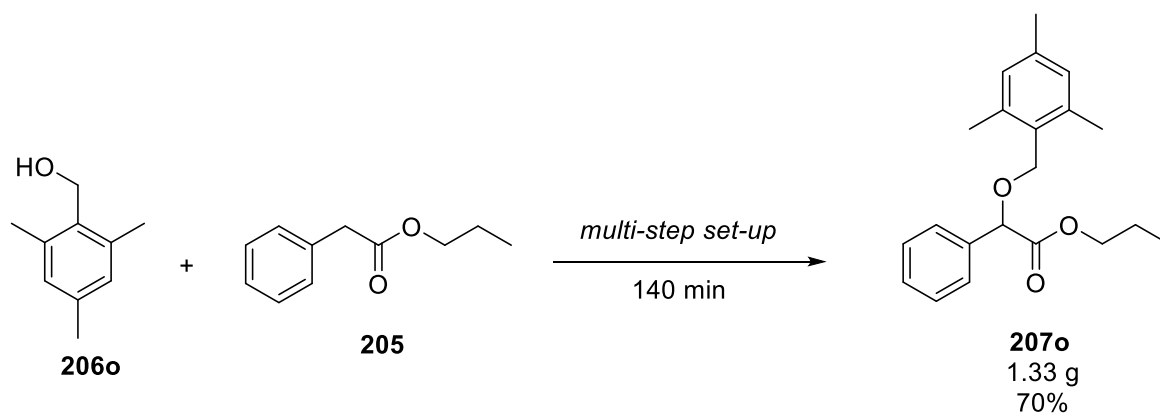
For the cyclopropanations, 5 equivalents of substrate were used instead of 1.7 equivalents as for the other substrates (Table 4.5, entries 1-3). A large excess (5-10 equiv.) of alkene is used in most cyclopropanation reactions with diazo compounds.²³ Yields were moderate in all cyclopropanation reactions but highly diastereoselective (*d.r.* > 98:2; 46-56% yield), the more nucleophilic 4-methoxystyrene gave a slightly improved yield (Table 4.5, entry 2). Thiol insertion using 4-bromothiophenol with the isobutyl substrate worked very well (75%, Table 4.5, entry 4). A very interesting reaction was the use of carbamates for the multi-step protocol, as the resulting products could subsequently be deprotected and give useful unnatural amino acids. The reaction with Boc-protected amine **206m** worked well, providing **207m** in 66% yield (Table 4.5, entry 5). In contrast, using 3-bromoaniline **198a** for an intermolecular N-H insertion gave a somewhat reduced yield (49%, Table 4.5, entry 6). The reason for this was that **207n** reacted with another molecule of 3-bromoaniline **198a** to give 28% of the corresponding amide product.

Table 4.5: Substrate scope for donor / acceptor carbene reactions

Entry	R of Ester	Substrate	Product	Yield [%]
1	<i>n</i> -Propyl	 206i	 207i	47

2	<i>n</i> -Propyl	 198d	 207j	56
3	<i>n</i> -Propyl	 206k	 207k	46
4	<i>iso</i> -butyl	 206l	 207l	75
5	<i>iso</i> -butyl	 206m	 207m	66
6	<i>iso</i> -butyl	 198a	 207n	49

After screening a diverse class of substrates, it was tested if the system was also scalable. For this purpose, 2,4,6-trimethylbenzyl alcohol was reacted with *n*-propyl phenylacetate using the same system by scaling out. The reaction mixture was collected for 140 min to give 1.33 g (4.1 mmol) of **207o** in 70% yield, demonstrating the scalability of the multi-step set-up (Scheme 63).



Scheme 63: Upscale of multi-step set-up

4.8 Conclusion & Outlook

In this chapter, a new protocol for the preparation and use of phenyl diazoacetates was described. The diazo transfer to make these diazo reagents starting from the corresponding esters was carefully studied for the thermal and kinetic properties. The switch from a batch to a continuous flow protocol made higher temperatures for this reaction accessible which led to much shorter reaction times (to 26 min down from 6 hours). The rapid optimisation of this continuous flow reaction was possible due to the use of in-line infrared spectroscopy. Subsequently, an efficient extraction protocol was developed to circumvent the need of column chromatography of the diazo species. The rapid diazo decomposition in multiple carbene insertion reactions was performed in flow using in-line infrared spectroscopy. Finally, a multi-step flow set-up was developed in which the diazo species was first prepared, then purified through liquid / liquid extraction in flow and finally used in a multitude of carbene reactions. The newly developed protocol proved sufficiently stable to provide access to gram quantities of products.

After having established this continuous flow protocol for donor / acceptor carbenes, the next chapter will use the same class of compounds for the construction of heterocycles. These reactions will provide rapid access to structurally complex molecules of biological interest.

References

- 1 H. M. L. Davies, J. R. Denton, *Chem. Soc. Rev.* **2009**, 38, 3061.
- 2 T. M. Gregg, M. K. Farrugia, J. R. Frost, *Org. Lett.* **2009**, 11, 4434.
- 3 H. M. L. Davies, L. Rusiniak, *Tetrahedron Lett.* **1998**, 39, 8811.
- 4 H. M. L. Davies, T. Hansen, M. R. Churchill, *J. Am. Chem. Soc.* **2000**, 122, 3063.
- 5 a) D.-H. Wang, J.-Q. Yu, *J. Am. Chem. Soc.* **2011**, 133, 5767; b) H. Wang, G. Li, K. M. Engle, J.-Q. Yu, H. M. L. Davies, *J. Am. Chem. Soc.* **2013**, 135, 6674.
- 6 J. Yang, H. Wu, L. Shen, Y. Qin, *J. Am. Chem. Soc.* **2007**, 129, 13794.
- 7 a) M. Regitz, *Angew. Chem. Int. Ed. Engl.* **1967**, 6, 733-749; b) M. Regitz, *Synthesis* **1972**, 351.
- 8 a) M. Regitz, J. Rüter, *Chem. Ber.* **1968**, 101, 1263; b) M. Regitz, F. Menz, *Chem. Ber.* **1968**, 101, 2622.
- 9 a) R. L. Danheiser, R. F. Miller, R. G. Brisbois, S. Z. Park, *J. Org. Chem.* **1990**, 55, 1959; b) D. W. Norbeck, J. B. Kramer, *J. Am. Chem. Soc.* **1988**, 110, 7217; c) D. F. Taber, R. B. Sheth, P. V. Joshi, *J. Org. Chem.* **2005**, 70, 2851.
- 10 F. W. Bollinger, L. D. Tuma, *Synlett* **1996**, 407.
- 11 a) H. Spencer, *Chem. Brit.* **1981**, 17, 106; b) D. Rewicki, C. Tuchscherer, *Angew. Chem. Int. Ed. Engl.* **1972**, 11, 44.
- 12 C. J. Cavender, V. J. Shiner, *J. Org. Chem.* **1972**, 37, 3567.
- 13 E. D. Goddard-Borger, R. V. Stick, *Org. Lett.* **2011**, 13, 2514.
- 14 N. Fischer, E. D. Goddard-Borger, R. Greiner, T. M. Klapötke, B. W. Skelton, J. Stierstorfer, *J. Org. Chem.* **2012**, 77, 1760.
- 15 J. S. Baum, D. A. Shook, H. M. L. Davies, H. D. Smith, *Synth. Comm.* **1987**, 17, 1709.
- 16 M. Kitamura, S. Kato, M. Yano, N. Tashiro, Y. Shratake, M. Sando, T. Okauchi, *Org. Biomol. Chem.* **2014**, 12, 4397.
- 17 F. Stoessel, *Process Saf. Environ.* **2009**, 87, 105.
- 18 F. Stoessel, H. Fierz, P. Lerena, G. Killé, *Org. Proc. Res. Dev.* **1997**, 1, 428.
- 19 For more information: F. Stoessel *Thermal Safety of Chemical Processes*, Wiley, Weinheim, **2008**.
- 20 F. E. Valera, M. Quaranta, A. Moran, J. Blacker, A. Armstrong, J. T. Cabral, D. G. Blackmond, *Angew. Chem. Int. Ed.* **2010**, 49, 2478.
- 21 C. J. Smith, N. Nikbin, S. V. Ley, H. Lange, I. R. Baxendale, *Org. Biomol. Chem.* **2011**, 9, 1938.
- 22 Picture obtained from Pierre Fabre company.
- 23 C. Qin, V. Boyarskikh, J. H. Hansen, K. I. Hardcastle, D. G. Musaev, H. M. L. Davies, *J. Am. Chem. Soc.* **2011**, 133, 19198.

5 Synthesis of heterocycles using diazo compounds

5.1 General Introduction

In the previous chapter, the use of donor / acceptor substituted diazo compounds for a wide range of reactivity was described. Herein, the application of this reactivity for the preparation of heterocyclic structures is discussed. Two particular structural frameworks were the targets of this work (Figure 32). Firstly, the bicyclic lactone **208** is the key intermediate in the preparation of the drug molecule milnacipran, as well as analogues of it.¹ Secondly, dihydroindoles such as **209** are privileged structures that have found widespread application as pharmaceuticals.²

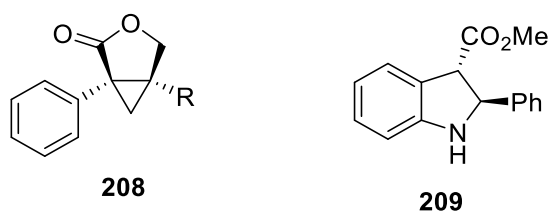
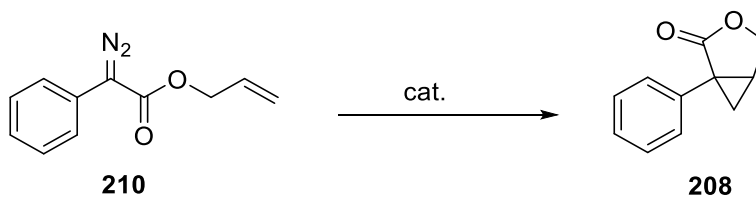


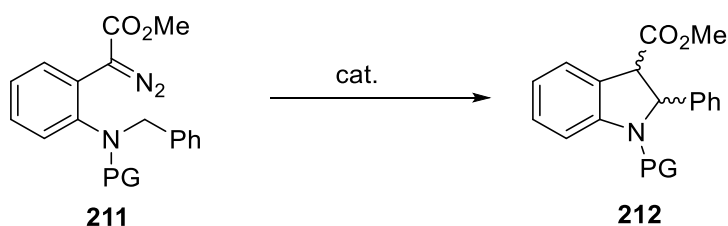
Figure 32: General structure of bicyclic lactone **208** and dihydroindole **209**

Lactone **208** can be prepared by several synthetic routes. The intramolecular cyclopropanation of allyl diazophenylacetate **210** provides a rapid way of generating the structural complexity of bicyclic lactone **208** from a simple starting material (see Scheme 64). Considering the structural similarity of allyl diazophenylacetate **210** to the diazo reagents discussed in chapter 4, a strategy of a diazo transfer reaction onto allyl phenylacetate followed by a continuous liquid / liquid extraction to isolate diazo reagent **210** could be envisioned.



Scheme 64: Synthesis of bicyclic lactone **208** via intramolecular cyclopropanation of **210**

The use of a diazo reagent for the synthesis of dihydroindoles **209** can be rationalised from an intramolecular C-H insertion reaction of the *ortho*-amino derivative of a diazo phenylacetate **211**. Controlling the stereochemistry of the two adjacent stereocentres in respect of diastereoselectivity and enantioselectivity would pose the main challenge in this synthesis. Interestingly, no flexible and highly stereoselective synthesis of dihydroindoles from diazo compounds is known to this date.



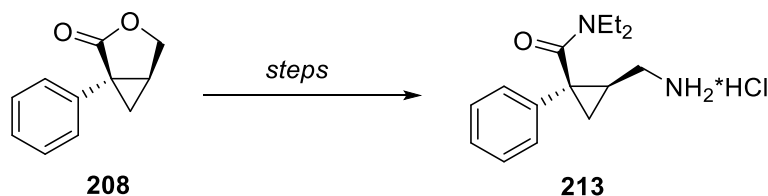
Scheme 65: Synthesis of dihydroindole scaffold **212** via intramolecular C-H insertion of **211**

The first part of this chapter will deal with the intramolecular cyclopropanation for the synthesis of lactone **208** whereas the second part will discuss the stereoselective formation of dihydroindoles.

5.2 Intramolecular Cyclopropanation

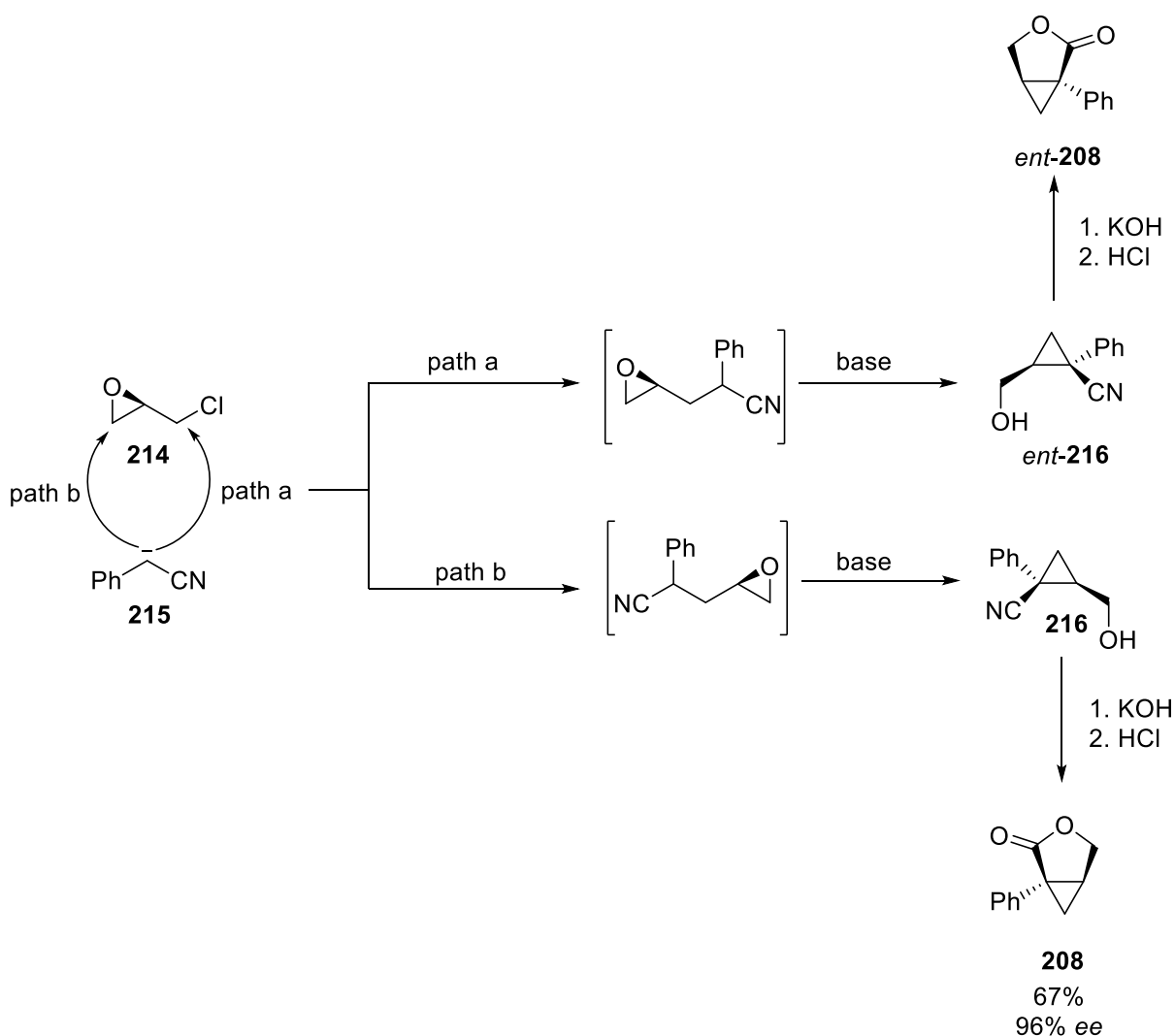
5.2.1 Introduction – Intramolecular cyclopropanation to bicyclic lactone

The importance of the bicyclic lactone **208** stems from its role in the preparation of levomilnacipran **213**, an important serotonin-norepinephrine reuptake inhibitor (SNRI).³ Levomilnacipran is the 1*S*,2*R* enantiomer of milnacipran. As a reuptake inhibitor of serotonin and norepinephrine it is more balanced than other SNRIs such as venlafaxine and duloxetine.⁴ The stereocentres and main features, such as the cyclopropane moiety of levomilnacipran **213**, are carried from the bicyclic lactone **208** (see Scheme 66). The lactone is ring-opened to generate the amide as well as the primary amine in a few relatively simple steps.

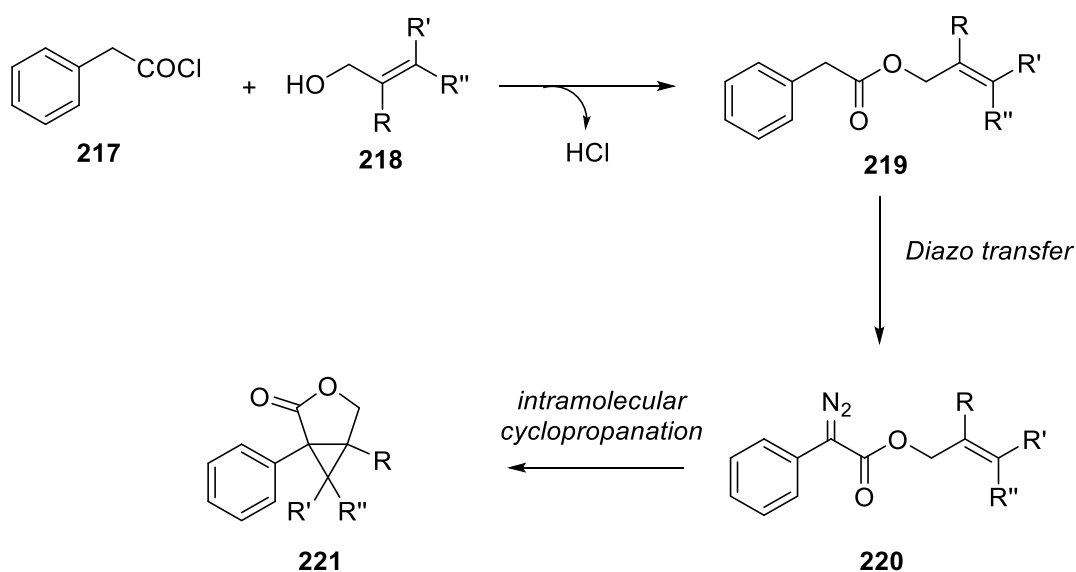


Scheme 66: Synthesis of 1*S*,2*R*-milnacipran **213** from lactone **208**

In one possible synthesis of the key lactone, **208** is generated by a cascade of reactions starting with non-racemic epichlorohydrin **214** and phenylacetonitrile **215**. Sodium amide deprotonates phenylacetonitrile **215** which then reacts as nucleophile with epichlorohydrin **214** to generate the cyclopropane moiety. Interestingly, from the stereochemical outcome of the reaction, the reaction pathway of the nucleophilic attack of phenylacetonitrile anion **215** onto epichlorohydrin **214** can be deduced.⁵ The high ee of 96% of **208** shows that path b completely dominates in which the electrophilic side is positioned at the epoxide (Scheme 67). The alcohol **216** obtained is subsequently transformed into lactone **208** via a two-step process. First, the nitrile functionality is hydrolysed with potassium hydroxide, then the carboxylate is protonated with HCl which leads to the intramolecular lactonisation to **208**.


 Scheme 67: Reaction pathway analysis *via* stereochemical rational

This approach to lactone **208** is scalable and the chiral pool strategy using (*R*)-epichlorohydrin **214** is relatively cheap. However, modifications on the substitution pattern of the system are difficult to install with this route. A diazo based approach to lactone **208**, in contrast, makes diverse substitution patterns easily accessible (Scheme 68). The desired modification would stem from the allyl alcohol used for the preparation of the diazo precursor allyl phenylacetate. Subsequent diazo transfer onto the methylene group of the phenylacetate generates diazo reagent **220** which could undergo an intramolecular cyclopropanation reaction to furnish highly substituted lactone **221**. The substituted milnacipran analogues that can be derived from the modified lactones **221** have already shown promising biological properties and are interesting target molecules in drug discovery.⁶

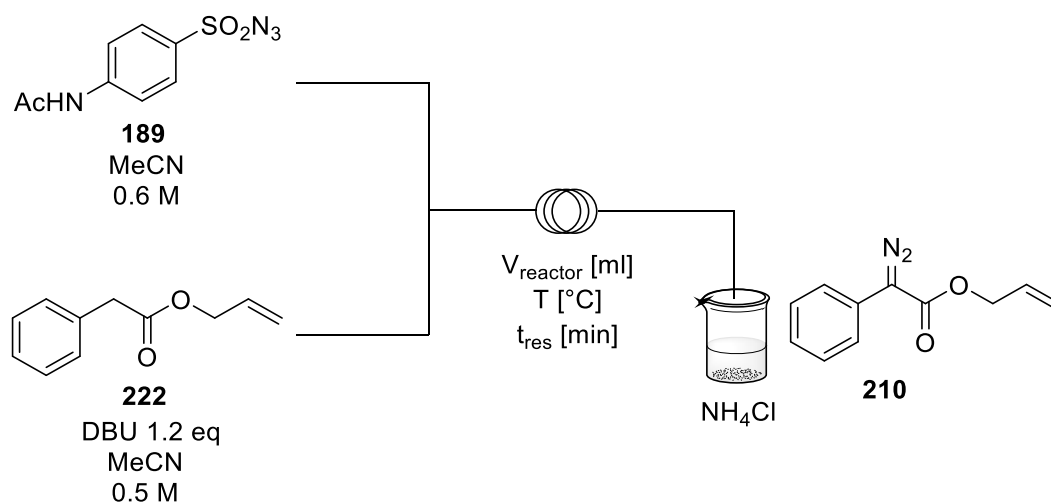


Scheme 68: The diazo based approach to substituted bicyclic lactones **221**; R = alkyl, H; R' = alkyl, H; R'' = alkyl, H

Doyle and Hu described in 2001 the stereochemically defined intramolecular cyclopropanation to lactone **208** from diazo allyl phenylacetate **210** using a chiral rhodium carboxamidate catalyst.⁷ High enantiomeric excess was achieved (up to 95% ee) providing a strong proof of concept for the generation of bicyclic lactone **208** from diazo reagent **210**. A similar approach was recently achieved using a spirobox ligand on an iron-based catalyst. Considering the high costs of rhodium catalysts, the comparatively cheap iron is a welcome replacement in this reaction.⁸ The disadvantage of the flexible diazo approach compared to the approach using epichlorohydrin described in Scheme 67 lies in the scalability of the reaction. The thermal risk of a large scale diazo approach using standard batch conditions was already discussed in section 4.3 and applies equally to the transformation of diazo allylphenylacetate **210** to lactone **208**. Consequently, a continuous flow approach to this reaction was sought to provide a large scale route to highly substituted lactone derivatives **221**.

5.2.2 Diazo Transfer in Flow

The diazo transfer onto allyl phenylacetate **222** was first optimised. For this purpose, a simple one-step flow set-up was designed (Scheme 69). The base that is commonly employed in diazo transfer reactions on phenylacetates, namely DBU, was added to allyl phenylacetate **222** in slight excess (1.2 eq). *p*-Acetamidobenzenesulfonyl azide **189** was charged into a separate syringe and the two acetonitrile solutions were pumped through a PTFE reaction coil. The outlet of the reaction was quenched in an aqueous NH₄Cl solution which, at a later stage of the project, was replaced by an aqueous sodium nitrite solution (see section 4.5).



Scheme 69: Continuous flow optimisation of diazo transfer reaction

The results of the diazo transfer reaction are shown in Table 5.1. At room temperature (22 °C), the ^1H NMR conversion of the diazo transfer reaction is low even at longer reaction times (Table 5.1, entries 1-2). An increase in the temperature to 60 °C leads to a great improvement in conversion at shorter reaction times (Table 5.1, entry 3) and reaches 70% conversion with a residence time of 30 minutes at 60 °C (Table 5.1, entry 4). A further increase in residence time led to only marginal improvements (Table 5.1, entries 5-6). Next, the impact of the concentration of the reaction on the reaction rate was investigated.

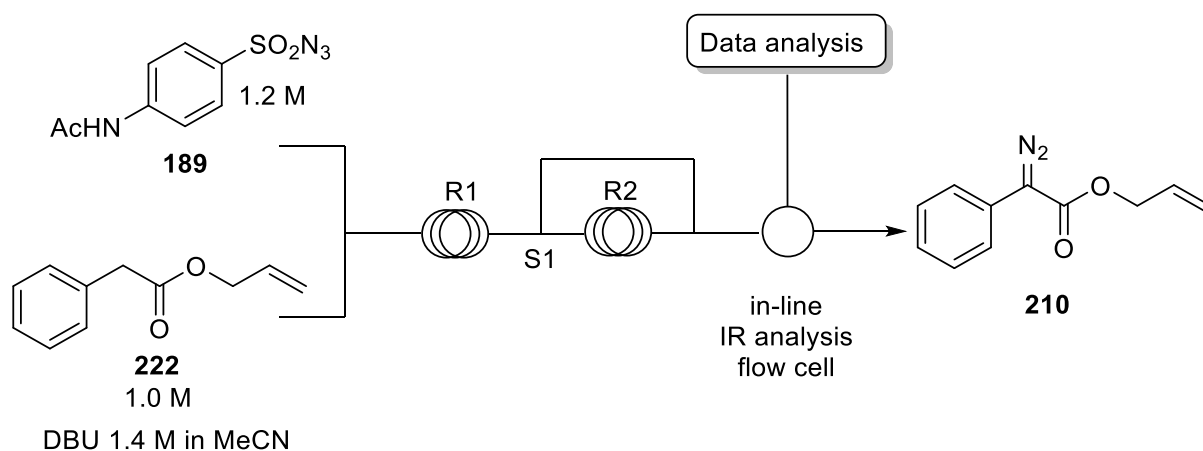
 Table 5.1: Results of diazo transfer onto allyl phenylacetate **222**

Entry	t_{res} [min]	V_{reactor} [ml]	T [°C]	Conversion [%] ^a
1	23	0.9	22	30
2	38	3	22	40
3	15	3	60	50
4	30	3	60	70
5	36	3.6	60	73
6	50	10	60	73

^a determined by ^1H NMR comparing peaks of starting material and product

To collect the data more rapidly, a set-up similar to the one in section 4.4 was used. The reaction was studied using in-line infrared spectroscopy in flow (Scheme 70). The results were confirmed qualitatively using offline HPLC analysis. The concentration of allyl phenylacetate was now doubled to 0.5 mol/L in the reaction coil. A switch (S1) was put in place after the first reactor of the flow system to optimise the reaction more rapidly. By using the switch, two data

points could be acquired without the need of restabilising the flow system after changing the reaction conditions.



Scheme 70: Diazo transfer optimised via in-line IR

The results of this approach are shown in Table 5.2. With this approach, yields were consistently higher than those shown in Table 5.1, demonstrating the importance of the concentration for the reaction rate. Short reaction times (8 min) and only moderately high temperatures (40 – 50 °C) gave diazo product **210** already in good yields (Table 5.2, entries 1 + 3). Longer residence times led to a further improvement of the reaction (Table 5.2, entries 2, 4-5, 7). Increasing the temperature over 60 °C gave only slightly higher yields (compare entry 4 with entries 5, 7). A further increase in residence time to 26 min (Table 5.2, entry 6) gave the highest conversion (93%). Compared to the results for methyl phenylacetate (section 4.4.2) the allyl phenylacetate **222** was a slightly more reactive substrate for the diazo transfer reaction.

Table 5.2: Diazo transfer using higher concentrated reaction medium

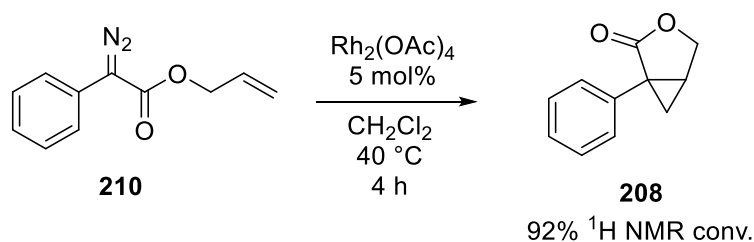
Entry	t_{res} [min]	T [°C]	Yield [%] ^a
1	8	40	64
2	14	50	80
3	8	50	66
4	14	60	84
5	14	65	86
6	26	65	93 ^b
7	14	75	86

^a determined by IR spectroscopy; ^b determined by ¹H NMR

With these results in hand, the intramolecular cyclopropanation of the diazo allyl phenylacetate was next investigated in continuous flow.

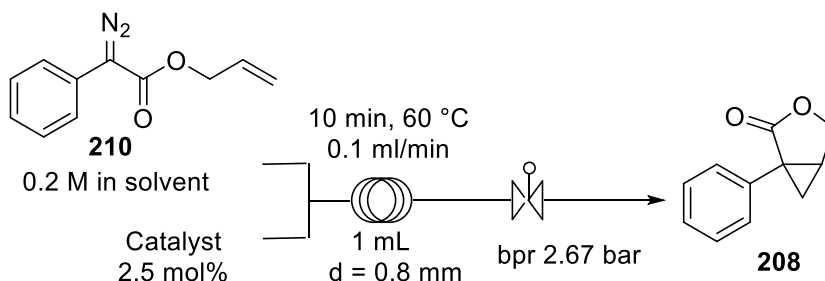
5.2.3 Intramolecular Cyclopropanation in Flow

The intramolecular cyclopropanation of purified diazo allyl phenylacetate **210** to lactone **208** under rhodium catalysis was first investigated in batch by slow addition of the diazo species to a dry dichloromethane solution (40 °C) containing rhodium acetate as the catalyst. The reaction was complete in 4 hours showing a conversion of 92% (¹H NMR) into the lactone without the formation of side products (Scheme 71).



Scheme 71: Batch cyclopropanation

This promising result was subsequently used to study the reaction under continuous flow conditions. In the continuous set-up (Scheme 72), solvents could be superheated due to the use of a back pressure regulator (Table 5.3, entries 1-3, 7).



Scheme 72: Flow set-up for intramolecular cyclopropanation

The conditions best comparable to the batch experiment provided only moderate yield (Table 5.3, entry 1). A possible reason for this could be the low solubility of the catalyst in CH_2Cl_2 . The catalyst was soluble when the reaction solution was prepared under vigorous stirring, however upon loading the syringe used for the addition of the reaction solutions, rhodium acetate started precipitating. Similar findings were observed in some of the other solvents (Table 5.3, entries 1, 3, 5-6). Therefore, the active catalyst loading within the reactor was lower than 2.5 mol% in these cases. The use of acetonitrile to improve the catalyst solubility led only to marginal improvements in the yield (Table 5.3, entry 2). Switching to rhodium octanoate, which is a more soluble catalyst, provided a significant improvement in the yield of lactone **208**.

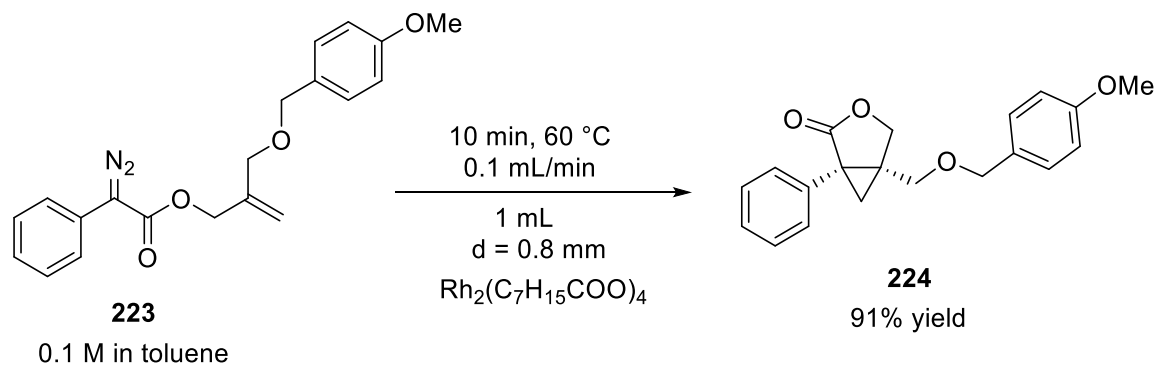
(Table 5.3, entries 3-5). Acetonitrile and dichloromethane as solvents showed similar results (Table 5.3, entries 3, 4). The use of toluene as solvent gave the highest yield (Table 5.3, entry 5). *n*-Hexane did not provide any access to product **208**, presumably due to the complete lack of catalyst solubility (Table 5.3, entry 6). The use of an iron catalyst known for the reaction with diazo compounds in cyclopropanation reactions did not result in any diazo decomposition and all of the starting material was recovered (Table 5.3, entry 7).⁹

Table 5.3: Continuous flow optimisation of intramolecular cyclopropanation

Entry	Solvent ^a	Catalyst [2.5 mol%]	Yield [%] ^b
1	CH ₂ Cl ₂	Rh ₂ (OAc) ₄	27
2	CH ₂ Cl ₂ /CH ₃ CN 9/1	Rh ₂ (OAc) ₄	31
3	CH ₂ Cl ₂	Rh ₂ (C ₇ H ₁₅ COO) ₄	63
4	CH ₃ CN	Rh ₂ (C ₇ H ₁₅ COO) ₄	56
5	Toluene	Rh ₂ (C ₇ H ₁₅ COO) ₄	82
6	<i>n</i> -C ₆ H ₁₄	Rh ₂ (C ₇ H ₁₅ COO) ₄	0
7	CH ₂ Cl ₂	Fe(III)TPPCI	0

^a all solvents were dried before use; ^b isolated yield

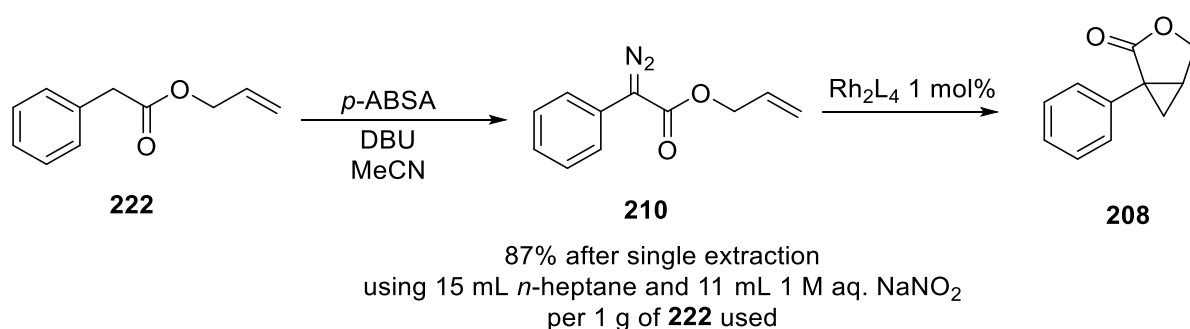
The best continuous flow conditions (Table 5.3, entry 5) were subsequently used for the assembly of a substituted lactone species **224** (Scheme 73). Diazo reagent **223** had been obtained by the diazo transfer reaction onto the corresponding allyl ester. The Pierre Fabre Company, who sponsored this work, had supplied this allyl ester to test the feasibility of the intramolecular cyclopropanation in flow on a complex substituted substrate. Fortunately, cyclopropane **224** was obtained in excellent yield (91%) in just 10 minutes residence time.



Scheme 73: Cyclization of substituted diazo ester **223** in flow

5.2.4 Two-step protocol

After optimising the two steps independently under continuous flow reaction condition, the feasibility of a two-step set-up with a liquid / liquid extraction in between the two synthetic steps was investigated. In analogy to section 4.5, a highly hydrophobic solvent was used to extract the diazo reagent from the acetonitrile solution that had been quenched before with an aqueous sodium nitrite solution. In a two-step batch experiment, diazo reagent **210** was first generated over three days to ensure that no residual starting material was present. The subsequent single extraction provided 87% of diazo allyl phenylacetate **210** (Scheme 74). The solution of *n*-heptane containing **210** was then added to a hot solution of rhodium acetate in the respective solvent.



Scheme 74: Feasibility test for the two step process to lactone **208**

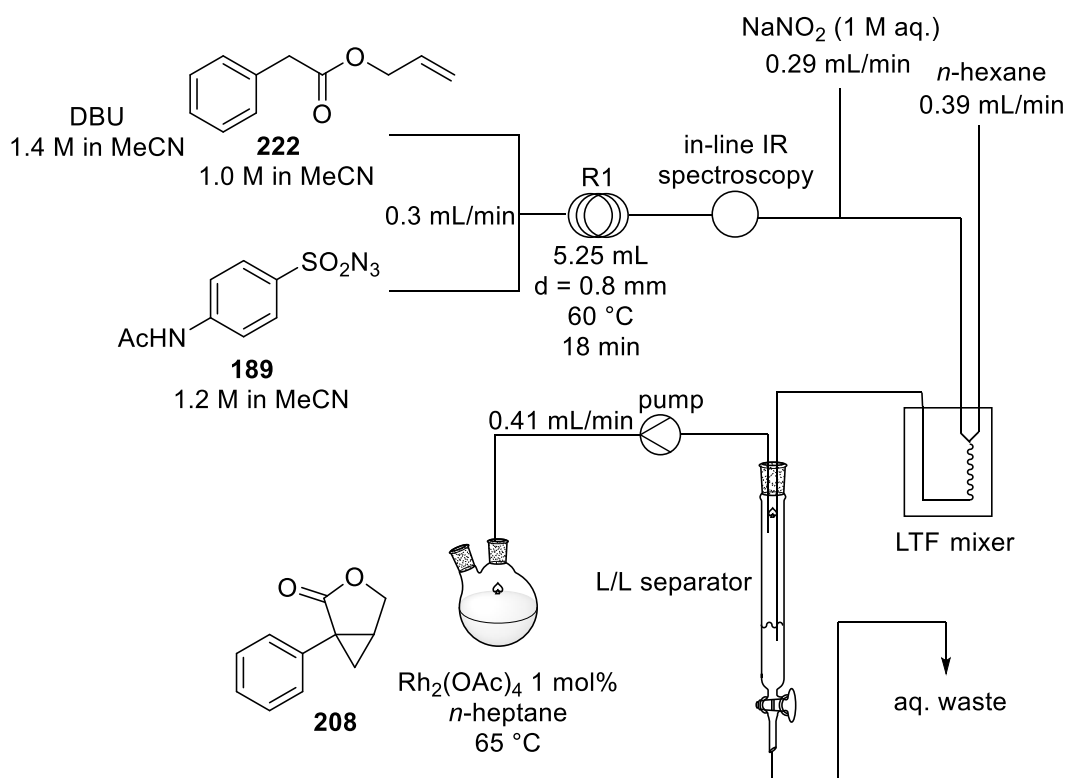
The results of this two-step experiment are shown in Table 5.4. Considering the difficulties in catalyst solubility observed in section 5.1.3, the solubility in different solvent systems in this two-step batch experiment was studied. Using rhodium acetate as catalyst, yields were identical in *n*-heptane and in a solvent mixture of chloroform and acetonitrile (Table 5.4, entries 1 + 3). A mixture of toluene and acetonitrile gave product **208** in slightly lower yield (Table 5.4, entry 2). The experiment in dichloromethane / acetonitrile required a longer reaction time due to the low boiling point of dichloromethane but gave very similar results to the other three experiments (Table 5.4, entry 4). Finally, the best result was obtained when rhodium octanoate was used as the catalyst in *n*-heptane, although catalyst was now completely insoluble (Table 5.4, entry 5). With regards to this observation, a two-step continuous flow into semi-batch approach seemed most applicable considering the insolubility of the rhodium catalysts in many solvents.

Table 5.4: Results of two-steps batch protocol

Entry	Catalyst	Solvent	Catalyst solubility	T [°C]	Time [h]	Yield [%] ^a
1	Rh ₂ (OAc) ₄	<i>n</i> -C ₇ H ₁₆	Insoluble	60	1	59
2	Rh ₂ (OAc) ₄	C ₆ H ₅ CH ₃ :CH ₃ CN 1:1	Traces of solid	60	1	44
3	Rh ₂ (OAc) ₄	CHCl ₃ :CH ₃ CN 1:1	Homogeneous	60	1	59
4	Rh ₂ (OAc) ₄	CH ₂ Cl ₂ :CH ₃ CN 1:1	Homogeneous	35	3.5	51
5	Rh ₂ (C ₇ H ₁₅ COO) ₄	<i>n</i> -C ₇ H ₁₆	Insoluble	60	1	79

^a Two-step yield of lactone **208** determined *via* quantitative HPLC

The continuous flow into semi-batch set-up is described in Scheme 75. In the first reactor coil, diazo reagent **210** is generated using the aforementioned method (section 5.1.2). The stability of this transformation is monitored *via* in-line infrared spectroscopy which is coupled directly after the reactor. Then a feed of aqueous sodium nitrite as quench solution is added, and the hydrophobic extraction solvent *n*-heptane is added next. The mixture then passes through a short glass mixer to ensure an efficient extraction. The reaction stream flows into a gravitational liquid / liquid separation system from which the organic layer is pumped out straight into a flask containing a hot solution of rhodium acetate in *n*-heptane.



Scheme 75: Continuous flow into semi-batch set-up A

No accumulation of the diazo reagent in the round bottom flask was observed making this a safe process towards lactone **208**. The gravitational phase separator used in this experiment was designed in a very similar way to the standard batch type extraction commonly used in organic chemistry laboratories. A narrow bore glass column was filled with aqueous sodium nitrite solution and then stabilised with the reaction stream running into the glass column (Figure 33). The aqueous layer was displaced from the separator *via* a siphon outlet whereas the organic layer was pumped out of the top.

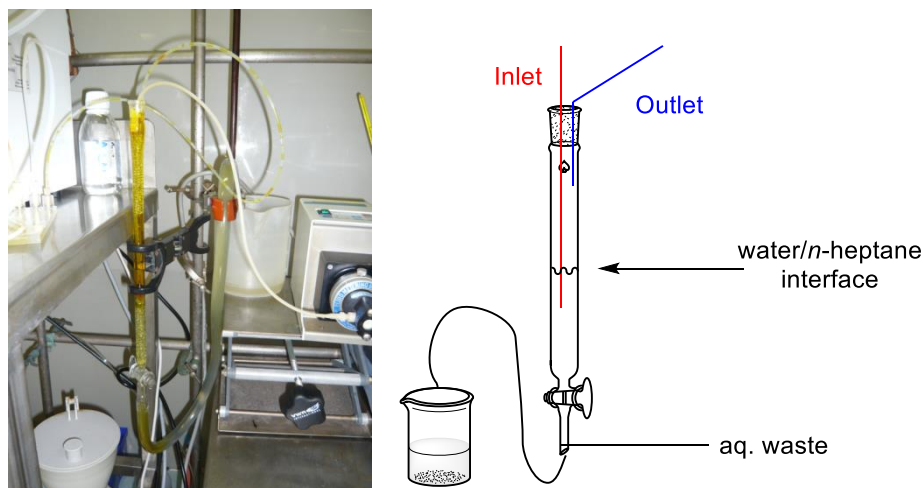


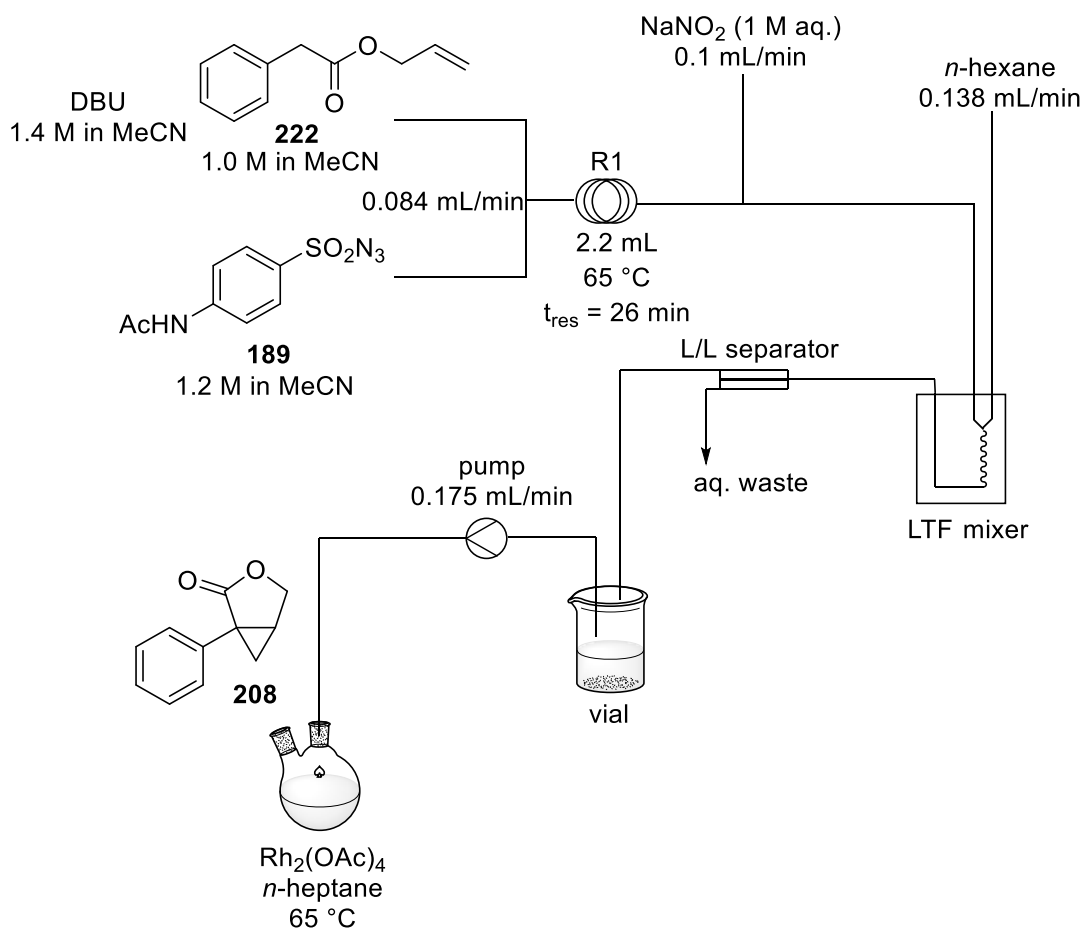
Figure 33: photo of gravitational separator (left); scheme of gravitational separator (right)

Using the set-up from Scheme 75, lactone **208** was obtained in only 31% HPLC yield after two steps. This yield was significantly lower than those observed in the two-step batch approach (e.g. Table 5.4, entry 1). An inefficient diazo transfer could be excluded as possible source of the drop in yield due to the in-line infrared analysis which showed the efficient conversion of allyl phenylacetate **222** into diazo allyl phenylacetate **210**. To determine the possibly detrimental impact of the liquid / liquid extraction on the yield of the transformation, an alternative extraction system was used. The membrane based phase separator used in chapter 4 was deemed applicable to this system (Figure 34). In this device, the organic solvent passes the hydrophobic membrane whereas the aqueous layer remains on the inlet side of the membrane, therefore providing an efficient phase separation.



Figure 34: Membrane separator

With this in mind, a set-up using the membrane separator was designed (Scheme 76). An advantage of this approach was the elimination of the dead volume that was required for the gravitational phase separator. Hence, smaller amounts of reagents were needed to run this experiment. Surprisingly, in this second set-up, using the rhodium acetate catalyst did not lead to any formation of lactone **208**. Switching to rhodium octanoate however provided lactone **208** in a slightly improved 33% isolated yield.



Scheme 76: Continuous flow into semi-batch set-up **B**

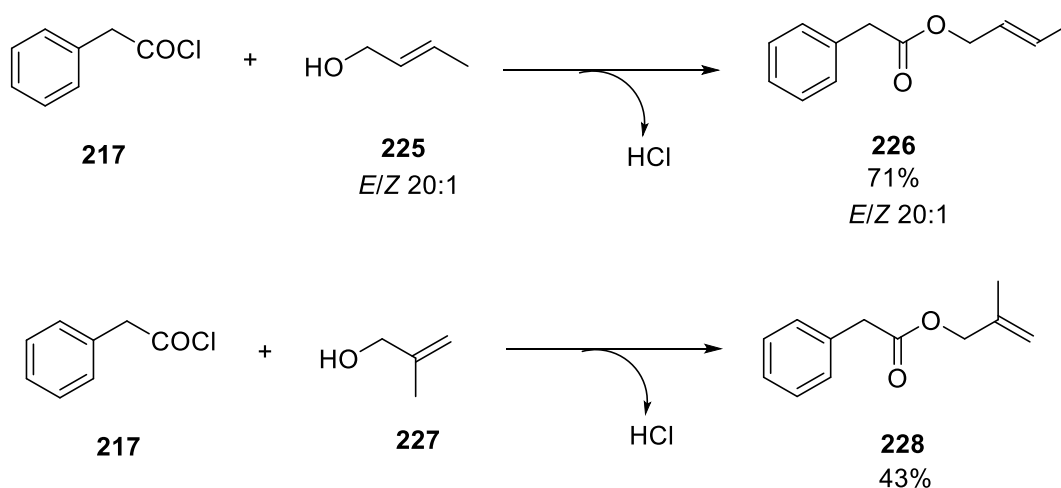
Finally, it was also investigated if the use of a completely continuous process would improve the yield of the transformation. Dichloromethane was used as solvent for the cyclisation as it provided a better solubility of the rhodium catalyst. The yield was surprisingly low, giving lactone **208** in 27% HPLC yield. An overview of the results is shown in Table 5.5. Although the yield is relatively low in all cases, it is interesting that the gravitational separation provided an acceptable yield with rhodium acetate (31%, Table 5.5, entry 1) whereas the membrane separation with the same catalyst only afforded a mixture of side products (Table 5.5, entry 2). The best result was obtained with a membrane separator using rhodium octanoate as the catalyst (Table 5.5, entry 3). These conditions were therefore used to test the feasibility of this method to make substituted analogues of lactone **208**.

Table 5.5: Two-step yields for continuous flow into semi-batch and completely continuous approach

Entry	Separation	Cyclisation	Catalyst (1 mol%)	Yield [%]
1	Gravitational	Semi-batch	Rh ₂ (OAc) ₄	31 ^a
2	Membrane	Semi-batch	Rh ₂ (OAc) ₄	0
3	Membrane	Semi-batch	Rh ₂ (C ₇ H ₁₅ COO) ₄	33 ^b
4	Gravitational	Continuous	Rh ₂ (C ₇ H ₁₅ COO) ₄	27 ^a

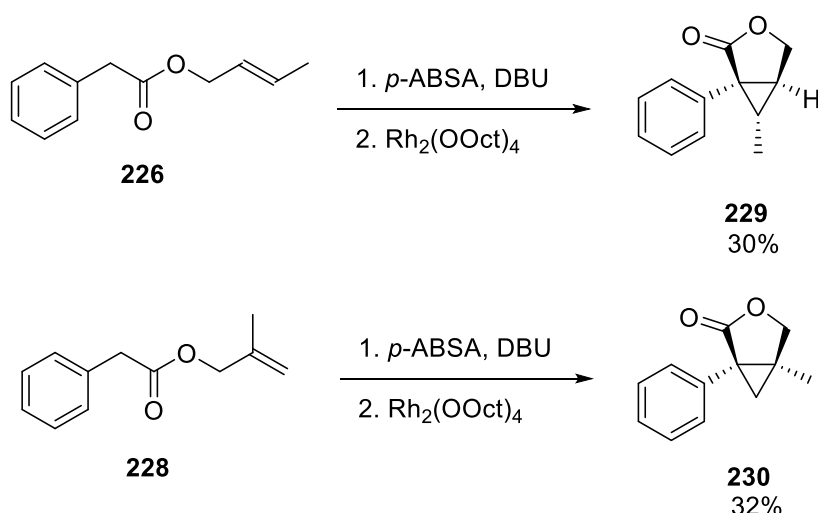
^a HPLC yield; ^b isolated yield

The two methyl substituted analogues of lactone **208** were obtained by reacting freshly prepared phenylacetyl chloride with the corresponding allylic alcohol (Scheme 77). Crotyl alcohol **225** reacted to give allyl product **226** in the same ratio of *E/Z* isomers. A procedure using the *in situ* formation of phenylacetyl chloride using phenylacetic acid and thionyl chloride in dichloromethane and adding to this the allylic alcohol provided very low yield. Therefore, the reaction had to be performed in two separate steps.



Scheme 77: Preparation of substituted allyl phenylacetates

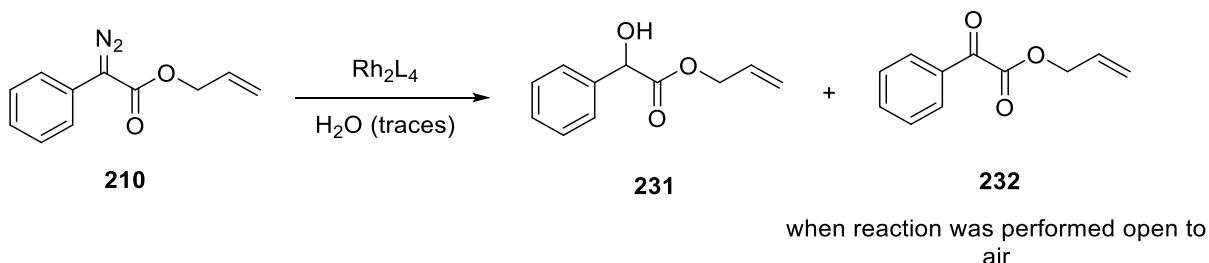
The substituted allyl phenylacetates **226** and **228** were subsequently subjected to the continuous flow into semi-batch protocol described in Scheme 76. The yields for these reactions were very similar to those for lactone **208**. Hence, compounds **229** and **230** were obtained in 30% and 32% yield over two steps, respectively (Scheme 78). Both compounds were obtained as single diastereoisomers.¹⁰


 Scheme 78: Synthesis of substituted lactone analogues **229** and **230**

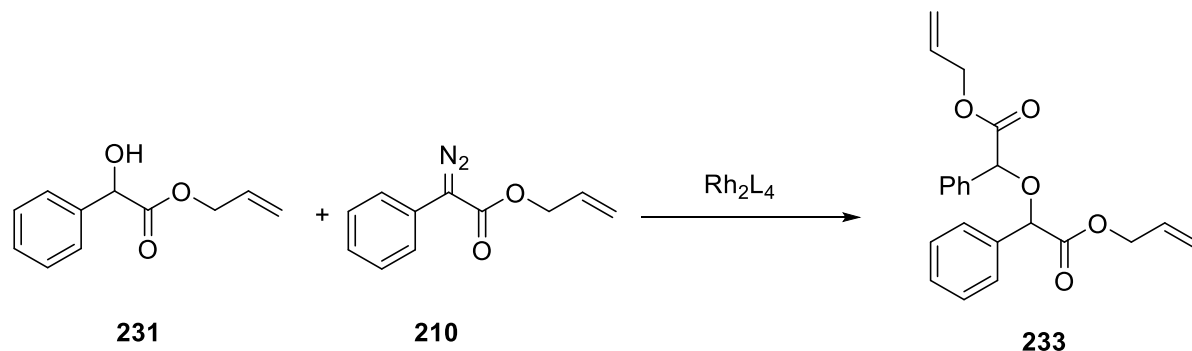
The overall yields of these processes were low and there was a lack in understanding of what factors led to the differences in results between the two-step batch approach and the continuous flow into semi-batch method. To gain a better understanding of the driving forces of the reaction, a detailed side product analysis was performed next.

5.2.5 Side product and error analysis

The crude reaction mixtures were subjected to LC/MS analysis and side products were isolated *via* flash column chromatography. Three main side products for the cyclisation of diazo allyl phenylacetate **210** to lactone **208** were found in all of the reactions above (Table 5.5, entries 1-4). The first one was α -hydroxyester **231**, the formation of which can be rationalised by the O-H insertion of the rhodium carbene derived from diazo reagent **210** into residual water. Interestingly, when the semi-batch transformation was performed open to air, the formation of α -ketoester **232** was also observed, most likely formed either by the oxidation of α -hydroxyester **231** or by the insertion of the metal carbene into oxygen (Scheme 79).¹¹


 Scheme 79: Possible explanation for the formation of compounds **231** and **232**

Another major side product was a dimeric structure with a mass of 366.15 g/mol. This mass would correspond to $m(\mathbf{231}) + m(\mathbf{210}) - m(\text{N}_2)$. Although several such structures can be imagined, isolation and purification of the product showed that ether **233** was formed as confirmed by characterisation of the compound. The best explanation for the formation of ether **233** is the reaction of α -hydroxyester **231** with diazo reagent **210** (Scheme 80). This is especially interesting as it shows that even 0.5 eq. of water could possibly lead to a complete consumption of the diazo reagent in O-H insertion reactions.



Scheme 80: Possible explanation for the formation of the dimeric side product **233**

The third side product was most difficult to analyse. The mass obtained from the LC/MS analysis was 215.09 g/mol. The mass of this compound corresponds to $m(\mathbf{210}) + m(\text{CH}_3\text{CN}) - m(\text{N}_2)$. Traces of acetonitrile could still be around in the cyclisation reaction as it was the solvent of the first reaction in this two-step process, the diazo transfer. However, it was first unclear what type of structure the reaction of acetonitrile with diazo allyl phenylacetate **210** would provide. Figure 35 shows some of the theories proposed at this stage of the project. Product **234** could be obtained via an intermolecular C-H insertion reaction of diazo reagent **210** with acetonitrile.¹² 2H-Azirine **235** could be formed by the insertion of the metal carbene into the C-N triple bond.¹³

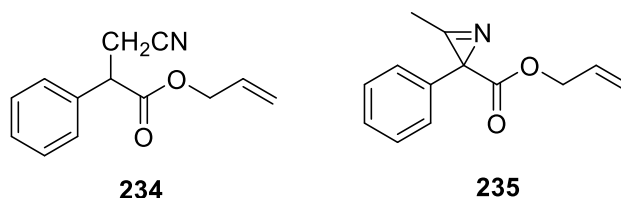
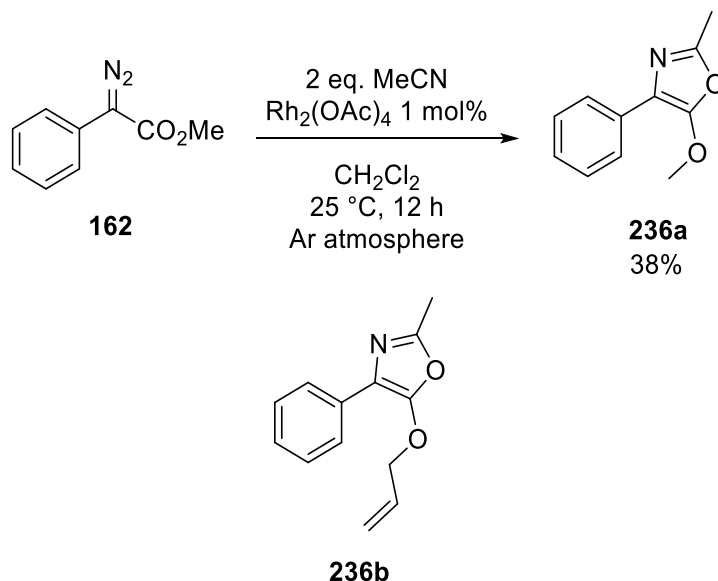


Figure 35: Hypothesised products from the reaction of acetonitrile with diazo allyl phenylacetate

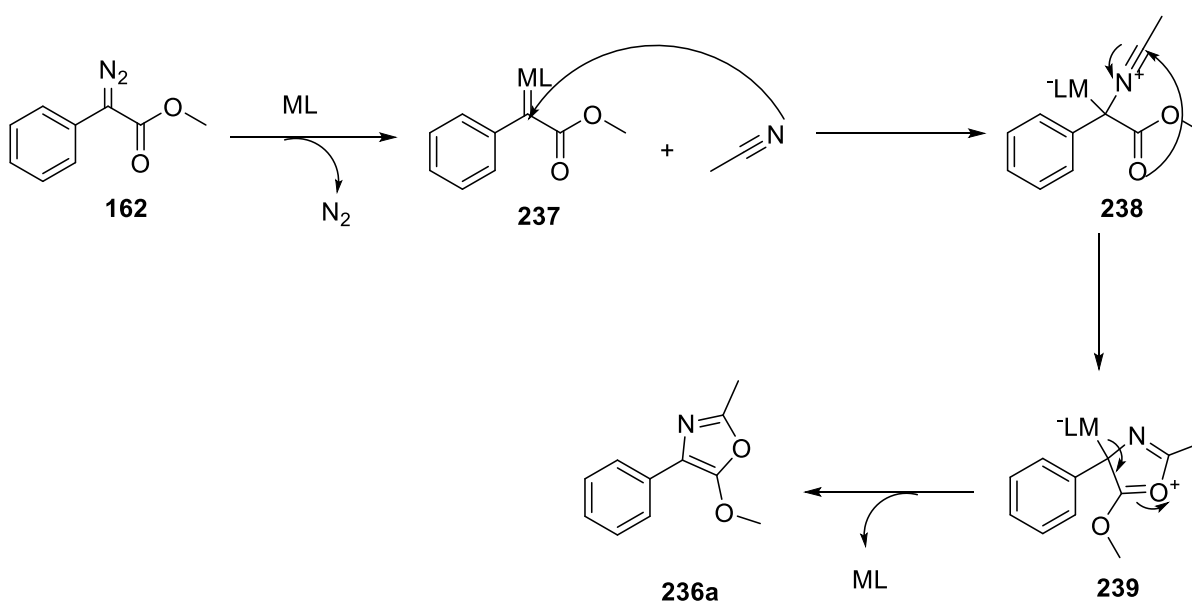
To determine the structure of the unknown product, the simpler diazo methyl phenylacetate **162** was treated with 2 eq. of acetonitrile in dichloromethane under rhodium acetate catalysis. Interestingly, neither the C-H insertion nor the insertion into the C-N triple bond was observed.

Instead, oxazole **236a** was formed in 38% yield (Scheme 81). Therefore, the side reaction of **210** with acetonitrile furnishes oxazole **236b**.



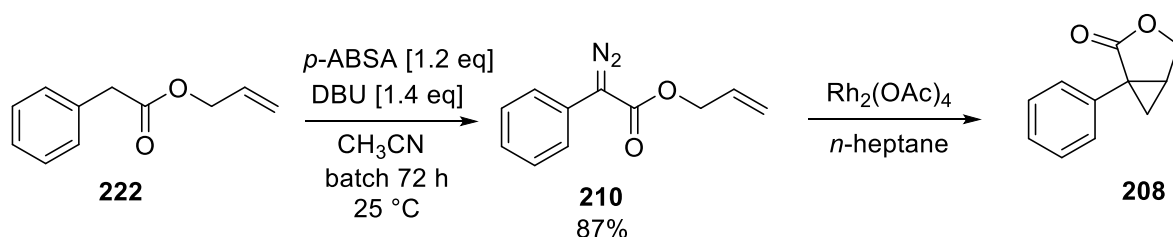
Scheme 81: Formation of oxazoles **236** from diazo methyl phenylacetate **162**

The reaction of diazo compounds with nitriles had already been described.¹⁴ The proposed mechanism of the reaction is shown in Scheme 82. First, metal catalysis cleaves off nitrogen from diazo methyl phenylacetate **162** to generate the corresponding donor / acceptor metal carbene **237**. Acetonitrile now attacks this metal carbene *via* the nitrogen lone pair to generate the zwitterionic moiety **238**. An intramolecular nucleophilic attack of the carbonyl oxygen occurs next onto the carbon of the nitrile functionality to form the five-membered ring **239** which finally provides oxazole **236a** after cleavage of the metal catalyst.



Scheme 82: Possible mechanism for the formation of oxazole **236a**

As the three main side products in the cyclisation reaction had been identified, the question was how easily they were formed and why they were formed in the continuous and semi-batch protocol but less in the two-step batch experiment. One possible explanation could have been the change in rhodium acetate batches that had been used in the experiments. As some of the experiments had been performed at different time points of the project, it had to be verified that the problem did not result from a malfunctioning or oxidised batch of rhodium acetate. Table 5.6 shows the results from this control experiment. All four experiments gave similar yields which were slightly lower than those obtained in Table 5.4. Interestingly, even in the batch experiment around ~ 10% of oxazole **236b** was formed.



Scheme 83: Test of rhodium acetate batches

Table 5.6: Rhodium acetate test

Entry	Rh ₂ (OAc) ₄ opened	Lactone 208 [%] ^a	Dimer 233 [%] ^a	Oxazole 236b [%] ^a	Yield [%] ^b
1	2011	75	5	8	45
2	2012	73	6	9	38
3	16.09.2014	81	2	8	45
4	16.10.2014 ^c	80	2	8	47

^a HPLC ratio; ^b two-step yield of lactone **208** determined by HPLC; ^c opened on the day of the experiment

Next, the impact on traces of water and acetonitrile in the reaction mixture was studied. For this purpose, the same reaction conditions as in Scheme 83 were used. As could be expected, the use of acetonitrile as solvent led to a diminished formation of lactone **208** and to an increased formation of the oxazole side product **236b** (Table 5.7, entry 1). The slight increase in α -hydroxyester **231** and ether **233** can possibly be explained by a greater water content in acetonitrile than in *n*-heptane. The addition of 0.1 equivalents of water into the reaction mixture had no strong impact on the reaction and lactone **208** was observed as main product in the reaction (Table 5.7, entry 2). However, when one equivalent of water was added to the reaction mixture, only traces of lactone **208** could be observed (Table 5.7, entry 3). α -Hydroxyester **231** and ether **233** were the only products observed in these reaction

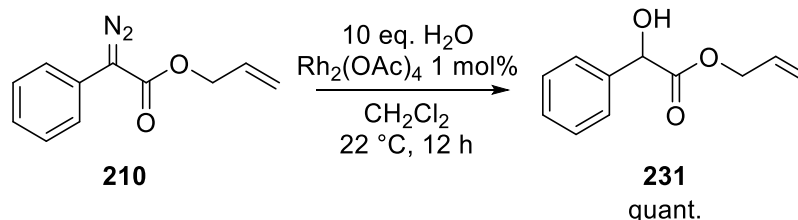
conditions. The ratio of these two products was shifted towards α -hydroxyester **231** compared to the experiments before. In absolute numbers, one equivalent of water represents only a small total amount of water. The reaction was performed on 1 g of diazo reagent **210** (4.95 mmol) which means a volume of 89 μ L water represents one equivalent. The reaction can therefore be classified as highly water-sensitive.

Table 5.7: Influence of acetonitrile and water on reaction conversion

Entry	Conditions	Lactone 208 [%] ^a	Alcohol 231 [%] ^a	Dimer 233 [%] ^a	Oxazole 236b [%] ^a
1	CH ₃ CN as solvent	45	8	11	26
2	0.1 eq H ₂ O added	73	5	6	10
3	1 eq H ₂ O added	1	57	27	1
4	10 eq H ₂ O added	0	99 ^b	0	0

^a HPLC ratio; ^b isolated yield

In fact, when 10 equivalents of water are used in similar reaction conditions (Scheme 84), α -hydroxyester **231** is obtained as the only product in quantitative yield. None of the dimeric ether **233** is found.

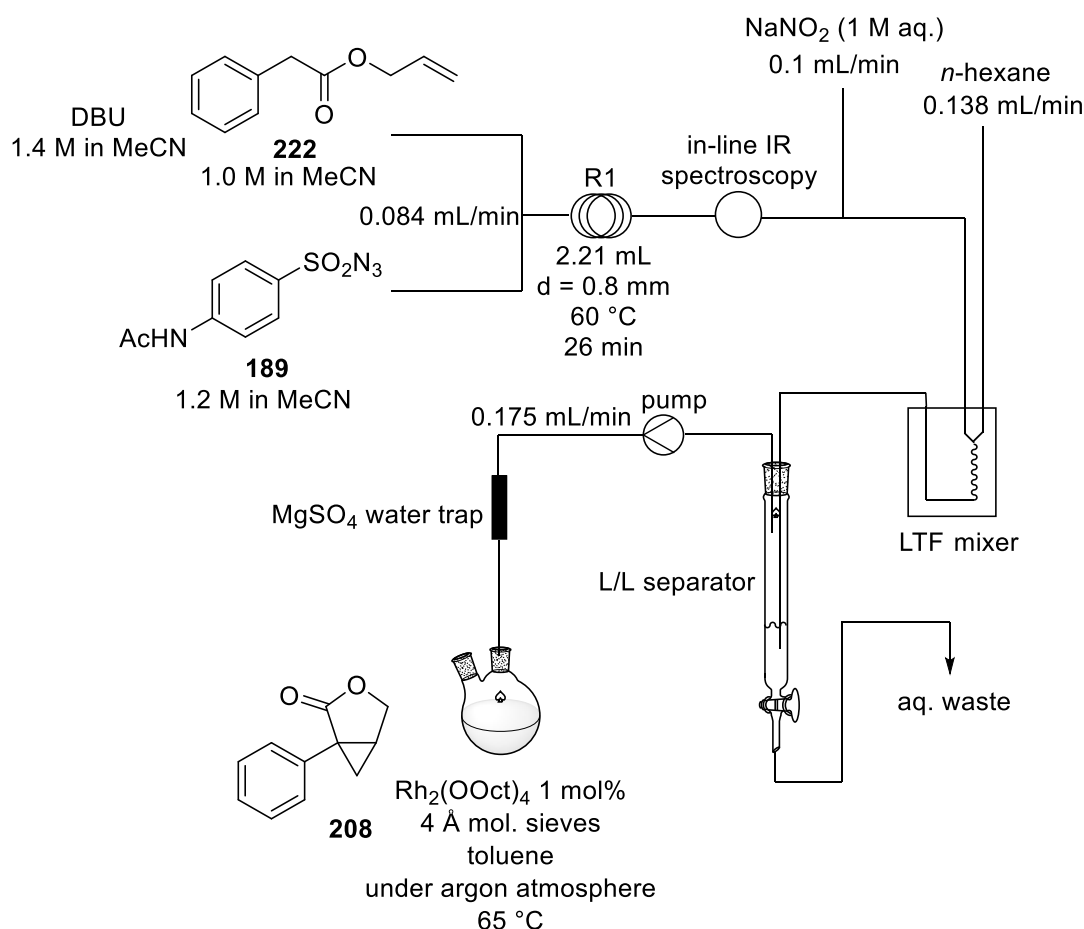


Scheme 84: Impact of water for the cyclisation

With this knowledge about the formed side products and the impact of water and acetonitrile on the reaction, ways to favour the intramolecular cyclopropanation were sought.

5.2.6 Modified two-step protocol

The goal of the modified two-step protocol was to minimize the water content in the final cyclisation reaction and to improve the yield of lactone **208**. The first alterations in the flow set-up to achieve this were to switch from technical grade solvents to dried solvents for the cyclisation, and to keep the round bottom flask for the cyclisation under dry conditions with molecular sieves as a drying agent. A gravitational separator was used instead of the membrane separator as it had given a higher yield in the cyclisation (Table 5.5, entries 1-2). Rhodium octanoate was chosen as catalyst as it had outperformed rhodium acetate (Table 5.5, entries 2-3).



Scheme 85: Modified continuous flow into semi-batch protocol

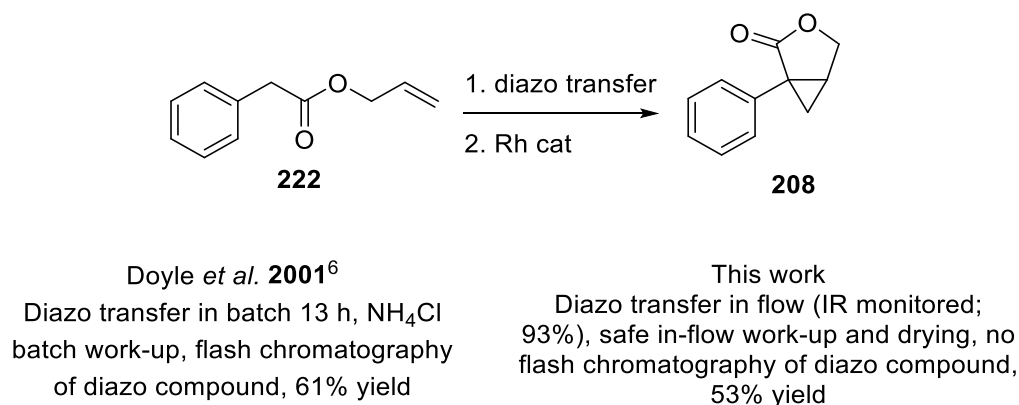
These modifications had a beneficial effect on the cyclisation reaction. The yield for the two-step continuous flow to semi-batch protocol was improved to 40% (Table 5.8, entry 1). Next, other ways to reduce the water content within the reaction were sought. A glass column was filled with MgSO_4 (dry) which was placed between the liquid / liquid extraction and the round bottom flask (Scheme 85). It was hoped that this would trap residual water impurities from the *n*-hexane stream containing the diazo reagent. The MgSO_4 water trap led to an improved yield of 53% (Table 5.8, entry 2). Increasing the amount of MgSO_4 , however, did not lead to further improvements (Table 5.8, entry 3).

Table 5.8: Results of the modification to trap water

Entry	MgSO_4 trap	Yield [%]
1	None	40
2	4 cm x 6 mm (1 g)	53
3	11 cm x 6 mm (2.7 g)	50

The results show that trapping water with MgSO_4 is a possible way of reducing the water content of a reaction after an in-flow liquid / liquid extraction. More detailed investigations into

the efficiency of different drying agents and the importance of the residence time of the reagent stream would be needed to develop generally applicable solvent drying systems in flow. The best result (Table 5.8, entry 2) gave almost the same yield as the one reported for the two-step batch protocol with column chromatography of the diazo reagent in between (61%, Scheme 86).⁴ However, the continuous flow generation of the diazo reagent with the subsequent in-line liquid / liquid separation and in-line drying as well as finally the diazo consumption made this a completely safe approach to the key building block **208**.



Scheme 86: Comparison standard batch protocol and this continuous flow approach

5.2.7 Upscale

For the upscale, larger reactor coils and faster flow rates (times 2.4) were chosen to keep the operating time down. The size of the narrow glass column for the liquid / liquid extraction and the amount of MgSO₄ for the water trapping were not altered. Two 50 mL syringes were used to pump acetonitrile solutions of allyl phenylacetate **222** (1 M) and *p*-acetamidobenzenesulfonyl azide **189** (1.2 M) into the flow system. The other three pumps used were the continuous pumps from the Vapourtec® E-Series (Figure 36). The set-up ran for eight hours with six hours collection time. With this method, 2 g of lactone **208** were obtained (33%). Dimeric ether **233** (1.69 g, 26%) was obtained as main side product indicating that in the upscale more water passed through the system and led to the significant drop in yield. There are two potential explanations for this. Firstly, the faster flow rates in the upscale led to a shorter residence time in the MgSO₄ water trap which made the drying less efficient. Secondly, the MgSO₄ water trap was saturated with water after some time of the experiment and then, water was not trapped efficiently anymore. In either case, a more efficient method for trapping water would be needed to make this process more reliable for scaling.



Figure 36: Upscale of the multistep process for the intramolecular cyclopropanation

In conclusion, the preparation of lactone **208** and substituted analogues was achieved using continuous flow technology. The optimisation of the multistep process towards lactone **208** proved more challenging than the general multistep protocol for donor / acceptor carbenes developed in Chapter 4. Through the careful analysis of side-products and competing reactions it was possible to determine the difficulties within the continuous flow system. This led to a system with which lactone **208** was obtained in 53% yield over two steps without isolation of the diazo species (compared to 61% in standard batch conditions). Unfortunately, the up-scale of the reaction furnished lactone **208** in much lower yield (33%). This shows that the system developed herein would require a more efficient and scalable drying protocol to be scalable to gram and decagram quantities without loss in yield.

5.3 Formation of dihydroindoles

In this section, the synthesis of dihydroindoles using diazo compounds is discussed. This is the only project which does not use continuous flow technology but rather classical batch experiments due to its exploratory nature. Instead, the focus will lie in the development of a high-yielding and stereoselective approach to dihydroindoles using diazo chemistry.

5.3.1 Introduction

Dihydroindoles, or indolines, are a key structure in many biologically active compounds. Highly complex natural products such as vinblastine,¹⁵ strychnine¹⁶ and physostigmine¹⁷ possess the indoline scaffold. Indoline moieties can also be found in drug molecules such as pentopril which is an important ACE inhibitor (Figure 37).¹⁸

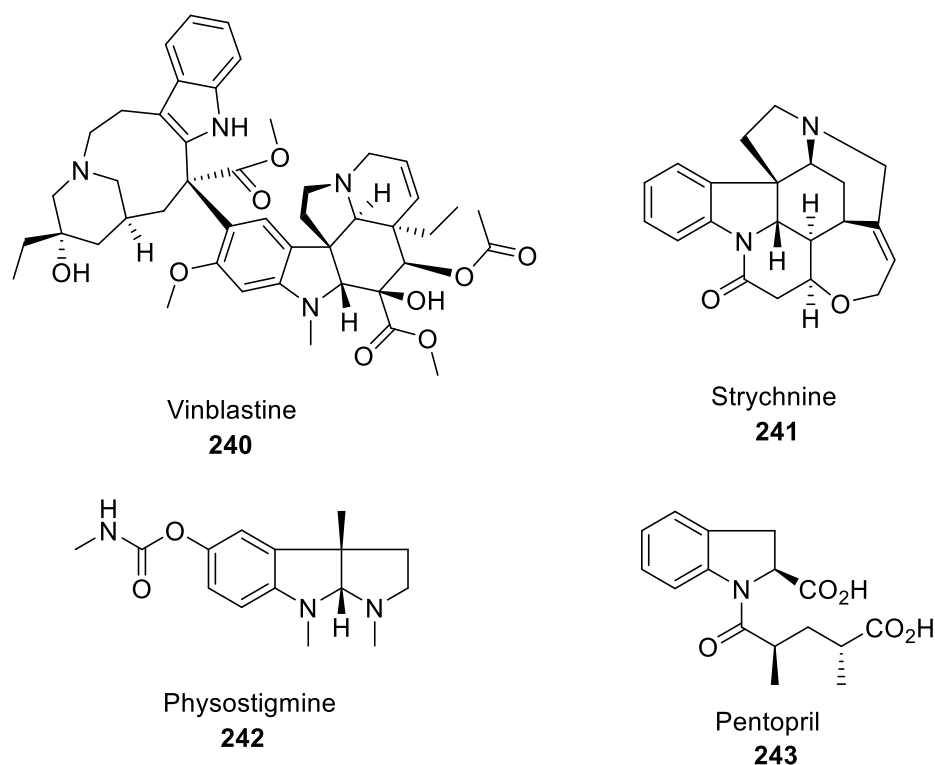
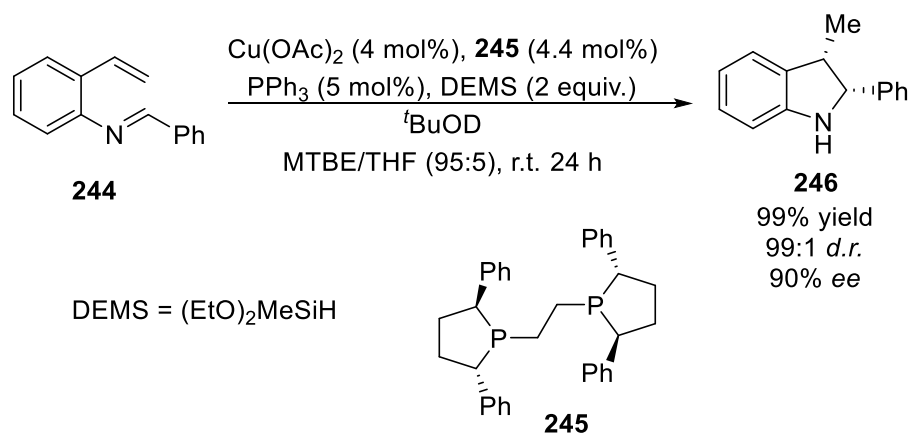


Figure 37: Indoline scaffolds in molecules of biological interest

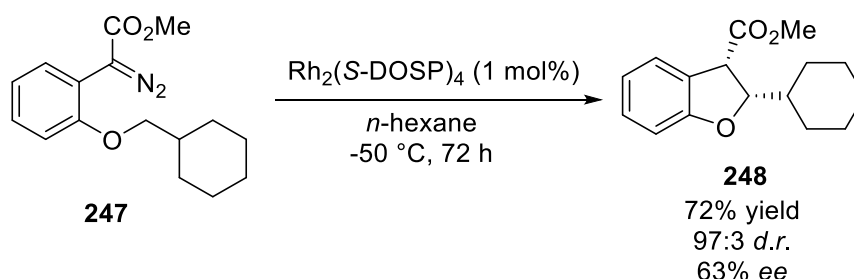
A standard protocol for the preparation of indolines is the copper-¹⁹ or palladium-catalysed aryl amination.²⁰ Intramolecular radical-mediated aryl aminations,²¹ as well as intramolecular carbolithiations,²² are other possible strategies to the indoline scaffold.²³ A very efficient and highly stereoselective synthesis to *cis* 2,3-disubstituted indolines was recently disclosed by Asci and Buchwald (Scheme 87).²⁴ Imine **244** was generated from the aniline analogue in a simple condensation with benzaldehyde. In the cyclisation reaction, the olefin moiety of imine **244** first inserts into the Cu-H bond of the chiral catalyst complex and subsequent cyclisation provides indoline **246** in excellent diastereo- and enantioselectivity.



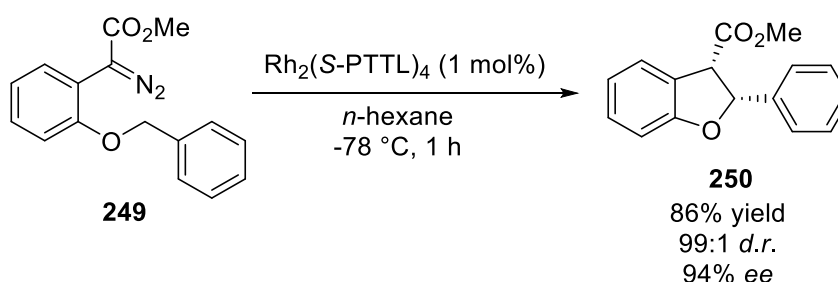
Scheme 87: Buchwald's asymmetric synthesis to indolines

The possibility of assembling the indoline structure *via* carbene type C-H insertion methodology has, however, received little attention. This stands in contrast to other five-membered cyclic molecules such as indanes and benzofuranes. Davies *et al.*²⁵ and Hashimoto and co-workers²⁶ investigated the rhodium-catalysed C-H insertion for the formation of benzofuranes in particular. The two research groups optimised the reaction in different ways. Davies used the $\text{Rh}_2(\text{DOSP})_4$ catalyst, whereas Hashimoto's group used $\text{Rh}_2(\text{PTTL})_4$. In both cases, the *cis* diastereomer was produced in large excess (Scheme 88). Davies found later that his newly developed $\text{Rh}_2(\text{S-PTAD})_4$ catalyst was also capable of performing the C-H insertion to form benzofuranes in excellent diastereomeric and enantiomeric excess (97:3 *d.r.*, 95% *ee*).²⁷

1. Davies, 2001

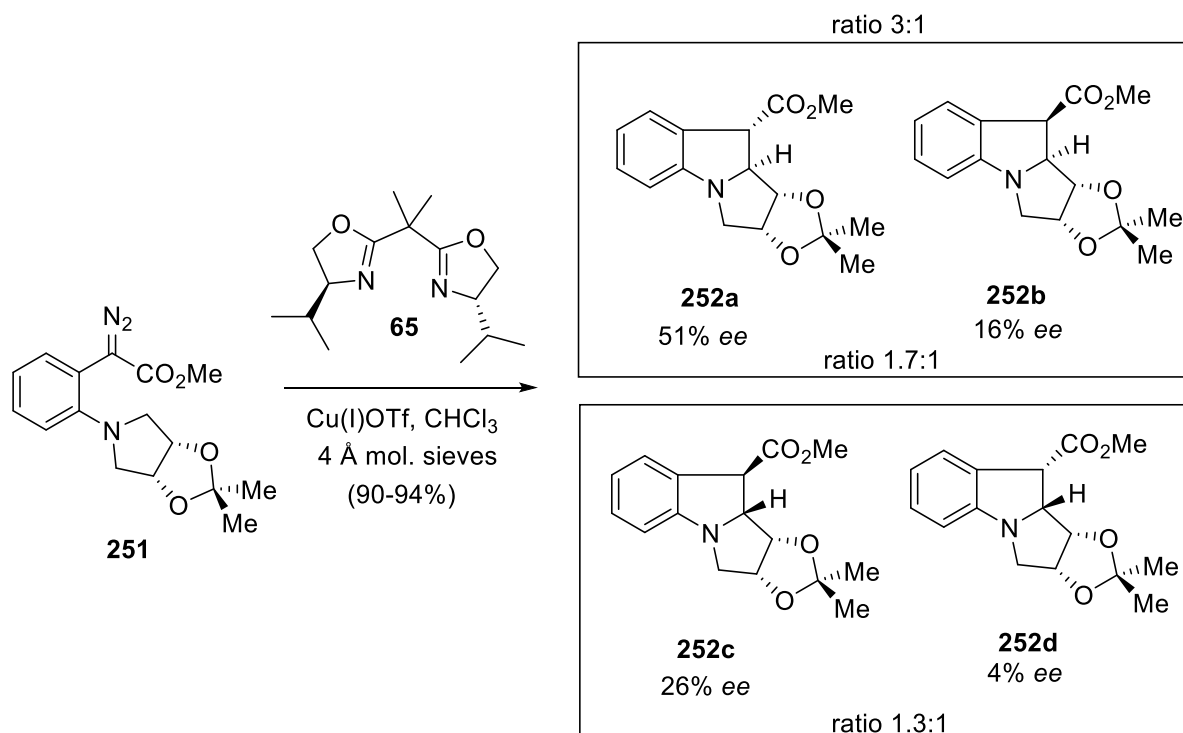


2. Hashimoto, 2002



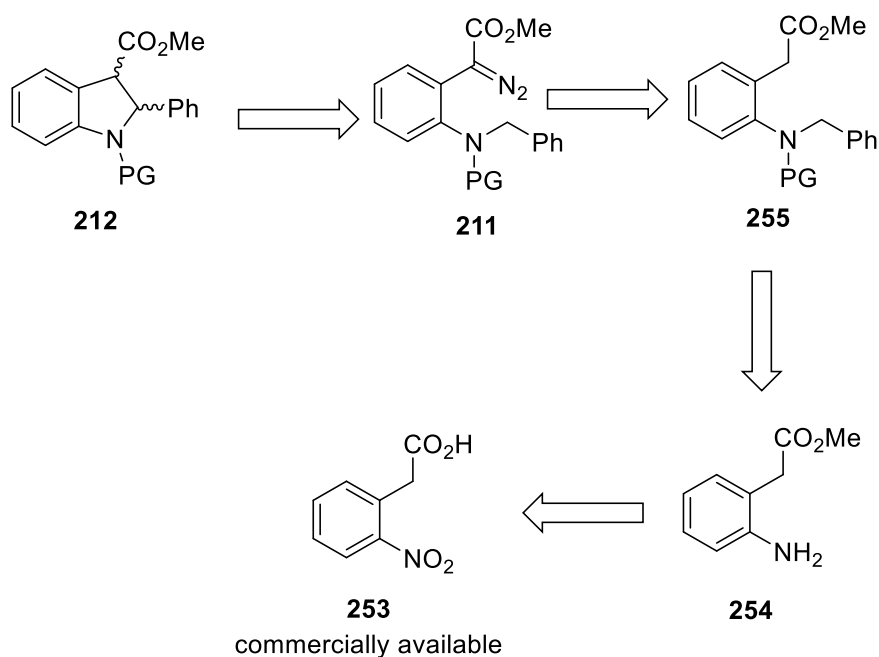
Scheme 88: Synthesis of benzofuranes using C-H insertion methodology

Considering these great advances in using C-H insertion chemistry for the assembly of five-membered heterocycles, it is surprising that only few reports exist on this strategy for the formation of indolines. Sulikowski *et al.* applied this strategy for the preparation of tetracyclic indoline compound **252** (Scheme 89).²⁸ The strategy gave low to modest enantioselectivities and formed all four different isomers providing an overall low selectivity towards one particular product. Interestingly, a copper catalyst proved more successful in inducing stereocontrol than rhodium catalysts.



Scheme 89: Sulikowski's approach to indolines

A more general approach to indolines *via* an asymmetric C-H insertion methodology was therefore sought. The retrosynthetic strategy is described below (Scheme 90). Diazo reagent **211** was envisioned as precursor of the C-H insertion reaction. The diazo reagent **211** could be prepared from ester **255** *via* a diazo transfer reaction. Amine **254** would be derived from commercially available 2-nitrophenylacetic acid **253** by esterification and subsequent reduction.

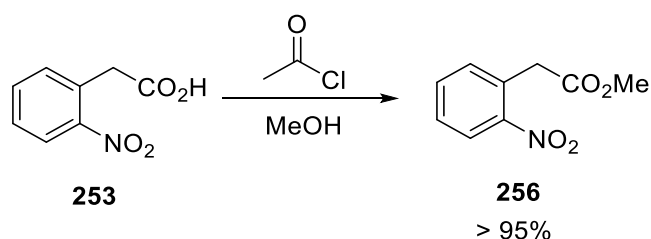


Scheme 90: Retrosynthetic strategy for indolines through C-H insertion methodology

This chapter discussing the stereoselective synthesis of dihydroindoles is divided into three segments. In this first one, the preparation of ester **255** is described (Section 5.3.2). After that, a detailed discussion of the diazo transfer to make diazo compound **211** is performed (Section 5.3.3). In the final segment, the C-H insertion chemistry to prepare dihydroindole **212** is presented.

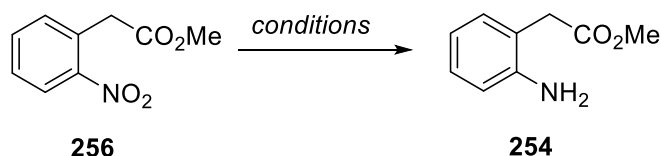
5.3.2 Synthesis of diazo transfer precursor

The first step towards the synthesis of indolines was the esterification of 2-nitrophenylacetic acid (Scheme 91). For this purpose, a mixed anhydride was formed *in situ* using acetyl chloride. In methanol, the mixed anhydride would then decompose into methyl ester **256**. Expectedly, this reaction proceeded in excellent yield.



Scheme 91: Esterification of 2-nitrophenylacetic acid **253**

Next, the reduction of the aromatic nitro group to the amine was performed (Scheme 92). For this purpose, several different reaction conditions were investigated (Table 5.9).



Scheme 92: Reduction of methyl 2-nitrophenylacetate **256**

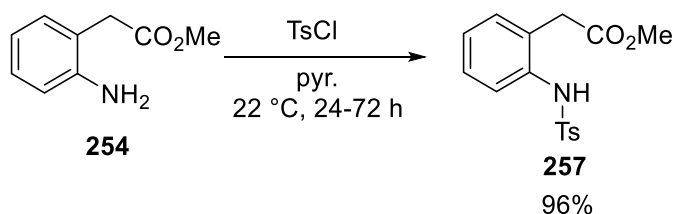
Transfer hydrogenations using nickel and iron catalysis proved unsuitable, with all of the starting material being recovered (Table 5.9, entries 1-2). Ammonium formate / methanol as hydrogen sources over Pd/C led to a complex reaction mixture (Table 5.9, entry 3). Zinc with acetic acid and water resulted in the reduction of the nitro group, however the strong acidic conditions also led to a partial cleavage of the methyl ester (Table 5.9, entry 4). In contrast, hydrogen gas using Pd/C as catalyst gave an excellent yield (99%) for the reduction (Table 5.9, entry 5). It should be mentioned that the resulting amine is unstable and has to be used within a few days in the next reaction to avoid decomposition. This is the reason why scaling the reaction using hydrogen gas and Pd/C proved difficult. When using a larger scale, the hydrogen balloons were refilled over a longer period of time over which the product had started to decompose. A scale of < 5 g proved best for this reaction. Finally, the use of tin(II)

chloride in ethanol resulted in an ester cleavage next to a partial reduction and was therefore not suitable for this transformation (Table 5.9, entry 6).

Table 5.9: Conditions tested for nitro group reduction

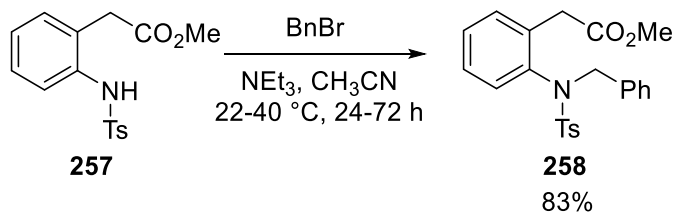
Entry	Reagents	Conditions	Yield [%]
1 ²⁹	N ₂ H ₄ , Raney Ni, MeOH	40 °C, 1 h	0; SM recovered
2 ³⁰	CaCl ₂ , Fe powder, EtOH, H ₂ O	60 °C, 20 h	0; SM recovered
3 ³¹	NH ₄ HCOO, Pd/C, MeOH	-10 °C, 4 h	0; complex product mixture
4 ³²	Zn, AcOH, H ₂ O	22 °C, 1.5 h	51; partly ester cleaved; all SM consumed
5 ²⁷	H ₂ (balloon), Pd/C, MeOH	22 °C, 24-72 h	99
6 ³³	SnCl ₂ , EtOH	70 °C, 1 h	0; ester cleaved

The next step in the preparation of indolines was the protection of the amine group. Tosyl chloride and pyridine were used for this purpose (Scheme 93). The reaction proceeded well (96%), however the work-up was tedious and pyridine as a solvent was undesirable due to its toxicity. Unfortunately, switching to triethylamine as the base in acetonitrile, led to a double tosylation instead to the formation of the desired product **257**.



Scheme 93: Tosylation of methyl 2-aminophenylacetate **254**

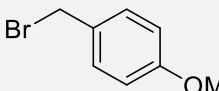
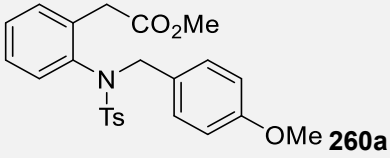
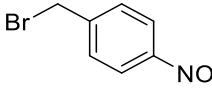
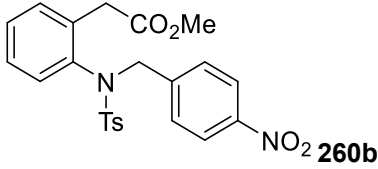
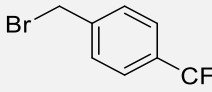
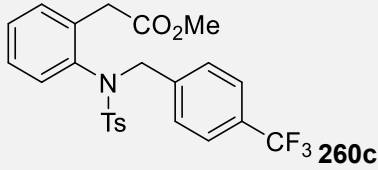
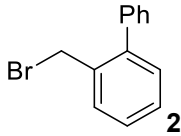
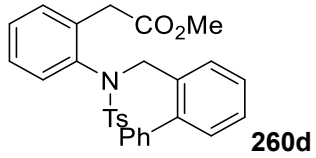
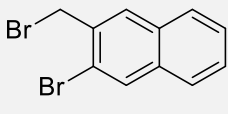
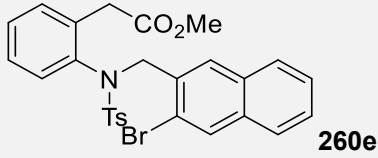
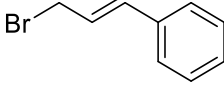
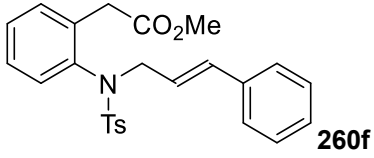
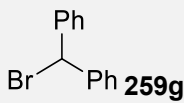
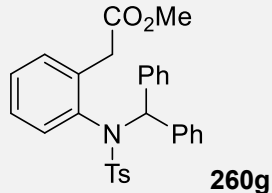
The benzylation of **257** was performed using NEt₃ as base in acetonitrile (Scheme 94). The yield of this reaction was good (83%), however the reaction time was long (24-72 h depending on scale). It was possible to speed the reaction up by heating to 40 °C (12 h). The use of DBU as base gave a complex product mixture.



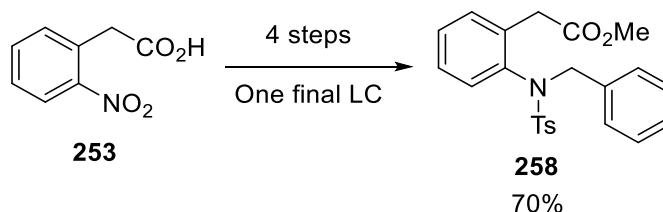
Scheme 94: Benzylation of tosyl amine **257**

To generate a range of substrates for the cyclisation later in the chapter, the electrophile of this reaction was diversified (Table 5.10). Yields were lower than in the previous benzylation as mixed fractions after the column purification were not further purified. However, a diverse set of benzyl substituents with electron-rich and electron-poor aromatic systems were obtained successfully (Table 5.10, entries 1-7).

 Table 5.10: Substrates made *via* amine addition onto electrophiles

Entry	Electrophile	Product	Yield [%]
1	 259a	 260a	71
2	 259b	 260b	42
3	 259c	 260c	57
4	 259d	 260d	68
5	 259e	 260e	34
6	 259f	 260f	18
7	 259g	 260g	36

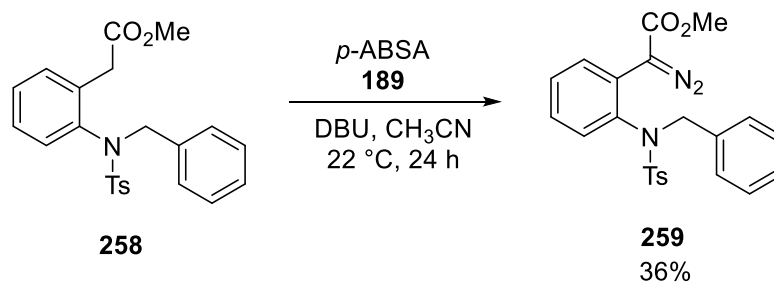
It was finally investigated if the crude reaction mixtures of the previous reactions could be carried through the four step synthesis with only a final column purification. The four steps from 2-nitrophenylacetic acid **253** could be successfully used to make diazo transfer precursor **258** in 70% yield without the need of multiple liquid column chromatography purifications.



Scheme 95: Four step process from 2-nitrophenylacetic acid

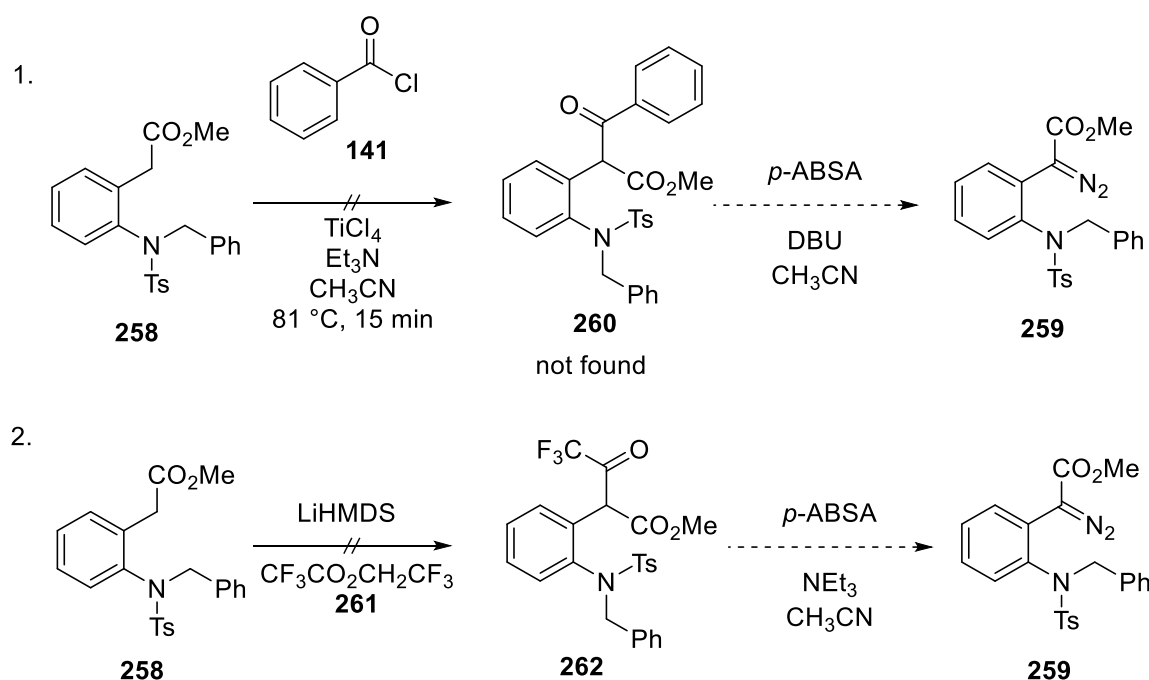
5.3.3 Diazo transfer

Having developed an efficient synthesis to compound **258**, the diazo transfer to generate diazo compound **259** was investigated next (Scheme 96). The standard diazo transfer conditions described in chapter 4 were repeated first for this reaction. Surprisingly, the yield of the transformation was significantly lower than all diazo transfer reactions performed previously. Changing the equivalents of DBU (1.4 - 4 equiv.) or of the diazo transfer reagent *p*-ABSA **189** (1.2 - 3 equiv.) had no strong impact on the reaction efficiency (yields between 25 and 36%). Although some starting material was also recovered (up to 10%), the main product was an unexpected side product (~ 45% yield).



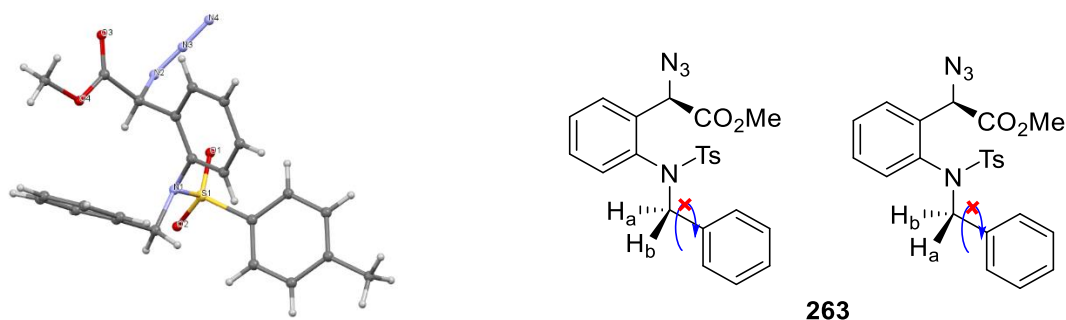
Scheme 96: Diazo transfer onto ester **258**

In section 4.1.1, it was described that deacylation reactions could be used for substrates insufficiently active for an efficient direct diazo transfer. Therefore, two common pre-functionalisation strategies were performed to generate more of the diazo reagent (Scheme 97). The benzoylation described by Taber *et al.*³⁴ using titanium(IV) chloride as the Lewis acid to generate the activated ester did not give any of the desired product **260**, but instead gave a mixture of undesired side products in the first reaction step (Scheme 97, 1). The use of Danheiser's method³⁵ to make trifluoroacetyl-functionalised ester **262** did not succeed either as only starting material **258** was recovered (Scheme 97, 2).



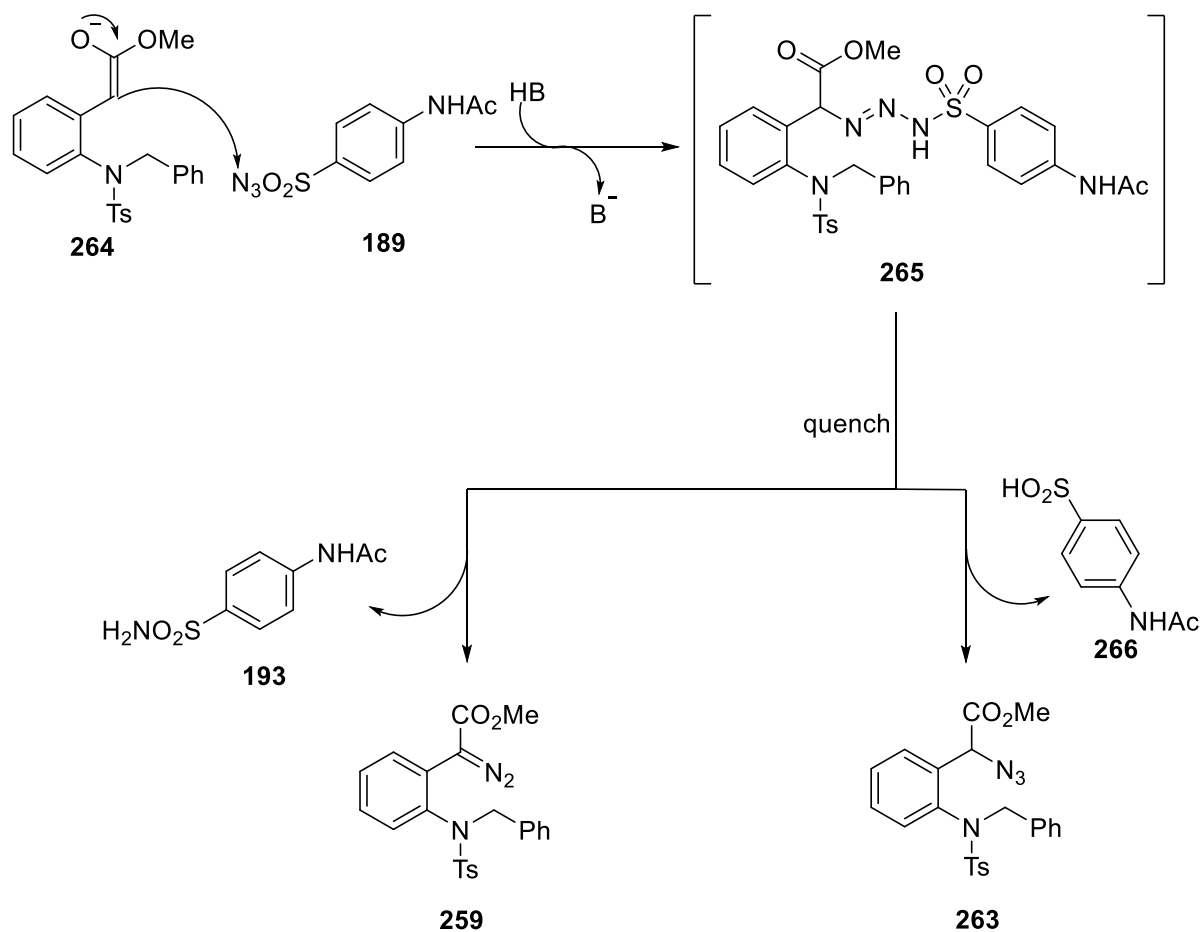
Scheme 97: Unsuccessful pre-functionalisation strategies for diazo transfer

Next, the diazo transfer reaction shown in Scheme 96 was studied in more detail. Through the characterisation of the side-product formed in the reaction a way to a higher yielding diazo transfer was sought. X-ray crystallography of the solid obtained after purification showed azide **263** as the side-product of the diazo transfer reaction (Figure 38, left). Azide **263** has two diastereotopic protons as the rotation of the molecule is hindered and therefore, the two benzylic protons split in the ^1H NMR (Figure 38, right). The competing formation of an azide in a diazo transfer reaction had already been described by Evans *et al.* before, albeit with completely different substrates.³⁶


 Figure 38: Side product of diazo transfer reaction, azide **263**; X-ray structure (left); diastereotopic protons H_a and H_b (right)

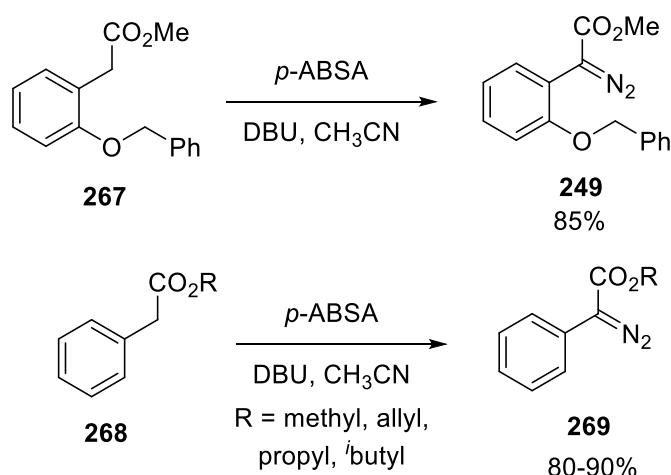
The formation of azide **263** can be rationalised from the decomposition of the intermediate triazene **265** (Scheme 98). In a first step, enolate **264** reacts with diazo transfer reagent $p\text{-ABSA}$ **189** to generate the triazene intermediate. Depending on the quench conditions as

well as the diazo transfer reagent employed, triazene **265** can decompose into diazo reagent **259** and sulfonyl amide **193** or into azide **263** and sulfinic acid **266**.³⁷



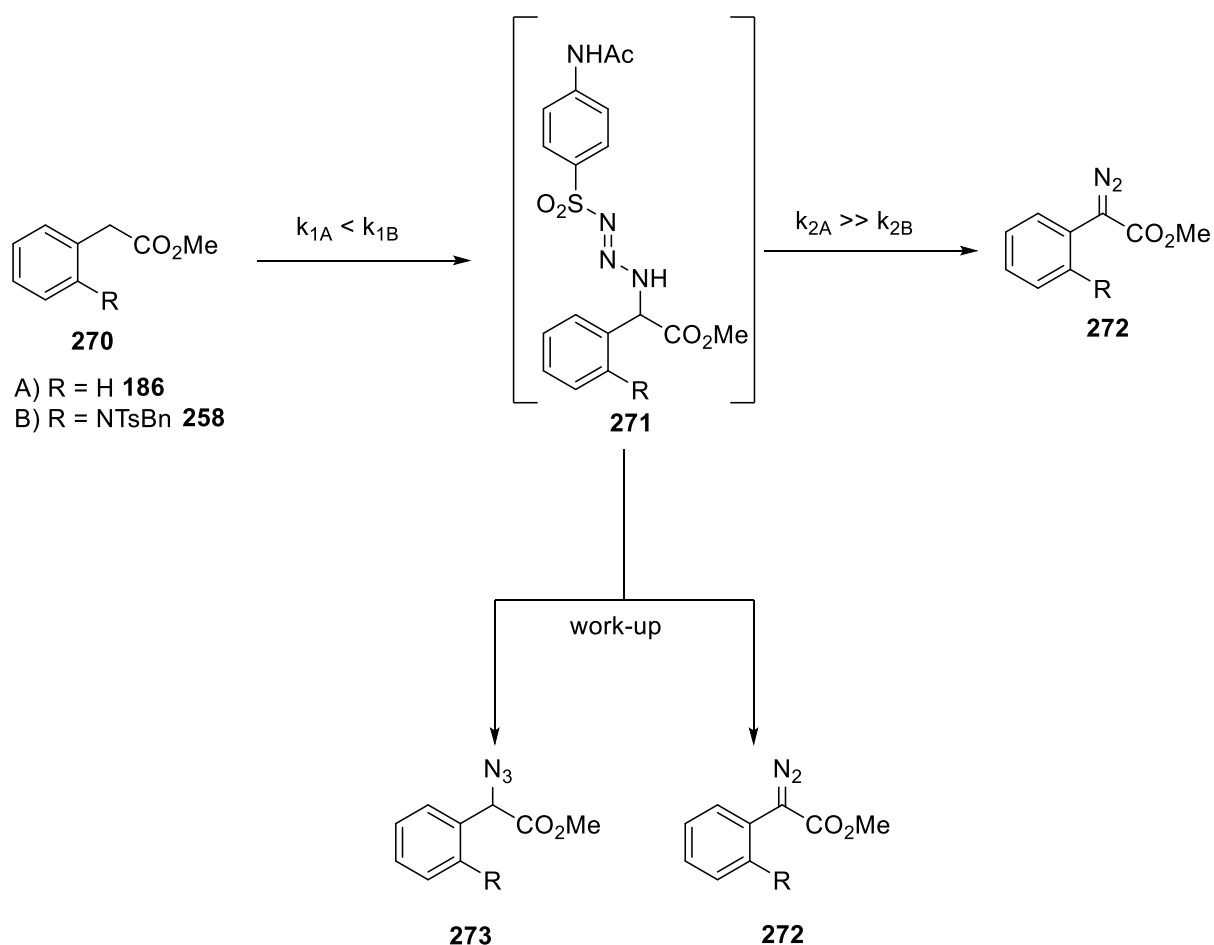
Scheme 98: Rationale for the formation of azide **263** in the diazo transfer reaction

Although azide **263** had been isolated, characterised and its formation rationalised, it was still unclear why the azide was formed in the diazo transfer reaction with amino reagent **258** but not in the reactions with alkyl phenylacetate **268** or *ortho*-benzyoxy methyl phenylacetate **267** which both provided the respective diazo product in high yields under standard diazo transfer conditions (Scheme 99). In all those reactions, no azide had been found.



Scheme 99: Diazo Transfer with other alkyl phenylesters

To get a better understanding into the particularity of the diazo transfer with amino reagent **258**, ^1H NMR studies of the diazo transfer reactions were performed. The substrates for these studies were methyl phenylacetate **186** and *o*-amino ester **258**. In both cases, an intermediate was formed in the ^1H NMR that later decomposed into the diazo product **272**, presumably a triazene moiety (Scheme 100). However, the rates of the formation and decomposition of this intermediate differed significantly in the case of two substrates. In the case of methyl phenylacetate **186** (A), the intermediate is formed slowly over time and decomposes relatively rapidly and selectively into the diazo product **272**. None of the intermediate is left after approx. one day (21 h) and only the diazo product **272** and some starting material **270** can be detected (by ^1H NMR). The kinetics behave differently for the *o*-amino substrate **258** (B). Here, the formation of intermediate triazene **271** is rapid and complete within 15 minutes. Therefore, the rate constant of the formation of the triazene is faster for the *o*-amino substrate **258** than for methyl phenylacetate **186** ($k_{1A} < k_{1B}$). In contrast, the decomposition of the triazene intermediate **271** is a lot faster for methyl phenylacetate **186** than for *o*-amino reagent **258** ($k_{2A} \gg k_{2B}$). In the latter case almost none of the triazene **271** is decomposed into the diazo reagent after 24 h. Therefore, when the work-up is performed, residual triazene **271** is still present in case of *o*-amino substrate **258** which then decomposes in the work-up conditions into azide **273** and diazo product **272**.



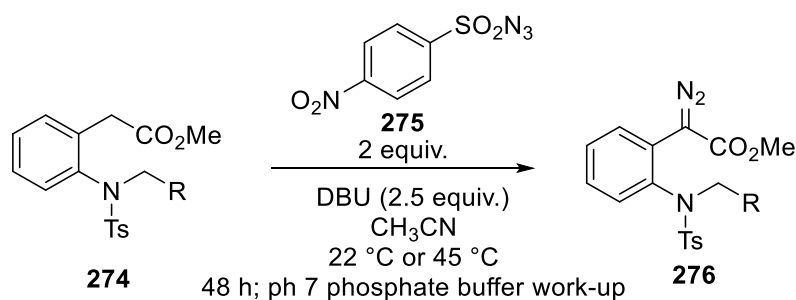
Scheme 100: Analysis of rate constants between two substrates in a diazo transfer reaction

With the understanding that triazene intermediate **271** was still present when the work-up was performed, reagents and conditions were tested to improve the yield of the diazo transfer reaction. It was found that it made no difference if acetonitrile or tetrahydrofuran were used as the solvent in the reaction (Table 5.11, entries 1-2). LiHMDS as the base did not provide any of the desired product, as no reaction took place (Table 5.11, entry 3). Mesyl azide did not work as the diazo transfer reagent under standard conditions, possibly due to the high acidity of the methyl group (Table 5.11, entry 4). In contrast, switching to *p*-nitrobenzenesulfonyl azide (*p*-NBSA) as the diazo transfer reagent led to a stark improvement in yield (Table 5.11, entry 5). Modifications in the work-up (use of phosphate buffer pH 7 instead of an ammonium chloride work-up), and the reaction temperature (45 °C), led to further improvements of the yield (Table 5.11, entries 6-7), giving diazo reagent **259** in a good yield of 64%. Under the optimised reaction conditions only traces of azide product **263** were recovered after the reaction.

Table 5.11: Optimisation of diazo transfer reaction

Entry	Transfer reagent	Base	Solvent	Conditions	Yield [%]
1	<i>p</i> -ABSA	DBU	MeCN	22 °C, 24-168 h	36
2	<i>p</i> -ABSA	DBU	THF	22 °C, 48 h	34
3	<i>p</i> -ABSA	LiHMDS	THF	Addition at -78 °C; then 22 °C for 24 h	0
4	MsN ₃	DBU	MeCN	22 °C, 24 h	0
5	<i>p</i> -NBSA	DBU	MeCN	22 °C; 48 h	50
6	<i>p</i> -NBSA	DBU	MeCN	22 °C, 48 h; pH 7 phosphate buffer work-up	61
7	<i>p</i> -NBSA	DBU	MeCN	45 °C; 48 h; pH 7 phosphate buffer work-up	64

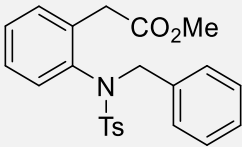
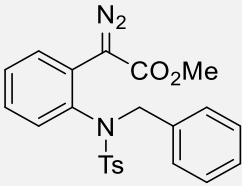
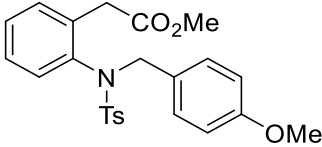
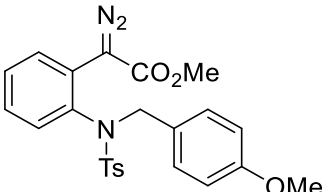
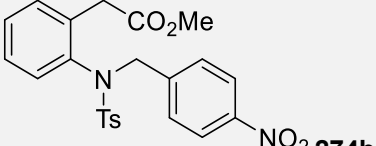
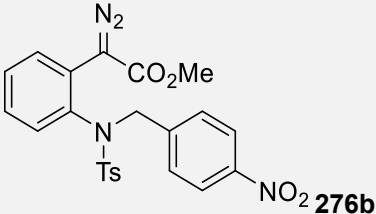
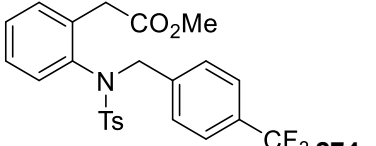
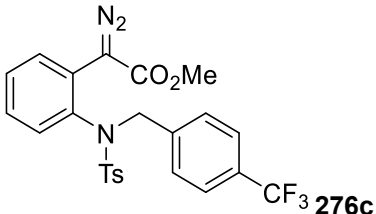
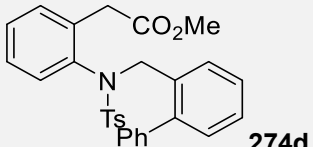
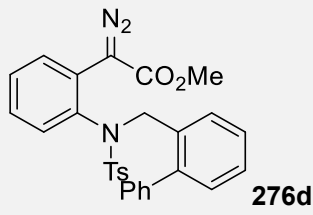
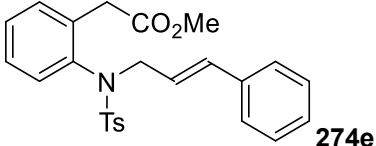
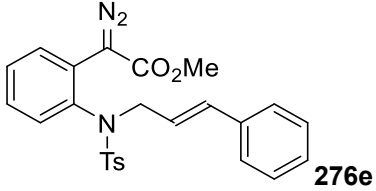
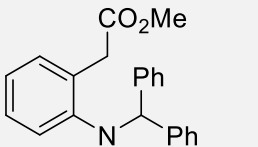
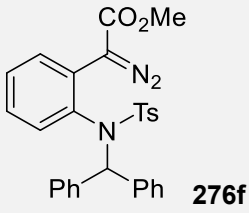
The optimised reaction conditions were used to perform the diazo transfer reaction on some of the substrates from the benzylation reaction (Table 5.12). The reaction was left stirring for 48 h at 22 or 45 °C with 2 equivalents *p*-NBSA **275** and 2.5 equivalents DBU (Scheme 101).



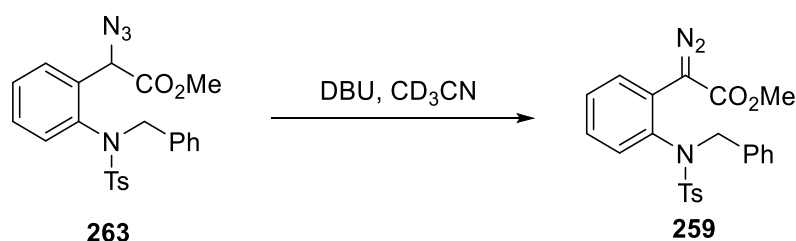
Scheme 101: Optimised diazo transfer conditions for substrate scope

The results of this approach are shown below (Table 5.12). Unfortunately, several substrates did not give the desired diazo product (Table 5.12, entries 3, 6-7). For those reactions that did result in the desired diazo compound, the yields were moderate to good (37-75%, Table 5.12, entries 1-2, 4-5). Broadening the scope of this reaction is part of ongoing studies.

Table 5.12: Substrate scope optimised diazo transfer

Entry	Starting material	Product	Yield [%]
1	 258	 259	64
2	 274a	 276a	52
3	 274b	 276b	0; decomp.
4	 274c	 276c	37
5	 274d	 276d	75
6	 274e	 276e	0; decomp.
7	 274f	 276f	0; complex mixture

During the studies on the diazo transfer reaction, a surprising discovery was made. The side-product of the diazo transfer reaction had been difficult to characterise and, before the full data set had become available, a theory had been that the side-product was in fact the triazene intermediate **271**. To test this hypothesis, the side-product was returned to the original standard diazo transfer conditions to see if further decomposition into the diazo product could be observed. Interestingly, this was the case and the formation of diazo product **259** was observed. Having established later the structure of azide **263**, this meant that there was a way of transforming the azide **263** into diazo compound **259**. ^1H NMR studies provided further evidence for this reaction. In fact, the reaction also proceeded when no diazo transfer reagent *p*-NBSA **275** was present (Scheme 102). Azide **263** reacted with DBU in deuterated acetonitrile to produce diazo compound **259**.

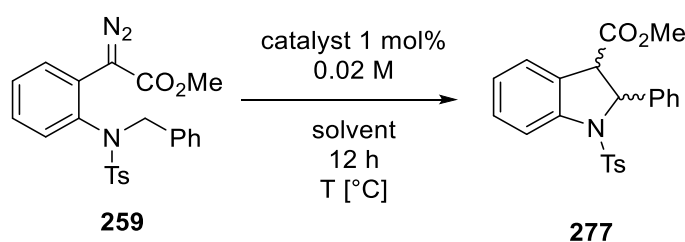


Scheme 102: Formation of diazo compound **259** from azide **263**

The reaction was completely unexpected and no report of this simple azide to diazo transformation could be found in the literature.³⁷ The reaction was finished within 10 minutes, highly exothermic and a strong gas evolution was observed. Further investigations into this reaction are part of ongoing studies.

5.3.4 C-H insertion for dihydroindoles

Having developed a route to diazo compounds of type **259**, the C-H insertion to dihydroindole **277** was investigated (Scheme 103). The separation of the diastereomers was possible *via* column chromatography (CH_2Cl_2 as mobile phase) and the enantiomers were separated *via* HPLC.



Scheme 103: Formation of dihydroindole **277**

First, the reaction was performed using an achiral rhodium acetate catalyst in dichloromethane (Table 5.13, entry 1). The reaction proceeded in excellent yield with an excess of the *trans* diastereomer (3.7:1). The selectivity for the *trans* diastereomer stands in contrast to the C-H insertion for the preparation of benzofuranes in which the *cis* diastereomer is preferentially formed (ratio 7:3 *cis* / *trans* under these reaction conditions, see Chapter 6). Next, the chiral $\text{Rh}_2(\text{S-DOSP})_4$ **62** catalyst was used for the cyclisation reaction under the same reaction conditions as $\text{Rh}_2(\text{OAc})_4$ (Table 5.13, entry 2). A slight drop in yield was observed whereas the diastereomeric ratio remained very similar (3.5:1). Enantiomeric excess for the two diastereomers was promising, although the minor *cis* diastereomer had the higher enantiomeric excess (60% *ee*). In the next two experiments, the reaction temperature was altered to investigate the impact of the temperature on the reaction selectivity. At an increased temperature (40 °C), the selectivity for the *trans* diastereomer dropped to 2.6:1 (Table 5.13, entry 3). The enantiocontrol of the reaction however remained almost unchanged to the experiment at room temperature. At a lower temperature (0 °C), the diastereomeric ratio was similar to that at room temperature (3.3:1) and the enantiomeric excess was slightly improved (Table 5.13, entry 4). In the case of the minor *cis* diastereomer, a good enantiomeric excess was achieved under these conditions (74%).

 Table 5.13: First optimisation set of C-H insertion for dihydroindole **277**

Entry	Conditions	Yield [%]	d.r. (<i>trans</i> : <i>cis</i>)	ee (<i>trans</i>) [%]	ee (<i>cis</i>) [%]
1	$\text{Rh}_2(\text{OAc})_4$, CH_2Cl_2 , 22 °C	92	3.7 : 1	-	-
2	$\text{Rh}_2(\text{S-DOSP})_4$, CH_2Cl_2 , 22 °C	77	3.5 : 1	41	60
3	$\text{Rh}_2(\text{S-DOSP})_4$, CH_2Cl_2 , 40 °C	86	2.6 : 1	37	64
4	$\text{Rh}_2(\text{S-DOSP})_4$, CH_2Cl_2 , 0 °C	79	3.3 : 1	45	74

The next aspect of the reaction that was altered was the choice of the catalyst. $\text{Rh}_2(\text{R-PTAD})_4$ had given excellent selectivities in the formation of benzofuranes²¹ and was therefore used in the formation of dihydroindole **277**. The reaction in dichloromethane provided moderate yields (52%) but with low diastereoselectivity (Table 5.14, entry 1). The enantiomeric excess for the *trans* diastereomer was very low (7%) whereas the enantiomeric excess of the *cis* diastereomer was higher (59%). These reaction conditions could provide a good starting point for an optimisation towards the stereoselective formation of the *cis* diastereomer. Interestingly, a very different reaction outcome was found when *n*-hexane was used as solvent with $\text{Rh}_2(\text{R-PTAD})_4$ as catalyst. The yield of this transformation was low (18%) and again, both diastereomers were formed in an approximately 1:1 ratio (Table 5.14, entry 2). However, the *trans* diastereomer now showed a higher *ee* than the in the prior experiments (58%).

Table 5.14: Use of Rh₂(*R*-PTAD)₄ for C-H insertion

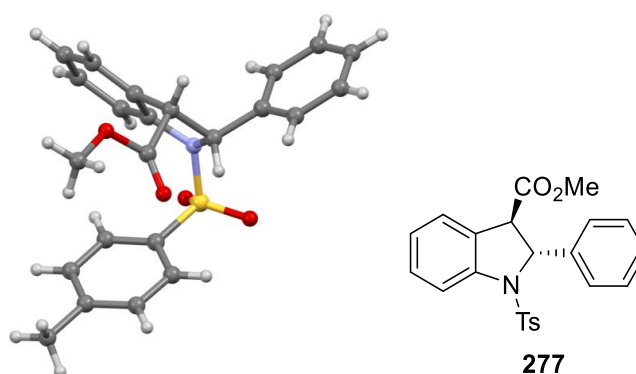
Entry	Conditions	Yield [%]	d.r. (trans:cis)	ee (trans) [%]	ee (cis) [%]
1	Rh ₂ (<i>R</i> -PTAD) ₄ , CH ₂ Cl ₂ , 22 °C	52	1 : 1	7	59
2	Rh ₂ (<i>R</i> -PTAD) ₄ <i>n</i> -hexane, 22 °C	18	1 : 1.1	58	40

The effect of an apolar solvent on the stereoselectivity of the *trans* diastereomer led to further investigations in this direction. Therefore, three reactions with apolar solvents were performed, using toluene (Table 5.15, entry 1), cyclohexane (Table 5.15, entry 2) and *n*-hexane (Table 5.15, entry 3) respectively. In toluene, the diastereoselectivity was favouring the *trans* diastereomer in a ratio of 5 to 1, the best *d.r.* to that point. Enantiocontrol for both diastereomers however, was only moderate. Much better results were achieved in cyclohexane and in *n*-hexane. In cyclohexane, the *d.r.* went up to 9.3 to 1 in favour of the *trans* diastereomer and the ee of this major diastereomer was good (72%). In *n*-hexane, the yield (81%), *d.r.* (13:1) and ee (83% for *trans*) were high. Interestingly, the formation of the *cis* indoline product was racemic in *n*-hexane. This suggests that the formation of the *cis* and the *trans* diastereomer occur *via* a different mechanism in *n*-hexane.

Table 5.15: Apolar solvents for the C-H insertion chemistry

Entry	Conditions	Yield [%]	d.r. (trans:cis)	ee (trans) [%]	ee (cis) [%]
1	Rh ₂ (<i>S</i> -DOSP) ₄ , toluene, 22 °C	-	5.2 : 1	42	53
2	Rh ₂ (<i>S</i> -DOSP) ₄ , cyclohexane, 22 °C	-	9.3 : 1	72	7
3	Rh ₂ (<i>R</i> -DOSP) ₄ , <i>n</i> -hexane, 22 °C	81	13 : 1	83	0

The best reaction conditions so far (Table 5.15, entry 3) were performed with both enantiomers of the chiral catalyst. The main enantiomer of the indoline **277** formed in the reaction using Rh₂(*S*-DOSP)₄ was crystallised to determine the absolute configuration of the enantiomer. The crystal structure is shown below (Figure 39, left). The *trans* configuration of the methyl ester and the adjacent phenyl group is apparent. Both stereocentres have a (*R*) configuration. The main product of this transformation is therefore methyl (2*R*, 3*R*)-2-phenyl-1-tosylindoline-3-carboxylate **277**.


 Figure 39: Determination of absolute stereochemistry of indoline **277**

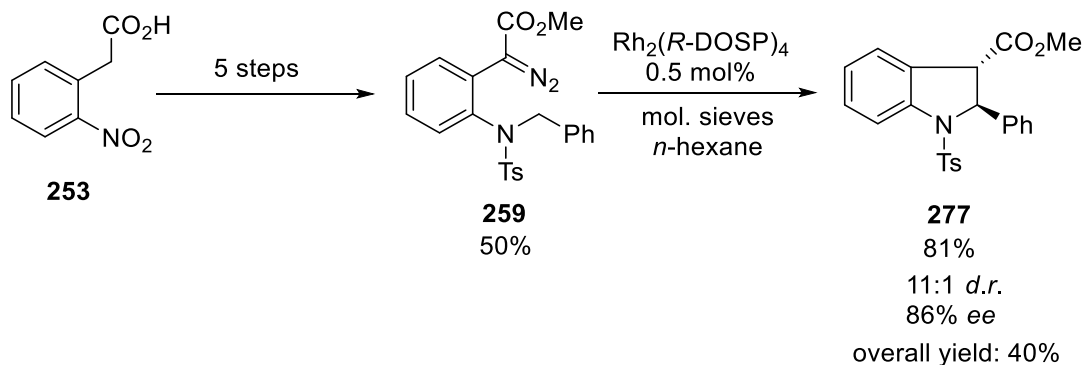
Further optimisations of the reaction conditions for the intramolecular C-H insertion were subsequently attempted. The reaction was performed in *n*-hexane at 0 °C, to investigate the impact of the temperature on the stereoselectivity (Table 5.16, entry 1). A stark improvement in the diastereoselectivity was observed, providing the *trans* diastereomer in 48:1 excess. In contrast, the enantiomeric excess of the *trans* diastereomer in fact dropped at this temperature to 73%. A reduction in the catalyst loading to 0.5 mol% was possible at room temperature, providing indoline **277** in good diastereomeric excess (11:1) and high enantiomeric excess (86%). A higher reaction temperature did not provide any improvements in terms of selectivity (Table 5.16, entry 3). A solvent mixture of *n*-hexane and cyclohexane gave indoline **277** in good *d.r.* but somewhat lower *ee* (74%).

Table 5.16: Last set of optimisation reactions for indoline formation

Entry	Conditions	Yield [%]	d.r. (<i>trans</i> : <i>cis</i>)	ee (<i>trans</i>) [%]	ee (<i>cis</i>) [%]
1	Rh ₂ (<i>R</i> -DOSP) ₄ , <i>n</i> -hexane, 0 °C	82	48 : 1	73	0
2	Rh ₂ (<i>R</i> -DOSP) ₄ , <i>n</i> -hexane, 22 °C; 0.5 mol% catalyst	81	11 : 1	86	0
3	Rh ₂ (<i>R</i> -DOSP) ₄ , <i>n</i> -hexane, 40 °C; 0.5 mol% catalyst	48	9 : 1	75	0
4	Rh ₂ (<i>R</i> -DOSP) ₄ , <i>n</i> -hexane / cyclohexane (1:1) 22 °C; 0.5 mol% catalyst	58	11 : 1	74	0

Having found good reaction conditions for the stereoselective intramolecular C-H insertion reaction, a scheme of the total reaction progressed towards indolines using diazo compounds can be described (Scheme 104). The overall yield is 40% over 6 steps. Diastereocontrol of the reaction is high, especially if compared to Sulikowski's difficulties for the C-H insertion reaction (Section 5.3.1). The enantiomeric excess is good although not excellent, however it

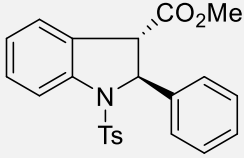
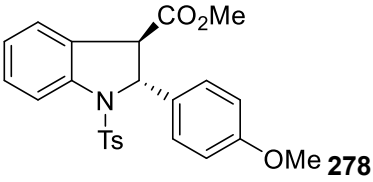
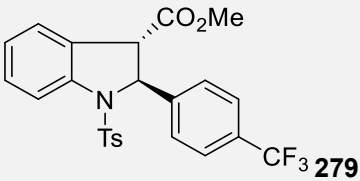
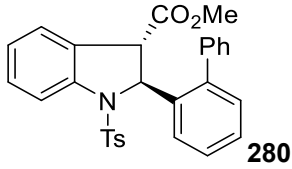
is a great step forward compared to the results obtained previously for dihydroindoles *via* C-H insertion technique (Section 5.3.1). It should also be pointed out that the product observed is the opposite diastereomer (*trans*) to Buchwald's highly efficient indoline (*cis*) synthesis (Section 5.3.1).¹⁸



Scheme 104: Synthesis of tosyl protected indoline in six steps

The scope of substrates for this transformation was investigated briefly as well. An electron-rich aromatic ring next to the C-H group is tolerated (80% yield, Table 5.17, entry 2) providing the product **278** with excellent diastereomeric excess (35:1). However, a sharp drop in enantiocontrol was observed (66% *ee*). Surprisingly, the methoxy substituted indoline **278** was obtained with the opposite enantiomer being the main product. Trifluoro-substituted product **279** was obtained in good yield (82%), however the diastereomeric excess was a lot lower than for the two previous indolines. The enantiomeric excess (72% *ee*) was slightly better than for the methoxy substituted derivative **278**. The sterically hindered compound **280** bearing a phenyl group in *ortho* position reacted very slowly and thus had a much lower yield (37%). However, the diastereomeric excess was good (13:1 *d.r.*) and enantiomeric excess of this compound was excellent (98% *ee*).

Table 5.17: Indoline products obtained from C-H insertion reaction

Entry	Product	Yield [%]	d.r. (trans:cis)	e.r. (ee%) (trans)	e.r.(ee%) (cis)
1	 277	81	11:1	92:8 (86)	50:50 (0)
2	 278	80	35:1	83:17 (66)	n.d.
3	 279	82	4.5:1	86:14 (72)	58:42 (16)
4	 280	37	13:1	99:1 (98)	n.d.

Overall, the reaction provided access to tosyl protected dihydroindoles in good yields (37-82% for the C-H insertion step; up to 36% over six steps), high excess of the *trans* diastereomer (up to 35:1) and good to excellent enantiomeric excess (up to 98% ee). The preparation of the dihydroindoles was performed in classical batch experiments. However, in a next step the use of flow chemistry for this transformation could be envisioned. Furthermore, the development of a broader substrate scope is part of ongoing studies.

5.4 Conclusion & Outlook

In this chapter, the use of diazo compounds for the rapid generation of heterocycles of biological interest has been discussed. Two different classes of heterocycles were synthesised by using two of the most important reactions of diazo compounds, the cyclopropanation of an alkene and the insertion into an unactivated C-H bond.

The studies on the intramolecular cyclopropanation for the continuous flow into semi-batch preparation of lactone **208** provided a safe synthesis of this key building block without the need of isolation of the diazo species. The presence of water had a detrimental effect to the cyclopropanation reaction and posed the main problem in the development of an efficient

multistep protocol. In-line liquid / liquid separation and subsequent drying of the diazo reagent solution using a cartridge filled with MgSO_4 were utilised to rectify this issue. Yields were satisfactory on small scale using these techniques, however a drop in yield was observed when an upscale of the reaction was studied.

In the second part of this chapter, the stereoselective synthesis of dihydroindoles through C-H insertion methodology was investigated. The diazo transfer *prior* to the C-H insertion reaction required optimisation as an azide was formed in a competing transformation. Through careful analysis of the reaction it was possible to improve the yield for the diazo transfer from 36% to 64%. The stereoselective C-H insertion subsequently was optimised to proceed in good yield as well as in high diastereomeric and enantiomeric excess. Through this route, indolines were accessible in 40% yield over six steps.

This final research chapter used the reactivity of diazo compounds for the synthesis of biologically active molecules and their precursors. This was done in a safe fashion (continuous flow, section 5.2) as well as in a highly stereoselective way (indolines, section 5.3). The next chapter will give a final overview of the entire thesis and an outlook into future research in the field of diazo compounds in continuous flow technology.

References

- 1 S. Shuto, S. Ono, Y. Hase, Y. Ueno, T. Noguchi, K. Yoshii, A. Matsuda, *J. Med. Chem.* **1996**, 39, 4844.
- 2 a) R. Silvestri, *J. Med. Chem.* **2013**, 56, 625; b) N. H. Greig, X.-F. Pei, T. T. Soncrant, D. K. Ingram, A. Brossi, *Med. Res. Rev.* **1995**, 15, 3.
- 3 S. Kasper, Y. Pletan, A. Solles, A. Tournoux, *Int. Clin. Psychopharmacol.* **1996**, 11, 35.
- 4 R. A. Sansone, L. A. Sansone, *Innov. Clin. Neurosci.* **2014**, 11, 37.
- 5 S. Shuto, S. Ono, Y. Hase, N. Kamiyama, H. Takada, K. Yamasihita, A. Matsuda, *J. Org. Chem.* **1996**, 61, 915.
- 6 J. Tamiya, B. Dyck, M. Zhang, K. Phan, B. A. Fleck, A. Aparicio, F. Jovic, J. A. Tran, T. Vickers, J. Grey, A. C. Foster, C. Chen, *Bioorg. Med. Chem. Lett.* **2008**, 18, 3328.
- 7 M. P. Doyle, W. Hu, *Adv. Synth. Catal.* **2001**, 343, 299.
- 8 J.-J. Shen, S.-F. Zhu, Y. Cai, H. Xu, X.-L. Xie, Q.-L. Zhou, *Angew. Chem. Int. Ed.* **2014**, 53, 13188.
- 9 B. Morandi, J. Cheang, E. M. Carreira, *Org. Lett.* **2011**, 13, 3080.
- 10 Possibly traces of another diastereomer were observed in case of **229** in the crude ¹H-NMR, however, isolation of this compound was unsuccessful and therefore determination of the structure was not possible.
- 11 For the reaction of a diazo compound with oxygen: K. P. Kornecki, J. F. Briones, V. Boyarskikh, F. Fullilove, J. Autschbach, K. E. Schrote, K. M. Lancaster, H. M. L. Davies, J. F. Berry, *Science* **2013**, 342, 351.
- 12 H. Tomioka, K. Suzuki, *Tetrahedron Lett.* **1989**, 30, 6353.
- 13 V. Piquet, A. Baceiredo, H. Gornitzka, F. Dahan, G. Bertrand, *Chem. Eur. J.* **1997**, 3, 1757.
- 14 M. P. Doyle, W. E. Buhro, J. G. Davidson, R. C. Elliott, J. W. Hoekstra, M. Oppenhuizen, *J. Org. Chem.* **1980**, 45, 3657.
- 15 For selected total syntheses of vinblastine: a) H. Ishikawa, D. A. Colby, S. Seto, P. Va, A. Tam, H. Kakei, T. J. Rayl, I. Hwang, D. L. Boger, *J. Am. Chem. Soc.* **2009**, 131, 4904; b) S. Yokoshima, H. Tokuyama, T. Fukuyama, *Chem. Rec.* **2010**, 10, 101.
- 16 For selected total syntheses of strychnine: a) R. B. Woodward, M. P. Cava, W. D. Ollis, A. Hunger, H. U. Daeniker, K. Schenker, *J. Am. Chem. Soc.* **1954**, 76, 4749; b) J. S. Cannon, L. E. Overman, *Angew. Chem. Int. Ed.* **2012**, 51, 4288.
- 17 For selected total syntheses of physostigmine: a) T. Bui, S. Syed, C. F. Barbas III, *J. Am. Chem. Soc.* **2009**, 131, 8758; b) G. Pandey, J. Khamrai, A. Mishra, *Org. Lett.* **2015**, 17, 952.
- 18 A. Rakhit, M. E. Hurley, V. Tipnis, J. Coleman, A. Rommel, H. R. Brunner, *J. Clin. Pharmacol.* **1986**, 26, 156.
- 19 G. Evano, N. Blanchard, M. Toumi, *Chem. Rev.* **2008**, 108, 3054.
- 20 a) J. P. Wolfe, R. A. Rennels, S. L. Buchwald, *Tetrahedron* **1996**, 52, 7525; b) B. H. Yang, S. L. Buchwald, *Org. Lett.* **1999**, 1, 35.
- 21 J. N. Johnston, M. A. Plotkin, R. Viswanathan, E. N. Prabhakaran, *Org. Lett.* **2001**, 3, 1009.
- 22 a) D. W. Zhang, L. S. Liebeskind, *J. Org. Chem.* **1996**, 61, 2594; b) W. F. Bailey, X. L. Jiang, *J. Org. Chem.* **1996**, 61, 2596.
- 23 For an overview on strategies to indolines see: a) S. Anas, H. B. Kagan, *Tetrahedron: Asymmetry* **2009**, 20, 2193; b) D. Liu, G. Zhao, L. Xiang, *Eur. J. Org. Chem.* **2010**, 3975.
- 24 E. Ascic, S. L. Buchwald, *J. Am. Chem. Soc.* **2015**, 137, 4666.
- 25 H. M. L. Davies, M. V. A. Grazini, E. Aouad, *Org. Lett.* **2001**, 3, 1475.
- 26 H. Saito, H. Oishi, S. Kitagaki, S. Nakamura, M. Anada, S. Hashimoto, *Org. Lett.* **2002**, 4, 3887.
- 27 R. P. Reddy, G. H. Lee, H. M. L. Davies, *Org. Lett.* **2006**, 8, 3437.

- 28 a) S. Lee, H.-J. Lim, K. L. Cha, G. A. Sulikowski, *Tetrahedron* **1997**, 53, 16521; b) G. Sulikowski, S. Lee, *Tetrahedron Lett.* **1999**, 8035.
- 29 D. Balcom, A. Furst, *J. Am. Chem. Soc.* **1953**, 75, 4334.
- 30 S. Chandrappa, K. Vinaya, T. Ramakrishnappa, K. S. Rangappa, *Synlett* **2010**, 3019.
- 31 S. Ram, R. E. Ehrenkauf, *Tetrahedron Lett.* **1984**, 25, 3415.
- 32 S. Castellano, C. Milite, P. Campiglia, G. Sbardella, *Tetrahedron Lett.* **2007**, 48, 4653.
- 33 F. D. Bellamy, K. Ou, *Tetrahedron Lett.* **1984**, 25, 839.
- 34 D. F. Taber, R. B. Sheth, P. V. Joshi, *J. Org. Chem.* **2005**, 70, 2851.
- 35 R. L. Danheiser, R. F. Miller, R. G. Brisbois, S. Z. Park, *J. Org. Chem.* **1990**, 55, 1959.
- 36 D. A. Evans, T. C. Britton, J. A. Ellman, R. L. Dorow, *J. Am. Chem. Soc.* **1990**, 112, 4011.
- 37 The only reports on azide to diazo transformations use phosphorus reagents, see section 1.2.5. For an overview on reactions of organoazides see: a) G. L'Abbé, *Chem. Rev.* **1969**, 69, 345; b) S. Bräse, C. Gil, K. Knepper, V. Zimmermann, *Angew. Chem. Int. Ed.* **2005**, 44, 5188.

6 Conclusion & Outlook

The chemical and pharmaceutical industries rely on highly efficient protocols for the generation of complex molecules at low costs and in high yields. Diazo compounds are the ideal functional group to help in this quest as they can be used to generate complexity rapidly, with high chemo-, regio- and stereocontrol. To date, the use of this highly useful class of compounds for the preparation of large quantities of valuable target molecules has been hindered due to the thermal profile of diazo compounds. Diazo compounds are highly energetic and prone to explosions, especially when heated or exposed to acidic conditions. In this thesis, protocols were developed to prepare and directly use diazo compounds safely by using continuous flow technology.

Five distinct projects using diazo compounds were investigated (Scheme 105). In the first project, ethyl diazoacetate **7** was prepared in flow and directly used in an aldol addition with aldehydes (Scheme 105, 1.). Yields were moderate to high with the majority of examples being obtained in around 80% yield. The β -hydroxy- α -diazoesters were subsequently used for a small set of reactions. The 1,2-hydride shift to obtain a β -ketoester was finally used in a three-step continuous flow set-up.

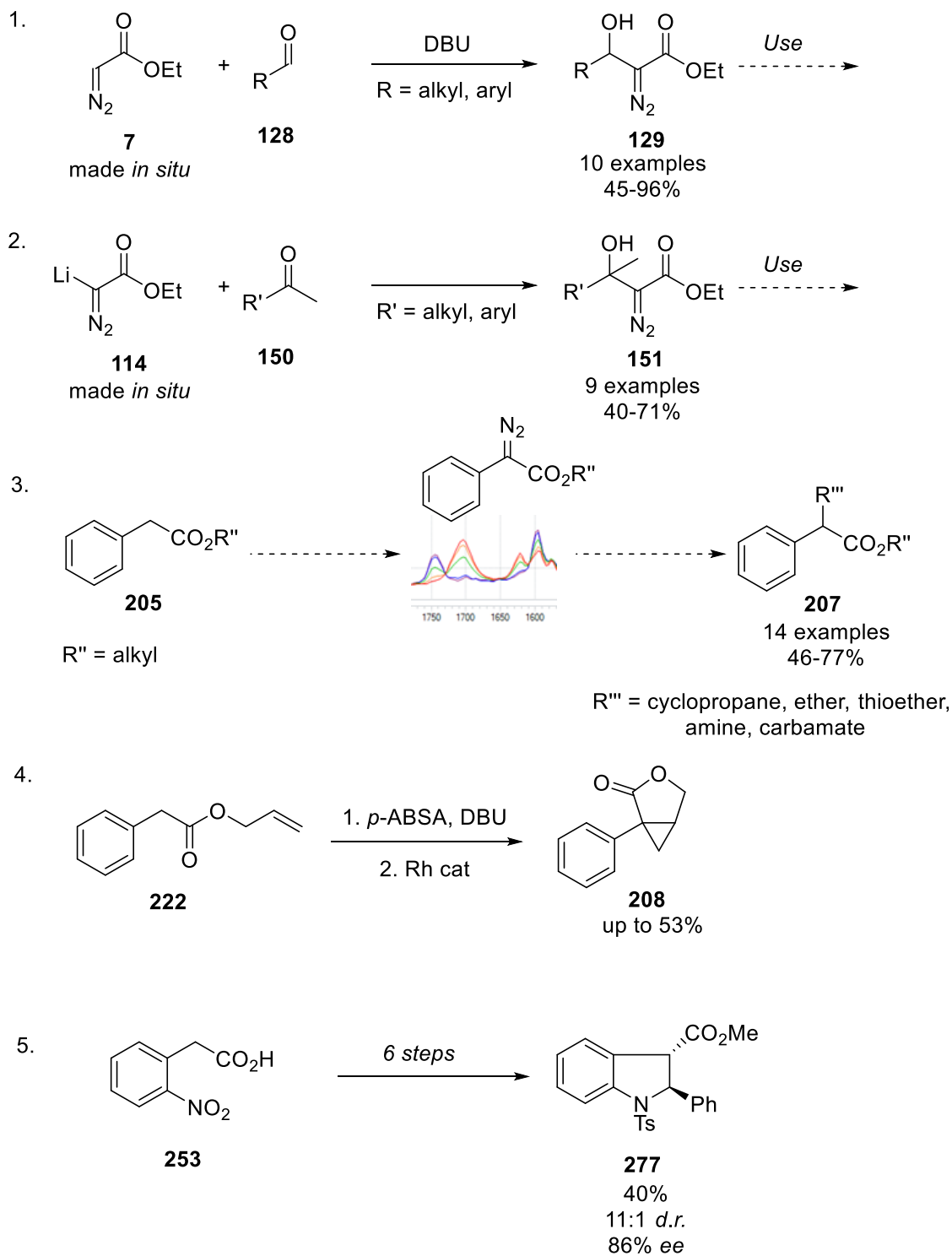
The second project expanded the scope of electrophiles that reacted with ethyl diazoacetate **7** by forming highly nucleophilic ethyl lithiodiazoacetate **114** (Scheme 105, 2.). Handling ethyl lithiodiazoacetate **114** in flow proved very challenging due to instability of this reagent at temperatures above $-55\text{ }^{\circ}\text{C}$. Nevertheless, a set of ketones was used successfully in this set-up with moderate to good yields (40-71%). The ring-opening of a lactone was less efficient, providing only 12% of the desired product.

In the third project, the chemistry of aryl diazoacetates was investigated in detail and transferred from batch into flow chemistry (Scheme 105, 3.). These reagents are precursors of highly versatile donor / acceptor carbenes. In-line infrared spectroscopy was used for the rapid optimisation of the diazo transfer as well as for the monitoring of the carbene insertion into multiple substrates. A multistep flow protocol was designed to access valuable synthetic targets with no need for isolation of the diazo intermediate.

Donor / acceptor carbenes were also used in the final two projects. The use of an allyl substituted ester of a diazo compound resulted in the formation of lactone **208** (Scheme 105, 4.). This reaction was performed in a continuous flow to semi-batch multistep protocol which gave access to this important compound in up to 53% yield.

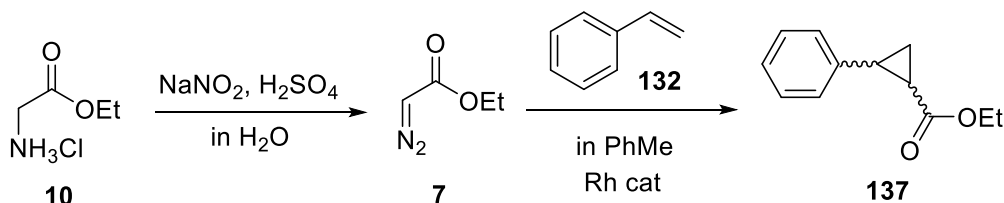
The stereodefined synthesis of indolines was achieved in the last project (Scheme 105, 5.). A six step synthesis to these products of biological interest was designed. The diazo transfer

proved more difficult than anticipated in this case but the yield was improved by carefully studying the side-product formed during the reaction. The final cyclisation reaction could be performed with up to excellent diastereomeric (up to 35:1) and enantiomeric excess (up to 98% ee).



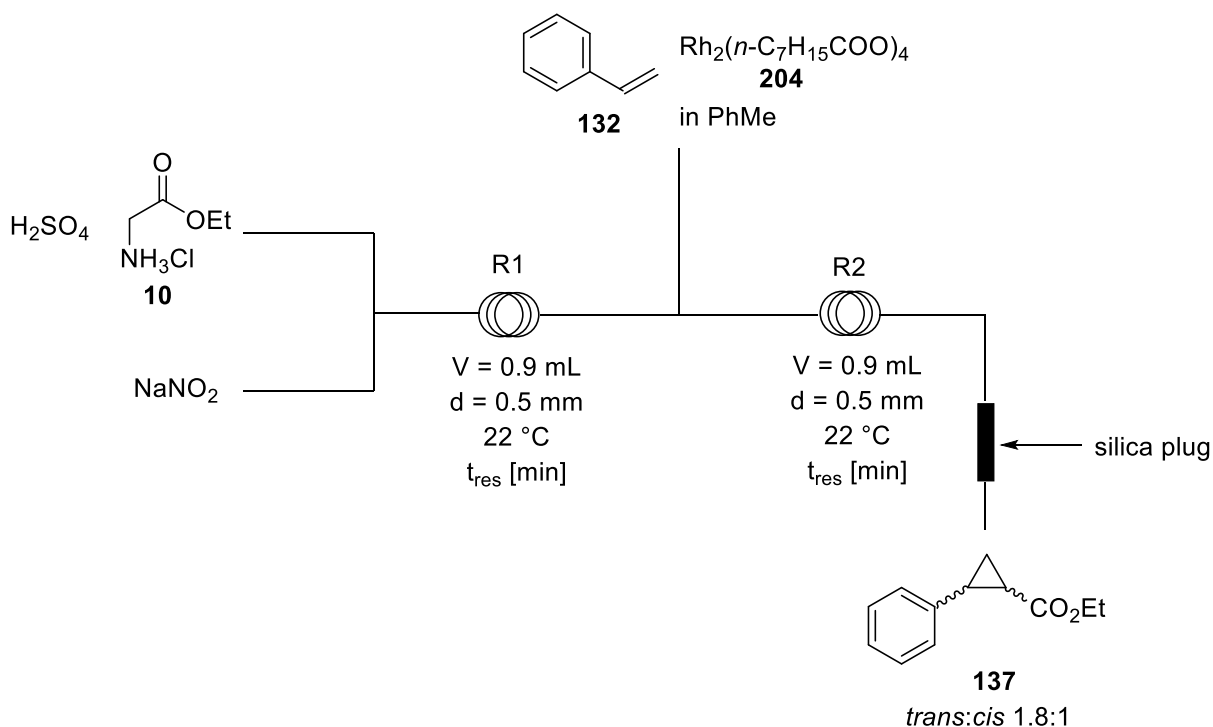
Scheme 105: Overview of thesis projects

During the course of this work there were also several projects that could not be completed and will be briefly mentioned in this section. During the work on ethyl diazoacetate **7**, it was studied if the *in situ* formation of EDA **7** could also be combined with a biphasic cyclopropanation reaction with styrene **132** (Scheme 106).



Scheme 106: Cyclopropanation of ethyl diazoacetate **7** with styrene **132**

The continuous flow set-up used for this transformation is shown in Scheme 107. In the first reactor, ethyl diazoacetate **7** was generated in a similar fashion as in the project of the aldol addition to aldehydes. Then, a solution containing styrene **132** and rhodium octanoate **204** in toluene was added to prepare the cyclopropane in a biphasic mixture.



Scheme 107: Continuous flow set-up for cyclopropanation of styrene **132**

Some preliminary results of this approach are shown in Table 6.1. The conversion of styrene **132** into the cyclopropane worked well with independently prepared ethyl diazoacetate **7** (Table 6.1, entry 1). For the *in situ* formation ethyl diazoacetate, the use of 1.25 equivalents of glycine ethyl ester hydrochloride **10** compared to styrene gave low conversions (Table 6.1, entries 2-3). Interestingly, reducing the residence time by half had a beneficial effect,

presumably due to better mixing because of the higher flow rates applied. The use of 2 equivalents of glycine ethyl ester hydrochloride **10** led to a strong increase in conversion (Table 6.1, entry 4). Reducing the catalyst loading to just 0.5 mol% proved detrimental to the reaction outcome (Table 6.1, entry 5). Changing the reaction conditions had no impact on the diastereomeric ratio which was around 1.8:1 in favour of the *trans* diastereomer in all cases (literature 1.5:1).¹

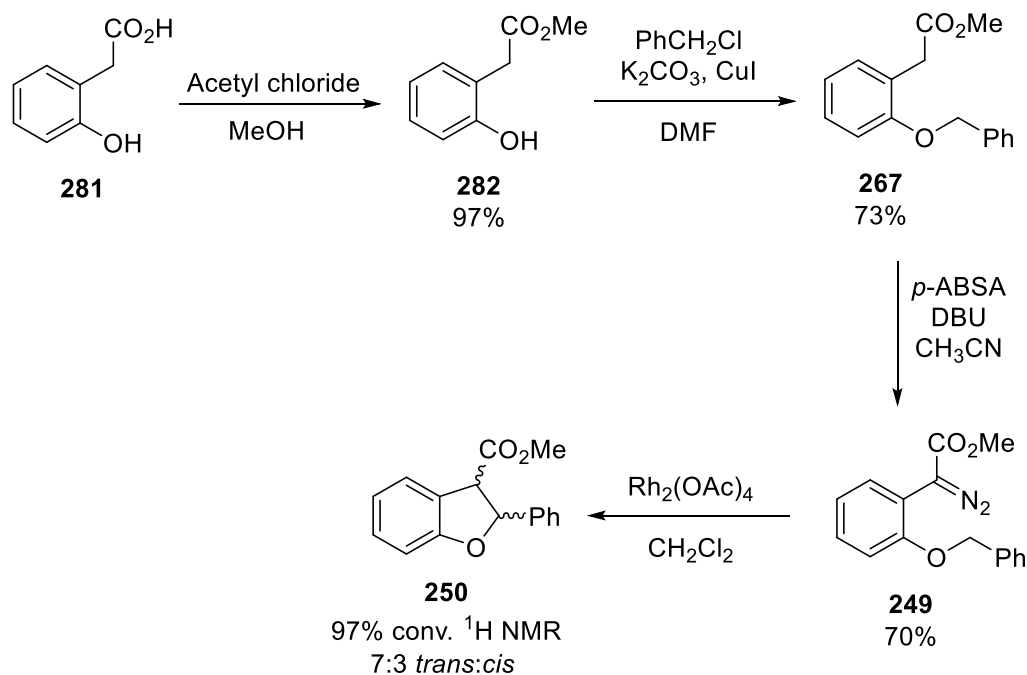
Table 6.1: Optimisation table for cyclopropanation of styrene

Entry	Equiv. glycine ethyl ester HCl	Cat. Loading [mol%]	t _{res} R1 / R2 [min]	Conversion [%] ^a
1^b	-	1	9 / 4.5	96
2	1.25	1	9 / 4.5	31
3	1.25	1	4.5 / 2.3	35
4	2	1	4.5 / 2.3	77
5	2	0.5	4.5 / 2.3	38

^a Conversion determined by ¹H NMR; ^b Independently synthesized ethyl diazoacetate (1.5 equiv.) was used

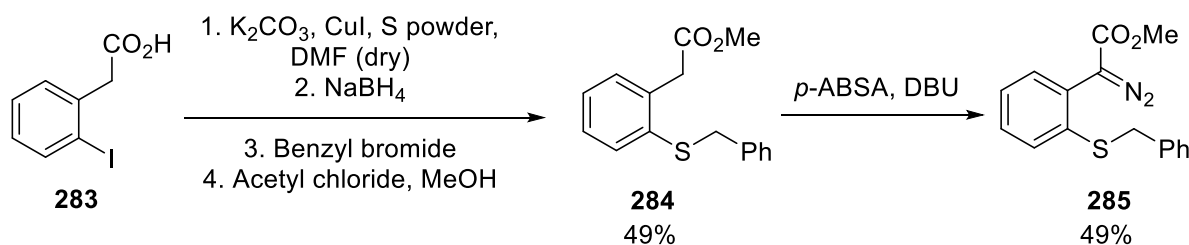
The preliminary results were encouraging and the development of a biphasic cyclopropanation of ethyl diazoacetate **7** should be possible in continuous flow. However, there have already been reports on cyclopropanations of ethyl diazoacetate in flow.²

During the studies on the preparation of dihydroindoles, similar approaches were studied for the preparation of benzofuranes and dihydrobenzo[*b*]thiophenes. The synthesis of benzofuranes was performed according to Davies *et al.* (Scheme 108). Diazo compound **249** was prepared readily from 2-hydroxyphenylacetic acid **281** in three steps (50% yield). The subsequent C-H insertion reaction to benzofurane **250** worked smoothly in batch with 97% conversion (¹H NMR) and in a diastereomeric ratio of 7:3 (*trans*:*cis*). The cyclisation was next studied in flow, and diazo compound **249** was converted into benzofurane **250** in 85% conversion (¹H NMR) with a slightly altered diastereomeric ratio of 6:4 (*trans*:*cis*) in 40 min residence time at 22 °C using rhodium acetate as the catalyst (1 mol%).



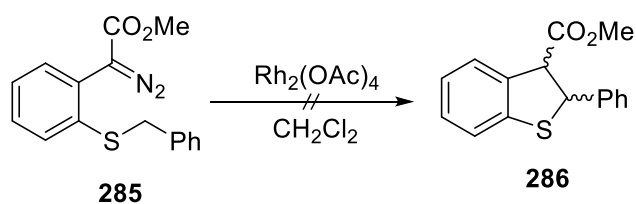
Scheme 108: Synthesis of dihydroindole **250** by C-H insertion methodology

The preparation of dihydrobenzo[*b*]thiophenes proved more difficult. The synthesis started from commercially available 2-iodophenylacetic acid **283** which was converted into thioether **284** in 49% yield (Scheme 109). However, this reaction did not prove scalable with yields dropping sharply (~ 10% yield) when moving to gram scale. The diazo transfer with *p*-ABSA and DBU provided diazo compound **285** in moderate yield (49%).



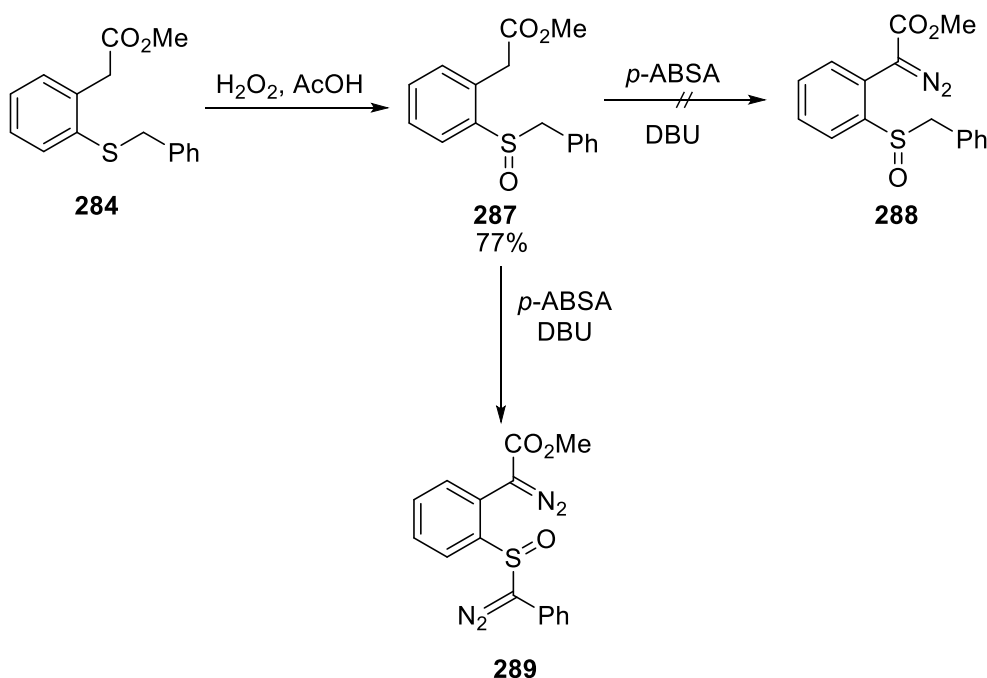
Scheme 109: Formation of diazo compound **285**

The cyclisation of the thioether diazo compound **285** resulted in a complex mixture of side-products, with no formation of the dihydrobenzo[*b*]thiophene **286** being observed (Scheme 110).



Scheme 110: Attempted C-H insertion for the formation of dihydrobenzo[*b*]thiophene **286**

Changing the oxidation state of the sulfur to a sulfoxide *prior* to the diazo transfer was attempted next (Scheme 111). Thioether **284** was readily transformed into the corresponding sulfoxide **287** using hydrogen peroxide (77%). Unfortunately, the subsequent diazo transfer did not furnish any of the diazo sulfoxide **288**, instead a mixture of multiple side-products was obtained. One of these side-products was compound **289** which had two diazo group in the molecule. The attempt of performing a cyclisation with this compound to the benzo[*b*]thiophene did not work.

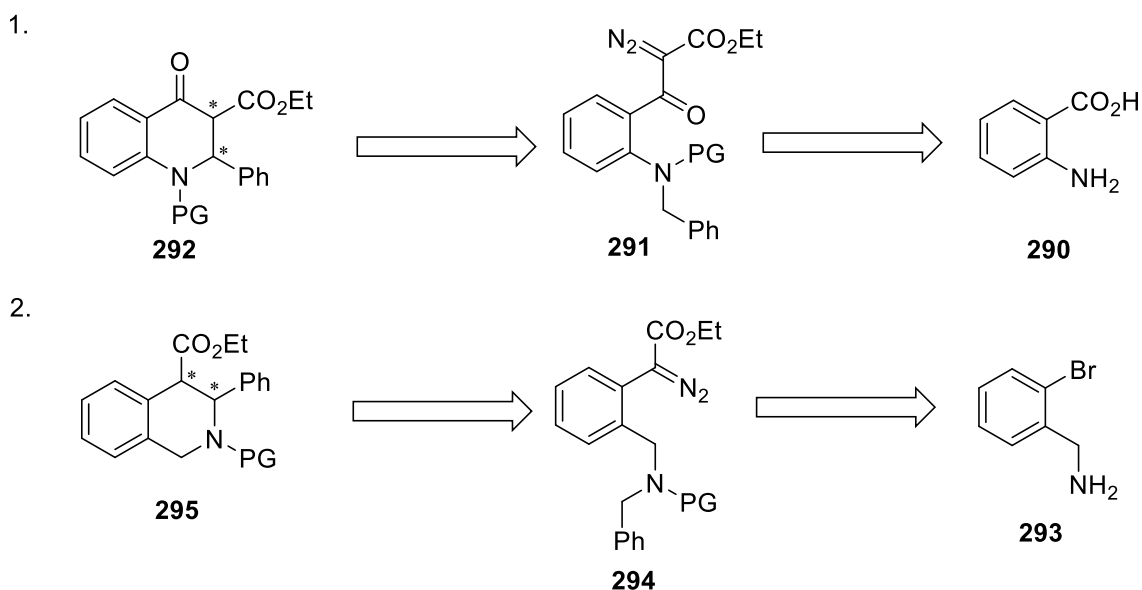


Scheme 111: Sulfoxide route

Although this project proved more challenging than the synthesis of dihydroindoles, it would be interesting to investigate these transformations further. In-depth optimisation studies on the C-H insertion of the sulfides could provide a catalyst system capable of producing the desired dihydrobenzo[*b*]thiophene **286**.

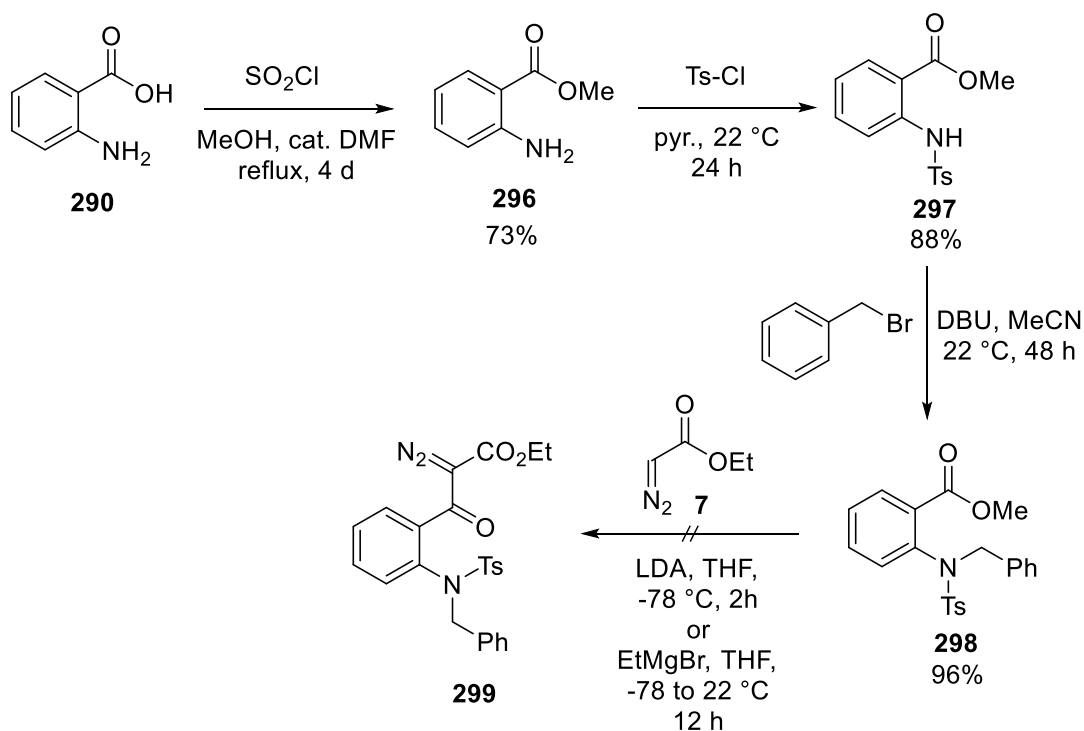
Another project that was started and received considerable attention in the course of this thesis was the stereoselective preparation of tetrahydroquinolines and tetrahydroisoquinolines from diazo compounds. The retrosynthetic strategy to these compounds is shown in

Scheme 112. For the formation of tetrahydroquinolines, a C-H insertion from the acceptor / acceptor substituted diazo compound **291** was envisioned (Scheme 112, 1.). As in the case of the indolines, two adjacent stereocenters are formed in this C-H insertion reaction. Anthranilic acid **290** was used to start this synthesis, a cheap and abundant compound. For the preparation of tetrahydroisoquinoline **295**, a similar approach was attempted (Scheme 112, 2.). 2-Bromobenzylamine **293** was chosen as starting material to access diazo compound **294**. An intramolecular C-H insertion reaction would then furnish tetrahydroisoquinoline **295**.



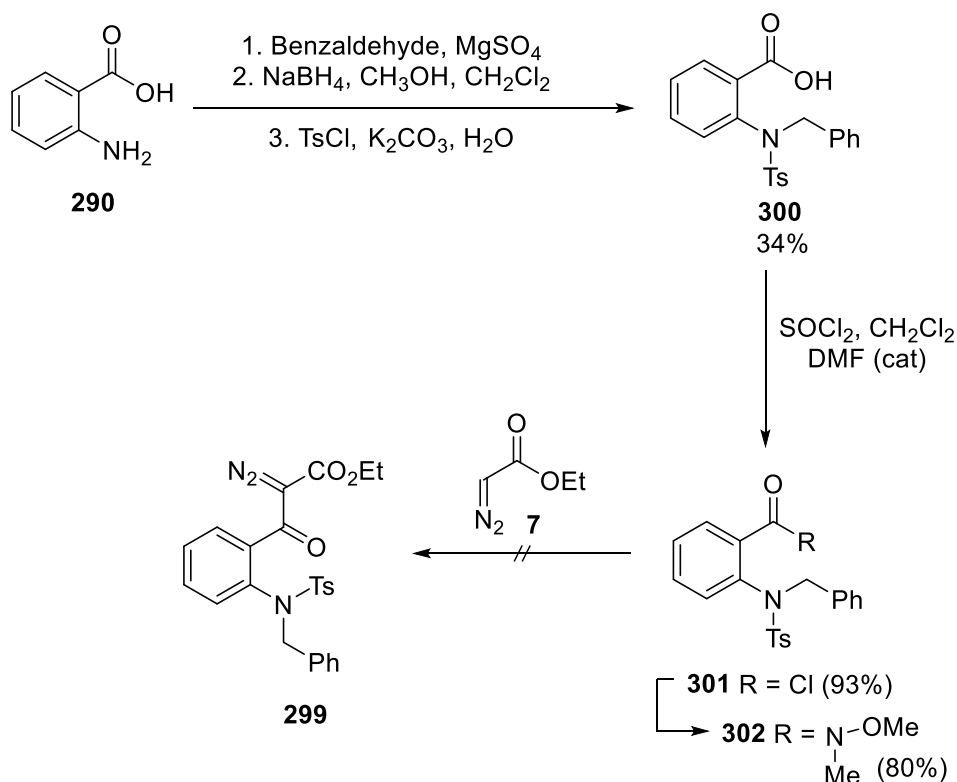
Scheme 112: Retrosynthetic strategy to tetrahydroquinoline **292** and tetrahydroisoquinoline **295**

The first approach to diazo compound **291** in the course of the preparation of tetrahydroquinoline **292** started with the methylation of anthranilic acid (73%). The methyl ester **296** was subsequently tosylated (88%) and benzylated (96%) to provide access to ester **298**. Treatment of ester **298** with ethyl diazoacetate and LDA did not lead to any product. The formation of a Grignard reagent of ethyl diazoacetate **7** and subsequent reaction with compound **298** also did not work (Scheme 113).

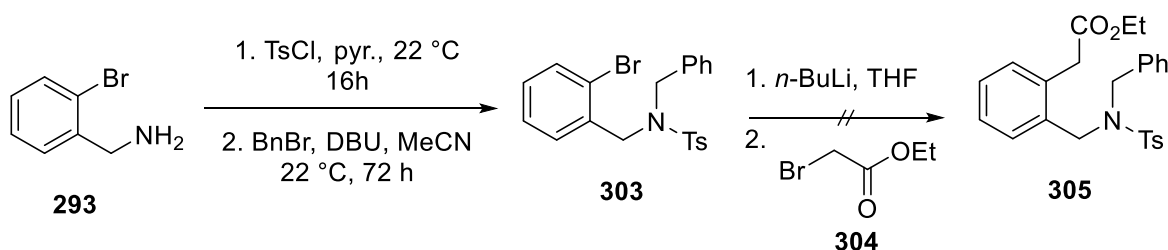


Scheme 113: Synthesis of diazo compound **299**

Therefore, the use of acyl chloride **301** as well as of Weinreb amide **302** for the reaction with ethyl diazoacetate **7** was investigated (Scheme 114). DBU was the base used for the reaction of acyl chloride **301** with ethyl diazoacetate **7**, however the desired product **299** was not found. Instead, a complex mixture of side-products was obtained. For the reaction of Weinreb amide **302**, LDA and ethyl diazoacetate were used at -78°C . Here, again none of the desired diazo compound **299** was observed.


 Scheme 114: Modified strategy to diazo compound **299**

The synthesis of tetrahydroisoquinolines from 2-bromobenzylamine **293** proved similarly difficult. Amine protection with tosyl chloride and benzylation worked smoothly (76%), however the subsequent lithium-halogen-exchange and reaction with ethyl bromoacetate resulted only in the recovery of the starting material **303**.


 Scheme 115: Synthesis of diazo precursor **305**

As indicated in Schemes 113 to 115, the formation of the six-membered heterocycles failed at the stage of the preparation of the respective diazo starting materials. It should, however, be possible to find efficient pathways to the two diazo compounds **291** and **294** to subsequently investigate the possibility of a stereoselective intramolecular C-H insertion reaction for tetrahydroquinolines and tetrahydroisoquinolines.

In conclusion, the chemistry of diazo compounds has been successfully expanded in this thesis. The use of continuous flow technology for the safe preparation and reaction of diazo

compounds was achieved. Preliminary studies into the use of diazo compounds for the stereoselective formation of heterocycles resulted in an efficient pathway to dihydroindoles. For the formation of dihydrobenzo[*b*]thiophenes, tetrahydroquinolines and tetrahydroisoquinolines further investigations will be required.

-
- 1 A. J. Anciaux, A. J. Hubert, A. F. Noels, N. Petiniot, P. Teyssie, *J. Org. Chem.* **1980**, *45*, 695.
 - 2 C. Aranda, A. Cornejo, J. M. Fraile, E. García-Verdugo, M. J. Gil, S. V. Luis, J. A. Mayoral, V. Martínez-Merino, Z. Ochoa, *Green Chem.* **2011**, *13*, 983.

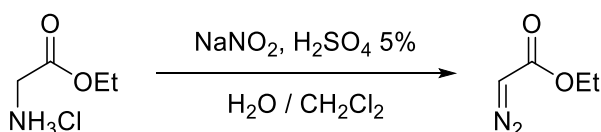
7 Experimental section

7.1 General methods

Reactions were carried out in standard reagent grade solvents. All chemicals were purchased from Sigma Aldrich, Alfa Aesar, Fisher Scientific, and Strem Chemicals and used without further purification. Reactions involving air- or moisture-sensitive reagents were carried out under an argon or nitrogen atmosphere using oven-dried glassware. For flow chemistry, KR Analytical Ltd Fusion 100 Touch syringe pumps, Vapourtec® E series pumps, Syrris® Asia pumps, and Ismatec piston pumps were used. Mixing systems used for flow chemistry were LTF®-MX mixer and Comet mixer. Mettler Toledo IR spectroscopy with flow diamond probe and flow silicon probe was used for reaction optimisation and kinetic studies. Thermal analyses were performed with a Setaram C80 calorimeter. Purifications were performed on a Biotage® Isolera system. Thin layer chromatography was performed on Merck Silica gel 60 F₂₅₄. Dry solvents were directly used from a MBRAUN® SPS-800 solvent purification system or distilled over CaH₂ (dichloromethane, diisopropylamine). HPLC measurements for chiral reactions were performed on a Shimadzu Class VP system with the following parts: auto injector: SIL-10AD; pump controller: LC-10AT; pump: FCV-10AL; degasser: DGU-14A; oven: CTO-10AS; system controller: SCL-10A; diode array detector: SPD-M10A. 2-Propanol and *n*-hexane (both HPLC grade purity) were used for HPLC analysis. Mass spectrometer were recorded at the EPSRC National Mass Spectrometry Facility in Swansea on a Waters Xevo G2-S and on a Thermo Scientific LTQ Orbitrap XL machine or at Cardiff University on a Water LCR Premier XE-tof. Ions were generated using atmospheric pressure ionisation technique (APCI), electrospray (ES), electron ionisation (EI) and nanospray ionisation (NSI). Infrared spectra were recorded on a Shimadzu FTIR IRAffinity-1S and on a Shimadzu FTIR IRAffinity-1 with the neat substance between NaCl disks. Melting points were recorded on a Gallenkamp variable heater. ¹H NMR and ¹³C NMR spectra were recorded on a Bruker Fourier 300 and a Bruker DPX 400 and referenced to the residual proton solvent peak (¹H: CDCl₃, δ 7.26; DMSO, δ 2.54) and solvent ¹³C signal (CDCl₃, δ 77.16). Signals were reported in ppm, multiplicity (s = singlet, d = doublet, t = triplet, q = quartet, quin = quintet, sex = sextet, hep = septet, m = multiplet, b = broad), coupling constants in Hertz.

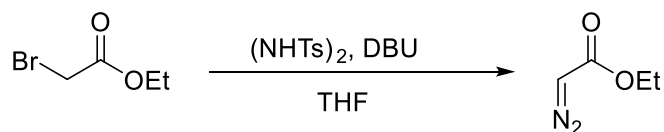
7.2 Experimentals Chapter 3

7.2.1 Synthesis of Ethyl diazoacetate in batch *via* diazotization



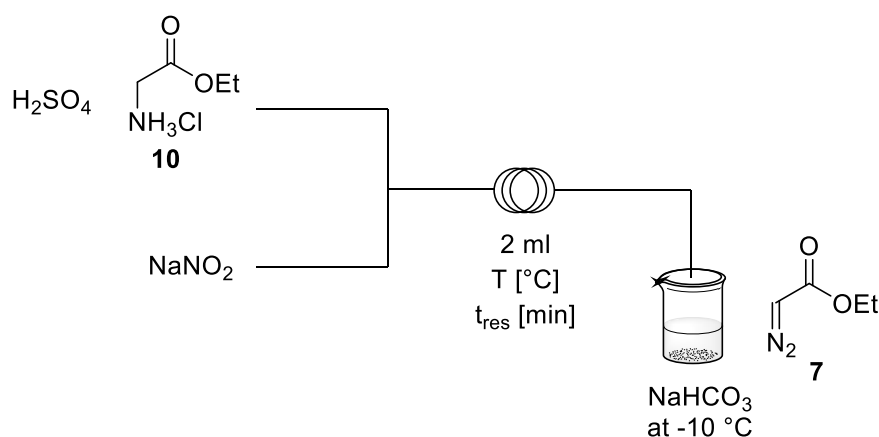
The reaction was performed following a known procedure.¹ Glycine ethyl ester hydrochloride (1.4 g, 10 mmol) was dissolved in a solvent mixture of 2.5 mL water and 5 mL dichloromethane in a 50 mL two-neck round bottom flask. The reaction mixture was flushed with N₂ (gas) and cooled to -10 °C (brine / ice cooling bath). Then, sodium nitrite (0.83 g, 12 mmol) dissolved in 2.5 mL water was added to the solution. Finally, sulfuric acid (5% w/w, 0.91 mL) was added dropwise. The reaction was left stirring for 15 min at -10 °C and subsequently poured into a beaker with aqueous saturated NaHCO₃ solution (15 mL) which was kept at -10 °C. The cold mixture was transferred into a cold separating funnel and extracted with cold dichloromethane (2 x 20 mL). The combined organic layers were washed with aqueous saturated NaHCO₃ solution (15 mL) and brine (15 mL) and dried over MgSO₄. The solvent was evaporated *in vacuo* at 30 °C to afford pure ethyl diazoacetate **7** (0.98 g, 8.6 mmol, 86%; containing ~ 10% CH₂Cl₂) as yellow, low boiling liquid. ¹H NMR (400 MHz, CDCl₃): δ = 4.67 (bs, 1H, CHN₂), 4.15 (q, *J* = 7.2 Hz, 2H, CH₂CH₃), 1.21 (t, *J* = 7.2 Hz, CH₂CH₃) ppm; ¹³C NMR (100 MHz, CDCl₃): δ = 170.0 (C=O), 61.2 (OCH₂), 46.5 (C=N₂), 14.8 (CH₃) ppm. Spectroscopic data was in accordance with the literature.²

7.2.2 Synthesis of Ethyl diazoacetate in batch from ethyl 2-bromoacetate



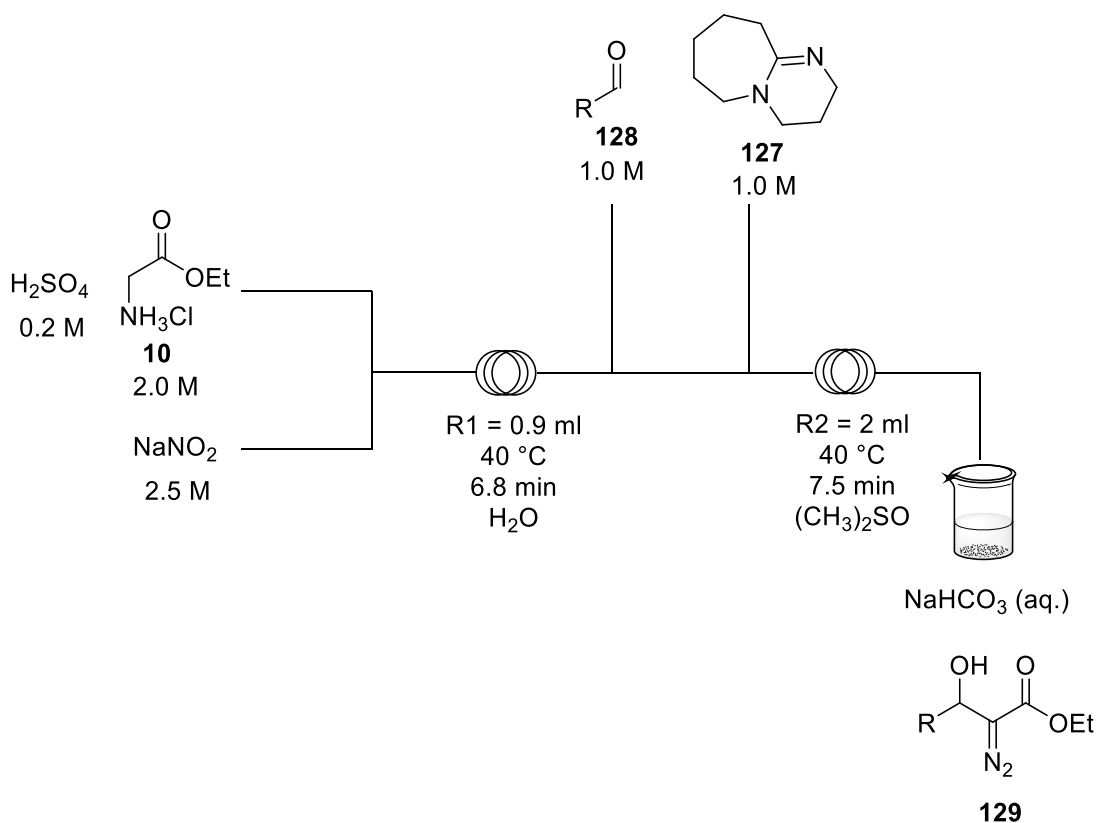
The reaction was performed following a known procedure.³ Ditosyl hydrazine (1.7 g, 5 mmol) was dissolved in THF (10 mL) under inert atmosphere (N₂). Then, ethyl 2-bromoacetate (0.28 mL, 2.5 mmol) was added and the mixture was cooled to 0 °C before the dropwise addition of DBU (1.87 mL, 12.5 mmol). The reaction mixture was left stirring at 0 °C for 10 min and was then transferred into a separating funnel, quenched with aqueous saturated NaHCO₃ solution (20 mL) and extracted with diethyl ether (2 x 20 mL). The combined organic layers were subsequently washed with aqueous saturated NaHCO₃ solution (20 mL) and brine (2 x 15 mL) and dried over MgSO₄. The solvent was evaporated *in vacuo* at 30 °C and the resulting yellow oil was purified *via* flash column chromatography (100% Petroleum ether) to afford ethyl diazoacetate **7** (0.22 g, 1.93 mmol, 77%) as yellow, low boiling liquid. Spectroscopic data was in accordance with the literature.²

7.2.3 Synthesis of Ethyl diazoacetate in flow

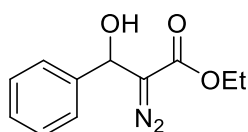


Glycine ethyl ester (11.17 g, 80 mmol) was dissolved in water and H_2SO_4 (5% w/w, 7.6 mL) was added to give a total volume of 100 mL. Sodium nitrite (6.9 g, 100 mmol) was dissolved in water to give a total volume of 100 mL. The two solutions were attached to the Vapourtec® E-Series pumps and pumped through a 2 mL flow reactor with a flow rate of 0.66 mL/min (0.33 mL/min each) and collected in saturated NaHCO_3 which was kept at $-10\text{ }^\circ\text{C}$. The work-up was performed according to the batch procedure (7.2.1). Ethyl diazoacetate **7** (5.5 g, 211 min coll time, 78%) was obtained as yellow liquid.

7.2.4 Two-step continuous flow system for α -diazo- β -hydroxyester

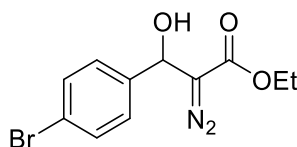


Glycine ethyl ester hydrochloride (1.12 g, 8 mmol) was dissolved in water (2.5 mL) and sulfuric acid (5% w/w, 0.76 mL) was added and a 4 mL syringe was equipped with the mixture. Next, NaNO₂ (664 mg, 10 mmol) was dissolved in water (3.9 mL) and another 4 mL syringe was equipped with this solution. The two syringes were connected to a flow set-up with a T-piece mixer and a 0.9 mL coil (PTFE, i.d. = 0.5 mm). 1,8-Diazabicycloundec-7-ene (DBU, 596 µL, 4 mmol) was dissolved in dimethyl sulfoxide (3.4 mL) and charged into a 4 mL syringe. Aldehyde (4 mmol) was dissolved in the required amount of DMSO to have a solution of exactly 4 mL volume. This mixture was charged into another 4 mL syringe. Both syringes were put to another syringe pump and connected with two T-pieces to the outlet of the first coil as well as to the inlet of the second coil. The second coil consisted of a 2 mL coil (PTFE, i.d. = 0.8 mm). The pumps were set to 4 mL/h and the entire set-up ran for 28 min to reach the steady state. Afterwards, the product was collected for 20 - 30 minutes in NaHCO₃ as quenching agent. Extraction was performed with CH₂Cl₂ (3 x 10 mL), the combined organic layers were washed with water thoroughly (3 x 10 mL) and dried over anhydrous MgSO₄. After evaporating the solvent *in vacuo*, the diazoalcohol was purified by column chromatography (*n*-hexane / ethyl acetate gradient from 100:0 to 85:15).



Ethyl 2-diazo-3-hydroxy-3-phenylpropanoate **106**

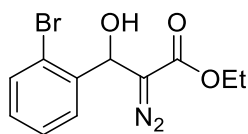
363 mg (30 min collection time; 82% yield) as thick yellow oil. ¹H NMR (400 MHz, CDCl₃): δ = 7.57 (m, 5H, ArH), 6.11 (d, *J* = 3.5 Hz, 1H, CHOH), 4.47 (q, *J* = 7.5 Hz, 2H, CH₂CH₃), 3.26 (brs, 1H, OH), 1.50 (t, *J* = 7.5 Hz, 3H, CH₂CH₃) ppm; ¹³C NMR (100 MHz, CDCl₃): δ = 166.8 (C=O), 139.2 (ArC), 129.1 (ArCH), 128.6 (ArCH), 126.0 (ArCH), 69.2 (COH), 61.6 (OCH₂), 15.0 (CH₃) ppm; MS (EI): *m/z* 220 (M⁺, 4%), 192 (8), 174 (28), 146 (19), 129 (100), 118 (20), 105 (93), 90 (21), 77 (79), 63 (16). Carbon of diazo species not detected. Spectroscopic data was in accordance with the literature.⁴



Ethyl 3-(4-bromophenyl)-2-diazo-3-hydroxypropanoate **129a**

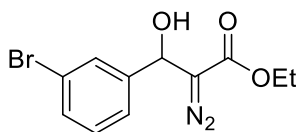
295 mg (20 min collection time; 74% yield) as yellow oil. ¹H NMR (400 MHz, CDCl₃): δ = 7.79 (m, 2H, ArH), 7.58 (m, 2H, ArH), 6.15 (d, *J* = 3.5 Hz, 1H, CHOH), 4.55 (q, *J* = 7 Hz, 2H, CH₂CH₃), 3.47 (brs, 1H, CHOH), 1.58 (t, *J* = 7.5 Hz, 3H, CH₂CH₃) ppm; ¹³C NMR (100 MHz,

CDCl_3): δ = 166.8 (C=O), 138.4 (ArC), 132.5 (ArCH), 128.1 (ArCH), 122.8 (ArC), 68.8 (COH), 61.8 (OCH₂), 15.0 (CH₃) ppm; MS (EI): m/z 300 (5%), 298 (M⁺, 5), 272 (49), 270 (55), 226 (87), 224 (90), 198 (39), 196 (32), 185 (100), 183 (99), 158 (91), 155 (91), 89 (84), 77 (55), 75 (61). Carbon of diazo species not detected. Spectroscopic data was in accordance with the literature.⁴



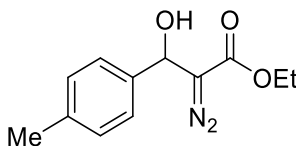
Ethyl 3-(2-bromophenyl)-2-diazo-3-hydroxypropanoate **129b**

421 mg (22 min collection time; 96% yield) as yellow oil. ¹H NMR (500 MHz, CDCl_3): δ = 7.71 (dd, J = 8, 1.5 Hz, 1H, ArH), 7.57 (dd, J = 8, 1 Hz, 1H, ArH), 7.39 (td, J = 7.5, 1.5 Hz, 1H, ArH), 7.20 (td, J = 8, 1.5 Hz, 1H, ArH), 6.09 (s, 1H, CHOH), 4.29 (m, 2H, CH₂CH₃), 3.34 (brs, 1H, CHOH), 1.30 (t, J = 7 Hz, 3H, CH₂CH₃) ppm; ¹³C NMR (125 MHz, CDCl_3): δ = 166.3 (C=O), 137.7 (ArC), 132.9 (ArCH), 127.8 (ArCH), 127.6 (ArCH), 121.6 (ArC), 68.8 (COH), 61.3 (OCH₂), 14.8 (CH₃) ppm. Carbon of diazo species not detected. Spectroscopic data was in accordance with the literature.⁵



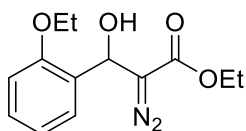
Ethyl 3-(3-bromophenyl)-2-diazo-3-hydroxypropanoate **129c**

362 mg (22 min collection time; 82% yield) as yellow oil. ¹H NMR (500 MHz, CDCl_3): δ = 7.61 (m, 1H, ArH), 7.46 (d, J = 8 Hz, 1H, ArH), 7.35 (d, J = 8 Hz, 1H, ArH), 7.26 (t, J = 7.5 Hz, 1H, ArH), 5.87 (s, 1H, CHOH), 4.28 (q, J = 7 Hz, 2H, CH₂CH₃), 3.09 (brs, 1H, CHOH), 1.30 (t, J = 7 Hz, 3H, CH₂CH₃) ppm; ¹³C NMR (125 MHz, CDCl_3): δ = 166.2 (C=O), 141.1 (ArC), 131.4 (ArCH), 130.5 (ArCH), 128.9 (ArCH), 124.5 (ArCH), 123.0 (ArC), 68.1 (COH), 61.4 (OCH₂), 14.5 (CH₃) ppm. Carbon of diazo species not detected. Spectroscopic data was in accordance with the literature.⁶



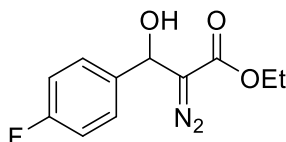
Ethyl 2-diazo-3-hydroxy-3-(*p*-tolyl)propanoate **129d**

203 mg (17 min collection time; 77% yield) as yellow oil. ^1H NMR (500 MHz, CDCl_3): δ = 7.31 (d, J = 8 Hz, 2H, ArH), 7.19 (d, J = 8 Hz, 2H, ArH), 5.88 (s, 1H, CHOH), 4.27 (q, J = 7 Hz, 2H, CH_2CH_3), 3.12 (brs, 1H, CHOH), 2.35 (s, 3H, ArCH_3), 1.29 (t, J = 7 Hz, 3H, CH_2CH_3) ppm; ^{13}C NMR (125 MHz, CDCl_3): δ = 166.5 (C=O), 138.2 (ArC), 135.6 (ArC), 129.4 (ArCH), 125.7 (ArCH), 68.7 (COH), 61.1 (OCH_2), 21.1 (CH_3), 14.5 (CH_3) ppm. Carbon of diazo species not detected. Spectroscopic data was in accordance with the literature.⁴



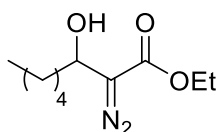
Ethyl 2-diazo-3-(2-ethoxyphenyl)-3-hydroxypropanoate **129e**

328 mg (22 min collection time; 85% yield) as yellow solid. ^1H NMR (500 MHz, CDCl_3): δ = 7.44 (d, J = 7.5 Hz, 1H, ArH), 7.28 (td, J = 8, 1.5 Hz, 1H, ArH), 6.98 (dt, J = 7.5, 1 Hz, 1H, ArH), 6.90 (d, J = 8 Hz, 1H, ArH), 5.90 (d, J = 6.5 Hz, 1H, CHOH), 4.25 (q, J = 7 Hz, 2H, $\text{CO}_2\text{CH}_2\text{CH}_3$), 4.08 (m, 2H, OCH_2CH_3), 3.62 (brs, 1H, CHOH), 1.42 (t, J = 7 Hz, 3H, OCH_2CH_3), 1.29 (t, J = 7 Hz, 3H, $\text{CO}_2\text{CH}_2\text{CH}_3$) ppm; ^{13}C NMR (125 MHz, CDCl_3): δ = 166.5 (C=O), 155.4 (ArC), 129.3 (ArCH), 127.2 (ArCH), 127.2 (ArC), 120.8 (ArCH), 111.2 (ArCH), 66.4 (COH), 63.7 (OCH_2), 60.9 (OCH_2), 14.8 (CH_3), 14.5 (CH_3) ppm. Carbon of diazo species not detected.



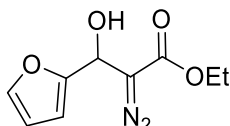
Ethyl 2-diazo-3-(4-fluorophenyl)-3-hydroxypropanoate **129f**

260 mg (20 minutes collection time; 1.09 mmol, 82%) as yellow oil. ^1H NMR (400 MHz, CDCl_3): δ = 7.68 (m, 2H, ArH), 7.35 (m, 2H, ArH), 6.17 (d, J = 3.5 Hz, 1H, CHOH), 4.55 (q, J = 7 Hz, 2H, CH_2CH_3), 3.36 (brs, 1H, CHOH), 1.57 (t, J = 7 Hz, 3H, CH_2CH_3) ppm; ^{13}C NMR (100 MHz, CDCl_3): δ = 167.0 (C=O), 163.5 (d, J = 234 Hz, ArCF), 135.4 (ArC), 128.2 (d, J = 9 Hz, ArCH), 116.3 (d, J = 20 Hz, ArCH), 68.8 (COH), 61.9 (OCH_2), 15.1 (CH_3) ppm; MS (EI): m/z 238 (M^+ , 4%), 182 (7), 164 (65), 136 (37), 123 (100), 108 (89), 95 (45), 75 (18). Carbon of diazo species not detected. Spectroscopic data was in accordance with the literature.⁴



Ethyl 2-diazo-3-hydroxy-octanoate **129g**

188 mg (20 min collection time; 66% yield) as pale yellow oil. ^1H NMR (400 MHz, CDCl_3): δ = 4.90 (dt, J = 4.5, 9.5 Hz, 1H, CHOH), 4.47 (q, J = 7 Hz, 2H, OCH_2CH_3), 2.80 (brs, 1H, CHOH), 1.86 (m, 2H, CH_2CHOH), 1.53 (m, 9H, $\text{CH}_2\text{CH}_2\text{CH}_2\text{CH}_3$), 1.12 (t, J = 7 Hz, 3H, OCH_2CH_3) ppm; ^{13}C NMR (100 MHz, CDCl_3): δ = 167.3 (C=O), 67.3 (COH), 61.6 (OCH_2), 34.5 (CH_2), 32.0 (CH_2), 25.8 (CH_2), 23.1 (CH_2), 15.1 (CH_3), 14.6 (CH_3) ppm; MS (EI): m/z 214 (M^+ , 5%), 154 (11), 143 (100), 130 (62), 115 (74), 99 (69), 87 (67), 69 (58), 55 (48). Carbon of diazo species not detected. Spectroscopic data was in accordance with the literature.⁵

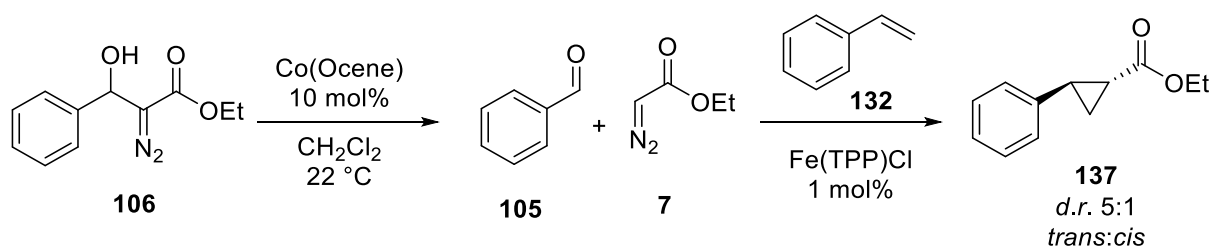


Ethyl 2-diazo-3-(furan-2-yl)-3-hydroxypropanoate **129h**

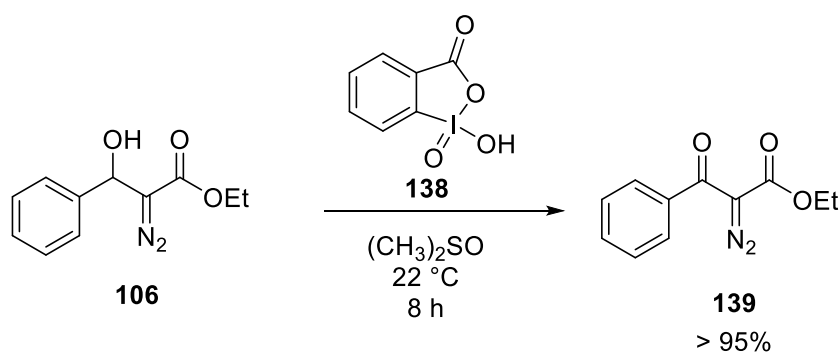
94 mg (15 min collection time; 45% yield) as yellow oil. ^1H NMR (400 MHz, CDCl_3): δ = 7.49 (t, J = 0.8 Hz, 1H, $\text{O}-\text{CH}=\text{C}$), 6.46 (m, 2H, $\text{CH}=\text{CH}$), 5.91 (d, J = 4.5 Hz, 1H), 5.64 (d, J = 5 Hz, 1H), 4.35 (q, J = 7 Hz, 2H), 1.38 (t, J = 7.5 Hz, 3H) ppm; ^{13}C NMR (125 MHz, CDCl_3): δ = 166.1 (C=O), 143.4 (ArC-O), 143.1 (ArCH-O), 110.7 (ArCH), 107.8 (ArCH), 63.9 (CHOH), 61.5 (OCH_2), 14.7 (CH_3) ppm; MS (EI): m/z 208 (M^+ , 18%), 190 (38), 162 (15), 143 (100), 121 (77), 97 (95), 91 (88), 84 (95), 77 (69), 66 (94), 55 (89). Carbon of diazo species not detected. Spectroscopic data was in accordance with the literature.⁵

Upscale: Glycine ethyl ester hydrochloride (11.2 g, 80 mmol) was dissolved in water with sulfuric acid (5% w/w, 7.6 mL) for a total volume of 40 mL. Sodium nitrite (6.9 g, 100 mmol) was dissolved in water for a total volume of 40 mL. Both solutions were pumped using the Vapourtec E-series with a flow rate of 0.67 mL/min through a reactor (0.88 mL, t_{res} = 1.3 min). Benzaldehyde (4.07 mL, 40 mmol) and DBU (6.0 mL, 40 mmol) were dissolved in dimethyl sulfoxide for a total volume of 80 mL and pumped into the continuous flow system with a flow rate of 0.67 mL/min. The combined solutions were pumped through a continuous flow reactor (10 mL, t_{res} = 7.5 min) and the system was stabilised for thirty minutes. Then, the reaction was collected for 115 min in NaHCO_3 (aq., sat.), extracted with dichloromethane (3 x 25 mL) and the combined organic fractions were washed with water (2 x 40 mL) and brine (40 mL). The organic layer was dried over MgSO_4 and evaporated *in vacuo*. Flash column chromatography furnished diazo alcohol **106** (6.05 g, 27 mmol, 72%) as yellow oil.

7.2.5 Cyclopropanation with styrene

Ethyl 2-phenylcyclopropane-1-carboxylate **137**

Iron(TPP)Cl (7 mg, 0.01 mmol) and Cobaltocene (19 mg, 0.1 mmol) were put into an oven-dried round bottom flask and flushed with argon. Then, dichloromethane (5 mL, dry, distilled over CaH_2) was added to the two catalysts and the reaction mixture was stirred at room temperature. Next, styrene **132** (0.36 mL, 3 mmol) and diazo alcohol **106** (0.22 g, 1 mmol) were added to the mixture under argon and the mixture was left stirring at room temperature for 12 h. Subsequent evaporation of the solvent *in vacuo* and flash column chromatography furnished cyclopropane **137** (107 mg, 0.56 mmol, 56% yield) as colourless oil. ^1H NMR (400 MHz, CDCl_3): δ = 7.24–7.10 (m, 3H, ArH), 7.05–7.00 (m, 2H, ArH), 4.09 (q, J = 7.1 Hz, 1H, OCH_2), 2.44 (ddd, J = 9.3, 6.5, 4.2 Hz, 1H, cyclopropCH- CO_2), 1.83 (ddd, J = 8.4, 5.3, 4.2 Hz, 1H, cyclopropCH), 1.53 (ddd, J = 9.6, 5.6, 3.0 Hz, cyclopropCH), 1.27–1.20 (m, 1H, cyclopropCH), 1.20 (t, J = 7.1 Hz, 3H, CH_3). Spectroscopic data was in accordance with the literature.⁷

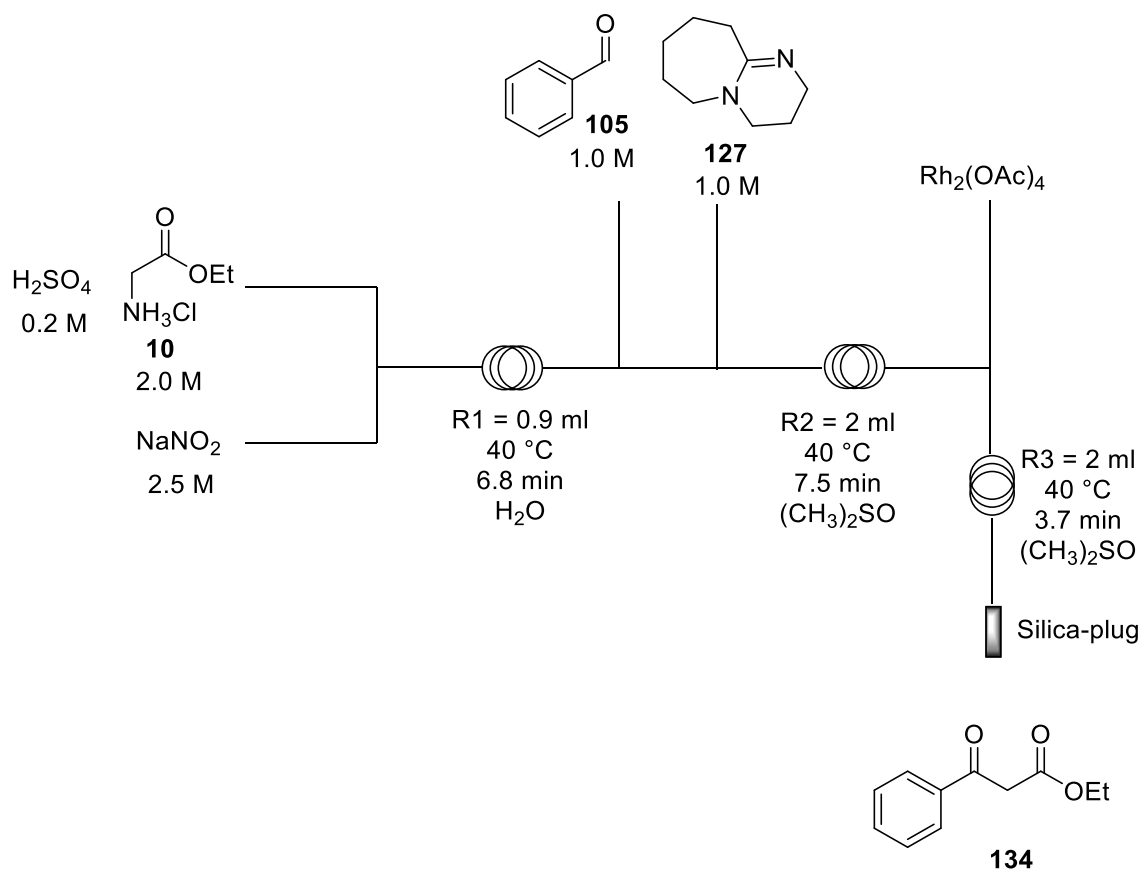
7.2.6 Oxidation of α -diazo- β -hydroxyester to α -diazo- β -ketoesterEthyl 2-diazo-3-oxo-3-phenylpropanoate **139**

Before preparation of α -diazo- β -ketoester, iodoxybenzoic acid (IBX) **138** was prepared following a standard procedure.⁸ A 250ml round bottom flask was fitted with a magnetic stirring bar and charged with a solution of oxone (12.9 g, 20.97 mmol) in water (52 mL). To this was added 2-Iodobenzoic acid (4.0 g, 16.13 mmol) and the solution was heated to 73°C and left stirring for three hours. Subsequently, the reaction mixture was cooled down slowly to 5°C

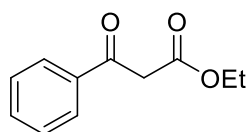
and then left at this temperature for 90 minutes with slow stirring to entice crystallisation. Finally, the solution was filtered to give a white solid which was washed with water (3 x 20 mL) and acetone (20 mL). After drying under *vacuo* the product was furnished as white solid (4.1 g, 14.8 mmol, 92%). ¹H NMR (400 MHz, d₆-DMSO): δ = 8.15 (d, *J* = 8.1 Hz, 1H, *ArH*), 8.03 (m, 2H, *ArH*), 7.84 (dt, *J* = 7.4, 1.2 Hz, 1H, *ArH*) ppm; ¹³C NMR (100 MHz, d₆-DMSO): δ = 167.9, 146.9, 133.7, 133.3, 131.8, 130.4, 125.3 ppm. Spectra in accordance to literature.⁹

Performed according to a known procedure.² Iodoxybenzoic acid **138** (420 mg, 1.5 mmol) was dissolved in dimethyl sulfoxide (10 mL), a process which takes around 20 min. Then, ethyl 2-diazo-3-hydroxy-3-phenylpropanoate **106** (220 mg, 1 mmol) was dissolved in dimethyl sulfoxide (3 mL) and added to the IBX solution over the course of one hour using a syringe pump. The solution was left stirring for 8 hours at 22 °C and was then quenched with aqueous saturated NaHCO₃ solution (20 mL). The solution was extracted with dichloromethane (2 x 20 mL) and the combined organic layers were washed with water (3 x 20 mL) and brine (20 mL). After drying over MgSO₄, the solvent was evaporated *in vacuo* to furnish pure diazoester **139** (216 mg, 0.99 mmol, 99%) as pale yellow oil. ¹H NMR (400 MHz, CDCl₃): δ = 7.86 (dd, *J* = 9.6, 1.4 Hz, 2H, *ArH*), 7.76 (tt, *J* = 7.5, 1.3 Hz, 1H, *ArH*), 7.66 (m, 2H, *ArH*), 4.48 (q, *J* = 7.1 Hz, 2H, CO₂CH₂), 1.49 (t, *J* = 7.1 Hz, 3H, CH₃) ppm. Spectroscopic data was in accordance with the literature.⁴

7.2.7 Three-step process

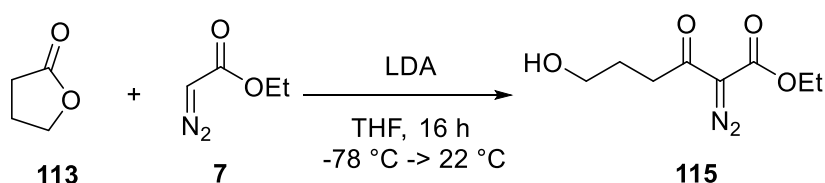


Syringes, pumps, reagents and flow set-up were built the way as described for the two-step procedure. Rhodium acetate dimer (0.025 mmol, 11 mg) was dissolved in a mixture water / DMSO (1:1) (10 mL). The solution was charged onto a 10 mL syringe and put on a third syringe pump which was calibrated on a flow rate of 16 mL/h to run through the third reactor (i.d. 0.8 mm, 2 mL). After the first two reactors had reached steady state, the third pump was started and collection commenced after another 4 min after the last reactor has reached steady state. The product was collected for 20-30 minutes in sat. NaHCO_3 solution. Extraction was performed with dichloromethane (3 x 10 mL), the combined organic layers were washed with water (3 x 10 mL) and dried over anhydrous MgSO_4 . After evaporating the solvent *in vacuo*, the β -ketoester was purified by column chromatography (*n*-hexane:EtOAc 98:2).

Ethyl 3-oxo-3-phenylpropanoate **134**

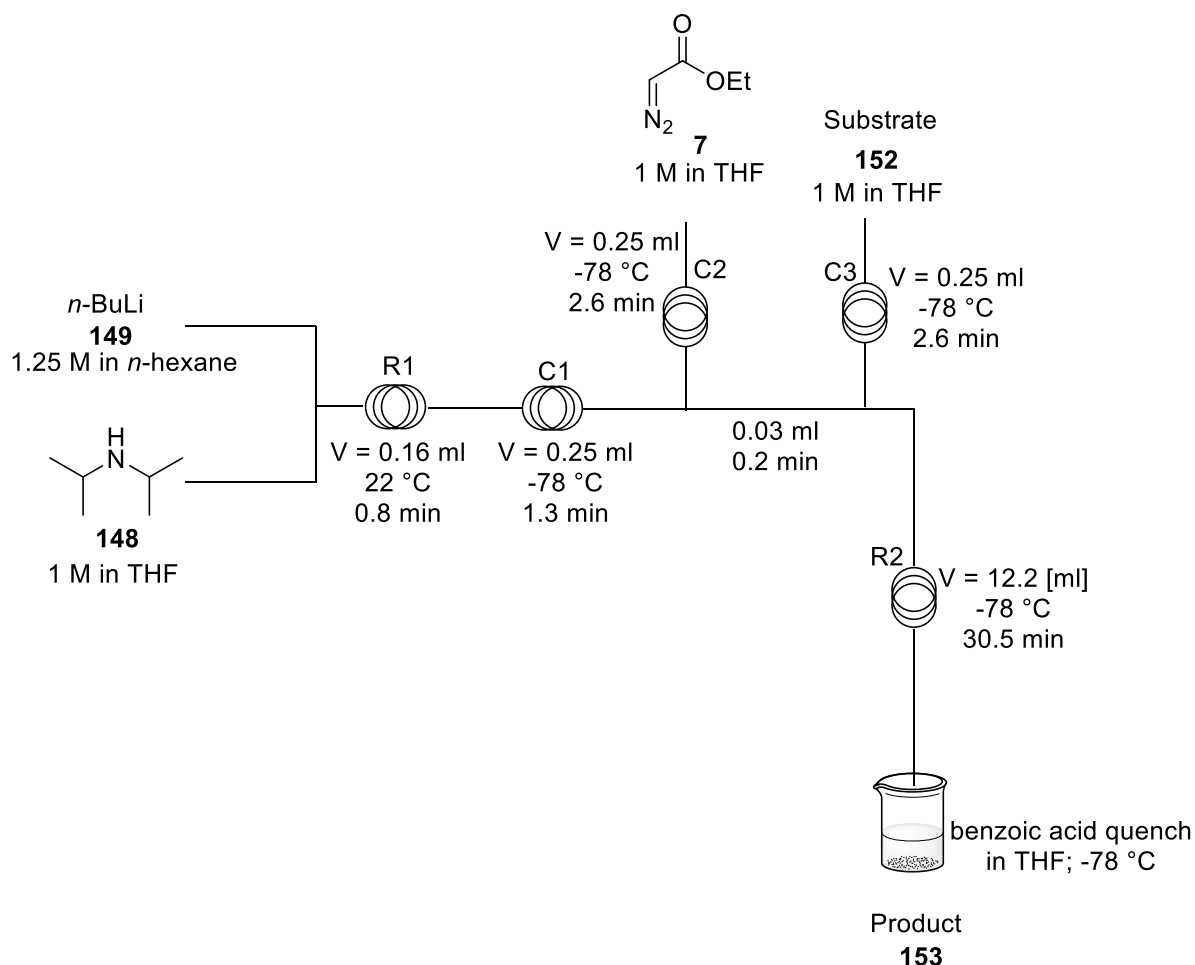
187 mg (20 min collection time; 73% yield) as colourless oil in both keto and enol form. Keto form: ^1H NMR (400 MHz, CDCl_3): δ = 7.88 (m, 2H, ArH), 7.39 (m, 3H, ArH), 4.14 (q, J = 7.0 Hz, 2H, CH_2CH_3), 3.92 (s, 2H, OCCH_2CO), 1.18 (t, J = 7.0 Hz, 3H, CH_3CH_2) ppm; ^{13}C NMR (100 MHz, CDCl_3): δ = 193.2 (C=O), 168.1 (C=O), 134.4 (ArC), 129.4 (ArCH), 60.9 (OCH_2), 40.6 (CH_2), 14.6 (CH_3) ppm; Enol form: ^1H NMR (400 MHz, CDCl_3): δ = 12.78 (s, 1H, OH), 7.70 (m, 2H, ArH), 7.53 (m, 2H, ArH), 7.34 (m, 1H, ArH), 5.60 (s, 1H, C=CH), 4.19 (q, J = 7.0 Hz, 2H, OCH_2CH_3), 1.26 (t, J = 7.0 Hz, 3H, OCH_2CH_3) ppm; ^{13}C NMR (100 MHz, CDCl_3): δ = 173.8 (COH), 172.0 (C=O), 134.0 (ArC), 131.8 (ArCH), 126.6 (ArCH), 88.0 (C=CH), 60.9 (OCH_2), 14.9 (CH_3) ppm; MS (EI): m/z 192 (M^+ , 64%), 164 (8), 147 (39), 120 (17), 105 (100), 91 (33), 77 (88), 65 (22). Spectroscopic data was in accordance with the literature.¹⁰

7.2.8 Lithiation reactions in batch



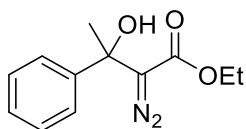
To a solution of γ -butyrolactone **113** (77 μL , 1 mmol) in THF (10 mL, dry) at $-78\text{ }^\circ\text{C}$ under a nitrogen atmosphere, ethyl diazoacetate **7** (106 μL , 1 mmol) and freshly prepared lithium diisopropylamide (2 mL, 0.5 M in THF, 1 mmol) were added. The reaction mixture was stirred at $-78\text{ }^\circ\text{C}$ for 3 h and was then warmed to $0\text{ }^\circ\text{C}$. At this temperature, the reaction mixture was quenched with aqueous ammonium chloride solution (1 M, 10 mL) and extracted with ethyl acetate (2 x 10 mL). The combined organic layers were washed with water (15 mL) and brine (15 mL) and dried over MgSO_4 . Subsequent evaporation of the solvent *in vacuo* and flash column chromatography afforded alcohol **115** (43 mg, 0.21 mmol, 21%) as yellow oil. ^1H NMR (400 MHz, CDCl_3): δ = 4.29 (q, J = 7.1 Hz, 2H, OCH_2), 3.67 (t, J = 7.0 Hz, 2H, CH_2), 2.97 (t, J = 7.0 Hz, 2H, CH_2), 2.33 (bs, 1H, OH), 1.90 (quint, J = 7.1 Hz, 2H, CH_2), 1.32 (t, J = 7.1 Hz, 3H, CH_3) ppm; ^{13}C NMR (75 MHz, CDCl_3): δ = 193.4 (C=O), 161.5 (C=O), 76.3 (C= N_2), 62.2 (CH_2OH or OCH_2), 61.6 (CH_2OH or OCH_2), 37.1 (CH_2), 27.3 (CH_2), 14.4 (CH_3) ppm. Spectroscopic data was in accordance with the literature.¹¹

7.2.9 Lithiation of ethyl diazoacetate in flow



Six round bottom flasks (2 x 250 mL, 4 x 100 mL) were dried overnight at 120°C in the oven. The next day, the continuous flow set-up was flushed for at least 45 minutes with $i\text{PrOH}$ at a flow rate of 0.5 mL/min . Subsequently, two round bottom flasks (2 x 250 mL) were flushed with argon, closed with a rubber septum, kept under argon and filled with *n*-hexane (150 mL, dry) and THF (200 mL, dry), respectively. The continuous flow set-up was flushed with THF (0.25 mL/min) for line A and C (both blue tubing; Vapourtec®) and for the line coming from the syringe pump. Line B (red tubing; Vapourtec®) was flushed with *n*-hexane (0.25 mL/min). The flushing with the dry solvents was performed for 45 minutes before cooling down the flow system to -78°C . It is important that no $i\text{PrOH}$ is left in the system when cooling it down as otherwise the pumps stall. A solution of ethyl diazoacetate **7** (1.5 M) in THF was prepared by addition of 2.4 mL of EDA (20.3 mmol of 90% EDA) to 12.6 mL THF in a dried RBF under argon with a rubber septum. A solution of diisopropylamine **148** (1.5 M) was prepared by addition of 3.2 mL freshly distilled diisopropylamine (22.5 mmol) to 11.8 mL THF in a dried RBF under argon with a rubber septum. A solution of the substrate (1.0 M) was prepared by

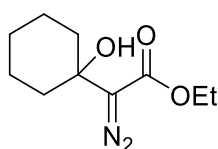
addition of substrate (10 mmol) to THF for a total volume of 10 mL in a dried RBF under argon with a rubber septum. A solution of *n*-BuLi (1.75 M) was prepared by addition of 10.5 mL of *n*-BuLi (2.5 M, 26.3 mmol) to 4.5 mL *n*-hexane in a dried RBF under argon with a rubber septum. The *n*-BuLi solution was kept at $-78\text{ }^{\circ}\text{C}$ in an acetone / dry ice bath for the time of the experiment to prevent degradation. Line A (blue tubing) was connected to the DIPA solution which was pumped with a flow rate of 0.1 mL/min. Line B (red tubing) was connected to the *n*-BuLi solution which was pumped with a flow rate of 0.1 mL/min. Line C (blue tubing) was connected to the EDA solution which was pumped with a flow rate of 0.1 mL/min. The substrate was pumped using a KD syringe pump 100 with a flow rate of 0.1 mL/min. The system was stabilised for 70 minutes with no tubing of the reactors being outside the $-78\text{ }^{\circ}\text{C}$ cooling bath to prevent decomposition of ethyl lithiodiazoacetate **114**. Then, a collection vial containing 0.61 g benzoic acid (5 mmol) in THF (5 mL, 1 M) was connected to the outlet of the flow reactor within the cooling bath and the flow stream was collected for 20-50 minutes. Afterwards, the pumps were switched back to the solvent lines and the flow system was cleaned using first the dry solvent lines (THF and *n*-hexane), then warming up the flow system to room temperature. Finally, the system was cleaned using *i*PrOH (0.5 mL/min; 1 h). The collected solution was dissolved in EtOAc (15 mL), washed with NaHCO_3 (15 mL). The aqueous layer was re-extracted with EtOAc (15 mL) and then, the combined organic layers were washed twice with NaHCO_3 (2 x 15 mL) and brine (20 mL), dried over MgSO_4 , filtered and evaporated *in vacuo*. The final diazo reagents were obtained after flash column chromatography.



Ethyl 2-diazo-3-hydroxy-3-phenylbutanoate **131**

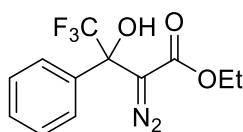
494 mg (34 min collection time, 62%) as yellow oil. ^1H NMR (300 MHz, CDCl_3): δ = 7.50-7.46 (m, 2H, ArH), 7.39-7.25 (m, 3H, ArH), 4.34 (bs, 1H, OH), 4.29 – 4.11 (m, 2H, CO_2CH_2), 1.72 (s, 3H, CH_3), 1.23 (t, J = 7.1 Hz, 3H, CH_2CH_3) ppm; ^{13}C NMR (75 MHz, CDCl_3): δ = 167.1 (C=O), 146.4 (ArC), 128.5 (ArCH), 127.8 (ArCH), 124.8 (ArCH), 73.4 (COH), 63.9 (C=N₂), 61.2 (CH_2), 29.3 (CH_3), 14.5 (CH_3) ppm; IR (neat): ν 3468b, 2982m, 2093s, 1687s, 1371m, 1312s, 1072m, 702m cm^{-1} . Spectroscopic data was in accordance with the literature.¹²

1.24 (t, $J = 7.1$ Hz, 3H, CH_3) ppm; ^{13}C NMR (75 MHz, CDCl_3): $\delta = 167.2$ (C=O), 159.8 (ArCOMe), 148.3 (ArC), 129.6 (ArCH), 117.1 (ArCH), 112.9 (ArCH), 110.9 (ArCH), 73.3 (COH), 61.2 (CH_2), 55.4 (OCH_3), 29.2 (CH_3), 14.5 (CH_3) ppm; IR (neat): ν 3481b, 2981m, 2093s, 1683s, 1601m, 1485m, 1371m, 1311s, 1053m cm^{-1} ; HRMS (ES): Exact mass calcd for $\text{C}_{13}\text{H}_{16}\text{N}_2\text{O}_4$ $[\text{M}+\text{Na}]^+$: 287.1008, Found: 287.1004; MS (ES): 551 (100%), 537 (12), 388 (28), 328 (14), 287 ($\text{M}+\text{Na}^+$, 18).



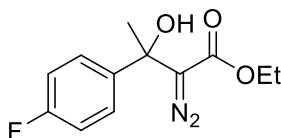
Ethyl 2-diazo-2-(1-hydroxycyclohexyl)acetate **153d**

345 mg (25 min collection time, 65%) as yellow oil. ^1H NMR (300 MHz, CDCl_3): $\delta = 4.23$ (q, $J = 7.1$ Hz, 2H, CO_2CH_2), 3.47 (bs, 1H, OH), 1.95-1.80 (m, 2H, CH_2), 1.80-1.63 (m, 4H, 2 x CH_2), 1.60-1.33 (m, 4H, 2 x CH_2), 1.28 (t, $J = 7.1$ Hz, 3H, CH_3) ppm; ^{13}C NMR (75 MHz, CDCl_3): $\delta = 167.4$ (C=O), 70.3 (COH), 62.8 (C= N_2), 60.9 (CH_2), 36.5 (2 x CH_2), 25.4 (CH_2), 22.1 (2 x CH_2), 14.6 (CH_3) ppm; HRMS: Exact mass calcd for $\text{C}_{10}\text{H}_{16}\text{N}_2\text{O}_3$ $[\text{M}]^+$: 212.1161, Found: 212.1161. Spectroscopic data was in accordance with the literature.¹³



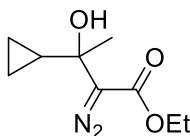
Ethyl 2-diazo-4,4,4-trifluoro-3-hydroxy-3-phenylbutanoate **153e**

406 mg (20 min collection time, 71%) as yellow oil. ^1H NMR (300 MHz, CDCl_3): $\delta = 7.68$ -7.64 (m, 2H, ArH), 7.48-7.41 (m, 3H, ArH), 6.44 (bs, 1H, OH), 4.37-4.22 (m, 2H, CO_2CH_2), 1.30 (t, $J = 7.1$ Hz, 3H, CH_3) ppm; ^{13}C NMR (75 MHz, CDCl_3): $\delta = 166.9$ (C=O), 134.8 (ArC), 129.6 (ArCH), 128.6 (ArCH), 126.4 (ArCH), 125.1 (q, $J = 286.7$ Hz, CF_3), 75.5 (q, $J = 31.7$, COH), 61.9 (OCH_2), 59.2 (C= N_2), 14.2 (CH_3) ppm; IR (neat): ν 3364b, 2986w, 2108s, 1678s, 1454m, 1373m, 1454s, 1173m, 1016w, 746w, 718m cm^{-1} ; HRMS (EI): Exact mass calcd for $\text{C}_{12}\text{H}_{11}\text{F}_3\text{N}_2\text{O}_3$ $[\text{M}]^+$: 288.0722, Found: 288.0723; MS (EI): m/z 288 (M^+ , 1%), 214 (57), 188 (32), 145 (40), 131 (16), 105 (100), 91 (26), 89 (31), 83 (40), 77 (62), 69 (28). Spectroscopic data was in accordance with the literature.¹⁴



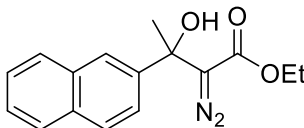
Ethyl 2-diazo-3-(4-fluorophenyl)-3-hydroxybutanoate **153f**

304 mg (20 min collection time, 60%) as yellow oil. ^1H NMR (300 MHz, CDCl_3): δ = 7.49-7.43 (m, 2H, ArH), 7.07-6.99 (m, 2H, ArH), 4.33 (bs, 1H, OH), 4.28-4.11 (m, 2H, CO_2CH_2), 1.68 (s, 3H, CH_3), 1.24 (t, J = 7.1 Hz, CH_3) ppm; ^{13}C NMR (75 MHz, CDCl_3): δ = 167.0 (C=O), 162.2 (d, J = 246.2 Hz, ArCF), 142.2 (ArC), 126.6 (d, J = 8.2 Hz, ArCH), 115.3 (d, J = 21.4 Hz, ArCH), 73.0 (COH), 63.8 (C=N₂), 61.3 (CH_2), 29.3 (CH_3), 14.4 (CH_3) ppm; IR (neat): ν 3464b, 2984m, 2087s, 1674s, 1602m, 1508s, 1371m, 1300s, 1225m, 1069m, 920w, 837m, 746m, 609m cm^{-1} ; HRMS (EI): Exact mass calcd for $\text{C}_{12}\text{H}_{13}\text{FN}_2\text{O}_3$ [M]⁺: 252.0910, Found: 252.0909; MS (EI): 252 (M^+ , 11%), 182 (44), 178 (65), 154 (24), 136 (88), 123 (99), 121 (48), 108 (27), 95 (62), 85 (98), 84 (100). Spectroscopic data was in accordance with the literature.¹⁵



Ethyl 3-cyclopropyl-2-diazo-3-hydroxybutanoate **153g**

189 mg (20 min collection time, 48%) as yellow, volatile oil. ^1H NMR (300 MHz, CDCl_3): δ = 4.28-4.21 (m, 2H, CO_2CH_2); 3.71 (bs, 1H, OH), 1.5 (s, 3H, CH_3), 1.29 (t, J = 7.1 Hz, 3H, CH_3), 1.13-1.04 (m, 1H, cyclopropH), 0.58-0.45 (m, 3H, cyclopropH) ppm; ^{13}C NMR (75 MHz, CDCl_3) δ = 166.4 (C=O), 68.4 (COH), 62.0 (C=N₂), 59.7 (OCH_2), 25.8 (CH_3), 19.2 (cyclopropCH), 13.3 (CH_3), 0.3 (cyclopropCH₂), 0.1 (cyclopropCH₂) ppm; IR (neat): ν 3482b, 2982m, 2093s, 1690s, 1371m, 1310m, 1186w, 1070m, 898w, 746w cm^{-1} ; HRMS: Exact mass calcd for $\text{C}_9\text{H}_{14}\text{N}_2\text{O}_3$ [M]⁺: 198.1004, Found: 198.1003; MS (EI): m/z 198 (M^+ , 44%), 191 (23), 190 (8), 183 (100), 180 (76).

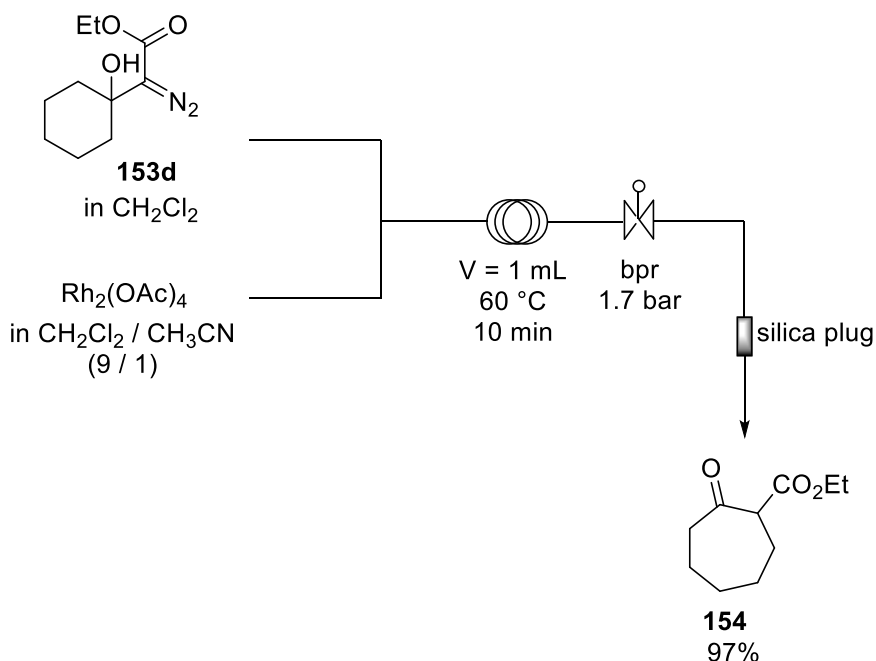


Ethyl 2-diazo-3-hydroxy-3-(naphthalen-2-yl)butanoate **153h**

227 mg (20 min collection time, 40%) as yellow oil. ^1H NMR (300 MHz, CDCl_3): δ = 8.01-7.85 (m, 4H, ArH), 7.61-7.49 (m, 3H, ArH), 4.56 (bs, 1H, OH), 4.31-4.12 (m, 2H, CO_2CH_2), 1.82 (s, 3H, CH_3), 1.24 (t, J = 7.0 Hz, 3H, CH_3) ppm; ^{13}C NMR (75 MHz, CDCl_3): δ = 167.1 (C=O),

143.7 (ArC), 133.1 (ArC), 132.9 (ArC), 128.4 (ArCH), 128.4 (ArCH), 127.6 (ArCH), 126.4 (ArCH), 126.2 (ArCH), 123.5 (ArCH), 123.1 (ArCH), 73.4 (COH), 63.9 (C=N₂), 61.2 (CH₂), 29.1 (CH₃), 14.4 (CH₃) ppm; IR (neat): ν 3435b, 2982m, 2089s, 1678s, 1506w, 1371m, 1304s, 1128w, 1067m, 860w, 822w, 752m, 478m cm⁻¹; HRMS (EI): Exact mass calcd for C₁₆H₁₆N₂O₃ [M]⁺: 284.1161, Found: 284.1169; MS (EI): m/z 284 (M⁺, 6%), 214 (27), 210 (39), 170 (99), 155 (100), 127 (99), 126 (69), 77 (22).¹⁵

7.2.10 Ring-expansion reaction of diazoalcohol



Ethyl 2-oxocycloheptane-1-carboxylate **154**

Diazo alcohol **153d** (234 mg, 1 mmol) was dissolved in dichloromethane (5 mL) and rhodium acetate (4.4 mg, 0.01 mmol, 1 mol%) was dissolved in a solution of dichloromethane / acetonitrile (9 / 1). Both solutions were pumped through a continuous flow set-up (see above) with a flow rate 0.1 mL/min. The system was stabilised for 30 min and then, the reaction mixture was collected for 75 min directly after the silica plug. Subsequently, the silica plug was washed with dichloromethane (2 x 5 mL) and the solvent was removed *in vacuo* to afford cycloheptane **154** as colourless oil (134 mg, 0.73 mmol, 97%). ¹H NMR (300 MHz, CDCl₃): δ = 4.23-4.13 (m, 2H, OCH₂), 3.53 (dd, *J* = 10.5, 4.1 Hz, 1H, CH), 2.68-2.53 (m, 2H, CH₂CO), 2.13-2.05 (m, 1H, CH₂), 1.99-1.80 (m, 4H, CH₂), 1.64-1.55 (m, 1H, CH₂), 1.48-1.41 (m, 2H, CH₂), 1.26 (t, *J* = 7.1 Hz, 3H, CH₃) ppm; ¹³C NMR (75 MHz, CDCl₃): δ = 209.3 (C=O), 170.7 (C=O), 61.2 (OCH₂), 59.1 (CHCO₂), 43.2 (CH₂), 29.8 (CH₂), 28.1 (CH₂), 27.7 (CH₂), 24.5 (CH₂), 14.2 (CH₃) ppm; HRMS (EI): Exact mass calcd for C₁₀H₁₆O₃ [M]⁺: 184.1099, Found: 184.1102; MS (EI): m/z 184 (M⁺, 56%), 156 (90), 138 (100), 128 (46), 110 (71), 101 (28), 99

(26), 88 (20), 82 (24), 73 (38), 67 (40), 55 (64). Spectroscopic data was in accordance with the literature.¹⁶

7.3 Experimentals Chapter 4

7.3.1 Calculation of rate constant of batch reaction

The following definitions were made to determine the order of the reaction: (a) $[ABSA]_0 \neq [ESTER]_0$ and (b) $[ABSA]/dt \sim [ESTER]/dt$ with $[ESTER]$ being the concentration of the starting material ester $[A]$ and $[ABSA]$ being the concentration of diazo transfer reagent $[B]$.

Kinetics for 2nd order reactions with $[A] \neq [B]$ are described by

$$\frac{dx}{dt} = k([A]_0 - x)([B]_0 - x)$$

Rearrangement of this term to

$$\frac{dx}{([A]_0 - x)([B]_0 - x)} = k dt$$

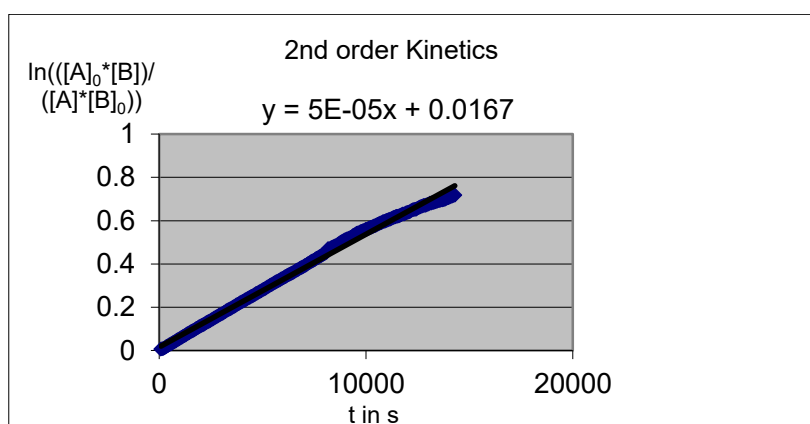
$$\int_0^x \frac{dx}{([A]_0 - x)([B]_0 - x)} = k \int_0^t dt$$

This gives

$$\frac{1}{[B]_0 - [A]_0} \ln \frac{[B][A]_0}{[A][B]_0} = kt$$

$$\ln \frac{[B][A]_0}{[A][B]_0} = k([B]_0 - [A]_0)t$$

A plot of the left term versus time allows to obtain $k([B]_0 - [A]_0)$ as slope.



With $y = k([B]_0 - [A]_0)t = 5 \times 10^{-5}t + 0.0167$ and therefore the slope being the first derivative of a function with $\frac{dx}{dt} y' = k([B]_0 - [A]_0) = 5 \times 10^{-5}$. With $[A]_0 = [Ester]_0 = 0.5 \frac{mol}{l}$ and $[B]_0 = [ABSA]_0 = 0.6 \frac{mol}{l}$, it follows $k = \frac{5 \times 10^{-5}}{[B]_0 - [A]_0} = 5 \times 10^{-4} M^{-1} s^{-1}$.

7.3.2 Calculation of rate constant for different temperatures in flow

Having determined the reaction order of the diazo transfer reaction, one can determine reaction rate constants from one time point.

$$kt = \frac{1}{[B]_0 - [A]_0} \ln \frac{[B][A]_0}{[A][B]_0}$$

The rate constants for different temperatures in continuous flow were thus:

$$k_{25^\circ C} = 6 \times 10^{-4} M^{-1} s^{-1}$$

$$k_{40^\circ C} = 1.8 \times 10^{-3} M^{-1} s^{-1}$$

$$k_{50^\circ C} = 3.6 \times 10^{-3} M^{-1} s^{-1}$$

$$k_{60^\circ C} = 6.5 \times 10^{-3} M^{-1} s^{-1}$$

7.3.3 Calculation of activation energy

By using the Arrhenius equation one can determine the activation energy of a reaction.

$$k = Ae^{-\frac{E_A}{RT}}$$

$$\Leftrightarrow \ln k = \ln A - \frac{1}{T} \frac{E_A}{R}$$

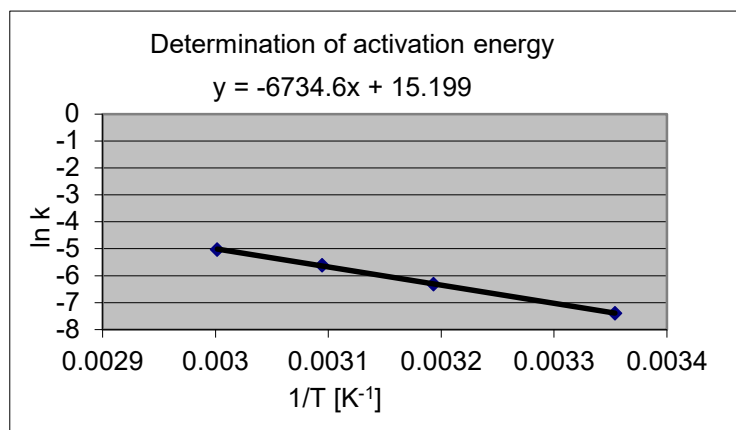
If one now plots $\ln(k)$ vs $1/T$, $\ln(A)$ will be the intercept with y and the slope will be $-E_A/R$.

$$y = \ln k = -\frac{1}{T} \frac{E_A}{R} + \ln A = -6734.6 \left(\frac{1}{T}\right) + 15.2$$

Therefore

$$-\frac{E_A}{R} = -6734.6 K$$

$$\Leftrightarrow E_A = 6734.6 K \times 8.314 J K^{-1} mol^{-1} = 56 kJ mol^{-1}$$



7.3.4 Calculation of T_{D24}

Calculation of T_{D24} is performed by using time to maximum rate in adiabatic conditions (TMR_{ad}) as defined by Stoessel.¹⁷

$$TMR_{ad} = \frac{c_p R T_0^2}{q_0 E_A} [s]$$

With c_p = specific heat capacity [kJ/(kg K)]; R = gas constant [J/(mol K)]; T_0 = initial temperature of runaway [K]; q_0 = heat release rate at T_0 [W/kg]; E_A = activation energy [J/mol].

Following assumptions are made according to [ii]: (a) activation energy of decomposition reaction is around 50 kJ/mol (this is a conservative estimate)¹⁸ (b) decomposition reaction obeys zero order kinetics (c) specific heat capacity of organic fluids is approx 1.7 kJ/(kg K).¹⁹

The heat release rate and the onset temperature are measured in differential scanning calorimetry.

7.3.5 Procedure thermal studies

For c80 studies methyl phenylacetate (1 mmol, 150 mg) and 1,8-diazabicyclo[5.4.0]undec-7-ene (DBU) (295 μ L) was dissolved in acetonitrile (1 mL). *p*-Acetamidobenzenesulfonyl azide (1.2 mmol, 300 mg) was dissolved in acetonitrile (1 mL).

7.3.6 Kinetic studies of diazo transfer

Calibration data

Methyl phenylacetate – Silicon flow probe

Experimental Section

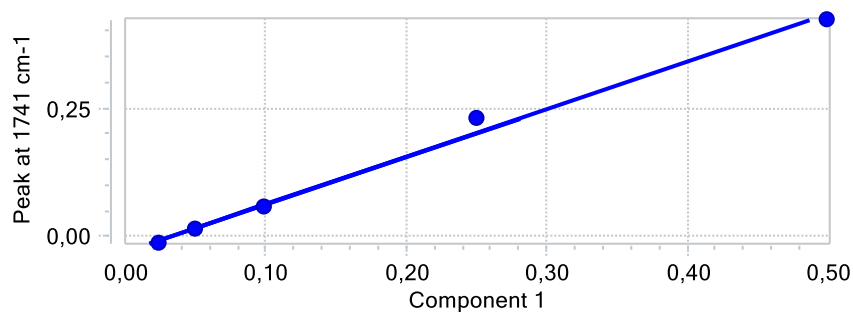
Spectrum Name	Actual	Peak	Regression Fit	Delta
Methyl phenylacetate 0,5M (100%)	0,5	0,420	0,486	0,013
Methyl phenylacetate 0,025M (5%)	0,025	-0,013	0,017	0,007
Methyl phenylacetate 0,25M (50%)	0,25	0,230	0,281	-0,031
Methyl phenylacetate 0,1M (20%)	0,1	0,055	0,092	0,007
Methyl phenylacetate 0,05M (10%)	0,05	0,014	0,047	0,002

R Squared: 0.992

Intercept: -0.030

Slope: 0.925

Peak: Peak at 1741 cm⁻¹



Diazo methyl phenylacetate – Silicon flow probe

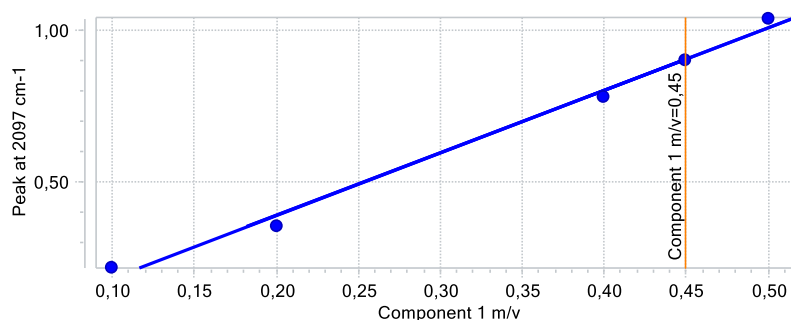
Spectrum Name	Actual	Peak	Regression Fit	Delta
Diazo methyl phenylacetate 0,10 M	0,0999	0,213	0,116	-0,016
Diazo methyl phenylacetate 0,45 M	0,44959	0,899	0,447	0,002
Diazo methyl phenylacetate 0,20 M	0,2	0,348	0,181	0,018
Diazo methyl phenylacetate 0,50 M	0,5	1,039	0,514	-0,014
Diazo methyl phenylacetate 0,40 M	0,4	0,778	0,389	0,010

R Squared: 0.992

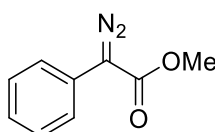
Intercept: -0.028

Slope: 2.074

Peak: Peak at 2097 cm⁻¹



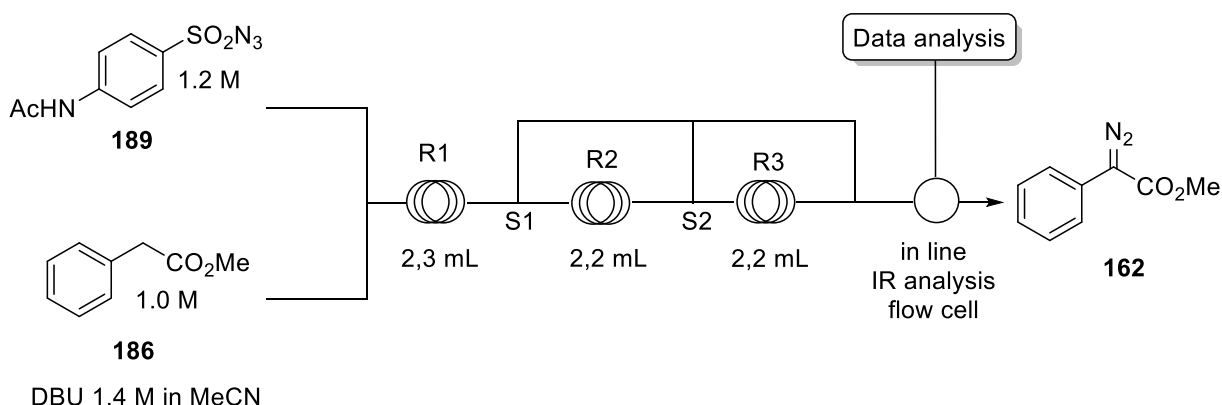
7.3.7 Procedure batch reaction diazo transfer



Methyl 2-diazo-2-phenylacetate **162**

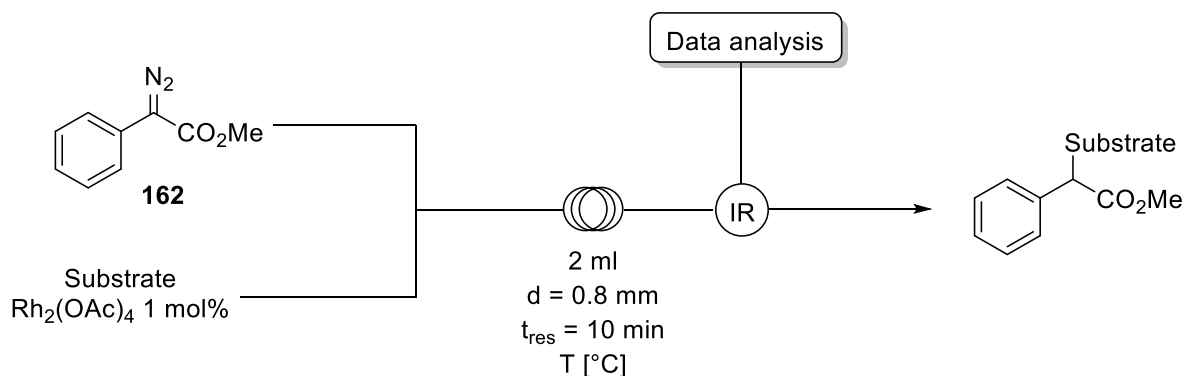
Methyl phenylacetate (1.5 g, 10 mmol) and 1,8-diazabicyclo[5.4.0]undec-7-ene (DBU) (14 mmol, 2.1 mL) were dissolved in acetonitrile to a total volume of 10 mL. This solution was then stirred in a flask and *p*-acetamidobenzenesulfonyl azide (12 mmol, 2.9 g), dissolved in acetonitrile to a total volume of 10 mL, was added slowly at room temperature. The mixture was pumped via a peristaltic pump through the IR silicon flow cell and constantly analyzed. After 24 h the reaction mixture was quenched with 1 M aqueous sodium nitrite solution (16 mL) and extracted with CH₂Cl₂ (3 x 15 mL). The combined organic layers were washed with brine (15 mL) and dried over MgSO₄. Purification was performed by dry-loading on a 20 g silica column and eluting with a Petrolether/EtOAc gradient 0-15% EtOAc over 25 column volumes. Subsequent combination of pure fractions afforded 2-diazo methylphenylacetate **162** (1.3 g, 7.4 mmol, 74% yield) as yellow-red oil. ¹H NMR (400 MHz, CDCl₃): δ 7.30 (dd, *J* = 8.6, 1.3 Hz, 2 H, ArH), 7.18 (t, *J* = 7.5 Hz, 2 H, ArH), 6.98 (tt, *J* = 7.4, 1.1 Hz, 1 H, ArH), 3.65 (s, 3 H, CH₃) ppm; ¹³C NMR (100 MHz, CDCl₃): δ 165.9, 129.2, 126.1, 125.7, 124.2, 52.3 ppm. As already described by other authors, the signal for C=N₂ was not observed.²⁰

7.3.8 Procedure flow reaction diazo transfer



Methyl phenylacetate (50 mmol, 7.51 g) and 1,8-diazabicyclo[5.4.0]undec-7-ene (DBU) (70 mmol, 10.5 mL) were dissolved in acetonitrile to a total volume of 50 mL. *p*-Acetamidobenzenesulfonyl azide (60 mmol, 14.5 g) was dissolved in acetonitrile to give a total volume of 50 mL, stirred vigorously for 5 minutes and then filtered. Both solutions were pumped each with a flow rate of 0.13 mL/min (total flow rate 0.26 mL/min) through the continuous flow set-up. IR data was analysed on reactor outlet and system stabilization was monitored via infrared analysis.

7.3.9 Diazo decomposition reactions



Rhodium acetate (0.054 mmol, 24 mg, 1 mol%) and 6.5 mmol substrate (1.2 equiv) were dissolved in a 9 / 1 mixture of chloroform / acetonitrile in a 20 mL measuring flask. Diazo methyl phenylacetate (5.4 mmol, 951 mg) was dissolved in *n*-heptane in a 20 mL measuring flask. The two solutions were pumped using a Syrris Asia syringe pump system through the continuous flow system with flow rates of 0.1 mL/min per pump (0.2 mL/min total flow rate) for a residence time of 10 minutes. At the end of the continuous flow system a back pressure regulator was attached with 6 bar back pressure as well as the infrared flow cell diamond probe with which the system was monitored.

Calibration data

Diazo methyl phenylacetate – Diamond flow probe

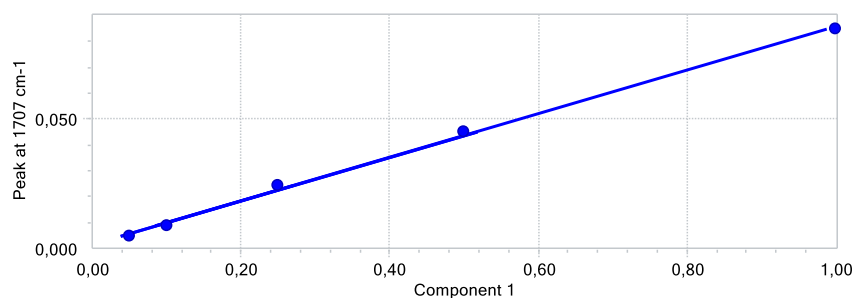
Spectrum Name	Actual	Peak	Regression Fit	Delta
Diazo 0,135 M (100%)	1	0,084	0,988	0,01
Diazo 0,014 M (10%)	0,1	0,008	0,084	0,015
Diazo 0,068 M (50%)	0,5	0,045	0,517	-0,017
Diazo 0,007 M (5%)	0,05	0,004	0,038	0,011
Diazo 0,034 M (25%)	0,25	0,024	0,271	-0,021

R Squared: 0.998

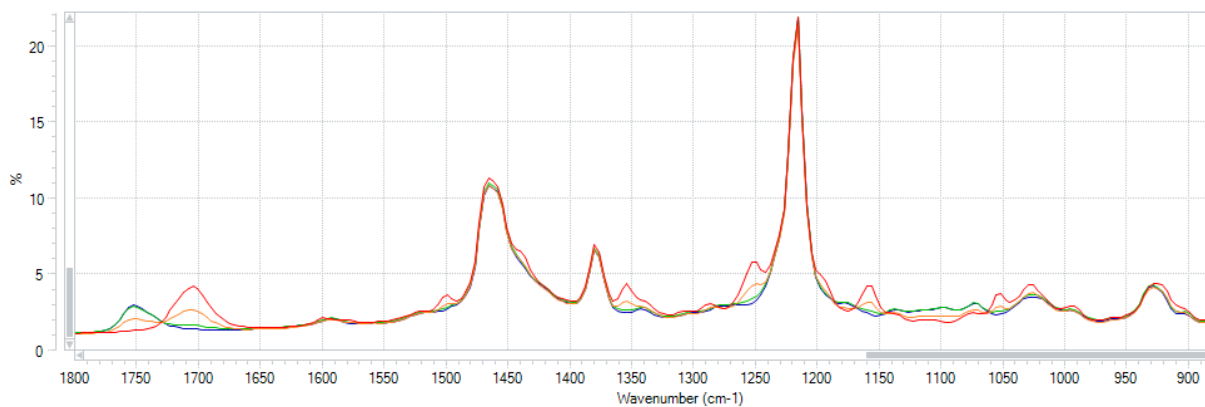
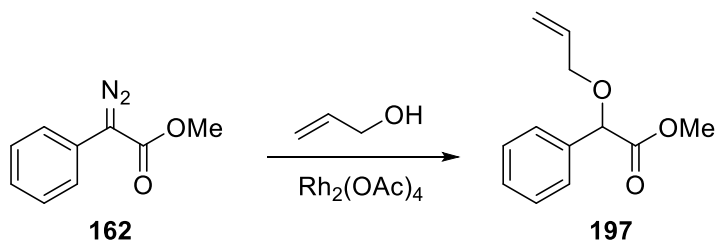
Intercept: 0.002

Slope: 0.084

Peak: Peak at 1707 cm⁻¹



In-line infrared and HPLC data

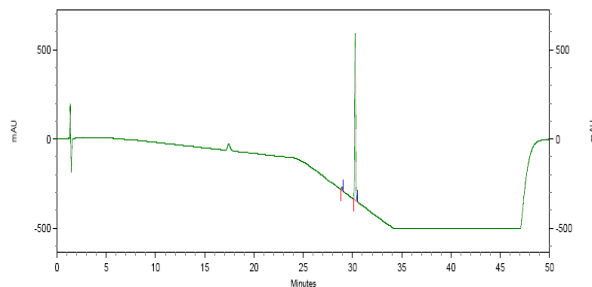


Red: 25 °C; 10 min residence time

Orange: 50 °C; 10 min residence time

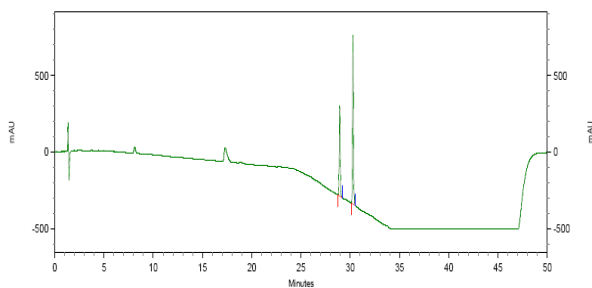
Green: 60 °C; 10 min residence time

Blue: 70 °C; 10 min residence time



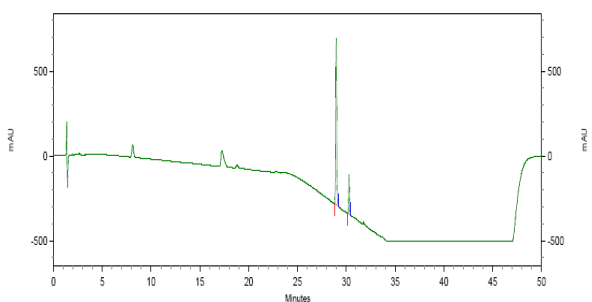
25 °C; 10 min res time

Res time	Peak	Area	Ratio [%]
28.93	Product 197	515229	2.1
30.26	Diazo 162	2465161	97.9



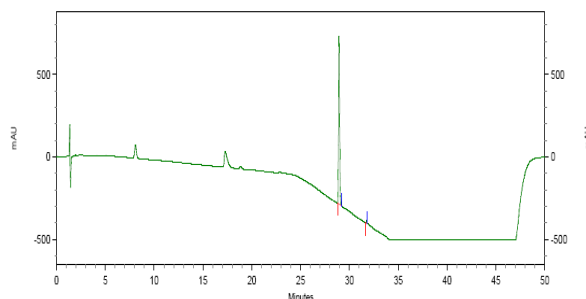
50 °C; 10 min res time

Res time	Peak	Area	Ratio [%]
28.93	Product 197	16085318	35.5
30.27	Diazo 162	29280589	64.5



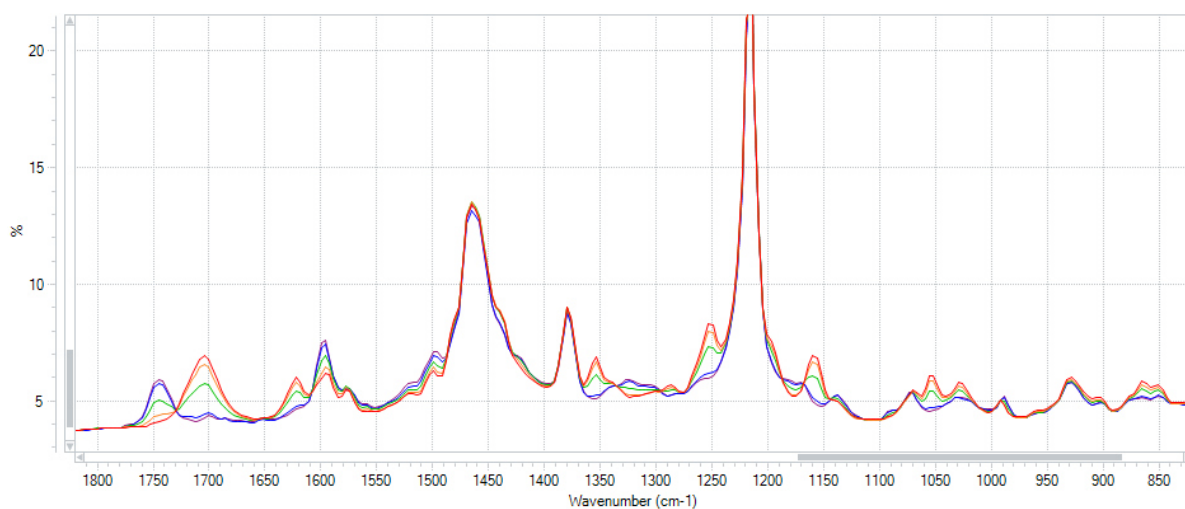
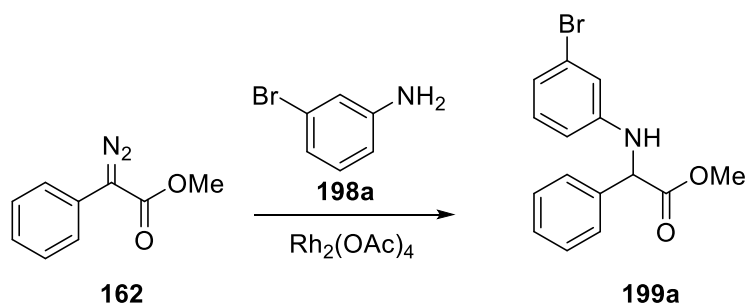
60 °C; 10 min res time

Res time	Peak	Area	Ratio [%]
28.96	Product 197	28201567	83.1
30.27	Diazo 162	5746451	16.9



70 °C; 10 min res time

Res time	Peak	Area	Ratio [%]
28.94	Product 197	29733243	100
30.26	Diazo 162	n.d.	n.d.



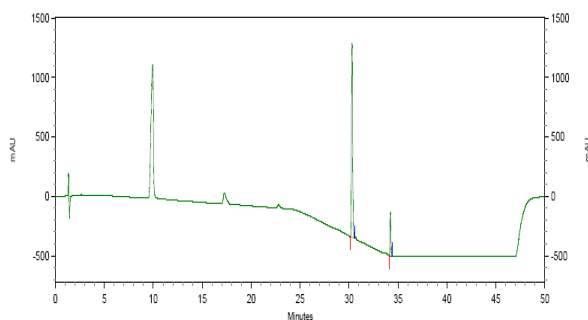
Red: 25 °C; 10 min residence time

Orange: 40 °C; 10 min residence time

Green: 50 °C; 10 min residence time

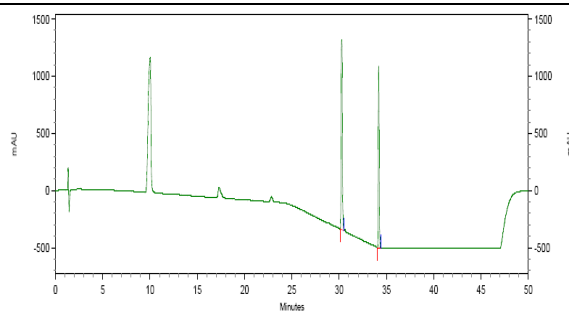
Blue: 60 °C; 10 min residence time

Violet: 70 °C; 10 min residence time



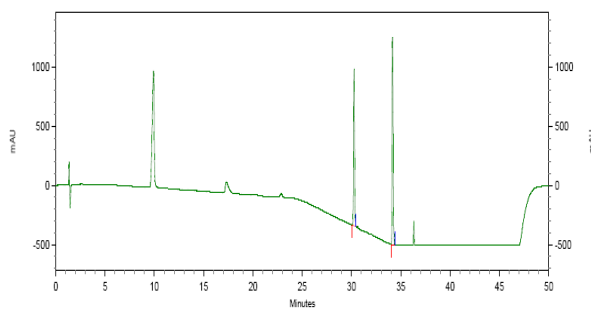
25 °C; 10 min res time

Res time	Peak	Area	Ratio [%]
30.30	Diazo 162	53614628	87.2
34.22	Product 199a	7878284	12.8



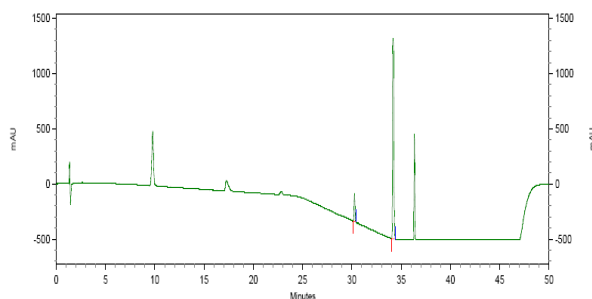
40 °C; 10 min res time

Res time	Peak	Area	Ratio [%]
30.26	Diazo 162	59135611	59.6
34.18	Product 199a	40098197	40.4



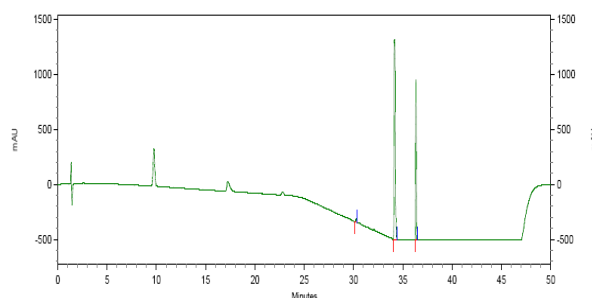
50 °C; 10 min res time

Res time	Peak	Area	Ratio [%]
30.25	Diazo 162	36237034	40.3
34.16	Product 199a	53576522	59.7



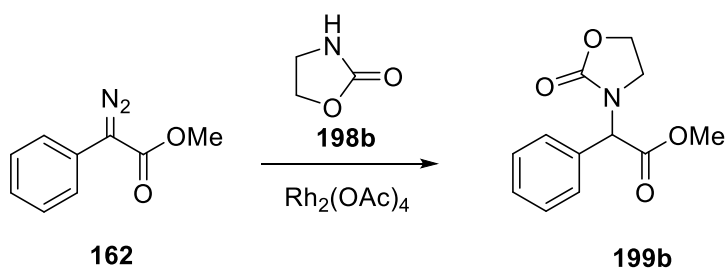
60 °C; 10 min res time

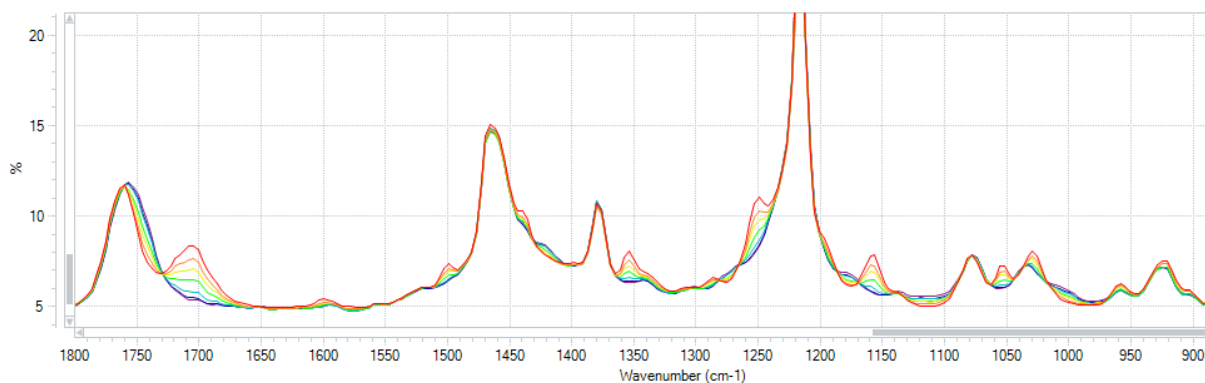
Res time	Peak	Area	Ratio [%]
30.27	Diazo 162	6298190	8.7
34.17	Product 199a	66441880	91.3



70 °C; 10 min res time

Res time	Peak	Area	Ratio [%]
30.25	Diazo 162	654446	0.7
34.16	Product 199a	67516044	67.5
36.33	Side Product 200	31909262	31.9





Red: 25 °C; 10 min residence time

Orange: 40 °C; 10 min residence time

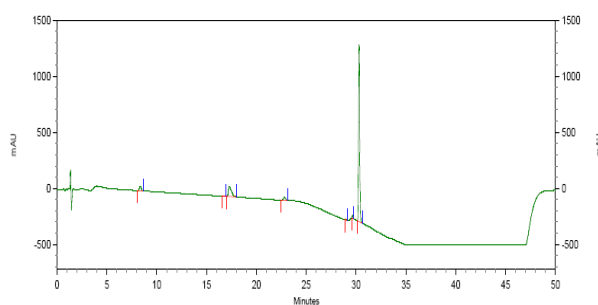
Yellow: 40 °C; 20 min residence time

Green: 50 °C; 10 min residence time

Turquoise: 50 °C; 20 min residence time

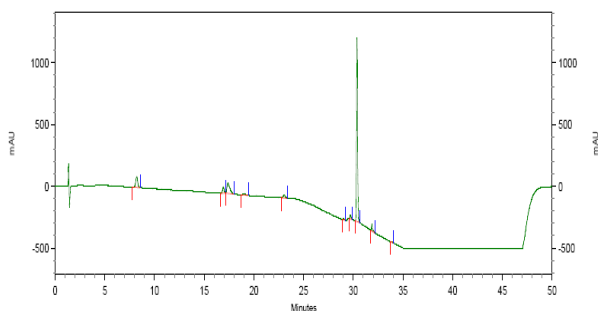
Blue: 60 °C; 10 min residence time

Violet: 70 °C; 10 min residence time



25 °C; 10 min res time

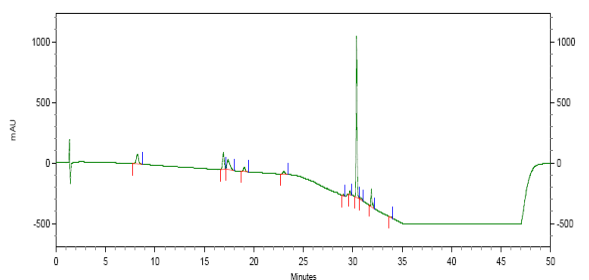
Res time	Peak	Area	Ratio [%]
8.21	Side Product I (m/z 166 g/mol)	1989722	3.6
16.93	Product 199b	206301	0.4
30.37	Diazo compound 162	52854507	96.0
31.87	Side Product II (m/z 314 g/mol)	n.d.	n.d.



Experimental Section

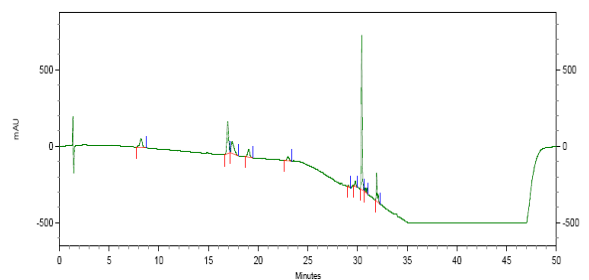
40 °C; 10 min res time

Res time	Peak	Area	Ratio [%]
8.21	Side Product I (m/z 166 g/mol)	4787803	9.0
16.93	Product 199b	2525733	4.7
30.37	Diazo compound 162	44637594	83.5
31.87	Side Product II (m/z 314 g/mol)	1515260	2.8



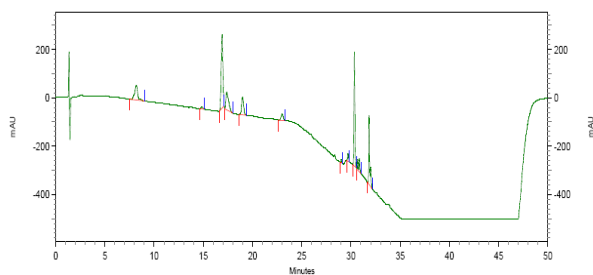
40 °C; 20 min res time

Res time	Peak	Area	Ratio [%]
8.23	Side Product I (m/z 166 g/mol)	5053063	9.4
16.92	Product 199bb	6917236	12.9
30.37	Diazo compound 162	37512901	70.0
31.87	Side Product II (m/z 314 g/mol)	4134985	7.7



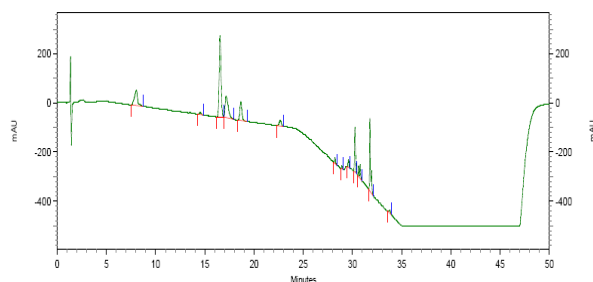
50 °C; 10 min res time

Res time	Peak	Area	Ratio [%]
8.23	Side Product I (m/z 166 g/mol)	3969253	8.5
16.93	Product 199b	10547757	22.6
30.42	Diazo compound 162	26861876	57.7
31.91	Side Product II (m/z 314 g/mol)	5213820	11.2



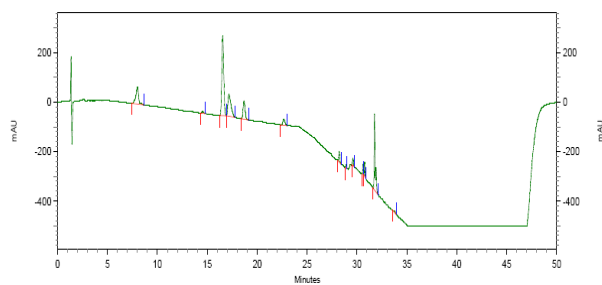
50 °C; 20 min res time

Res time	Peak	Area	Ratio [%]
8.20	Side Product I (m/z 166 g/mol)	5123830	12.6
16.89	Product 199b	15273949	37.5
30.35	Diazo compound 162	12171320	29.9
31.84	Side Product II (m/z 314 g/mol)	8151861	20.0



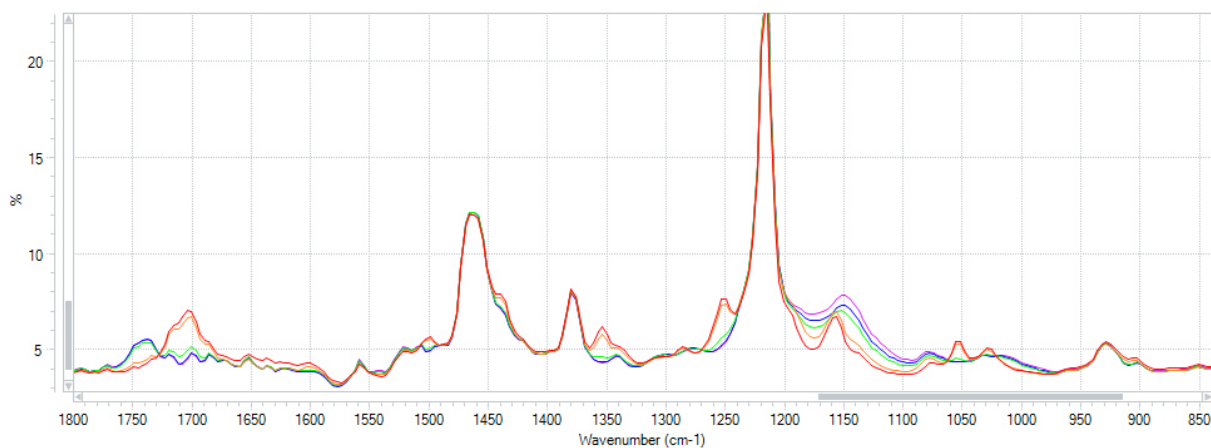
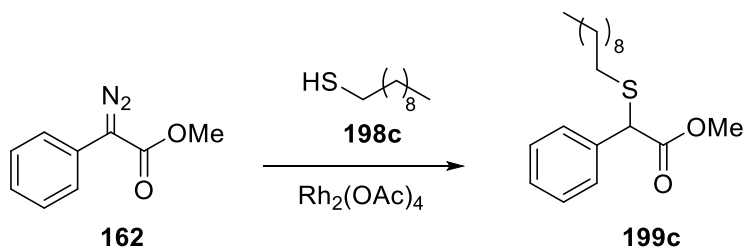
60 °C; 10 min res time

Res time	Peak	Area	Ratio [%]
8.04	Side Product I (m/z 166 g/mol)	5510911	15.2
16.55	Product 199b	17603962	48.5
30.25	Diazo compound 162	4689962	12.9
31.77	Side Product II (m/z 314 g/mol)	8510762	23.4



70 °C; 10 min res time

Res time	Peak	Area	Ratio [%]
8.01	Side Product I (m/z 166 g/mol)	5128904	16.3
16.55	Product 199b	17213506	15.7
30.25	Diazo compound 162	n.d.	n.d.
31.76	Side Product II (m/z 314 g/mol)	9141908	29.0



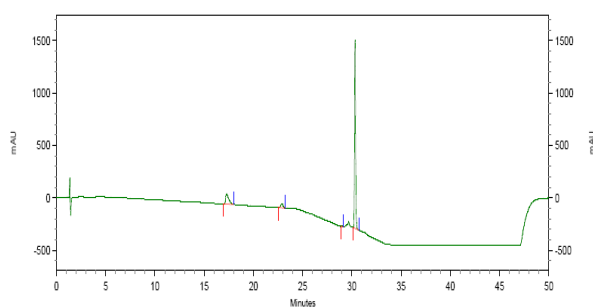
Red: 25 °C; 10 min residence time

Orange: 40 °C; 10 min residence time

Green: 60 °C; 10 min residence time

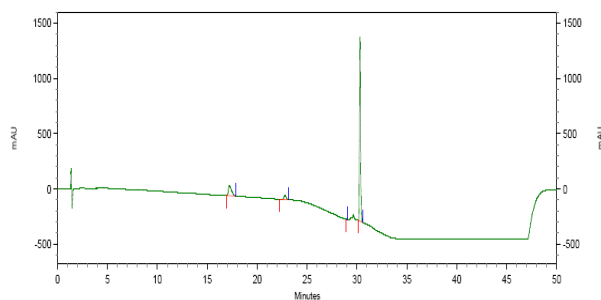
Blue: 60 °C; 20 min residence time

Violet: 70 °C; 10 min residence time



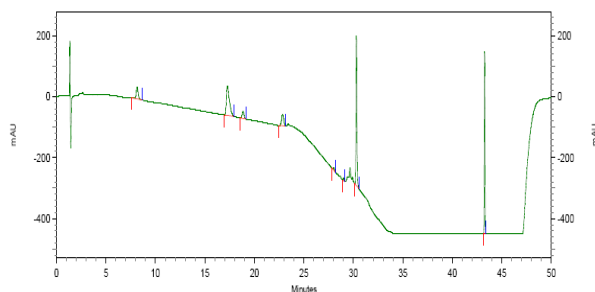
25 °C; 10 min res time

Res time	Peak	Area	Ratio [%]
8.16	Side Product I (m/z 166 g/mol)	n.d.	n.d.
30.31	Diazo 162	55928188	100
43.26	Product 199c	n.d.	n.d.



40 °C; 10 min res time

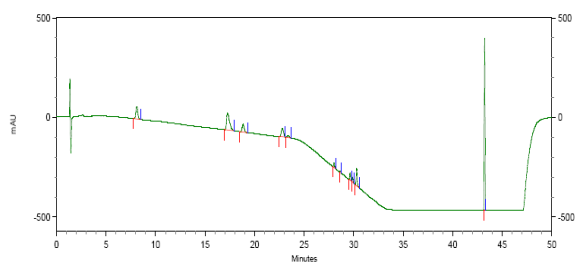
Res time	Peak	Area	Ratio [%]
8.16	Side Product I (m/z 166 g/mol)	n.d.	n.d.
30.31	Diazo 162	48462012	100
43.26	Product 199c	n.d.	n.d.



60 °C; 10 min res time

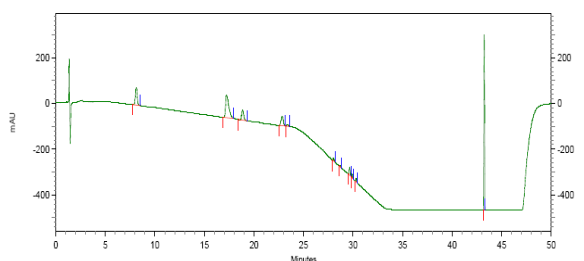
Res time	Peak	Area	Ratio [%]
8.16	Side Product I (m/z 166 g/mol)	2101040	7.5
30.31	Diazo 162	12834174	45.8
43.26	Product 199c	13070386	46.7

Experimental Section



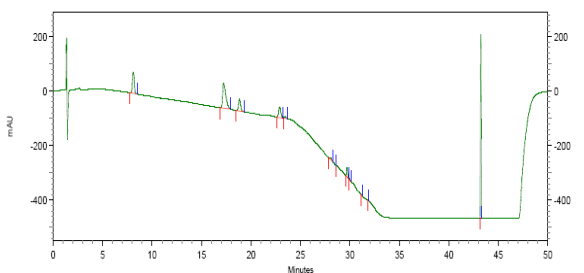
60 °C; 20 min res time

Res time	Peak	Area	Ratio [%]
8.11	Side Product I (m/z 166 g/mol)	3362813	13.2
30.30	Diazo 162	2399161	9.4
43.22	Product 199c	19715115	77.4



70 °C; 10 min res time

Res time	Peak	Area	Ratio [%]
8.13	Side Product I (m/z 166 g/mol)	3999225	18.6
30.31	Diazo 162	389204	1.8
43.23	Product 199c	17082063	79.6



80 °C; 10 min res time

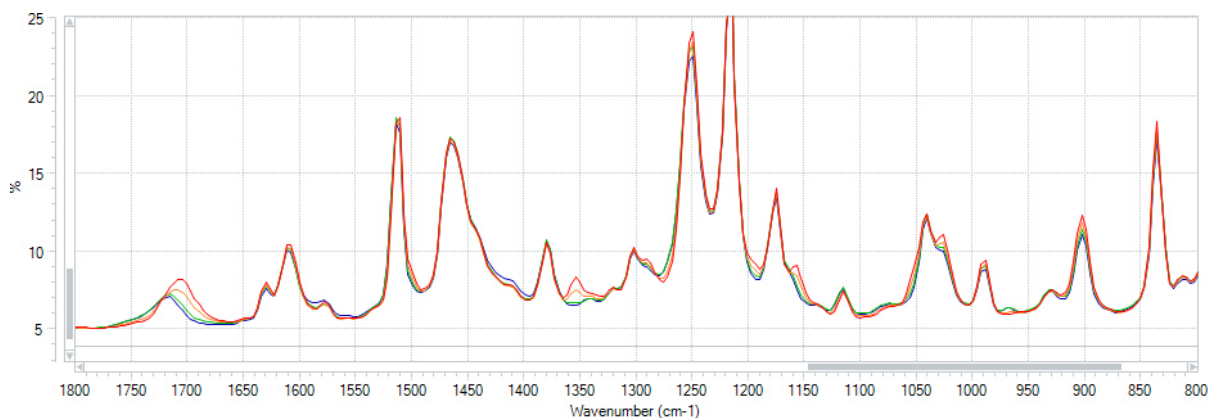
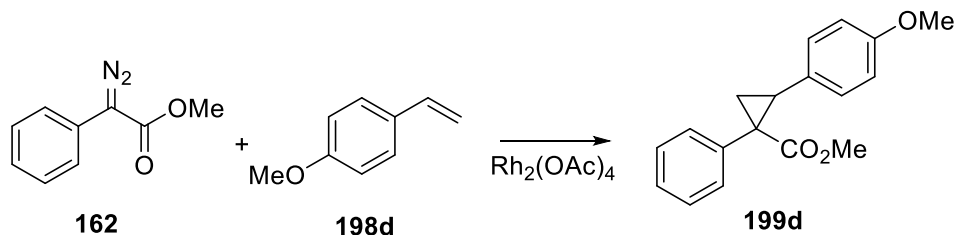
Res time	Peak	Area	Ratio [%]
8.11	Side Product I (m/z 166 g/mol)	4129163	22.3
30.31	Diazo 162	n.d.	n.d.

43.23

Product **199c**

14357947

77.7

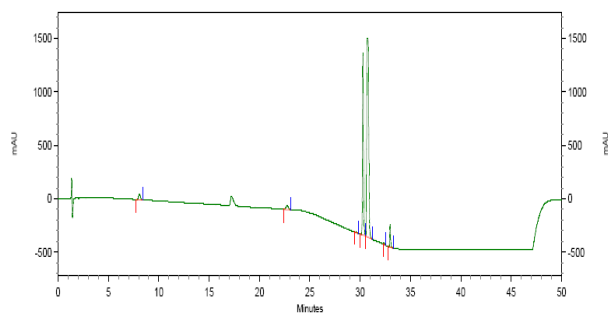


Red: 25 °C; 10 min residence time

Orange: 40 °C; 10 min residence time

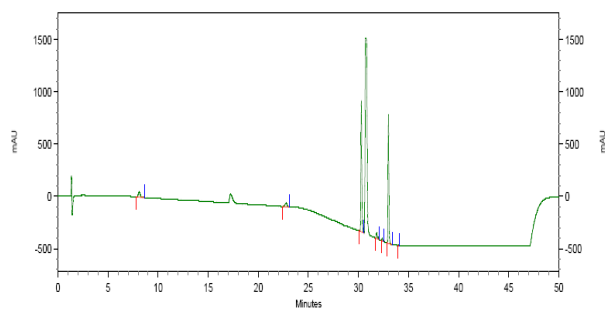
Green: 50 °C; 10 min residence time

Blue: 60 °C; 10 min residence time



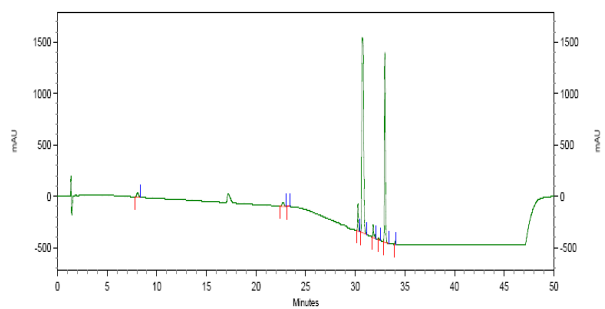
25 °C; 10 min res time

Res time	Peak	Area	Ratio [%]
8.09	Side Product I (m/z 166 g/mol)	2695569	4.6
30.28	Diazo 162	50490152	87.0
30.75	4-Vinylanisole 198d	102192092	n.d.
32.98	Product 199d	4832989	8.4



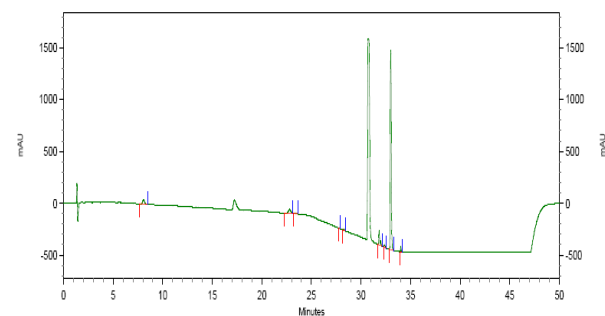
40 °C; 10 min res time

Res time	Peak	Area	Ratio [%]
8.12	Side Product I (m/z 166 g/mol)	2655378	4.0
30.29	Diazo 162	33901249	51.6
30.75	4-Vinylanisole 198d	n.d.	n.d.
32.99	Product 199d	29096940	44.3



50 °C; 10 min res time

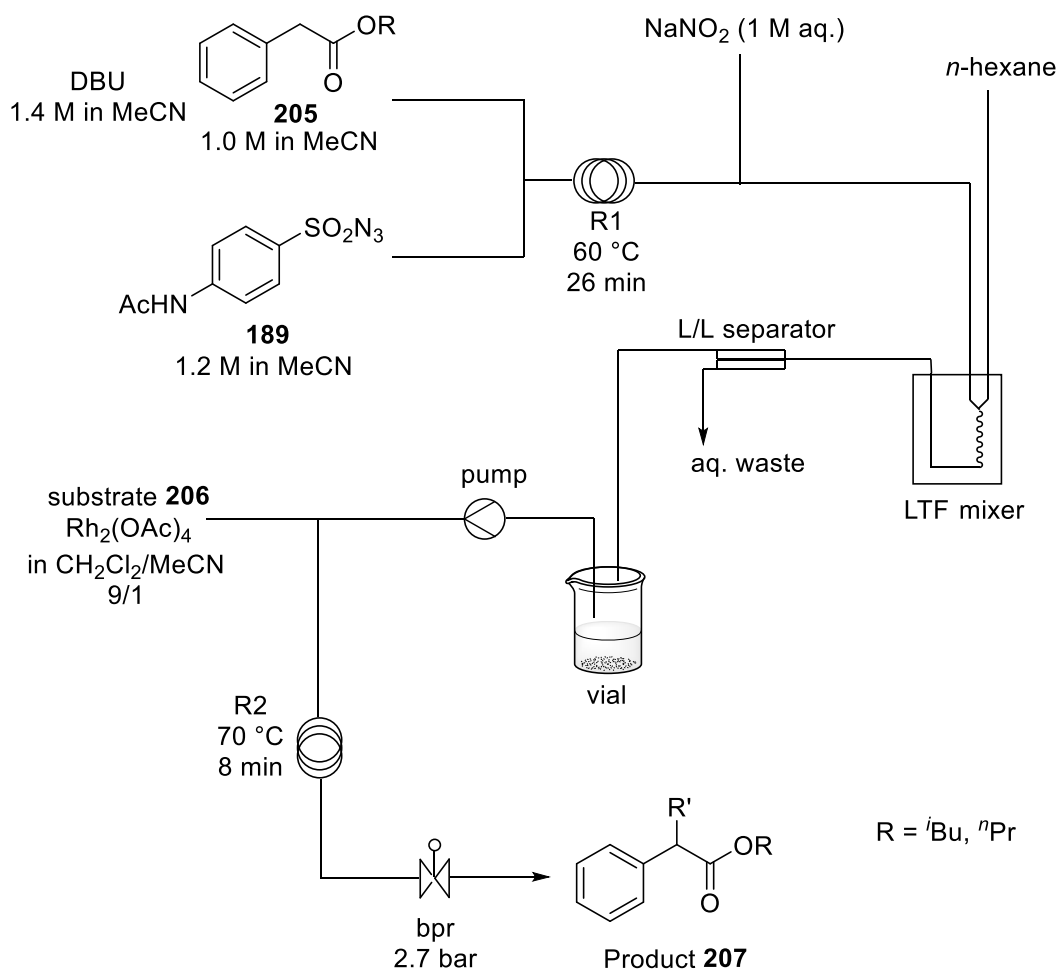
Res time	Peak	Area	Ratio [%]
8.09	Side Product I (m/z 166 g/mol)	2284010	3.9
30.27	Diazo 162	5849581	9.9
30.71	4-Vinylanisole 198d	100648928	n.d.
32.99	Product 199d	51141528	86.3



60 °C; 10 min res time

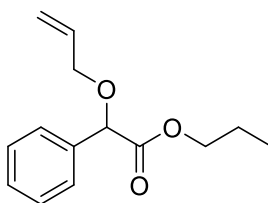
Res time	Peak	Area	Ratio [%]
8.08	Side Product I (m/z 166 g/mol)	2300500	3.9
30.29	Diazo 162	n.d.	n.d.
30.75	4-Vinyanisole 198d	n.d.	n.d.
33.01	Product 199d	56026549	96.1

7.3.10 Multistep process in flow



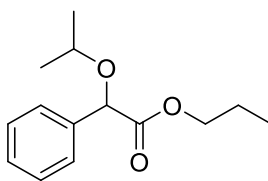
Alkyl 2-phenylacetate (5 mmol) was dissolved in acetonitrile and DBU (8.7 mmol, 1.31 mL, 1.7 equiv.) was added in a 10 ml measuring flask. *p*-Acetamidobenzenesulfonyl azide (6 mmol, 1.44 g, 1.2 equiv) was dissolved in acetonitrile in a 10 ml measuring flask. Both solutions were charged into 10 ml BD plastic syringes in a syringe pump and connected to the continuous flow set-up. Residence time for the first reaction was 26 minutes at 60 °C with a flow rate of 0.042 ml/min per pump (0.084 ml/min flow rate first reactor). 1 M NaNO₂ aqueous solution was pumped via the Vapourtec E series pump (blue tubing) with a flow rate of 0.101 ml/min

into the system. *n*-Hexane was pumped *via* the Vapourtec E series pump (red tubing) with a flow rate of 0.138 ml/min into the system. The system was stabilized for 55 minutes before collection of the organic layer into a collection vial started. The collection vial was connected after one minute (so that the bottom of the collection vial is covered) to the Vapourtec E series pump (red tubing) which pumps out of the collection vial with a flow rate of 0.175 ml/min. The substrate (5.2 mmol, 1.7 eq) and Rh₂(OAc)₄ (0.032 mmol, 14 mg, 1 mol%) were dissolved in chloroform with 1 ml acetonitrile in a 10 ml measuring flask. The solution was pumped through the flow circuit with 0.175 ml/min for a residence time of 8 minutes at 70 °C. The system was stabilized for 20 minutes before collecting for 20 -35 minutes. Solvent was evaporated and the crude material was directly purified via flash liquid chromatography with *n*-hexane/ethyl acetate gradient (0-8% EtOAc) on 25 g columns for 15-20 column volumes.



Propyl 2-(allyloxy)-2-(phenylacetate) **207a**

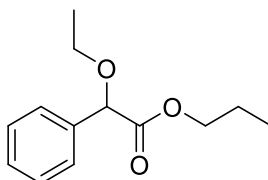
112 mg (20 min collection time; 72%) as colourless oil. ¹H NMR (300 MHz, CDCl₃): δ = 7.49 – 7.43 (m, 2H, ArH), 7.41 – 7.29 (m, 3H, ArH), 5.95 (m, 1H, allylH), 5.29 (dq, *J* = 17.2, 1.6 Hz, 1H, CH=CH₂), 5.23 (dq, *J* = 10.3, 1.6 Hz, 1H, CH=CH₂), 4.93 (s, 1H, CHCOR), 4.12 – 4.04 (m, 4H, 2 x OCH₂), 1.60 (sex, *J* = 7.3 Hz, 2H, CH₂CH₃), 0.83 (t, *J* = 7.4 Hz, 3H, CH₂CH₃) ppm; ¹³C NMR (75 MHz, CDCl₃): δ = 170.9 (C=O), 136.5 (ArC), 133.8 (C=C), 129.3 (ArCH), 128.6 (ArCH), 127.2 (ArCH), 118.2 (C=C), 79.8 (CHOR), 70.4 (OCH₂), 66.7 (OCH₂), 21.9 (CH₂), 10.2 (CH₃) ppm; IR (neat): ν 3027w, 2980w, 2968w, 2890w, 1747s, 1732s, 1454m, 1260m, 1203m, 1175s, 1098s, 1071m, 1058m, 1030m, 991m, 923m, 728m, 695s cm⁻¹; HMRS (APCI): Exact mass calcd for C₁₄H₁₉O₃ [M+H]⁺: 235.1334, Found: 235.1332; MS (APCI): *m/z* 235 (M+H⁺, 100%), 209 (31), 176 (62), 132 (54), 115 (45).



Propyl 2-isopropyl-2-phenylacetate **207b**

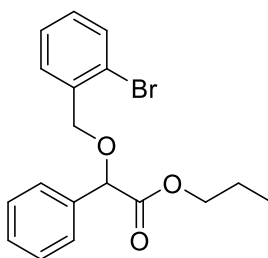
114 mg (20 min collection time; 72%) as colourless oil. ¹H NMR (300 MHz, CDCl₃): δ = 7.53 - 7.41 (m, 2H, ArH), 7.40 – 7.28 (m, 3H, ArH), 4.98 (s, 1H, CHOR), 4.07 (t, *J* = 6.7 Hz, 2H, CO₂CH₂), 3.69 (sept, *J* = 6.1 Hz, 1H, OCH(CH₃)₂), 1.61 (sex, *J* = 7.1 Hz, 2H, CH₂CH₃),

1.23 (dd, $J = 16.3, 6.1$ Hz, 6H, $\text{CH}(\text{CH}_3)_2$), 0.84 (t, $J = 7.5$ Hz, 3H) ppm; ^{13}C NMR (75 MHz, CDCl_3): $\delta = 171.6$ (C=O), 137.4 (ArC), 128.5 (ArCH), 128.4 (ArCH), 127.1 (ArCH), 78.5 (CHOR), 70.9 (OCH), 66.6 (OCH_2), 22.1 (CH_2), 21.9 (CH_3), 10.2 (CH_3) ppm; IR (neat): ν 2970m, 2931m, 2881m, 1749s, 1729m, 1454m, 1378m, 1249m, 1203m, 1171s, 1099s, 1058m, 1003m, 926m, 728m, 696s cm^{-1} ; HMRS (EI): Exact mass calcd for $\text{C}_{14}\text{H}_{21}\text{O}_3$ $[\text{M}+\text{H}]^+$: 237.1485, Found: 237.1486; MS (EI): m/z 236 (M^+ , 7%), 177 (13), 149 (100), 135 (19), 107 (100), 106 (96), 90 (59), 83 (62), 79 (99), 51 (24), 41 (64).



Propyl 2-ethoxy-2-phenylacetate **207c**

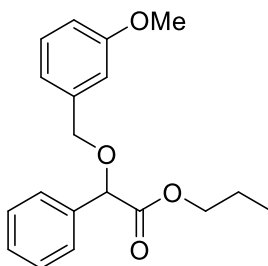
244 mg crude yield; 212 mg used for purification; 149 mg (30 min collection time; 77%) as colourless liquid. ^1H NMR (400 MHz, CDCl_3): $\delta = 7.49 - 7.43$ (m, 2H, ArH), 7.39 – 7.27 (m, 3H, ArH), 4.87 (s, 1H, CHOR), 4.07 (ddt, $J = 7.8, 3.9$ Hz, 2H, $\text{CO}_2\text{CH}_2\text{CH}_2$), 3.56 (ddq, $J = 37.3, 9.0, 7.0$ Hz, 2H, OCH_2CH_3), 1.67 – 1.54 (sex, $J = 7.1$ Hz, 2H, CH_2CH_3), 1.28 (t, $J = 7.0$ Hz, 3H, OCH_2CH_3), 0.83 (t, $J = 7.4$ Hz, 3H, CH_2CH_3) ppm; ^{13}C NMR (75 MHz, CDCl_3): $\delta = 171.2$ (C=O), 136.9 (ArC), 128.6 (ArCH), 128.6 (ArCH), 127.2 (ArCH), 80.9 (CHOR), 66.7 (OCH_2), 65.3 (OCH_2), 21.9 (CH_2), 15.2 (CH_3), 10.2 (CH_3) ppm; IR (neat): ν 2973s, 2937m, 2880m, 1750s, 1455w, 1267m, 1175s, 1114s, 729m, 697m cm^{-1} ; HMRS (NSI): Exact mass calcd for $\text{C}_{13}\text{H}_{19}\text{O}_3$ $[\text{M}+\text{H}]^+$: 223.1329, Found: 223.1329; MS (NSI): m/z 240 (57%), 223 ($\text{M}+\text{H}^+$, 100), 177 (89).



Propyl 2-(2-bromophenoxy)-2-phenylacetate **207d**

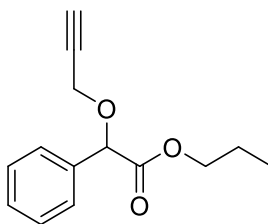
625 mg crude yield; 585 mg used for purification; 281 mg (35 min collection time; 71%) as colourless liquid. ^1H NMR (400 MHz, CDCl_3): $\delta = 7.59$ (dd, $J = 7.7, 1.7$ Hz, 1H, ArH), 7.54 – 7.49 (m, 3H, ArH), 7.43 – 7.28 (m, 3H, ArH), 7.16 (td, $J = 7.8, 1.7$ Hz, 1H, ArH), 5.02 (s, 1H, CHOR), 4.73 (d, $J = 13.0$ Hz, 1H, OCH_2Ar), 4.65 (d, $J = 13.0$ Hz, 1H, OCH_2Ar), 4.11 (t, $J = 6.6$ Hz, 2H, $\text{CO}_2\text{CH}_2\text{CH}_2$), 1.69 – 1.55 (sex, $J = 7.3$ Hz, 2H, CH_2CH_3), 0.85 (t, $J = 7.4$ Hz, 3H, CH_2CH_3) ppm; ^{13}C NMR (75 MHz, CDCl_3): δ 170.8 (C=O), 136.9 (ArC), 136.4 (ArC), 132.5 (ArCH), 129.3 (ArCH), 129.1 (ArCH), 128.8 (ArCH), 128.7 (ArCH), 127.5 (ArCH), 127.3

(ArCH), 122.6 (ArC), 80.7 (CHOR), 70.7 (OCH₂), 66.9 (OCH₂), 21.9 (CH₂), 10.1 (CH₃) ppm; IR (neat): ν 2967s, 2936m, 2878m, 1748s, 1441m, 1265m, 1205m, 1178m, 1122m, 1025m, 752m, 697m cm⁻¹; HMRS (NSI): Exact mass calcd for C₁₈H₂₀BrO₃ [M+H]⁺: 363.0590, Found: 363.0594; MS (NSI): m/z 383 (19%), 382 (100), 381 (19), 380 (M+NH₄⁺, 98), 348 (7), 347 (35), 346 (7), 345 (36), 303 (7), 177 (7).



Propyl 2-((3-methoxybenzyl)oxy)-2-phenylacetate **207e**

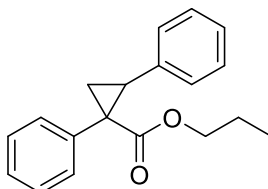
519 mg crude yield; 495 used for purification; 215 mg (30 min collection time; 72%) as yellow oil. ¹H NMR (300 MHz, CDCl₃): δ 7.53 – 7.46 (m, 2H, ArH), 7.43 – 7.34 (m, 3H, ArH), 7.29 – 7.23 (m, 1H, ArH), 6.95 (ddd, *J* = 4.6, 2.0, 1.1 Hz, 2H, ArH), 6.87 (ddd, *J* = 8.2, 2.6, 1.0 Hz, 1H, ArH), 4.95 (s, 1H, CHCOR), 4.61 (s, 2H, OCH₂Ar), 4.10 (td, *J* = 6.7, 0.9 Hz, 2H, CO₂CH₂CH₂), 3.82 (s, 3H, OCH₃), 1.69 – 1.54 (sex, *J* = 7.4 Hz, 2H, CH₂CH₃), 0.85 (t, *J* = 7.4 Hz, 3H, CH₂CH₃) ppm; ¹³C NMR (75 MHz, CDCl₃): δ = 170.9 (C=O), 159.8 (ArCOMe), 138.8 (ArC), 136.5 (ArC), 129.5 (ArC), 128.7 (ArC), 128.6 (ArC), 127.4 (ArC), 120.3 (ArC), 113.6 (ArC), 113.3 (ArC), 79.6 (CHOR), 70.9 (OCH₂), 66.8 (OCH₂), 55.3 (OCH₃), 21.9 (CH₂), 10.2 (CH₃) ppm; IR (neat): ν 2967s, 2879m, 2835m, 1747s, 1600m, 1587m, 1490m, 1456m, 1267s, 1176s, 1104m, 1053m, 785m, 732m, 696m cm⁻¹; HMRS (NSI): Exact mass calcd for C₁₉H₂₃O₄ [M+H]⁺: 315.1591, Found: 315.1593; MS (NSI): m/z 646 (27%), 332 (M+NH₄⁺, 100), 297 (28), 209 (21).



Propyl 2-phenyl-2-(prop-2-yn-1-yloxy)acetate **207f**

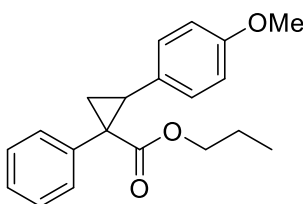
216 mg crude yield; 203 mg used for purification; 126 mg (30 min collection time; 58%) as yellow liquid. ¹H NMR (300 MHz, CDCl₃): δ = 7.52 – 7.44 (m, 2H, ArH), 7.43 – 7.34 (m, 3H, ArH), 5.22 (s, 1H, CHOR), 4.33 (dd, *J* = 16.0, 2.4 Hz, 1H, OCH₂C), 4.18 (dd, *J* = 16.0, 2.4 Hz, 1H, OCH₂C), 4.10 (td, *J* = 6.7, 2.7 Hz, 2H, CO₂CH₂), 2.50 (t, *J* = 2.4 Hz, 1H, CCH), 1.78 – 1.46 (sex, *J* = 7.3 Hz, 2H, CH₂CH₃), 0.84 (t, *J* = 7.4 Hz, 3H, CH₂CH₃) ppm; ¹³C NMR (75 MHz,

CDCl₃): δ = 170.4 (C=O), 135.6 (ArC), 128.9 (ArCH), 128.7 (ArCH), 127.6 (ArCH), 78.7 (CHOR), 78.6 (CCH), 75.6 (CCH), 66.9 (OCH₂), 56.2 (OCH₂), 21.9 (CH₂), 10.2 (CH₃) ppm; IR (neat): ν 3288s, 3968s, 2938m, 2880m, 1747s, 1455m, 1266m, 1207m, 1180m, 1100m, 731m, 698m cm⁻¹; HMRS (NSI): Exact mass calcd for C₁₄H₁₇O₃ [M+H]⁺: 233.1172, Found: 233.1174; MS (NSI): m/z 487 (31%), 271 (10), 250 (100), 233 (M+H⁺, 72), 177 (69).



Propyl 1,2-diphenylcyclopropane-1-carboxylate **207i**

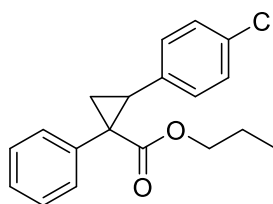
285 mg crude yield; 280 mg used for purification; 164 mg (30 min collection time, 47%) as colourless liquid. ¹H NMR (300 MHz, CDCl₃): δ = 7.18 – 7.09 (m, 3H, ArH), 7.10 – 6.98 (m, 5H, ArH), 6.83 – 6.75 (m, 2H, ArH), 4.16 – 3.96 (m, 2H, CO₂CH₂), 3.11 (dd, *J* = 9.3, 7.3 Hz, 1H, cyclopropCH), 2.14 (dd, *J* = 9.3, 4.9 Hz, 1H, cyclopropCH₂), 1.88 (dd, *J* = 7.3, 4.9 Hz, 1H, cyclopropCH₂), 1.65 – 1.49 (m, 2H, CH₂CH₃), 0.83 (t, *J* = 7.4 Hz, 3H, CH₂CH₃) ppm; ¹³C NMR (100 MHz, CDCl₃): δ = 174.2 (C=O), 136.9 (ArC), 135.2 (ArC), 132.3 (ArCH), 128.4 (ArCH), 127.2 (ArCH), 126.6 (ArCH), 67.2 (OCH₂), 38.0 (C), 33.3 (C), 22.3 (C), 20.6 (CH₂), 10.7 (CH₃) ppm; IR (in CH₂Cl₂): ν 3054m, 2972m, 1710m, 1421w, 1170m, 1093m, 895m cm⁻¹; HMRS (NSI): Exact mass calcd for C₁₉H₂₁O₂ [M+H]⁺: 281.1536, Found: 281.1535; MS (NSI): m/z 319 (3%), 298 (37), 281 (M+H⁺, 100), 239 (13), 221 (5).



Propyl 2-(4-methoxyphenyl)-1-phenylcyclopropane-1-carboxylate **207j**

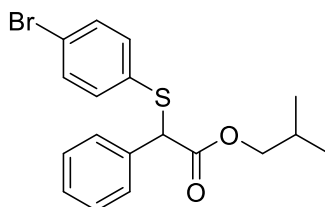
1.12 g crude yield; 1.05 g used for purification; 200 mg (30 min collection time, 56%) as colourless solid, m.p. 39-43 °C. ¹H NMR (300 MHz, CDCl₃): δ = 7.18 – 7.09 (m, 3H, ArH), 7.08 – 6.97 (m, 2H, ArH), 6.74 – 6.65 (m, 2H, ArH), 6.64 – 6.54 (m, 2H, ArH), 4.11 – 3.92 (m, 2H, CO₂CH₂), 3.69 (s, 3H, OCH₃), 3.04 (dd, *J* = 9.4, 7.3 Hz, 1H, cyclopropCH), 2.11 (dd, *J* = 9.4, 4.9 Hz, 1H, cyclopropCH₂), 1.80 (dd, *J* = 7.3, 4.9 Hz, 1H, cyclopropCH₂), 1.61 – 1.48 (m, 2H, CH₂CH₃), 0.81 (t, *J* = 7.4 Hz, 3H, CH₂CH₃) ppm; ¹³C NMR (75 MHz, CDCl₃): δ = 173.9 (C=O), 158.0 (ArCOMe), 135.0 (ArC), 131.9 (ArCH), 129.0 (ArCH), 128.5 (ArC), 127.6 (ArCH), 126.8 (ArCH), 113.2 (ArCH), 66.7 (OCH₂), 55.1 (OCH₃), 37.3 (C), 32.5 (C), 21.9 (C), 20.3 (CH₂),

10.3 (CH₃) ppm; IR (in CH₂Cl₂): ν 3055m, 2970m, 1709m, 1516m, 1265s, 1168m, 1035m, 833m cm⁻¹; HRMS (NSI): Exact mass calcd for C₂₀H₂₂O₃ [M+H]⁺: 311.1642, Found: 311.1643; MS (NSI): m/z 349 (8%), 328 (20), 311 (M+H⁺, 100), 269 (5), 251 (17), 161 (13).



Propyl 2-(4-chlorophenyl)-1-phenylcyclopropane-1-carboxylate **207k**

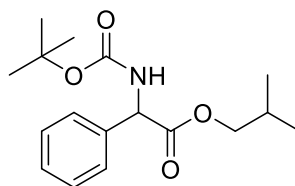
181 mg (30 min collection time; 46%) as colourless liquid. ¹H NMR (300 MHz, CDCl₃): δ = 7.04 (dt, *J* = 3.9, 1.6 Hz, 3H, ArH), 6.93 (ddd, *J* = 6.4, 2.9, 1.6 Hz, 4H, ArH), 6.63 – 6.56 (m, 2H, ArH), 4.04 – 3.83 (m, 2H, CO₂CH₂), 2.98 (dd, *J* = 9.3, 7.2 Hz, 1H, cyclopropCH), 2.05 (dd, *J* = 9.3, 5.0 Hz, 1H, cyclopropCH₂), 1.73 (dd, *J* = 7.2, 5.0 Hz, 1H, cyclopropCH₂), 1.46 (dt, *J* = 7.5, 6.6 Hz, 2H, CH₂CH₃), 0.72 (t, *J* = 7.4 Hz, 3H, CH₂CH₃) ppm; ¹³C NMR (75 MHz, CDCl₃): δ = 173.9 (C=O), 135.2 (ArC), 134.2 (ArC), 132.0 (ArCH), 131.9 (ArCH), 129.0 (ArCH), 128.5 (ArCH), 127.6 (ArCH), 127.1 (ArCH), 126.8 (ArC), 66.7 (OCH₂), 37.3 (C), 32.2 (C), 21.9 (C), 20.4 (CH₂CH₃), 10.3 (CH₂CH₃) ppm; IR (neat): ν 2968s, 2878m, 1714s, 1495m, 1254s, 1207m, 1169m, 1092m, 829m, 700m, 566m cm⁻¹; HRMS (NSI): Exact mass calcd for C₁₉H₁₉ClO₂ [M+H]⁺: 315.1148, Found: 315.1146; MS (NSI): m/z 350 (20%), 332 (51), 318 (7), 317 (32), 316 (20), 315 (M+H⁺, 100), 273 (14), 237 (7), 177 (9).



Isobutyl 2-((4-bromophenyl)thio)-2-phenylacetate **207l**

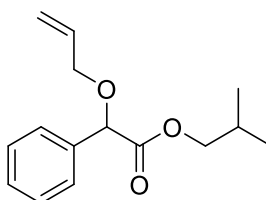
702 mg crude yield; 674 mg used for purification; 344 mg (30 min collection time, 75%) as colourless liquid. ¹H NMR (300 MHz, CDCl₃): δ = 7.47 – 7.18 (m, 9H, ArH), 4.89 (s, 1H, CHSR), 3.86 (d, *J* = 6.6 Hz, 2H, CO₂CH₂), 1.85 (hep, *J* = 6.7 Hz, 1H, CH(CH₃)₂), 0.83 (d, *J* = 6.7 Hz, 6H, CH₃) ppm; ¹³C NMR (75 MHz, CDCl₃): δ = 170.1 (C=O), 135.3 (ArC), 134.0 (ArCH), 132.9 (ArC), 132.0 (ArCH), 128.7 (ArCH), 128.5 (ArCH), 128.4 (ArCH), 122.2 (ArC), 71.8 (CS), 56.4 (CH₂), 27.6 (CH), 18.9 (CH₃) ppm; IR (neat): ν 2962s, 2873m, 1735s, 1472s, 1282m, 1145s, 1008s, 817m, 728m, 696s cm⁻¹; HMRS (APCI): Exact mass calcd for C₁₈H₂₀BrO₂S [M+H]⁺: 379.0362, Found: 379.0356; MS (APCI): m/z 382 (4%), 381 (25), 380 (4), 379 (M+H⁺, 24), 326

(3), 325 (33), 324 (3), 323 (32), 307 (11), 305 (12), 279 (22), 277 (22), 193 (15), 191 (16), 151 (7), 137 (100), 119 (9).



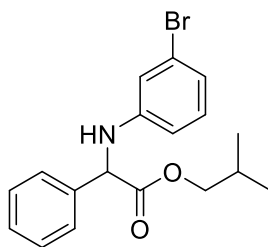
Isobutyl 2-((*tert*-butoxycarbonyl)amino)-2-phenylacetate **207m**

572 mg crude yield; 557 mg used for purification; 249 mg (30 min collection time, 66%) as colourless solid, m.p. 28-31 °C. ^1H NMR (300 MHz, CDCl_3): δ = 7.41 – 7.26 (m, 5H, ArH), 5.70 – 5.53 (m, 1H, NH), 5.32 (d, J = 7.5 Hz, 1H, CHN), 3.98 – 3.80 (m, 2H, CO_2CH_2), 1.85 (hept, J = 6.7 Hz, 1H, $\text{CH}(\text{CH}_3)_2$), 1.43 (s, 9H, $(\text{CH}_3)_3$), 0.80 (dd, J = 6.8, 1.8 Hz, 6H, $(\text{CH}_3)_2$) ppm; ^{13}C NMR (75 MHz, CDCl_3): δ = 171.2 (C=O), 154.8 (C=O), 137.2 (ArC), 128.8 (ArCH), 128.3 (ArCH), 127.1 (ArCH), 80.1 (CO), 71.7 (CHN), 57.7 (OCH_2), 28.3 (CH or $(\text{CH}_3)_3$), 27.6 (CH or $(\text{CH}_3)_3$), 18.8 ($(\text{CH}_3)_2$) ppm; IR (in CH_2Cl_2): ν 3435s, 3063m, 2968s, 2876m, 1716s, 1494s, 1348m, 1107m, 1053m, 997m, 850m cm^{-1} ; HMRS (NSI): Exact mass calcd for $\text{C}_{17}\text{H}_{26}\text{NO}_4$ [$\text{M}+\text{H}$] $^+$: 308.1856, Found: 308.1857; MS (NSI): m/z 637 (57%), 615 (85), 330 (18), 308 ($\text{M}+\text{H}^+$, 54), 252 (87), 208 (100). Spectroscopic data was in accordance with the literature.²¹



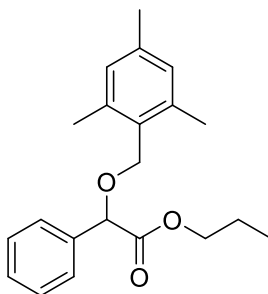
Isobutyl 2-(allyloxy)-2-phenylacetate **207h**

299 mg crude yield; 287 mg used for purification; 185 mg (30 min collection time, 62%) as colourless liquid. ^1H NMR (300 MHz, CDCl_3): δ = 7.49 – 7.43 (m, 2H, ArH), 7.40 – 7.28 (m, 3H, ArH), 5.95 (m, 1H, allylH), 5.29 (dq, J = 17.3, 1.6 Hz, 1H, OCH_2), 5.25 – 5.17 (dq, J = 10.4, 1.2 Hz, 1H, OCH_2), 4.94 (s, 1H, CHOR), 4.07 (dd, J = 5.8, 1.2 Hz, 2H, OCH_2), 3.89 (dd, J = 6.7, 1.5 Hz, 2H, CO_2CH_2), 1.87 (hept, J = 6.7 Hz, 1H, CH), 0.82 (dd, J = 6.8, 0.9 Hz, 6H, CH_3) ppm; ^{13}C NMR (75 MHz, CDCl_3): δ = 170.9 (C=O), 136.6 (CH), 133.8 (ArC), 128.7 (ArC), 128.6 (ArCH), 127.3 (ArCH), 118.2 (CH_2), 79.7 (CHOR), 71.1 (OCH_2), 70.4 (OCH_2), 27.7 (CH), 18.9 (CH_3) ppm; IR (neat): ν 2963m, 2874m, 1751s, 1469w, 1454w, 1256m, 1204m, 1174m, 1100m, 1015m, 924m, 730m, 697m cm^{-1} ; HMRS (NSI): Exact mass calcd for $\text{C}_{15}\text{H}_{21}\text{O}_3$ [$\text{M}+\text{H}$] $^+$: 249.1485, Found: 249.1488; MS (NSI): m/z 519 (34%), 287 (8), 271 (34), 266 (100), 249 ($\text{M}+\text{H}^+$, 95), 191 (28), 175 (8).



Isobutyl 2-((3-bromophenyl)amino)-2-phenylacetate **207n**

491 crude yield; 480 mg used for purification; 217 mg (30 min collection time, 49%) as colourless solid, m.p. 84-88 °C. ^1H NMR (300 MHz, CDCl_3): δ = 7.54 – 7.42 (m, 2H, ArH), 7.41 – 7.26 (m, 3H, ArH), 6.95 (t, J = 8.0 Hz, 1H, ArH), 6.80 (ddd, J = 7.9, 1.8, 0.9 Hz, 1H, ArH), 6.71 (t, J = 2.1 Hz, 1H, ArH), 6.45 (ddd, J = 8.2, 2.4, 1.0 Hz, 1H, ArH), 5.12 (bs, 1H, NH), 5.04 (s, 1H, CHN), 4.00 – 3.82 (m, 2H, OCH_2), 1.87 (hep, J = 6.7 Hz, 1H, CH), 0.81 (dd, J = 6.7, 2.5 Hz, 6H, CH_3) ppm; ^{13}C NMR (75 MHz, CDCl_3): δ = 171.4 (C=O), 147.1 (ArC-N), 137.2 (ArC), 130.5 (ArC), 128.9 (ArC), 128.4 (ArC), 127.1 (ArC), 123.1 (ArC), 120.8 (ArC), 116.1 (ArC), 111.9 (ArC), 71.8 (OCH_2), 60.4 (CN), 27.6 (CH), 18.8 (CH_3) ppm; IR (in CH_2Cl_2): ν 3412m, 3053m, 2964m, 2876m, 1732s, 1597s, 1496s, 1481m, 1421m, 1321m, 1265s, 1168m, 1070m cm^{-1} ; HMRS (NSI): Exact mass calcd for $\text{C}_{18}\text{H}_{21}\text{BrNO}_2$ $[\text{M}+\text{H}]^+$: 362.0756, Found: 362.0748. Spectroscopic data was in accordance with the literature.²²



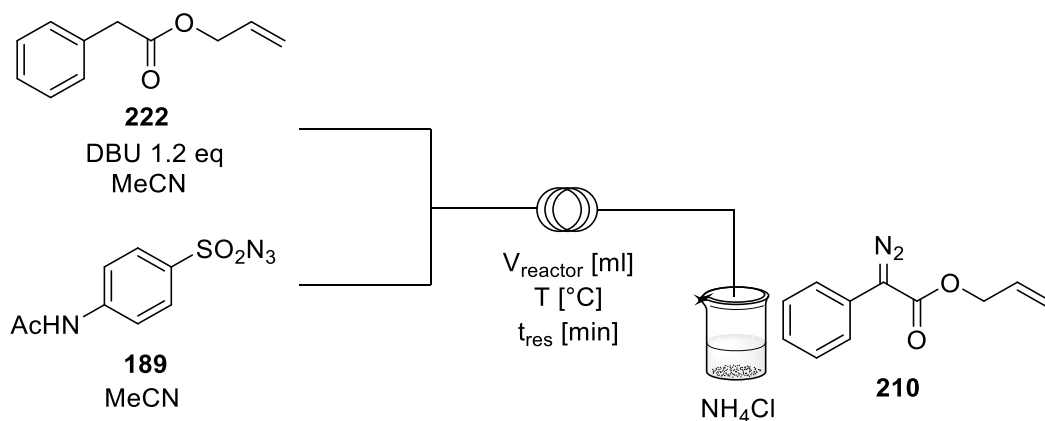
Propyl 2-phenyl-2-((2,4,6-trimethylbenzyl)oxy)acetate **207o**

3.003 g crude yield; 2.995 g used for purification; 1.33 g (140 min collection time, 70%) as colourless oil. ^1H NMR (400 MHz, CDCl_3): δ = 7.48 – 7.44 (m, 2H, ArH), 7.38 – 7.30 (m, 3H, ArH), 6.85 (s, 2H, ArH), 4.91 (s, 1H, CHOR), 4.69 (d, J = 10.6 Hz, 1H, OCH_2), 4.57 (d, J = 10.6 Hz, 1H, OCH_2), 4.09 (td, J = 6.7, 1.3 Hz, 2H, OCH_2), 2.33 (s, 6H, o-CH_3), 2.26 (s, 3H, p-CH_3), 1.68 – 1.56 (m, 2H, CH_2CH_3), 0.85 (t, J = 7.4 Hz, 3H, CH_2CH_3) ppm; ^{13}C NMR (100 MHz, CDCl_3): δ = 171.5 (C=O), 138.7 (ArCH), 138.3 (ArC), 137.2 (ArCH), 130.7 (ArCH), 129.3 (ArCH), 128.7 (ArC), 127.5 (ArC), 80.42 (CHOR), 67.1 (OCH_2), 66.3 (OCH_2), 22.3 (CH_3), 21.4 (CH_3), 20.0 (CH_3) ppm; IR (neat): ν 2967s, 2879m, 1748s, 1614m, 1454s, 1264m, 1202m, 1175s, 1098s, 1071m, 851m, 725m, 697s cm^{-1} ; HMRS (NSI): Exact mass calcd for

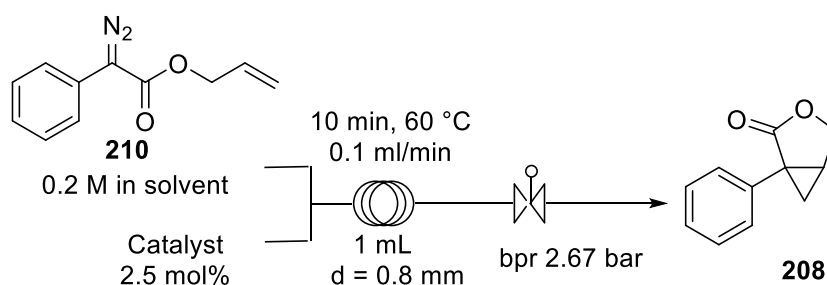
$C_{21}H_{27}O_3NH_4$ $[M+NH_4]^+$: 344.2220, Found: 344.2220; MS (NSI): m/z 670 (34%), 365 (5), 349 (13), 344 ($M+NH_4^+$, 100).

7.4 Experimentals Chapter 5

7.4.1 Experimentals intramolecular cyclopropanation

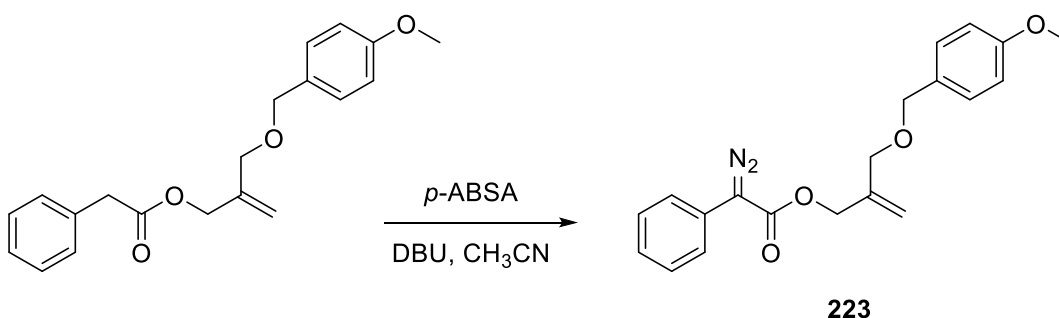


Optimisation diazo transfer in flow for Allyl 2-diazo-2-phenylacetate Allyl phenylacetate (35.24 g, 200 mmol) and DBU (42.6 ml, 280 mmol, 1.4 eq) were dissolved in acetonitrile for a total volume of 200 ml. *p*-Acetamidobenzenesulfonyl azide (57.66g, 240 mmol, 1.2 eq) was dissolved in a total volume of 200 ml acetonitrile and subsequently filtered to remove residual solids. The two solutions were pumped through the flow system using Asia syringe pumps with flow rates of 0.5 ml/min each (combined flow rate 1 ml/min) for a residence time of 8.2 min and of 0.3 ml/min each (combined flow rate 0.6 ml/min) for a residence time of 13.7 min. The reaction mixture was analysed using in-line infrared with the consumption of starting material used to determine the yield of the transformation. Calibration of allyl phenylacetate gave a R^2 of 0.993. Extraction of allyl 2-diazo-2-phenylacetate was performed using *n*-heptane (15 ml) and 1M $NaNO_2$ (11 ml) solution per 1 g allyl phenylacetate used. 964 mg Allyl 2-diazo-2-phenylacetate **210** (collection time 19 min, 4.77 mmol) was obtained without further purification in 84% yield as yellow oil. 1H NMR (400 MHz, $CDCl_3$): δ = 7.46-7.51 (m, 2H, ArH), 7.36-7.42 (m, 2H, ArH), 7.16-7.22 (m, 1H, ArH), 5.92-6.04 (m, 1H, allylH), 5.37 (ddd, J = 17.2, 3.0, 1.5 Hz, 1H, $CH_2=CH$), 5.28 (ddd, J = 10.4, 2.5, 1.2 Hz, 1H, $CH_2=CH$), 4.78 (dt, J = 5.6, 1.4 Hz, 1H, OCH_2) ppm; ^{13}C (100 MHz, $CDCl_3$): δ = 165.2 (C=O), 132.1 (C=C), 128.9 (ArCH), 125.9 (ArCH), 125.4 (ArC), 123.9 (ArCH), 118.4 (C=C), 65.4 (OCH_2) ppm. Spectroscopic data was in accordance with the literature.²³



Optimisation cyclopropanation in flow for 1-phenyl-3-oxabicyclo[3.1.0]hexan-2-one **208**

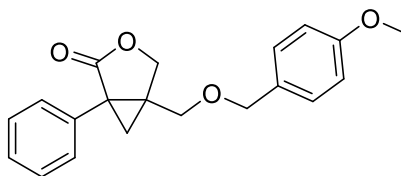
Allyl 2-diazo-2-phenylacetate **210** (202 mg, 1 mmol) was dissolved in the reaction solvent to give the total volume of 5 ml. Catalyst (0.025 mmol, 2.5 mol%) was dissolved in the reaction solvent to give the total volume of 5 ml. Both solutions were charged into 5 ml syringes and pumped using a KR Analytical Ltd Fusion 100 Touch syringe pump with a combined flow rate of 0.1 ml/min through a 1 ml reaction coil (residence time 10 minutes). The system was stabilized for 30 minutes and then collected for 60 minutes by running through a silica plug to quench the reaction mixture. The silica plug was washed with CH₂Cl₂ and the solvent was evaporated *in vacuo*. The crude reaction mixture was purified using column chromatography (10 g SNAP Ultra, 9:1 *n*-Hexane:EtOAc). 1-Phenyl-3-oxabicyclo[3.1.0]hexan-2-one **208** was obtained as colourless oil (for yields see Table 5.3, entries 1-7)). ¹H NMR (400 MHz, CDCl₃): δ = 7.48-7.27 (m, 5H, ArH), 4.47 (dd, *J* = 9.27, 4.6 Hz, 1H, CO₂CH₂), 4.31 (d, *J* = 9.27 Hz, 1H, CO₂CH₂), 2.57 (dt, *J* = 7.8, 4.6 Hz, 1H, CH), 1.66 (dd, *J* = 7.8, 4.86 Hz, 1H, CH₂), 1.38 (t, *J* = 4.58 Hz, 1H, CH₂) ppm. ¹³C NMR (100 MHz, CDCl₃): δ = 176.5 (C=O), 134.5 (ArC), 129.1 (ArCH), 128.8 (ArCH), 128.2 (ArCH), 68.6 (OCH₂), 32.2 (C), 25.5 (CH), 20.6 (CH₂) ppm; HRMS (APCI): exact mass calcd. for C₁₁H₁₀O₂ [M+H]⁺: 175.0754, Found: 175.0751; MS (EI): *m/z* 195 (8%), 177 (16), 175 (M+H⁺, 100), 161 (6), 157 (17). Spectroscopic data was in accordance with the literature.²³



2-(((4-methoxybenzyl)oxy)methyl)allyl 2-diazo-2-phenylacetate **223**

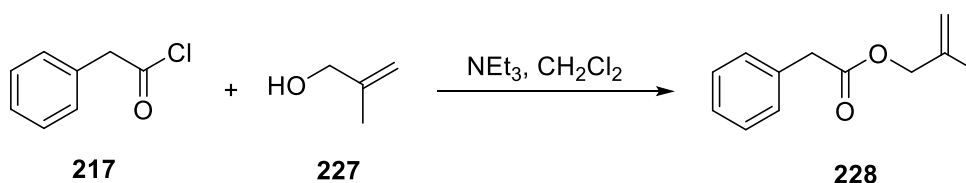
Ester (652 mg, 2 mmol) and *p*-ABSA (577 mg, 2.4 mmol) were dissolved in acetonitrile (4 mL). Then, DBU (419 μL, 2.8 mmol) was added slowly and the reaction mixture was left stirring at 22 °C for 72 h. Sodium nitrite solution (1 M, 7.2 mL) was added and the mixture was extracted

with *n*-hexane (10.4 mL) to give diazo compound **223** (701 mg, 1.99 mmol, 99%) as yellow oil in sufficient purity for the cyclisation reaction. ^1H NMR (400 MHz, CDCl_3): δ = 7.48 (m, 2H, *ArH*), 7.38 (m, 2H, *ArH*), 7.27 (m, 2H, *ArH*), 7.19 (m, 1H, *ArH*), 6.86 (m, 2H, *ArH*), 5.28 (d, J = 4.6 Hz, 2H, $\text{C}=\text{CH}_2$), 4.83 (s, 2H, OCH_2), 4.45 (s, 2H, OCH_2), 4.04 (s, 2H, OCH_2), 3.78 (s, 3H, OCH_3) ppm; ^{13}C NMR (75 MHz, CDCl_3): δ = 164.7 (C=O), 159.2 (ArCO), 140.5 (ArC), 129.9 (ArC), 129.3 (ArC), 128.9 (ArC), 125.8 (ArC), 125.3 (ArC), 123.9 (ArC), 115.5 (C=C), 113.7 (C=C), 71.8 (OCH_2), 70.3 (OCH_2), 64.9 (OCH_2), 63.3 (C=N₂), 55.1 (OCH_3) ppm; IR (neat): ν 2934w, 2085s, 1701s, 1512s, 1449m, 1242s, 1152m, 1032m, 756m cm^{-1} ; HRMS (EI): exact mass calcd. for $\text{C}_{20}\text{H}_{20}\text{N}_2\text{O}_4$ $[\text{M}]^+$: 352.1423, Found: 352.1414; MS (EI): m/z 324 (M^+ , 13%), 250 (15), 224 (26), 186 (100), 174 (31), 158 (42), 135 (94), 129 (97), 121 (100), 105 (100), 91 (45), 77 (100), 63 (23).



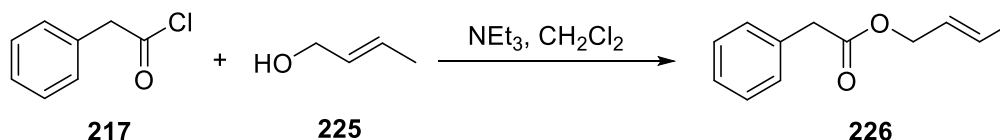
5-(((4-Methoxybenzyl)oxy)methyl)-1-phenyl-3-oxabicyclo[3.1.0]hexan-2-one **224**

Prepared following procedure for cyclopropanation in flow. The reaction mixture was collected for 60 minutes (combined flow rate 0.1 ml/min) and subsequently purified as described above. Lactone **224** (178 mg, 91%) was obtained as colourless oil. ^1H NMR (400 MHz, CDCl_3): δ = 7.24 (m, 5H, *ArH*), 6.98 (m, 2H, *ArH*), 6.74 (m, 2H, *ArH*), 4.45 (d, J = 9.06 Hz, 1H, OCH_2), 4.27 (d, J = 9.06 Hz, 1H, OCH_2), 4.22 (d, J = 11.56 Hz, 1H, OCH_2), 4.15 (d, J = 11.56 Hz, 1H, OCH_2), 3.70 (s, 3H, OCH_3), 3.40 (d, J = 10.73 Hz, 1H, OCH_2), 3.15 (d, J = 10.73 Hz, 1H, OCH_2), 1.63 (d, J = 5.13 Hz, 1H, cyclopropH), 1.31 (d, J = 5.13 Hz, 1H, cyclopropH). ^{13}C NMR (75 MHz, CDCl_3): δ = 176.5 (C=O), 159.3 (ArC-OMe), 131.2 (ArC), 130.4 (ArC), 129.6 (ArC), 129.2 (ArC), 128.6 (ArC), 128.2 (ArC), 113.8 (ArC), 72.9 (OCH_2), 70.1 (OCH_2), 68.3 (OCH_2), 55.3 (OCH_3), 36.8 (C), 35.3 (C), 20.5 (CH_2) ppm; IR (neat): ν 3958m, 2908m, 2858m, 1770s, 1612m, 1512s, 1454w, 1361m, 1303w, 1249s, 1091s, 1037m, 1014m, 910s cm^{-1} ; HMRS (EI): exact mass calcd for $\text{C}_{20}\text{H}_{20}\text{O}_4$ $[\text{M}]^+$: 324.1362, Found: 324.1360; MS (EI): m/z 324 (M^+ , 35%), 219 (34), 186 (46), 135 (32), 121 (100), 84 (35).



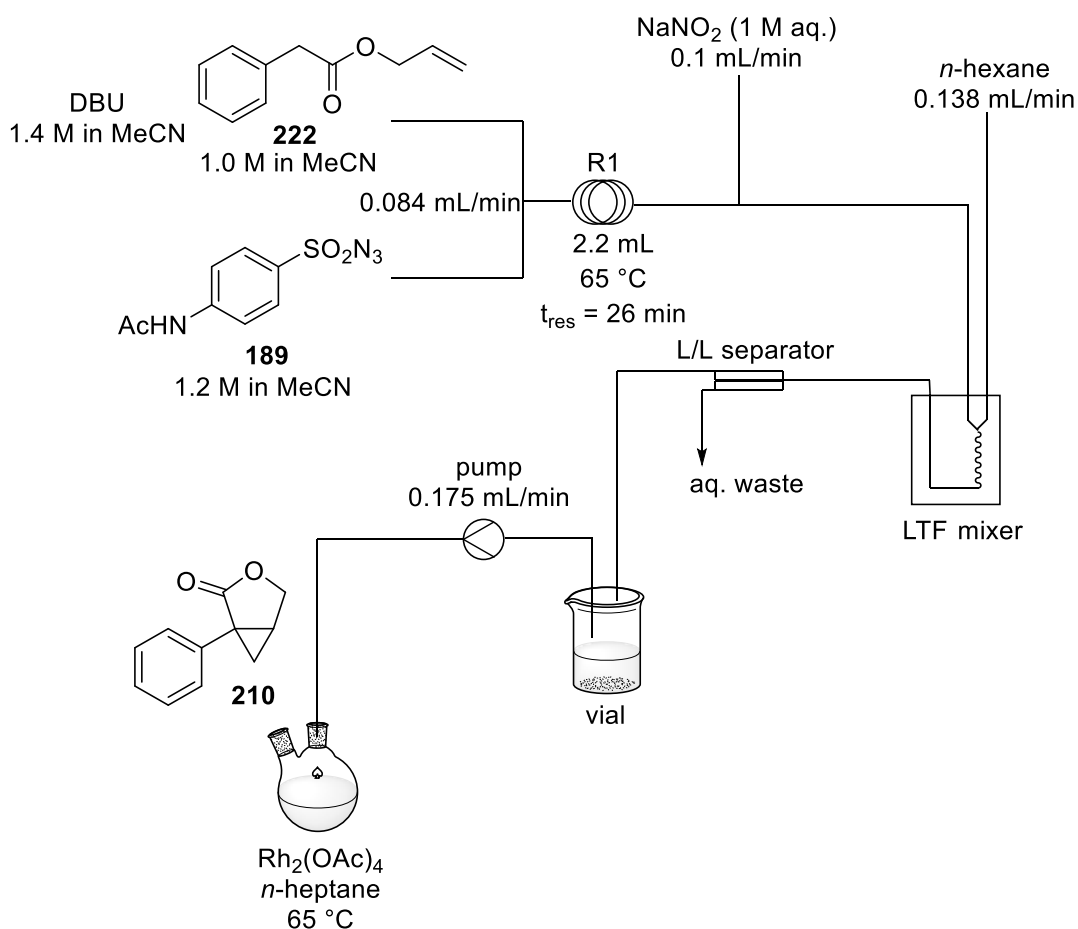
2-Methylallyl 2-phenylacetate **228**

2-Methylprop-2-en-1-ol **227** (1.68 mL, 20 mmol) was dissolved in dichloromethane (3 mL) in a 25 mL round bottom flask, triethylamine (2.1 mL, 15 mmol) was added and the mixture was cooled to 0 °C. Then, freshly prepared phenylacetyl chloride **217** (1.32 mL, 10 mmol) was added *via* syringe pump over one hour. The reaction mixture was left stirring for 12 h, then the mixture was concentrated *in vacuo* and dissolved in ethyl acetate (15 mL). The organic fraction was washed with water (15 mL) and brine (20 mL) and dried over MgSO₄. Subsequently, the solvent was evaporated *in vacuo* and the crude red oil was purified using flash column chromatography (20 g column, gradient *n*-hexane / ethyl acetate from 100:0 to 70:30) to afford 2-methylallyl 2-phenylacetate **228** (810 mg, 4.3 mmol, 43%) as red oil. ¹H NMR (400 MHz, CDCl₃): δ = 7.22 (m, 5H, ArH), 4.84 (d, *J* = 5.27 Hz, 2H, C=CH₂), 4.44 (s, 2H, OCH₂), 3.60 (s, 2H, CH₂), 1.64 (s, 3H, CH₃) ppm. Spectroscopic data was in accordance with the literature.²³

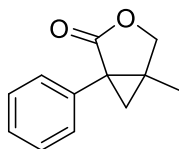


(*E*)-but-2-en-1-yl 2-phenylacetate **226**

Crotyl alcohol **225** (*E/Z* mixture (20:1), 1.7 mL, 20 mmol) was dissolved in dichloromethane (5 mL) in a 25 mL round bottom flask, triethylamine (2.1 mL, 15 mmol) was added and the mixture was cooled to 0 °C. Then, freshly prepared phenylacetyl chloride **217** (1.32 mL, 10 mmol) was added *via* syringe pump over one hour. The reaction mixture was left stirring for 12 h, then the mixture was concentrated *in vacuo* and dissolved in ethyl acetate (15 mL). The organic fraction was washed with water (15 mL) and brine (20 mL) and dried over MgSO₄. Subsequently, the solvent was evaporated *in vacuo* to afford but-2-en-1-yl 2-phenylacetate **226** (1.35 g, 7.1 mmol, 71%) as brown-red oil in sufficient purity for the next reaction (*E/Z* 20:1). ¹H NMR (400 MHz, CDCl₃): δ = 7.33 (m, 5H, ArH), 5.78 (dqt, *J* = 15.4, 6.6, 1.1 Hz, 1H, OCH₂CH=CH), 5.63 (dtq, *J* = 15.4, 6.4, 1.5 Hz, 1H, CH=CHCH₃), 4.55 (dt, *J* = 6.5, 1.1 Hz, 2H, OCH₂), 3.65 (dq, *J* = 6.3, 1.0 Hz, 2H, CH₂), 1.73 (s, 3H, CH₃) ppm. Spectroscopic data was in accordance with the literature.²⁴

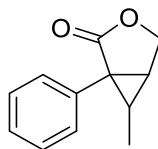


2-step continuous flow / semi-batch protocol Allyl ester (4 mmol) was dissolved in acetonitrile and DBU (0.84 ml, 5.6 mmol, 1.4 eq) was added to give a total volume of 4 ml. *p*-ABSA (1.15 g, 4.8 mmol, 1.2 eq) was dissolved in acetonitrile to give a total volume of 4 ml. Both solutions were charged into 5 ml syringes. Flow rates were put to 0.042 ml/min for the ester and sulfonyl azide solution on a syringe pump. 1 M aqueous sodium nitrite quench solution was pumped *via* Vapourtec pump (blue tubing) with a flow rate of 0.101 ml/min and *n*-heptane (red tubing) for the extraction was pumped with a flow rate of 0.158 ml/min. After passing the L/L phase separator, the aqueous layer was discarded and the organic layer was added to the solution. Rh₂(OOct)₄ (10.1 mg, 1 mol%) was dissolved in *n*-heptane (5 ml) and stirred at 65 °C. Addition of organic layer stream was performed for 30 minutes and the mixture stirred at 65 °C for another 30 minutes. Subsequently, solvent was evaporated *in vacuo* and the reaction mixture was purified *via* flash chromatography on an automated purification system using a 20g silica column.



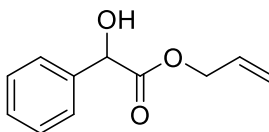
5-Methyl-1-phenyl-3-oxabicyclo[3.1.0]hexan-2-one **230**

63 mg (32% yield; 161 mg of 198 mg of the crude reaction mixture were used for purification) of **230** were obtained as colourless oil. ^1H NMR (250 MHz, CDCl_3): δ = 7.35-7.15 (m, 5H, ArH), 4.30 (d, J = 9.1 Hz, 1H, OCH_2), 4.12 (d, J = 9.1 Hz, 1H, OCH_2), 1.55 (d, J = 4.9 Hz, 1H, CH_2), 1.32 (d, J = 4.9, 1H, CH_2), 1.09 (s, 3H, CH_3) ppm. ^{13}C NMR (63 MHz, CDCl_3): δ = 177.6 (C=O), 132.2 (ArC), 130.4 (ArCH), 128.9 (ArCH), 128.2 (ArCH), 73.4 (OCH_2), 37.1 (C), 31.4 (C), 22.8 (CH_2), 15.4 (CH) ppm; HRMS (APCI): exact mass calcd for $\text{C}_{12}\text{H}_{13}\text{O}_2$ $[\text{M}+\text{H}]^+$: 189.0910, Found: 189.0913. Spectroscopic data was in accordance with the literature.²⁵



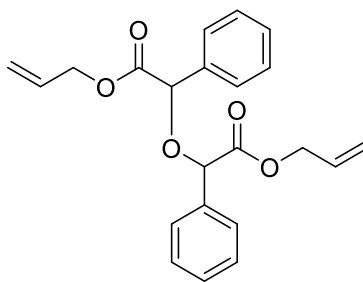
6-Methyl-1-phenyl-3-oxabicyclo[3.1.0]hexan-2-one **229**

66 mg (30% yield; 196 mg of 211 mg of the crude reaction mixture were used for purification) of **229** were obtained as colourless oil. ^1H NMR (400 MHz, CDCl_3): δ = 7.44-7.28 (m, 5H, ArH), 4.42 (dd, J = 9.1, 4.5 Hz, 1H, OCH_2), 4.32 (d, J = 9.1 Hz, 1H, OCH_2), 2.30 (t, J = 4.5 Hz, 1H, CH), 1.50-1.42 (m, 1H, CH), 0.80 (d, J = 6.1 Hz, 3H, CH_3) ppm. ^{13}C NMR (100 MHz, CDCl_3): δ = 176.7, 130.6, 128.8, 128.2, 68.7, 37.2, 28.9, 26.4, 13.6 ppm. HRMS (APCI): exact mass calcd for $\text{C}_{12}\text{H}_{13}\text{O}_2$ $[\text{M}+\text{H}]^+$: 189.0910, Found: 189.0910; MS (APCI): m/z 395 (2%), 377 (47), 206 (5), 189 ($\text{M}+\text{H}^+$, 100). Spectroscopic data was in accordance with the literature.²⁶

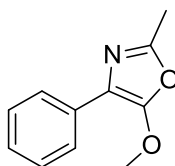


Allyl 2-hydroxy-2-phenylacetate **231**

Obtained as colourless oil. ^1H NMR (300 MHz, CDCl_3): δ = 7.48-7.41 (m, 2H, ArH), 7.39-7.28 (m, 3H, ArH), 5.90-5.73 (m, 1H, allylH), 5.20 (s, 2H, $\text{CH}=\text{CH}_2$), 5.16 (dq, J = 5.14, 1.27 Hz, 1H, CHOH), 4.60-4.68 (m, 2H, OCH_2), 3.40 (bs, 1H, OH) ppm. ^{13}C NMR (75 MHz, CDCl_3): δ = 173.3 (C=O), 138.3 (ArC), 131.2 (CH), 128.6 (ArCH), 128.5 (ArCH), 126.6 (ArCH), 118.7 (CH_2), 72.9 (COH), 66.4 (OCH_2) ppm. Spectroscopic data was in accordance with the literature.²⁷

Diallyl 2,2'-oxybis(2-phenylacetate) **233**

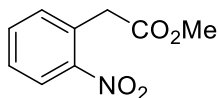
Obtained as pale yellow oil. ^1H NMR (300 MHz, CDCl_3): δ = 7.33-7.50 (m, 5H, ArH), 5.76-5.90 (m, 1H, allylH), 5.13-5.24 (m, 2H, $\text{C}=\text{CH}_2$), 5.04 (d, J = 2.0 Hz, 1H, CHOR), 4.57-4.64 (m, 2H, OCH_2) ppm. ^{13}C NMR (75 MHz, CDCl_3): δ = 169.8 (C=O), 135.5 (ArC), 131.5 (CH), 128.9 (ArCH), 127.6 (ArCH), 127.5 (ArCH), 118.4 (CH_2), 78.7 (CHOR), 65.7 (OCH_2) ppm; IR (neat): ν 3066m, 2085m, 1817w, 1801w, 1747s, 1685m, 1647w, 1496m, 1454m, 1361w, 1246m, 1203m, 1173s, 1103m, 987m, 935m, 732m, 698m cm^{-1} ; HMRS (EI): exact mass calcd for $\text{C}_{22}\text{H}_{25}\text{O}_5$ $[\text{M}]^+$: 366.1467, Found: 366.1468; MS (EI): m/z 366 (M^+ , 2%), 281 (80), 176 (74), 148 (29), 119 (22), 106 (44), 105 (100), 91 (100), 77 (92).

5-methoxy-2-methyl-4-phenyloxazole **236**

Methyl 2-diazo-2-phenylacetate **162** (176 mg, 1 mmol) was dissolved in dry CH_2Cl_2 (4 ml) and added *via* syringe pump over 1 h to a solution containing $\text{Rh}_2(\text{OAc})_4$ (4.42 mg, 0.01 mmol; 1 mol%) in dry CH_2Cl_2 (4 ml) under argon atmosphere (Schlenk dried flask) at reflux. After completion of the reaction (*via* TLC analysis) the reaction mixture was cooled down to room temperature and then the solvent was evaporated *in vacuo*. The crude reaction mixture was immediately purified *via* flash column chromatography (12 g silica column with 0%-10% EtOAc in *n*-hexane over 25 column volumes) to furnish 71 mg of **236** (38%) as colourless oil. ^1H NMR (300 MHz, CDCl_3): δ = 7.74-7.79 (m, 2H, ArH), 7.30-7.38 (m, 2H, ArH), 7.18 (tt, J = 8.37, 1.27 Hz, 1H, ArH), 4.00 (s, 3H, OCH_3), 2.41 (s, 3H, CH_3) ppm. ^{13}C NMR (75 MHz, CDCl_3): δ = 154.3 (C=N), 151.9 (C-OMe), 131.4 (ArC), 128.5 (ArCH), 126.3 (ArCH), 124.8 (ArCH), 114.5 (C), 60.1 (OCH_3), 14.3 (CH_3) ppm. IR (neat): ν 3028w, 2949w, 1743s, 1647s, 1599s, 1500w, 1449m, 1369m, 1221s, 1173m, 1016m, 766m, 731m cm^{-1} . HRMS (APCI): Exact mass calc for $\text{C}_{11}\text{H}_{12}\text{NO}_2$ $[\text{M}+\text{H}]^+$: 190.0868, Found: 190.0862; MS (APCI): m/z 190 ($\text{M}+\text{H}^+$, 100%), 175 (25), 164 (28), 144 (32), 136 (18), 114 (14).

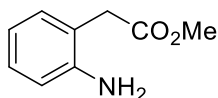
7.4.2 Experimentals Dihydroindoles

7.4.2.1 Synthesis of tosyl protected amine **257**



Methyl 2-(2-nitrophenyl)acetate **256**

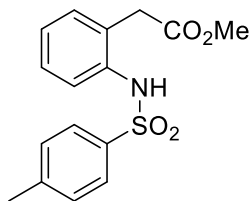
2-nitrophenylacetic acid (10 g, 55 mmol) was dissolved in 100 mL of methanol and the solution was cooled down at 0 °C before addition of acetyl chloride (9.8 mL, 138 mmol). The reaction was stirred overnight at room temperature and checked by TLC (*n*-hexane / EtOAc 4:1). The solvent was evaporated in *vacuo* and the residual oil washed with a saturated solution of NaHCO₃ (20 mL) and extracted with ether (3 x 25 mL). Subsequently, the combined organic fractions were washed with water (20 mL) and brine (20 mL), dried over MgSO₄ and concentrated in *vacuo* to afford 10.7 g of **256** (99% yield) as a yellow oil that solidified at room temperature (22 °C), m.p.: 36-40 °C. ¹H NMR (300 MHz, CDCl₃): δ = 8.13 (dd, *J* = 8.1, 0.9 Hz, 1H, Ar*H*), 7.62 (td, *J* = 7.5, 1.3 Hz, 1H, Ar*H*), 7.49 (td, *J* = 8.1, 1.4 Hz, 1H, Ar*H*), 7.37 (dd, *J* = 7.6, 1.0 Hz, 1H, Ar*H*), 4.04 (s, 2H, CH₂), 3.72 (s, 3H, CH₃) ppm; ¹³C NMR (75 MHz, CDCl₃): δ = 170.4 (C=O), 148.7 (ArC), 133.6 (ArCH), 133.3 (ArCH), 129.7 (ArC), 128.6 (ArCH), 125.3 (ArCH), 52.3 (CH₂), 39.6 (CH₃) ppm; HRMS (NSI): Exact mass calc for C₉H₉NO₄NH₄ [M+NH₄]⁺: 213.0870, Found: 213.0868; MS (NSI): *m/z* 234 (7%), 218 (13), 213 (M+NH₄⁺, 100), 196 (77), 164 (25). Spectroscopic data was in accordance with the literature.²⁸



Methyl 2-(2-aminophenyl)acetate **254**

A two-neck flask was evacuated and filled with N₂ twice; 10% Pd/C (233 mg) was added to the flask and the residue was washed with a small amount of CH₂Cl₂. Methanol (20 mL) was added carefully before addition of methyl 2-(2-nitrophenyl)acetate **256** (4 g, 21 mmol) dissolved in a small amount of methanol. Subsequently, the flask was evacuated and filled with N₂ twice, evacuated again and filled with H₂ (balloon). The H₂ balloon was refilled whenever all H₂ had been consumed. The reaction was stirred at room temperature for 48 h and monitored by TLC (ethyl acetate / *n*-hexane 1:4). The mixture was filtered through celite and the solvent was evaporated in *vacuo* to afford 3.3 g of methyl 2-(2-aminophenyl)acetate **254** (98% yield) as a red oil. ¹H-NMR (300 MHz, CDCl₃): δ = 7.15-7.06 (m, 2H, Ar*H*), 6.80-6.68 (m, 2H, Ar*H*), 4.07 (bs, 2H, NH), 3.71 (s, 3H, CH₃), 3.59 (s, 2H, CH₂) ppm; ¹³C NMR (75 MHz, CDCl₃): δ = 172.2 (C=O), 145.4 (ArC), 131.1 (ArCH), 128.5 (ArCH), 119.4 (ArC), 118.9

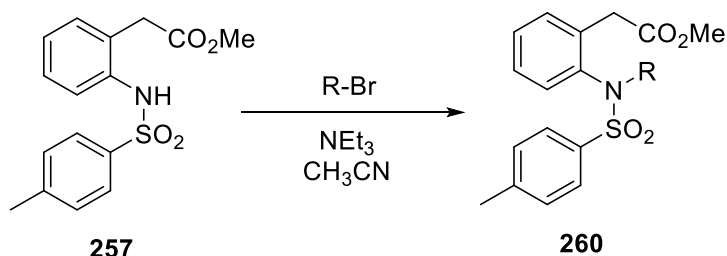
(ArCH), 116.5 (ArCH), 52.1 (CH₃), 38.2 (CH₂) ppm. Spectroscopic data was in accordance with the literature.²⁸



Methyl 2-(2-((4-methylphenyl)sulfonamido)phenyl)acetate **257**

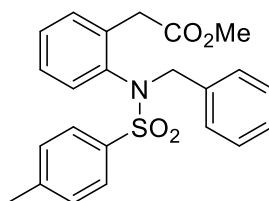
A solution of methyl 2-(2-aminophenyl)acetate **254** (3 g, 18 mmol) in pyridine (20 mL) was cooled down to 0 °C. *p*-Toluenesulfonyl chloride (4.16 g, 22 mmol) was added dropwise. The reaction was stirred at room temperature for 24 h and monitored *via* TLC (ethyl acetate / *n*-hexane 1:4). Hydrochloric acid (1 M, 25 mL) was added and the reaction mixture was extracted with ethyl acetate (2 x 20 mL), the organic layer was washed with hydrochloric acid (1 M, 20 mL) and water (2 x 20 mL) and then, dried over MgSO₄. Subsequent evaporation of the solvent in *vacuo* followed by liquid column chromatography furnished methyl 2-(2-((4-methylphenyl)sulfonamido)phenyl)acetate **257** (5.57 g, 96% yield) as a pale orange solid, m.p. 82-85 °C. ¹H NMR (300 MHz, CDCl₃): δ = 7.96 (bs, 1H, NH), 7.52 (d, *J* = 8.3 Hz, 2H, ArH), 7.26-6.95 (m, 6H, ArH), 3.54 (s, 3H, CO₂CH₃), 3.24 (s, 2H, CH₂), 2.26 (s, 3H, CH₃) ppm; ¹³C NMR (75 MHz, CDCl₃): δ = 172.6 (C=O), 143.7 (ArC), 137.2 (ArC), 135.4 (ArC), 131.1 (ArC), 129.7 (ArC), 128.6 (ArC), 128.5 (ArC), 127.0 (ArC), 126.5 (ArC), 125.9 (ArC), 52.5 (CH₃), 37.7 (CH₂), 21.5 (CH₃) ppm; IR (neat): ν 3226bm, 1708s, 1597m, 1587m, 1496m, 1435m, 1417m, 1336s, 1278s, 1238w, 1157s, 1089s, 1010s, 947m, 920m, 819m, 742m, 661s cm⁻¹; HRMS (NSI): Exact mass calc. for C₁₆H₁₇NO₄SNH₄ [M+NH₄]⁺: 320.0951, Found: 320.0955; MS (NSI): *m/z* 661 (28%), 358 (21), 343 (73), 337 (73), 320 (M+NH₄⁺, 100), 288 (46), 244 (6), 199 (7), 149 (5).

7.4.2.2 Benzylation of tosyl protect amine **257**



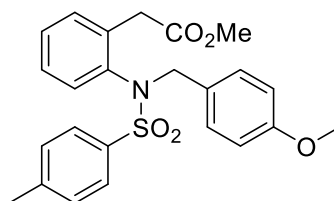
General procedure for the functionalisation of methyl 2-(2-((4-methylphenyl)sulfonamido)phenyl)acetate **260**. A solution of starting material **257** (2.57 g, 8.1 mmol) was dissolved in acetonitrile (25 mL). After the addition of triethylamine (2.2 mL, 16.1 mmol), the reaction

mixture was cooled down to 0 °C. Next, benzyl bromide was added (1.15 mL, 9.7 mmol) dropwise and the reaction mixture was stirred at room temperature for around 48 h until no starting material was detected anymore (monitored via TLC, ethyl acetate / *n*-hexane 1:4). Subsequently, the solvent was evaporated *in vacuo* and the residual oil was dissolved in dichloromethane (15 mL), and washed with water (20 mL) and brine (20 mL). After drying over MgSO₄, the mixture was concentrated *in vacuo* and purified *via* column chromatography.



Methyl 2-(2-((*N*-benzyl-4-methylphenyl)sulfonamido)phenyl)acetate **258**

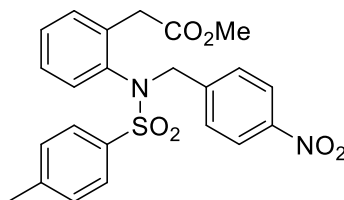
2.74 g (6.7 mmol, 83%) obtained as pale, pink solid, m.p. 78-81 °C. ¹H NMR (300 MHz, CDCl₃): δ = 7.45 (d, *J* = 8.3 Hz, 2H, *ArH*), 7.21-6.91 (m, 10H, *ArH*), 6.48 (dd, *J* = 8.0, 1.0 Hz, 1H, *ArH*), 4.92 (d, *J* = 13.6 Hz, 1H, NCH₂), 4.12 (d, *J* = 13.6, 1H, NCH₂), 3.50-3.38 (m, 5H, CH₃ and CH₂), 2.30 (s, 3H, CH₃) ppm; ¹³C NMR (75 MHz, CDCl₃): δ = 171.6 (C=O), 143.8 (*ArCH*), 137.7 (*ArC*), 136.2 (*ArC*), 135.5 (*ArC*), 135.2 (*ArC*), 131.4 (*ArC*), 129.6 (*ArC*), 129.4 (*ArC*), 128.5 (*ArC*), 128.4 (*ArC*), 128.2 (*ArC*), 128.0 (*ArC*), 127.9 (*ArC*), 127.5 (*ArC*), 56.1 (NCH₂), 51.8 (CH₃), 35.8 (CH₂), 21.6 (CH₃) ppm; IR (neat): ν 3062w, 3032w, 2949w, 1722s, 1597m, 1492m, 1348s, 1263s, 1161s, 1091m, 885m, 812s, 705s, 657s, 549s cm⁻¹; HMRS (NSI): Exact Mass calcd for C₂₃H₂₃NO₄S [M+H]⁺: 410.1421; Observed data: 410.1418.



Methyl 2-(2-((*N*-(4-methoxybenzyl)-4-methylphenyl)sulfonamido)phenyl)acetate **260a**

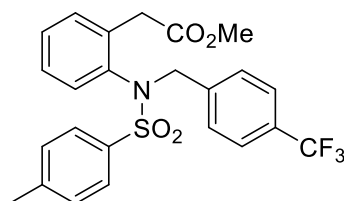
Performed according to the general procedure on a 0.63 mmol scale; **260a** (196 mg, 0.43 mmol, 71%) was obtained as a pale yellow solid, m.p. 108-110 °C. ¹H NMR (300 MHz, CDCl₃): δ = 7.64-7.54 (m, 2H, *ArH*), 7.35-7.23 (m, 4H, *ArH*), 7.10 (td, *J* = 7.5, 1.8 Hz, 1H, *ArH*), 7.06-7.00 (m, 2H, *ArH*), 6.76-6.68 (m, 2H, *ArH*), 6.59 (dd, *J* = 8.0, 1.2 Hz, 1H, *ArH*), 4.97 (d, *J* = 13.5 Hz, 1H, NCH₂), 4.23 (d, *J* = 13.5 Hz, 1H, NCH₂), 3.75 (s, 3H, ArOCH₃), 3.60 (s, 3H, CO₂CH₃), 3.55 (bs, 2H, CH₂), 2.47 (s, 3H, CH₃) ppm; ¹³C NMR (75 MHz, CDCl₃): δ = 171.6 (C=O), 159.2 (*ArCO*), 143.7 (*ArCH*), 137.6 (*ArC*), 136.3 (*ArC*), 135.9 (*ArC*), 131.4 (*ArC*), 130.7 (*ArC*), 129.5 (*ArC*), 128.4 (*ArC*), 128.3 (*ArC*), 128.0 (*ArC*), 127.4 (*ArC*), 127.2 (*ArC*), 113.7

(ArC), 55.5 (CH₃), 55.1 (CH₃), 51.7 (NCH₂), 35.7 (CH₂), 21.5 (CH₃) ppm; IR (neat): ν 2953w, 2835w, 1737s, 1614m, 1587m, 1514s, 1436m, 1340s, 1271m, 1244s, 1157s, 1028s, 873s, 694s, 653s, 574s cm⁻¹; HRMS (NSI): Exact mass calc. for C₂₄H₂₅NO₅SNH₄ [M+NH₄]⁺: 457.1792, Found: 457.1788; MS (NSI): m/z 491 (10%), 462 (23), 457 (M+NH₄⁺, 100), 440 (60), 433 (2).



Methyl 2-(2-((4-methyl-*N*-(4-nitrobenzyl)phenyl)sulfonamido)phenyl)acetate **260b**

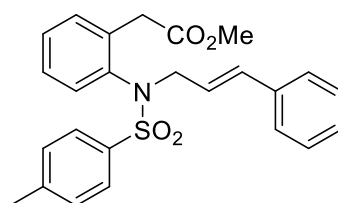
Performed according to the general procedure on 0.63 mmol scale; **260b** (120 mg, 0.26 mmol, 42%) was obtained as a yellow solid, m.p. 102-110 °C. ¹H NMR (300 MHz, CDCl₃): δ = 8.00 (d, *J* = 8.8 Hz, 2H, ArH), 7.48 (d, *J* = 8.3 Hz, 2H, ArH), 7.32-7.14 (m, 6H, ArH), 7.04 (td, *J* = 7.9, 1.9 Hz, 1H, ArH), 6.51 (dd, *J* = 8.0, 0.9 Hz, 1H, ArH), 5.00 (d, *J* = 14.0 Hz, 1H, NCH₂), 4.30 (d, *J* = 14.0 Hz, 1H, NCH₂), 3.58-3.38 (m, 5H, CH₂ and CH₃), 2.38 (s, 3H, CH₃) ppm; ¹³C NMR (75 MHz, CDCl₃): δ = 171.4 (C=O), 147.6 (ArC), 144.3 (ArC), 142.9 (ArC), 137.5 (ArC), 135.9 (ArC), 134.9 (ArC), 131.7 (ArC), 130.2 (ArC), 129.8 (ArC), 128.9 (ArC), 128.1 (ArC), 128.0 (ArC), 127.9 (ArC), 123.7 (ArC), 55.4 (CH₃), 51.9 (NCH₂), 35.9 (CH₂), 21.7 (CH₃) ppm; IR (neat): ν 3066w, 2949w, 2854w, 1737s, 1597m, 1519s, 1435m, 1338s, 1207m, 1155s, 1105m, 1085m, 1064m, 854m, 815m, 711s, 690s, 650s, 569s, 557s cm⁻¹; HRMS (NSI): Exact mass calc. for C₂₃H₂₂N₂O₆SNH₄ [M+NH₄]⁺: 472.1537, Found: 472.1531; MS (NSI): m/z 491 (22%), 477 (26), 472 (M+NH₄⁺, 100), 455 (60), 445 (10), 423 (10).



Methyl 2-(2-((4-methyl-*N*-(4-trifluoromethyl)benzyl)phenyl)sulfonamido)phenyl)acetate **260c**

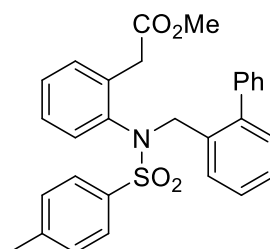
Performed according to the general procedure on 0.63 mmol scale; **260c** (170 mg, 0.36 mmol, 57%) was obtained as pale pink solid, m.p. 101-105 °C. ¹H NMR (300 MHz, CDCl₃): δ = 7.45 (d, *J* = 8.2 Hz, 2H, ArH), 7.36 (d, *J* = 8.1 Hz, 2H, ArH), 7.29-7.10 (m, 6H, ArH), 7.01 (td, *J* = 8.3, 1.4 Hz, 1H, ArH), 6.51 (d, *J* = 7.9 Hz, 1H, ArH), 4.96 (d, *J* = 13.9 Hz, 1H, NCH₂), 4.22 (d, *J* = 13.9 Hz, 1H, NCH₂), 3.54 (d, *J* = 16.8 Hz, 1H, CH₂), 3.44 (s, 3H, CH₃), 3.41 (d, *J* = 17.1 Hz, 1H, CH₂), 2.34 (s, 3H, CH₃) ppm; ¹³C NMR (75 MHz, CDCl₃): δ = 171.4 (C=O), 144.0 (ArC),

139.5 (ArC), 137.6 (ArC), 136.0 (ArC), 135.2 (ArC), 131.5 (ArC), 130.0 (q, $J = 32.2$ Hz, ArC-CF₃), 129.7 (ArC), 129.6 (ArC), 128.7 (ArC), 128.1 (ArC), 128.0 (ArC), 127.7 (ArC), 125.3 (q, $J = 3.7$ Hz, ArC), 124.0 (q, $J = 272.1$ Hz, CF₃), 55.6 (CH₃), 51.6 (NCH₂), 35.8 (CH₂), 21.5 (CH₃) ppm; IR (neat): ν 2954w, 2922w, 1726s, 1620w, 1595w, 1492m, 1438m, 1423m, 1348m, 1323s, 1271m, 1159s, 1109s, 1089s, 1066s, 1020s, 848m, 812m, 707m, 698m, 657m, 634m, 547s, 451w cm⁻¹; HRMS (NSI): Exact mass calc. for C₂₄H₂₂F₃NO₄S [M+NH₄]⁺: 495.1560, Found: 495.1547; MS (NSI): 972 (18%), 495 (M+NH₄⁺, 100), 477 (M⁺, 54), 446 (12), 199 (2).



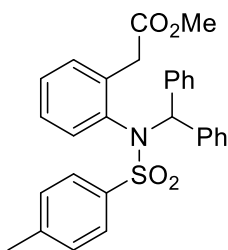
Methyl 2-(2-((*N*-cinnamyl-4-methylphenyl)sulfonamido)phenyl)acetate **260f**

Performed according to the general procedure on 0.63 mmol scale; **260f** (48 mg, 0.11 mmol, 18%) was obtained as pink solid, m.p. 106-110 °C. ¹H NMR (300 MHz, CDCl₃): δ = 7.49 (d, $J = 8.2$ Hz, 2H, ArH), 7.33 (d, $J = 7.0$ Hz, 1H, ArH), 7.23-7.10 (m, 8H, ArH), 7.04 (td, $J = 7.6$, 1.1 Hz, 1H, ArH), 6.54 (d, $J = 7.8$ Hz, 1H, ArH), 6.23 (d, $J = 15.8$ Hz, 1H, HC=CHAr), 6.02 (dt, $J = 15.7$, 6.9 Hz, HC=CHAr), 4.41 (dd, $J = 14.2$, 6.2 Hz, 1H, NCH₂), 4.04 (d, $J = 16.4$ Hz, 1H, CH₂), 3.97 (dd, $J = 14.3$, 6.7 Hz, 1H, NCH₂), 3.59 (d, $J = 16.4$ Hz, 1H, CH₂), 3.46 (s, 3H, CH₃), 2.36 (s, 3H, CH₃) ppm; ¹³C NMR (75 MHz, CDCl₃): δ = 171.9 (C=O), 143.7 (9), 138.2, 136.3, 136.2, 135.6, 134.4, 131.5, 129.5, 128.6, 128.5, 128.4, 128.1, 127.8, 127.6, 126.5, 123.4, 54.6 (1), 51.8 (10), 36.5 (3), 21.5 (21) ppm; IR (neat): ν 3034w, 2947m, 2856w, 1730s, 1595m, 1490m, 1433m, 1313m, 1257s, 1184m, 1153s, 881m, 657s, 580s cm⁻¹; HRMS (NSI): Exact mass calc. for C₂₅H₂₅NO₄SNH₄ [M+NH₄]⁺: 453.1843, Found: 453.1837; MS (NSI): m/z 888 (43%), 453 (M+NH₄⁺, 100), 437 (M⁺, 84), 288 (9).



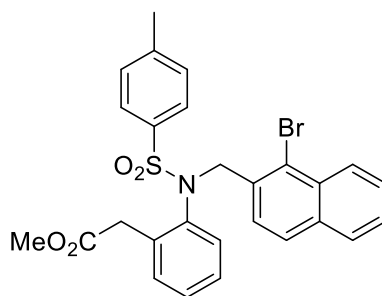
Methyl 2-(2-((*N*-([1,1'-biphenyl]-2-ylmethyl)-4-methylphenyl)sulfonamido)phenyl)acetate **260d**

Performed according to the general procedure on 0.63 mmol scale; **260d** (207 mg, 0.43 mmol, 68%) was obtained as pale yellow solid, m.p. 94-96 °C. ¹H NMR (300 MHz, CDCl₃): δ = 7.74 (dd, *J* = 7.8, 1.0 Hz, 1H, *ArH*), 7.38, (t, *J* = 8.3 Hz, 2H, *ArH*), 7.28 (td, *J* = 7.5, 1.3 Hz, 1H, *ArH*), 7.24-7.00 (m, 9H, *ArH*), 6.95 (dd, *J* = 7.6, 1.2 Hz, 1H, *ArH*), 6.80 (td, *J* = 7.9, 1.7 Hz, 1H, *ArH*), 6.63-6.57 (m, 2H, *ArH*), 6.04 (dd, *J* = 8.1, 0.9 Hz, 1H, *ArH*), 4.92 (d, *J* = 13.9 Hz, 1H, NCH₂), 4.17 (d, *J* = 13.9 Hz, 1H, NCH₂), 3.44 (s, 5H, CH₂ and CH₃), 2.34 (s, 3H, CH₃) ppm; ¹³C NMR (75 MHz, CDCl₃): δ = 171.6 (C=O), 143.6 (ArC), 142.3 (ArC), 140.3 (ArC), 137.7 (ArC), 136.1 (ArC), 135.5 (ArC), 132.9 (ArC), 131.3 (ArC), 130.8 (ArC), 129.9 (ArC), 129.5 (ArC), 129.2 (ArC), 128.2 (ArC), 128.1 (ArC), 128.0 (ArC), 127.8 (ArC), 127.7 (ArC), 127.5 (ArC), 127.4 (ArC), 126.6 (ArC), 52.2 (CH₃), 47.0 (NCH₂), 35.6 (CH₂), 21.6 (CH₃) ppm; IR (neat): ν 3062w, 3028w, 2956w, 2929w, 1743s, 1342s, 1203m, 1190m, 1153s, 1087m, 1057m, 867m, 817m, 759m, 692s, 653s, 547s cm⁻¹; HRMS (NSI): Exact mass calc. for C₂₉H₂₇NO₄SNH₄ [M+NH₄]⁺: 503.1999, Found: 503.1985; MS (NSI): *m/z* 988 (34%), 503 (M+NH₄⁺, 100), 488 (35), 320 (13), 288 (25), 167 (15).



Methyl 2-((*N*-benzhydryl-4-methylphenyl)sulfonamido)phenyl)acetate **260g**

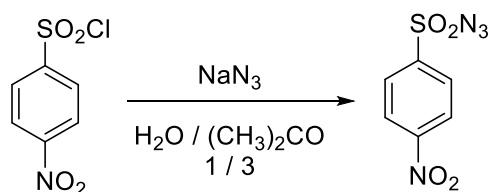
Performed according to the general procedure on a 0.63 mmol scale; **260g** (111 mg, 0.23 mmol, 36%) was obtained as colourless oil. ¹H NMR (300 MHz, CDCl₃): δ = 7.47 (d, *J* = 8.3 Hz, 2H, *ArH*), 7.44-7.23 (m, 14H, *ArH*), 7.06 (td, *J* = 8.0, 1.7 Hz, 1H, *ArH*), 6.58 (dd, *J* = 8.0, 1.0 Hz, 1H, *ArH*), 6.52 (s, 1H, NCH), 3.66 (s, 3H, CO₂CH₃), 3.60 (d, *J* = 1.5 Hz, CH₂), 2.52 (s, 3H, CH₃) ppm; ¹³C NMR (75 MHz, CDCl₃): δ = 171.7 (C=O), 143.5 (ArC), 139.1 (ArC), 138.9 (ArC), 137.3 (ArC), 137.1 (ArC), 136.9 (ArC), 132.2 (ArC), 131.6 (ArC), 129.8 (ArC), 129.6 (ArC), 129.2 (ArC), 128.6 (ArC), 128.3 (ArC), 128.2 (ArC), 128.1 (ArC), 127.7 (ArC), 127.5 (ArC), 126.8 (ArC), 70.1 (NCH), 51.8 (CH₃), 36.4 (CH₂), 21.5 (CH₃) ppm; IR (neat): ν 3061w, 3030w, 2949w, 1735s, 1597m, 1492m, 1448m, 1435m, 1338s, 1155s, 1089m, 1008m, 813w, 704s, 665m, 563s cm⁻¹; HRMS (NSI): Exact mass calc. for C₂₉H₂₇NO₄SNH₄ [M+NH₄]⁺: 503.1999, Found: 503.1990; MS (NSI): *m/z* 988 (13%), 503 (M+NH₄⁺, 95), 433 (3), 351 (6), 199 (5), 167 (100).



Methyl 2-(2-((N-((1-bromonaphthalen-2-yl)methyl)-4-methylphenyl)sulfonamido)phenyl)acetate **260e**

Performed according to the general procedure on a 0.63 mmol scale; **260e** (115 mg, 0.21 mmol, 34%) was obtained as pale yellow solid, m.p. 141-144 °C. ^1H NMR (300 MHz, CDCl_3): δ = 8.10 (d, J = 8.3 Hz, 1H, ArH), 7.69-7.34 (m, 7H, ArH), 7.23 (d, J = 8.0 Hz, 2H, ArH), 7.14 (td, J = 6.4, 1.1 Hz, 2H, ArH), 7.05-6.96 (m, 1H, ArH), 6.65 (dd, J = 8.1, 0.9 Hz, 1H, ArH), 5.30 (d, J = 13.9 Hz, 1H, NCH_2), 4.71 (d, J = 13.9 Hz, 1H, NCH_2), 3.50 (q, J = 13.3 Hz, 2H, CH_2), 3.11 (s, 3H, CH_3), 2.38 (s, 3H, CH_3) ppm; ^{13}C NMR (75 MHz, CDCl_3): δ = 171.4 (C=O), 143.9 (ArC), 137.5 (ArC), 136.2 (ArC), 135.1 (ArC), 134.1 (ArC), 132.7 (ArC), 132.2 (ArC), 131.3 (ArC), 129.6 (ArC), 128.5 (ArC), 128.4 (ArC), 128.3 (ArC), 128.2 (ArC), 128.0 (ArC), 127.8 (ArC), 127.7 (ArC), 127.4 (ArC), 127.4 (ArC), 126.8 (ArC), 124.8 (ArC), 56.3 (NCH_2), 51.5 (CH_3), 35.8 (CH_2), 21.6 (CH_3) ppm; IR (neat): ν 3003w, 1742s, 1340s, 1307m, 1211m, 1157s, 1072m, 993m, 854m, 816s, 716s, 660s cm^{-1} ; HRMS (APCI): Exact mass calc. for $\text{C}_{27}\text{H}_{24}\text{BrNO}_4\text{S}$ $[\text{M}+\text{Na}]^+$: 560.0507, Found: 560.0521; MS (APCI): m/z 563 (29%), 562 (98), 561 (31), 560 ($\text{M}+\text{Na}^+$, 100), 105 (12).

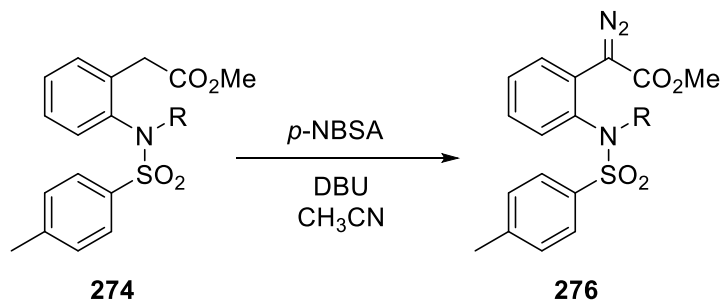
7.4.2.3 Diazo Transfer



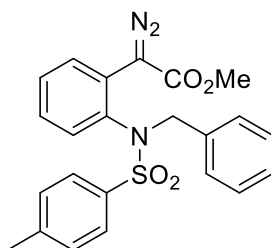
p-Nitrobenzylsulfonyl azide **275**

Prepared according to standard procedure.²⁹ A solution of *p*-nitrobenzenesulfonyl chloride (90%, 600 mg, 2.4 mmol) in acetone (6 mL) was cooled down to 0 °C. Then, a solution of sodium azide (264 mg, 4.1 mmol) in water (2 mL) was slowly added to the reaction mixture. The reaction mixture was left stirring for 16 h at room temperature. Afterwards, the mixture was concentrated *in vacuo* at 25 °C and the residual oil was dissolved in diethyl ether (10 mL) and washed with water (10 mL) and sodium carbonate (5% w/w, 10 mL). The organic layer was dried over MgSO_4 and concentrated *in vacuo* to furnish *p*-nitrobenzylsulfonyl azide **275**

(508 mg, 2.23 mmol, 93%) as yellow solid, m.p. 100-102 °C. ^1H NMR (300 MHz, CDCl_3): δ = 8.47 (d, J = 9.2 Hz, 2H, ArH), 8.17 (d, J = 9.2 Hz, 2H, ArH) ppm; ^{13}C NMR (75 MHz, CDCl_3): δ = 151.2 (ArC), 143.7 (ArC), 128.9 (ArCH), 125.0 (ArCH) ppm; IR (neat): ν 3107m, 2318w, 2140s, 1604m, 1527s, 1404m, 1348s, 1155s, 1109m, 1083s, 1012m, 854s, 761s, 742s, 731s, 680s, 603s, 459s cm^{-1} . Spectroscopic data was in accordance with the literature.³⁰



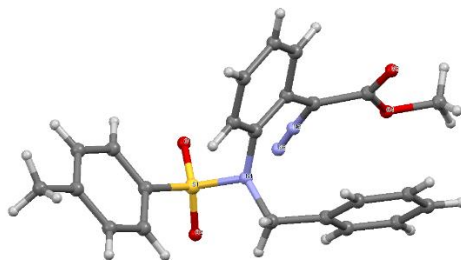
General procedure for the diazo transfer. A solution containing the specific ester (1 mmol) and *p*-NBSA (456 mg, 2 mmol) in acetonitrile (4 mL) was cooled down to 0 °C. DBU (374 μL , 2.5 mmol) was added dropwise. The reaction stirred for 48 h at room temperature or 45 °C. Then, the reaction mixture was cooled down to 0 °C and a pH 7 phosphate buffer (10 mL) was added to quench the reaction. The reaction mixture was extracted with dichloromethane (2 x 20 mL) and the combined organic fractions were washed with pH 7 phosphate buffer (10 mL), and brine (15 mL) and then dried over MgSO_4 . The solvent was evaporated *in vacuo* at 30 °C and the crude reaction mixture was purified *via* flash column chromatography.



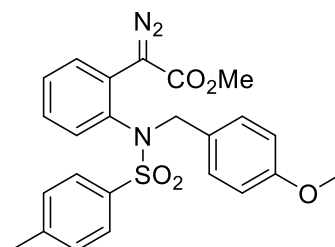
Methyl 2-(2-((*N*-benzyl-4-methylphenyl)sulfonamido)phenyl)-2-diazoacetate **259**

Performed according to the general procedure at 45 °C on a 1 mmol scale; **259** (280 mg, 0.64 mmol, 64%) was obtained as yellow solid, m. p. 110-112 °C (decomp.). ^1H NMR (400 MHz, CDCl_3): δ = 7.64 (d, J = 8.2 Hz, 2H, ArH), 7.46 (dd, J = 7.8, 1.0 Hz, 1H, ArH), 7.33 (d, J = 8.2 Hz, 2H, ArH), 7.26 (d, J = 7.6 Hz, 1H, ArH), 7.13-7.22 (m, 3H, ArH), 7.05-7.11 (m, 3H, ArH), 6.54 (dd, J = 8.1, 1.0 Hz, 1H, ArH), 5.08 (bs, 1H, NCH_2), 4.07 (bs, 1H, NCH_2), 3.61 (s, 3H, CO_2CH_3), 2.46 (s, 3H, CH_3) ppm; ^{13}C NMR (75 MHz, CDCl_3): δ = 166.0 (C=O), 144.0 (ArC), 136.9 (ArC), 135.8 (ArC), 134.4 (ArC), 131.2 (ArC), 130.4 (ArC), 129.7 (ArC), 129.5 (ArC), 128.7 (ArC), 128.4 (ArC), 128.3 (ArC), 128.1 (ArC), 127.9 (ArC), 127.6 (ArC), 60.5 (C=N₂), 56.9 (NCH_2), 51.7 (CH_3), 21.6 (CH_3) ppm; IR (neat): ν 3064w, 3032w, 2954w, 2924w,

2096s, 1693s, 1494m, 1429m, 1344s, 1242m, 1159s, 1151s, 1045m, 1029s, 858m, 812m, 717s cm^{-1} ; HRMS (NSI): Exact Mass calcd for $\text{C}_{23}\text{H}_{21}\text{N}_3\text{O}_4\text{SNa}$ $[\text{M}+\text{Na}]^+$: 458.1145; Observed data: 458.1142.

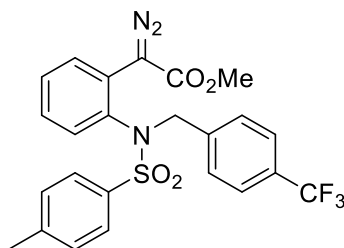


Crystal structure of diazo compound **259**: CCDC 1441276



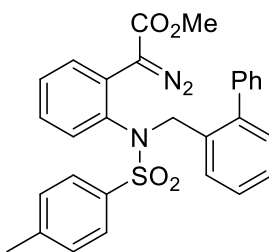
Methyl 2-diazo-2-(2-((*N*-(4-methoxybenzyl)-4-methylphenyl)sulfonamido)phenyl)acetate
276a

Performed according to the general procedure at 22 °C on a 0.31 mmol scale; **276a** (72 mg, 0.16 mmol, 52%) obtained as yellow solid, m.p. 132-135 °C. ^1H NMR (300 MHz, CDCl_3): δ = 7.69-7.63 (m, 2H, ArH), 7.49 (dd, J = 8.0, 1.5 Hz, 1H, ArH), 7.34 (d, J = 8.2 Hz, 2H, ArH), 7.29 (td, J = 7.5, 1.4 Hz, 1H, ArH), 7.09 (td, J = 7.9, 1.6 Hz, 1H, ArH), 6.99 (d, J = 8.7 Hz, 2H, ArH), 6.69 (d, J = 8.7 Hz, 2H, ArH), 6.55 (dd, J = 8.0, 1.2 Hz, 1H, ArH), 5.06 (d, J = 13.2 Hz, 1H, NCH_2), 4.03 (d, J = 13.2 Hz, 1H, NCH_2), 3.74 (s, 3H, OCH_3), 3.65 (s, 3H, OCH_3), 2.48 (s, 3H, CH_3) ppm; ^{13}C NMR (75 MHz, CDCl_3): δ = 166.1 (C=O), 159.4 (ArCO), 144.0 (ArC), 136.9 (ArC), 136.0 (ArC), 131.2 (ArC), 130.7 (ArC), 129.7 (ArC), 128.7 (ArC), 128.5 (ArC), 128.3 (ArC), 128.1 (ArC), 127.6 (ArC), 126.5 (ArC), 113.8 (ArC), 56.4 (OCH_3 or NCH_2), 55.1 (OCH_3 or NCH_2), 51.6 (C=N₂), 30.9 (CH_3), 21.7 (CH_3) ppm; IR (neat): ν 2953w, 2096s, 1703s, 1612w, 1589w, 1512m, 1492m, 1435m, 1340s, 1263s, 1240s, 1149s, 1028s, 877m, 813m, 758s, 727s, 658s, 607s cm^{-1} ; HRMS (NSI): Exact mass calc. for $\text{C}_{24}\text{H}_{23}\text{N}_3\text{O}_4\text{SNa}$ $[\text{M}+\text{Na}]^+$: 488.1251, Found: 488.1245; MS (NSI): m/z 494 (31%), 491 (87), 488 ($\text{M}+\text{NH}_4^+$, 20), 474 (6), 460 (5), 455 (100), 438 (92), 419 (12).



Methyl 2-diazo-2-(2-((4-methyl-*N*-(4-(trifluoromethyl)benzyl)phenyl)sulfonamido)phenyl)acetate **276c**

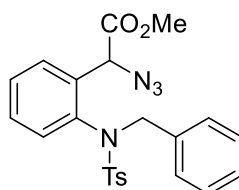
Performed according to the general procedure at 22 °C on a 0.35 mmol scale; **276c** (67 mg, 0.13 mmol, 37%) was obtained as yellow solid, m.p. 116-118 °C. ¹H NMR (400 MHz, CDCl₃): δ = 7.67 (d, *J* = 8.3 Hz, 2H, *ArH*), 7.51-7.42 (m, 3H, *ArH*), 7.36 (d, *J* = 8.0 Hz, 2H, *ArH*), 7.31 (td, *J* = 7.6, 1.4 Hz, 1H, *ArH*), 7.26 (d, *J* = 7.9 Hz, 2H, *ArH*), 6.58 (dd, *J* = 8.0, 1.2 Hz, 1H, *ArH*), 5.15 (bs, 1H, *NCH*₂), 4.10 (bs, 1H, *NCH*₂), 3.60 (s, 3H, CO₂CH₃), 2.49 (s, 3H, CH₃) ppm; ¹³C NMR (125 MHz, CDCl₃): δ = 165.8 (C=O), 144.4 (*ArC*), 138.6 (*ArC*), 137.1 (*ArC*), 135.6 (*ArC*), 131.7 (*ArC*), 130.3 (q, *J* = 30 Hz, *ArC*-CF₃), 129.8 (*ArC*), 129.7 (*ArC*), 129.1 (*ArC*), 128.4 (*ArC*), 128.3 (*ArC*), 128.1 (*ArC*), 127.9 (*ArC*), 125.3 (q, *J* = 3.7 Hz, *ArC*), 124.0 (q, *J* = 273.5 Hz, CF₃), 109.9 (*ArC*), 60.2 (C=N₂), 56.5 (*NCH*₂), 51.8 (CH₃), 21.8 (CH₃) ppm; IR (neat): ν 2954w, 2926w, 2096s, 1741w, 1695s, 1618w, 1597w, 1492m, 1448w, 1435m, 1421w, 1323s, 1240s, 1161s, 1111s, 1066s, 1020s, 817m, 713s, 661s, 547s cm⁻¹; HRMS (ES): Exact mass calc. for C₂₄H₂₀F₃N₃O₄SNa [M+Na]⁺: 526.1024, Found: 526.0999; MS (ES): *m/z* 541 (52%), 526 (M+Na⁺, 100), 498 (21), 353 (14), 105 (10).



Methyl 2-(2-((*N*-([1,1'-biphenyl]-2-ylmethyl)-4-methylphenyl)sulfonamido)phenyl)-2-diazoacetate **276d**

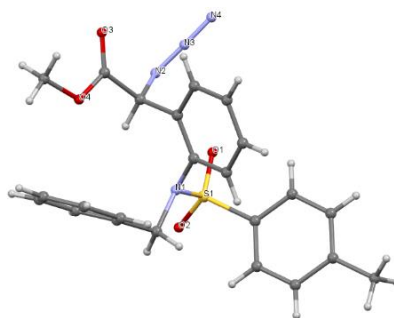
Performed according to the general procedure at 45 °C on a 0.3 mmol scale; **276d** (115 mg, 0.23 mmol, 75%) was obtained as yellow solid, m.p. 144-146 (decomp.). ¹H NMR (300 MHz, CDCl₃): δ = 7.90 (dd, *J* = 7.8, 1.2 Hz, 1H, *ArH*), 7.58 (d, *J* = 8.3 Hz, 2H, *ArH*), 7.42 (dd, *J* = 8.0, 1.5 Hz, 1H, *ArH*), 7.37 (td, *J* = 7.6, 1.5 Hz, 1H, *ArH*), 7.32-7.21 (m, 5H, *ArH*), 7.13-6.96 (m, 4H, *ArH*), 6.81 (td, *J* = 8.0, 1.6 Hz, 1H, *ArH*), 6.61-6.55 (m, 2H, *ArH*), 6.03 (dd, *J* = 8.1, 1.1 Hz, 1H, *ArH*), 5.04 (bs, 1H, *NCH*₂), 4.17 (bs, 1H, *NCH*₂), 3.59 (s, 3H, CH₃), 2.44 (s, 3H, CH₃) ppm; ¹³C NMR (75 MHz, CDCl₃): δ = 165.9 (C=O), 143.9 (*ArC*), 142.2 (*ArC*), 140.1 (*ArC*), 137.5

(ArC), 136.1 (ArC), 132.5 (ArC), 131.8 (ArC), 130.5 (ArC), 129.9 (ArC), 129.7 (ArC), 129.0 (ArC), 128.4 (ArC), 128.3 (ArC), 128.1 (ArC), 128.0 (ArC), 127.9 (ArC), 127.8 (ArC), 127.6 (ArC), 127.3 (ArC), 126.3 (ArC), 60.2 (C=N₂), 53.1 (C), 51.7 (C), 21.6 (CH₃) ppm; IR (neat): ν 3062w, 2953w, 2102s, 1693s, 1431m, 1342s, 1255m, 1238m, 1155s, 1045m, 854m, 712s, 659s, 569s, 542s cm⁻¹; HRMS (APCI): Exact mass calc. for C₂₉H₂₅N₃O₄SNa [M+Na]⁺: 534.1463, Found: 534.1453; MS (APCI): m/z 534 ([M+Na]⁺, 25%), 295 (18), 156 (15), 123 (48), 115 (100), 83 (71).



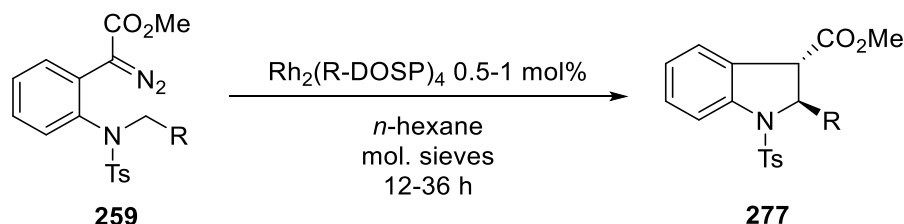
Methyl 2-azido-2-(2-((*N*-benzyl-4-methylphenyl)sulfonamido)phenyl)acetate **263**

As a pale yellow solid, m.p. 115-119 °C. ¹H NMR (300 MHz, CDCl₃): δ = 7.51 (dd, *J* = 8.3, 2.9 Hz, 4H, ArH), 7.17 (m, 23H, ArH), 6.57 (t, *J* = 7.1, 2H, ArH), 5.48 (s, 1H, CHN₃), 5.26 (s, 1H, CHN₃), 5.02 (d, *J* = 13.4 Hz, 1H, NCH₂), 4.90 (d, *J* = 13.9 Hz, 1H, NCH₂), 4.33 (d, *J* = 13.9 Hz, 1H, NCH₂), 4.11 (d, *J* = 13.4 Hz, 1H, NCH₂), 3.69 (s, 3H, CO₂CH₃), 3.38 (s, 3H, CO₂CH₃), 2.38 (s, 3H, CH₃), 2.37 (s, 3H, CH₃) ppm; ¹³C NMR (75 MHz, CDCl₃): δ = 169.5 (C=O), 169.4 (C=O), 144.1 (ArC), 144.0 (ArC), 137.9 (ArC), 137.7 (ArC), 135.9 (ArC), 135.6 (ArC), 135.2 (ArC), 135.1 (ArC), 135.0 (ArC), 134.7 (ArC), 129.7 (ArC), 129.6 (ArC), 129.5 (ArC), 129.4 (ArC), 129.2 (ArC), 129.1 (ArC), 129.0 (ArC), 128.8 (ArC), 128.6 (ArC), 128.4 (ArC), 128.3 (ArC), 128.2 (ArC), 128.0 (ArC), 127.9 (ArC), 60.1 (CHN₃), 59.9 (CHN₃), 56.3 (NCH₂), 56.3 (NCH₂), 52.8 (OCH₃), 52.7 (OCH₃), 21.6 (2 x CH₃) ppm; IR (neat): ν 3062w, 3030w, 2954m, 2926m, 2875w, 2850w, 2100s, 1735s, 1595m, 1490m, 1456m, 1448m, 1436m, 1354s, 1257w, 1211s, 1161s, 1089s, 1029s, 867m, 758m, 661s, 522m, 476w cm⁻¹; HRMS: Exact Mass calcd for C₂₃H₂₂N₄O₄SNH₄ [M+NH₄]⁺: 468.1700; Observed Data: 468.1695.

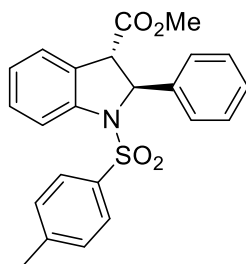


Crystal structure of azide **263**: CCDC 1441277

7.4.2.4 C-H insertion reaction

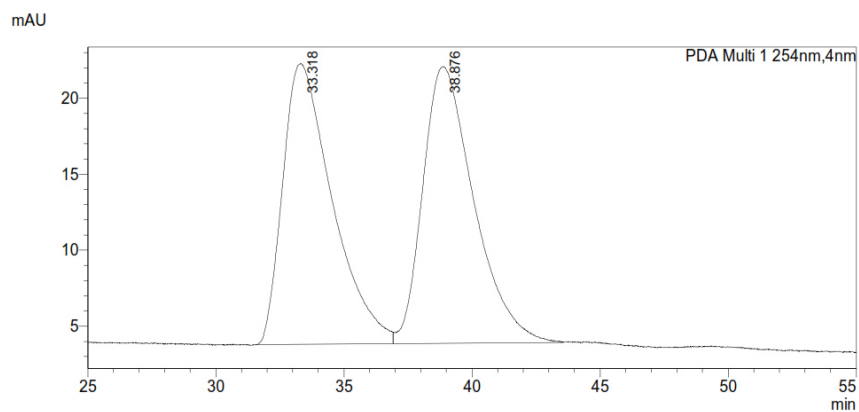


General procedure for C-H insertion reaction. An oven-dried 25 mL round bottom flask was equipped with a magnetic stirring bar and flushed with argon. Molecular sieves (3 Å, 1.2 g), and $\text{Rh}_2(\text{R-DOSP})_4$ (4.4 mg, 0.002 mmol, 1 mol%) were dissolved in *n*-hexane (dry, 10 mL). Subsequently, diazo compound **259** (100 mg, 0.23 mmol) was added and the reaction mixture was stirred at 22 °C under an argon atmosphere until all diazo compound was consumed (TLC analysis; 12-36 h). Then, the reaction mixture was passed through a short silica-plug which was washed with CH_2Cl_2 (3 x 5 mL). The reaction mixture was concentrated *in vacuo* and purified *via* column chromatography to afford the corresponding indoline.

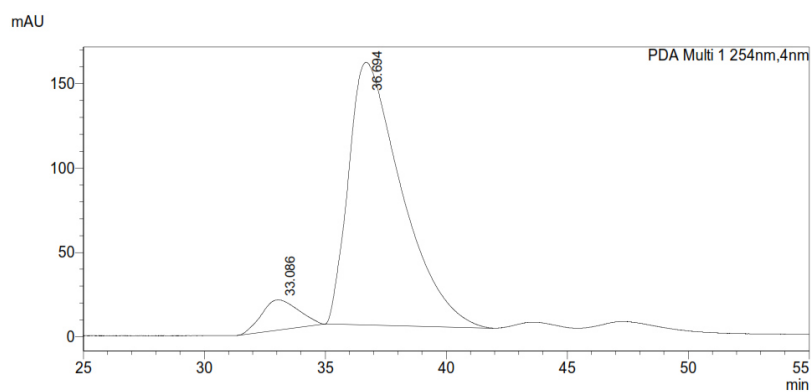


Methyl (2S,3S)-2-phenyl-1-tosylindoline-3-carboxylate **277**:

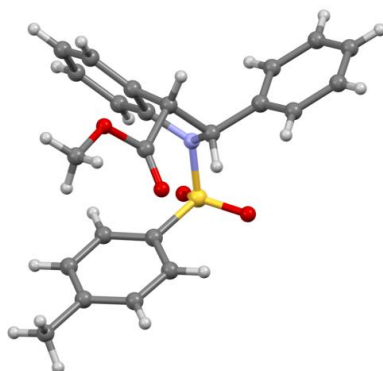
Performed according to the general procedure on a 0.23 mmol scale (100 mg); **277** (76 mg, 0.19 mmol, 81%, 11:1 *d.r.*; 92.5:7.5 *e.r.*) as colourless solid, m.p. 130-134 °C. ^1H NMR (300 MHz, CDCl_3): δ = 7.78 (d, J = 8.2 Hz, 1H, ArH), 7.66 (d, J = 8.3 Hz, 2H, ArH), 7.42-7.25 (m, 7H, ArH), 7.21 (d, J = 8.0 Hz, 2H, ArH), 7.08 (td, J = 7.5, 0.9 Hz, 1H, ArH), 5.79 (d, J = 3.7 Hz, 1H, NCH), 3.93 (d, J = 3.7 Hz, 1H, CHCO_2Me), 3.56 (s, 3H, CO_2CH_3), 2.38 (s, 3H, CH_3) ppm; ^{13}C NMR (75 MHz, CDCl_3): δ = 170.6 (C=O), 144.0 (ArC), 142.2 (ArC), 141.8 (ArC), 134.7 (ArC), 129.5 (ArC), 129.4 (ArC), 128.8 (ArC), 127.9 (ArC), 127.6 (ArC), 127.4 (ArC), 126.3 (ArC), 125.8 (ArC), 124.4 (ArC), 115.7 (ArC), 66.9 (NCH), 55.7 (C), 52.7 (C), 21.6 (CH_3) ppm; IR (neat): ν 3032w, 2954w, 1732s, 1597m, 1477m, 1354s, 1238m, 1166s, 1155s, 1103m, 1089m, 1014m, 952m, 810m, 678s, 570s, 543s cm^{-1} ; HMRS: Exact Mass calcd for $\text{C}_{23}\text{H}_{21}\text{NO}_4\text{SNH}_4$ $[\text{M}+\text{NH}_4]^+$: 425.1530; Observed Data: 425.1525; ee: 85%, determined by HPLC analysis: Chiracel® OD-H (0.46 cm x 25 cm), *n*-hexane / *i*-PrOH 99:1, 1.0 mL/min, 10 °C, 254 nm, T_{res} (minor, (*R,R*)-isomer) = 33.1 min, T_{res} (major, (*S,S*)-isomer) = 36.7 min; $[\alpha]_D^{20}$: -40° (c 0.1, CHCl_3).



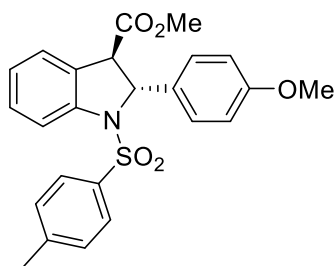
Peak#	Ret. Time	Area%
1	33.318	49.594
2	38.876	50.406
Total		100.000



Peak#	Ret. Time	Area%
1	33.086	7.423
2	36.694	92.577
Total		100.000

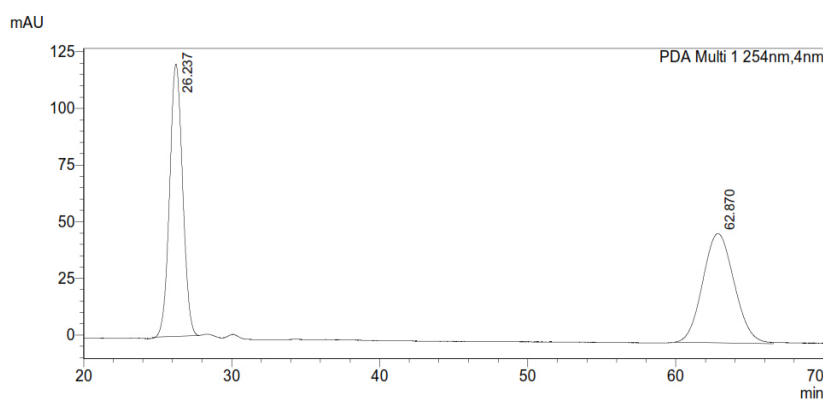


Crystal structure of (2*R*,3*R*)-isomer of **277**: CCDC 1441275

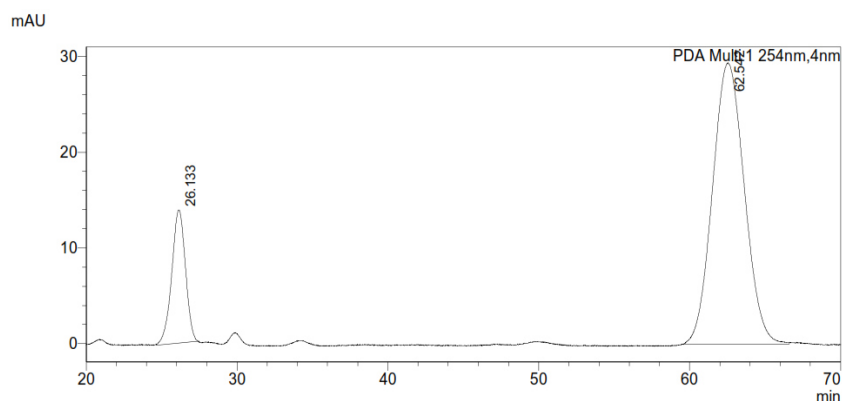


Methyl (2*R*,3*R*)-2-(4-methoxyphenyl)-1-tosylindoline-3-carboxylate **278**

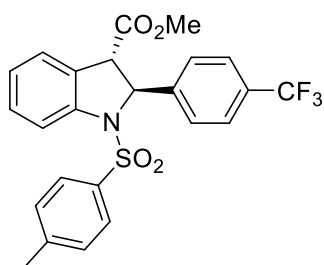
Performed according to the general procedure on 0.086 mmol scale (40 mg); **278** (30 mg, 0.069 mmol, 80%, 35:1 *d.r.*, 83:17 *e.r.*) was obtained as pale yellow solid, m.p. 60-64 °C. ¹H NMR (300 MHz, CDCl₃): δ = 7.65 (d, *J* = 8.2 Hz, 1H, Ar*H*), 7.56 (d, *J* = 8.3 Hz, 2H, Ar*H*), 7.28-7.16 (m, 4H, Ar*H*), 7.10 (d, *J* = 8.1 Hz, 2H, Ar*H*), 6.98 (td, *J* = 7.5, 1.0 Hz, 1H, Ar*H*), 6.76 (td, *J* = 8.9, 2.2 Hz, 2H, Ar*H*), 5.63 (d, *J* = 3.7 Hz, 1H, NCH), 3.82 (d, *J* = 3.7 Hz, 1H, CHCO₂Me), 3.71 (s, 3H, OCH₃), 3.47 (s, 3H, OCH₃), 2.28 (s, 3H, CH₃); ¹³C NMR (75 MHz, CDCl₃): δ = 170.1 (C=O), 159.3 (ArC-OMe), 143.9 (ArC), 141.8 (ArC), 134.8 (ArC), 134.4 (ArC), 129.4 (ArC), 127.6 (ArC), 127.4 (ArC), 127.1 (ArC), 126 (ArC), 124.3 (ArC), 115.6 (ArC), 114.2 (ArC), 66.6 (NCH), 55.9 (C), 55.7 (C), 55.3 (C), 21.6 (CH₃) ppm; IR (neat): 2937w, 1740s, 1512m, 1477m, 1460m, 1362m, 1217m, 1163s, 1105m, 1090m, 1026m, 812m, 706m, 658m cm⁻¹; HRMS (APCI): Exact mass calc. for C₂₄H₂₃NO₅S [M+H]⁺: 438.1375, Found: 438.1375; MS (APCI): *m/z* 438 (M+H⁺, 75%), 413 (41), 406 (60), 381 (58), 353 (54), 330 (75), 305 (25), 283 (52), 282 (47), 251 (83), 115 (44), 105 (100); ee: 66%, determined by HPLC analysis: YMC Chiral Amylose-C S-5 μm (25 cm), *n*-hexane / *i*-PrOH: 85:15, 1.0 mL/min, 10 °C, 254 nm, T_{res} (minor, (*S,S*)-isomer) = 26.1 min, T_{res} (major, (*R,R*)-isomer) = 62.5 min; [α]_D²⁰: +30° (c 0.1, CHCl₃).



Peak#	Ret. Time	Area%
1	26.237	50.805
2	62.870	49.195
Total		100.000

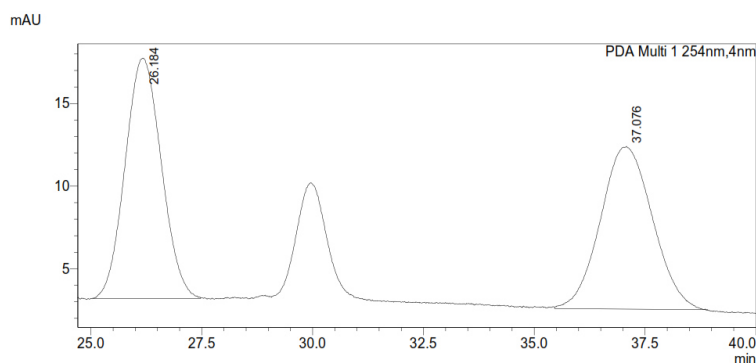


Peak#	Ret. Time	Area%
1	26.133	16.924
2	62.542	83.076
Total		100.000

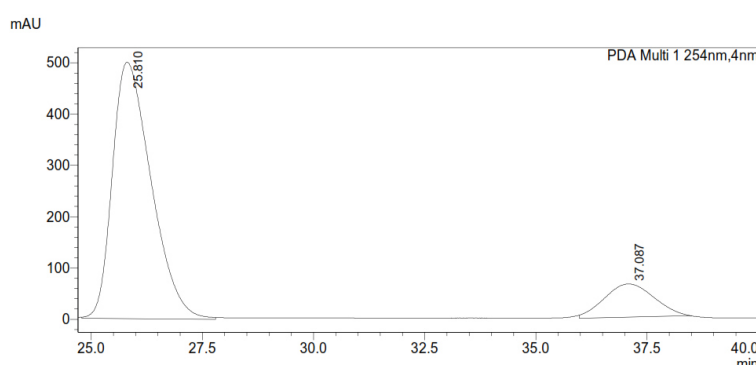


Methyl (2S,3S)-1-tosyl-2-(4-(trifluoromethyl)phenyl)indoline-3-carboxylate **279**:

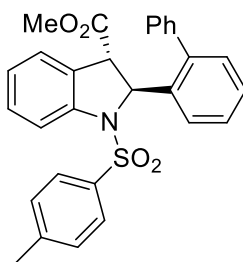
Performed according to the general procedure on a 0.12 mmol scale (58 mg); **279** (45 mg, 0.09 mmol, 82%, 4.5:1 *d.r.*, 86:14 *e.r.*) was obtained as colourless solid, m.p. 66-70 °C. ¹H NMR (300 MHz, CDCl₃): δ = 7.78 (d, *J* = 8.2 Hz, 1H, Ar*H*), 7.65 (d, *J* = 8.3 Hz, 2H, Ar*H*), 7.59 (d, *J* = 8.3 Hz, 2H, Ar*H*), 7.50 (d, *J* = 8.4 Hz, 2H, Ar*H*), 7.38-7.32 (m, 1H, Ar*H*), 7.30-7.25 (m, 1H, Ar*H*), 7.20 (d, *J* = 8.0 Hz, 2H, Ar*H*), 7.09 (td, *J* = 7.5, 0.9 Hz, 1H, Ar*H*), 5.81 (d, *J* = 3.8 Hz, 1H, NCH), 3.87 (d, *J* = 3.8 Hz, 1H, CHCO₂Me), 3.57 (s, 3H, CO₂CH₃), 2.35 (s, 3H, CH₃) ppm; ¹³C NMR (75 MHz, CDCl₃): δ = 170.3 (C=O), 146.1 (ArC), 144.3 (ArC), 141.6 (ArC), 134.3 (ArC), 130.0 (q, *J* = 32.6 Hz, ArC-CF₃), 129.7 (ArC), 129.6 (ArC), 127.6 (ArC), 126.8 (ArC), 126.4 (ArC), 126.3 (ArC), 126.0 (q, *J* = 3.7 Hz, ArC), 124.6 (ArC), 123.7 (q, *J* = 222.6 Hz, CF₃), 115.8 (ArC), 66.9 (NCH), 55.3 (C), 52.8 (C), 21.6 (CH₃) ppm; IR (neat): 2955w, 2925w, 1736s, 1597w, 1477m, 1462m, 1358s, 1323s, 1161s, 1109s, 1089s, 1066m, 812m, 752m, 656m; HRMS (APCI): Exact mass calc. for C₂₄H₂₁NO₄SF₃ [M+H]⁺: 476.1143, Found: 476.1154; MS (APCI): *m/z* 508 (34%), 478 (10), 477 (29), 476 (M+H⁺, 100), 326 (5), 321 (12), 155 (3); *ee*: 72%, determined by HPLC analysis: YMC Chiral Amylose-C S-5 μm (25 cm), *n*-hexane / *i*-PrOH: 95: 5, 1.0 mL/min, 10 °C, 254 nm, T_{res} (major, (S,S)-isomer) = 25.8 min, T_{res} (minor, (R,R)-isomer) = 37.1 min; [α]_D²⁰: -30° (c 0.1, CHCl₃).



Peak#	Ret. Time	Area%
1	26.184	50.731
2	37.076	49.269
Total		100.000



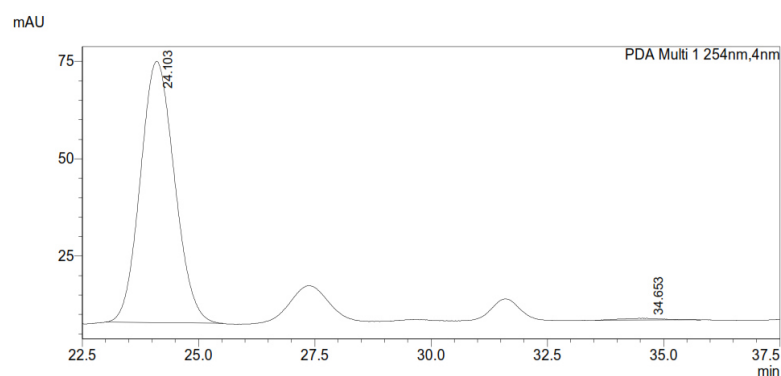
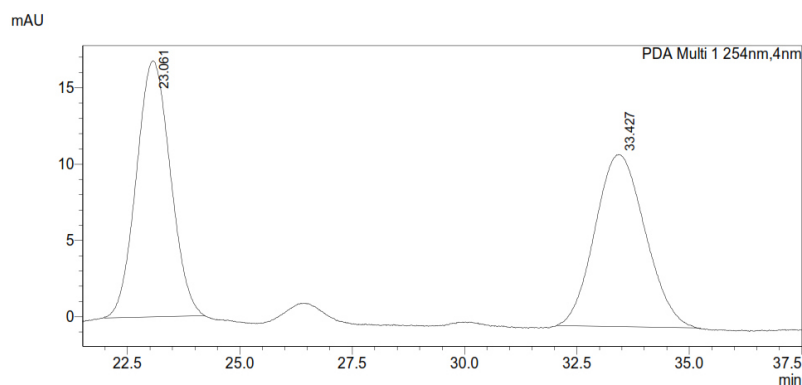
Peak#	Ret. Time	Area%
1	25.810	85.774
2	37.087	14.226
Total		100.000



Methyl (2S,3S)-2-([1,1'-biphenyl]-2-yl)-1-tosylindoline-3-carboxylate **280**:

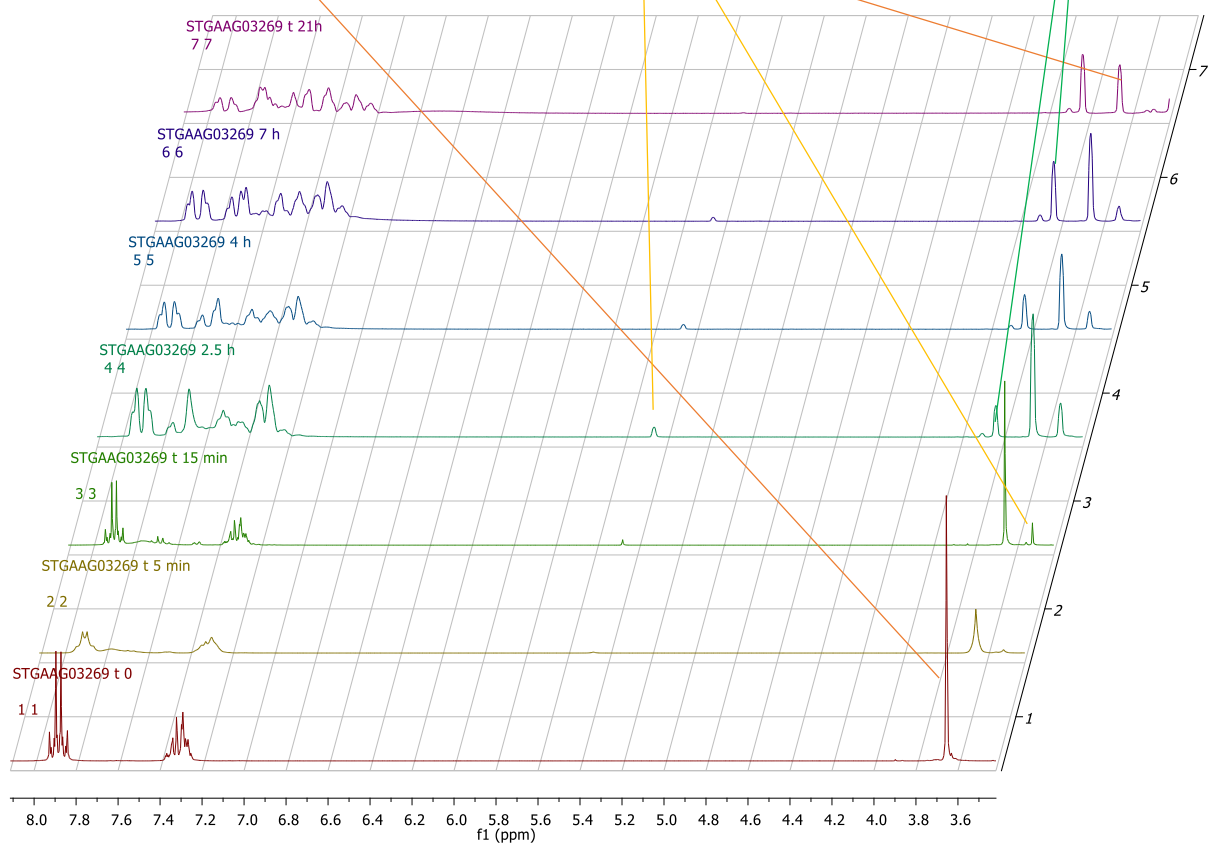
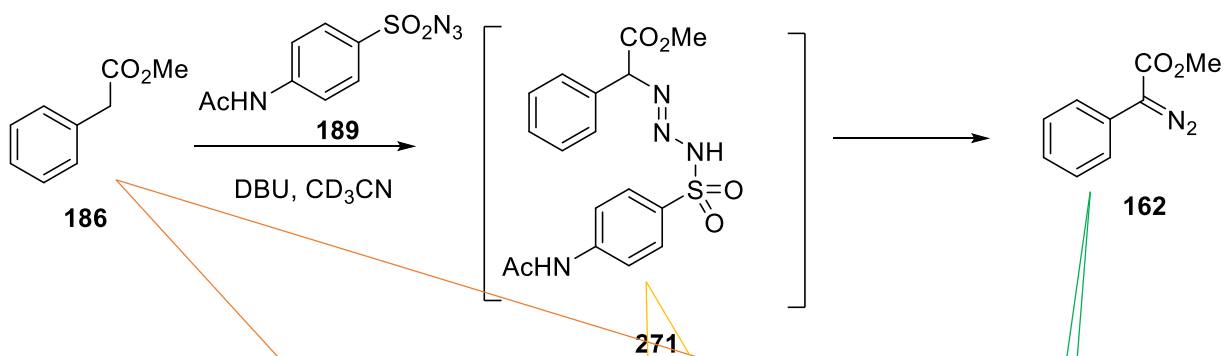
Performed according to the general procedure on a 0.1 mmol scale (53 mg); 6f (18 mg, 0.037 mmol, 37%, 13:1 *d.r.*, 99:1 *e.r.*) was obtained as colourless solid, m.p.199-201 °C. ¹H NMR (300 MHz, CDCl₃): δ = 7.75 (d, *J* = 8.2 Hz, 1H, *ArH*), 7.51-7.38 (m, 8H, *ArH*), 7.35-7.30 (m, 2H, *ArH*), 7.29-7.25 (m, 2H, *ArH*), 7.14-7.08 (m, 3H, *ArH*), 7.00 (td, *J* = 7.5, 1.0 Hz, 1H, *ArH*), 5.83 (d, *J* = 3.6 Hz, 1H, *NCH*), 3.76 (d, *J* = 3.6 Hz, 1H, *CHCO₂Me*), 3.14 (s, 3H, *CO₂CH₃*), 2.31 (s, 3H, *CH₃*) ppm; ¹³C NMR (75 MHz, CDCl₃): δ = 170.1 (C=O), 143.8 (ArC), 142.1 (ArC), 140.7 (ArC), 140.5 (ArC), 139.9 (ArC), 134.5 (ArC), 130.0 (ArC), 129.8 (ArC), 129.5 (ArC),

129.3 (ArC), 128.4 (ArC), 128.3 (ArC), 127.7 (ArC), 127.5 (ArC), 127.4 (ArC), 127.3 (ArC), 125.6 (ArC), 125.5 (ArC), 124.2 (ArC), 115.3 (ArC), 64.0 (C), 55.9 (C), 52.1 (C), 21.5 (CH₃) ppm; IR (neat): 2983w, 1735s, 1356m, 1228.7m, 1217m, 1167m, 1091w, 959w, 752m, 692m cm⁻¹; HRMS (APCI): Exact mass calc. for C₂₉H₂₆NO₄S [M+H]⁺: 484.1583, Found: 484.1573; MS (APCI): m/z 507 (31%), 506 (100), 484 (M+H⁺, 32), 329 (5); ee: 98%, determined by HPLC analysis: YMC Chiral Amylose-C S 5 μm (25 cm), *n*-hexane / *i*-PrOH: 95:5, 1.0 mL/min, 10 °C, 254 nm, T_{res} (major, (S,S)-isomer) = 24.1 min, T_{res} (minor, (R,R)-isomer) = 34.6 min; [α]_D²⁰: -45° (c 0.1, CHCl₃).

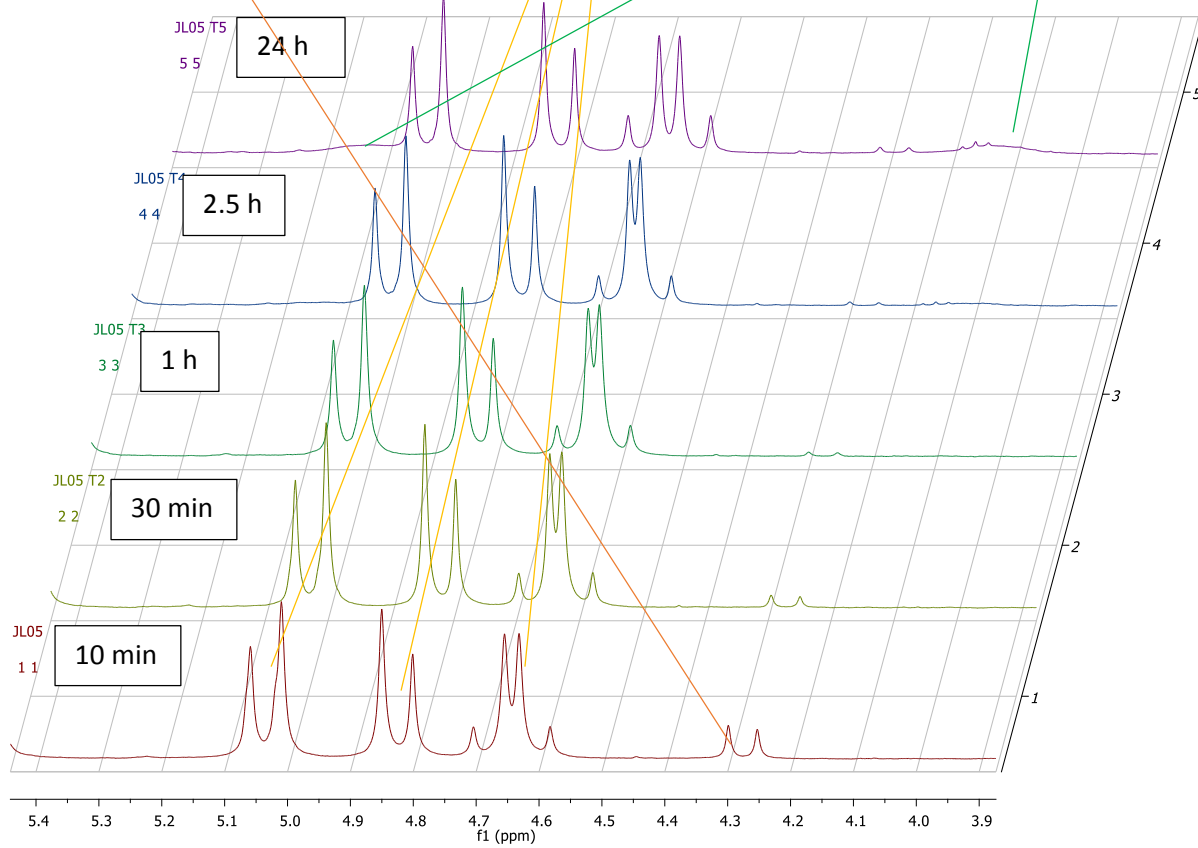
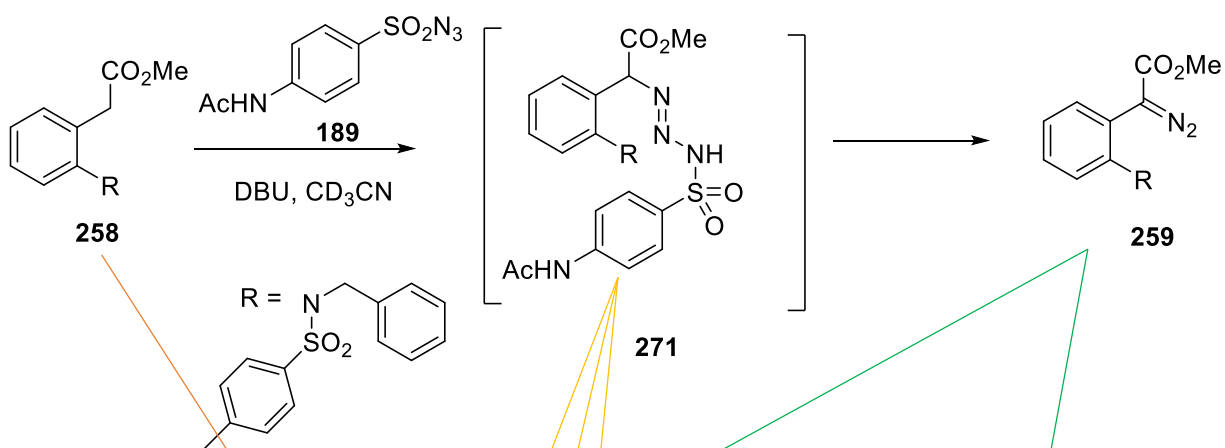


7.4.2.5 ^1H NMR studies

7.4.2.5.1 Diazo Transfer with methyl phenylacetate **186**



7.4.2.5.2 Diazo transfer with ester 258



References

- 1 E. B. Womack, A. B. Nelson, *Org. Synth.* **1944**, 24, 56.
- 2 M. Ranocchiari, A. Mezzetti, *Organometallics* **2009**, 28, 3611.
- 3 T. Toma, J. Shimokawa, T. Fukuyama, *Org. Lett.* **2007**, 9, 3195.
- 4 M. O. Erhunmwunse, P. G. Steel, *J. Org. Chem.* **2008**, 73, 8675.
- 5 P. R. Likhar, S. Roy, M. Roy, M. S. Subhas, M. L. Kantam, *Catal. Commun.* **2009**, 10, 728.
- 6 W. Wang, K. Shen, X. Hu, J. Wang, X. Liu, X. Feng, *Synlett* **2009**, 10, 1655.
- 7 H. Krawczyk, K. Wąsek, J. Kędzia, J. Wojciechowski, W. M. Wolf, *Org. Biomol. Chem.* **2008**, 6, 308.
- 8 M. Frigerio, M. Santagostino, S. Sputore, *J. Org. Chem.* **1999**, 64, 4537.
- 9 M. Frigerio, M. Santagostino, *Tetrahedron Lett.* **1994**, 35, 8019.
- 10 R. A. Maurya, K.-I. Min, D.-P. Kim, *Green Chem.* **2014**, 16, 116.
- 11 C. J. Moody, R. J. Taylor, *J. Chem. Soc. Perkin Trans. I* **1989**, 721.
- 12 A. Padwa, Y. S. Kulkarni, Z. Zhang, *J. Org. Chem.* **1990**, 55, 4144.
- 13 M. P. Doyle, M. Yan, W. Hu, L. S. Gronenberg, *J. Am. Chem. Soc.* **2003**, 125, 4692.
- 14 H.-F. Cui, L. Wang, L.-J. Yang, J. Nie, Y. Zheng, J.-A. Ma, *Tetrahedron* **2011**, 67, 8470.
- 15 F. Benfatti, S. Yilmaz, P. G. Cozzy, *Adv. Synth. Catal.* **2009**, 351, 1763.
- 16 B. Darses, I. N. Michaelides, F. Sladojevich, J. W. Ward, P. R. Rzepa, D. J. Dixon, *Org. Lett.* **2012**, 14, 1684.
- 17 F. Stoessel, H. Fierz, P. Lerena, G. Killé, *Org. Proc. Res. Dev.* **1997**, 1, 428.
- 18 J.-M. Dien, H. Fierz, F. Stoessel, G. Killé, *Chimia* **1994**, 48, 542.
- 19 F. Stoessel, *Chem. Eng. Process* **1993**, 89, 68.
- 20 E. Tayama, T. Yanaki, H. Iwamoto, E. Hasegawa, *Eur. J. Org. Chem.* **2010**, 6719.
- 21 M. J. O. Anteunis, C. Van der Auwera, L. Vanfleteren, F. Borremans, *Bull. Soc. Chim. Belges* **1988**, 97, 135.
- 22 H. Saito, T. Uchiyama, M. Miyake, M. Anada, S. Hashimoto, T. Takabatake, S. Miyairi, *Heterocycles*, **2010**, 81, 1149.
- 23 M. P. Doyle, W. Hu, *Adv. Synth. Catal.* **2001**, 343, 299.
- 24 T. Momose, N. Toyooka, T. Ikuta, H. Yanagino, *Heterocycles* **1990**, 30, 789.
- 25 M. P. Doyle, S. B. Davies, W. Hu, *Org. Lett.* **2000**, 2, 1145.
- 26 J. Barluenga, F. Aznar, I. Gutiérrez, J. A. Martín, *Org. Lett.* **2002**, 4, 2719.
- 27 S. K. Alamsetti, G. Sekar, *Chem. Commun.* **2010**, 46, 7235.
- 28 S. Lee, H.-J. Lim, K. L. Cha, G. A. Sulikowski, *Tetrahedron* **1997**, 53, 16521.
- 29 F. de Nanteuil, J. Waser, *Angew. Chem. Int. Ed.* **2011**, 50, 12075.
- 30 J. Waser, B. Gaspar, H. Nambu, E. M. Carreira, *J. Am. Chem. Soc.* **2006**, 128, 11693.